NAVAL POSTGRADUATE SCHOOL

MONTEREY, CALIFORNIA

THESIS

TOWARD QUANTIFYING THE IMPACT OF ATMOSPHERIC FORCING ON ARCTIC SEA ICE VARIABILITY USING THE NPS 1/12 DEGREE PAN-ARCTIC COUPLED ICE-OCEAN MODEL

by

Hsien-Liang R. Tseng

March 2010

Thesis Co-Advisors: Wieslaw Maslowski
Rebecca E. Stone

Approved for public release; distribution is unlimited

REPORT DOCUMENTATION PAGE			Form Approved OMB No. 0704-0188
Public reporting burden for this collection of information is estimated to average 1 hour per response, including the time for reviewing instruction, searching existing data sources, gathering and maintaining the data needed, and completing and reviewing the collection of information. Send comments regarding this burden estimate or any other aspect of this collection of information, including suggestions for reducing this burden, to Washington headquarters Services, Directorate for Information Operations and Reports, 1215 Jefferson Davis Highway, Suite 1204, Arlington, VA 22202-4302, and to the Office of Management and Budget, Paperwork Reduction Project (0704-0188) Washington DC 20503.			
1. AGENCY USE ONLY ***(Leave blank)***	**2. REPORT DATE** March 2010	**3. REPORT TYPE AND DATES COVERED** Master's Thesis	
4. TITLE AND SUBTITLE Toward Quantifying the Impact of Atmospheric Forcing on Arctic Sea Ice Variability Using the NPS 1/12 Degree Pan-Arctic Coupled Ice-Ocean Model		**5. FUNDING NUMBERS**	
6. AUTHOR(S) Tseng, Hsien-Liang R.			
7. PERFORMING ORGANIZATION NAME(S) AND ADDRESS(ES) Naval Postgraduate School Monterey, CA 93943-5000		**8. PERFORMING ORGANIZATION REPORT NUMBER**	
9. SPONSORING /MONITORING AGENCY NAME(S) AND ADDRESS(ES) N/A		**10. SPONSORING/MONITORING AGENCY REPORT NUMBER**	
11. SUPPLEMENTARY NOTES The views expressed in this thesis are those of the author and do not reflect the official policy or position of the Department of Defense or the U.S. Government. IRB Protocol number _____.			
12a. DISTRIBUTION / AVAILABILITY STATEMENT Approved for public release; distribution is unlimited		**12b. DISTRIBUTION CODE** **A**	

13. ABSTRACT (maximum 200 words)

The rapid Arctic sea ice decline since the 1970s has propelled the United States into a state of urgency for updating its defense plan as Arctic and non-Arctic nations alike are taking an interest in the newfound natural resources of an ice-declining Arctic. In line with the National Security Presidential Directive-66, we quantify the amount of anomalous sea ice variability (aSIV) that anomalous atmospheric forcing parameters explain using partial covariance analysis. A one-system approach where the NPS Model sea ice parameters are the direct output of the atmospheric forcing parameters input is employed. Atmospheric forcing fields of 2-m temperature, downward shortwave and longwave fluxes, 10-m zonal and meridional winds and stresses, are from the European Centre for Medium-Range Weather Forecasts Reanalysis-15 and Operational Products. Locations of interest are the Central Arctic seas, and locations along the Northwest Passage (NWP) and the Northern Sea Route (NSR). Results show that the atmospheric parameter having the largest influence on aSIV is anomalous surface air temperature. This occurs during the cooling months and averages 4-39% of aSAT contribution to aSIV in the Central Arctic, 9-16% along the NWP, and 11-25% along the NSR. Results also suggest that atmospheric forcing alone does not explain all of aSIV.

14. SUBJECT TERMS Arctic Sea Ice, Sea Ice Extent, Sea Ice Thickness, Sea Ice Volume, Coupled Ice-Ocean Model, Partial Correlation Coefficient, Surface Air Temperature, Arctic Oscillation, Atmospheric Forcing, Oceanic Forcing			**15. NUMBER OF PAGES** 200
			16. PRICE CODE
17. SECURITY CLASSIFICATION OF REPORT Unclassified	**18. SECURITY CLASSIFICATION OF THIS PAGE** Unclassified	**19. SECURITY CLASSIFICATION OF ABSTRACT** Unclassified	**20. LIMITATION OF ABSTRACT** UU

NSN 7540-01-280-5500 Standard Form 298 (Rev. 2-89)
Prescribed by ANSI Std. 239-18

THIS PAGE INTENTIONALLY LEFT BLANK

Approved for public release; distribution is unlimited

TOWARD QUANTIFYING THE IMPACT OF ATMOSPHERIC FORCING ON ARCTIC SEA ICE VARIABILITY USING THE NPS 1/12 DEGREE PAN-ARCTIC COUPLED ICE-OCEAN MODEL

Hsien-Liang R. Tseng
Captain, United States Air Force
B.S., University of California at Los Angeles, 2004

Submitted in partial fulfillment of the
requirements for the degrees of

MASTER OF SCIENCE IN METEOROLOGY
MASTER OF SCIENCE IN PHYSICAL OCEANOGRAPHY

from the

NAVAL POSTGRADUATE SCHOOL
March 2010

Author: Hsien-Liang R. Tseng

Approved by: Wieslaw Maslowski
Thesis Co-Advisor

Rebecca E. Stone
Thesis Co-Advisor

Philip Durkee
Chairman, Department of Meteorology

Jeffrey Paduan
Chairman, Department of Oceanography

THIS PAGE INTENTIONALLY LEFT BLANK

ABSTRACT

The rapid Arctic sea ice decline since the 1970s has propelled the United States into a state of urgency for updating its defense plan as Arctic and non-Arctic nations alike are taking an interest in the newfound natural resources of an ice-declining Arctic. In line with the National Security Presidential Directive-66, we quantify the amount of anomalous sea ice variability (aSIV) that anomalous atmospheric forcing parameters explain using partial covariance analysis. A one-system approach where the NPS Model sea ice parameters are the direct output of the atmospheric forcing parameters input is employed. Atmospheric forcing fields of 2-m temperature, downward shortwave and longwave fluxes, 10-m zonal and meridional winds and stresses, are from the European Centre for Medium-Range Weather Forecasts Reanalysis-15 and Operational Products. Locations of interest are the Central Arctic seas, and locations along the Northwest Passage (NWP) and the Northern Sea Route (NSR). Results show that the atmospheric parameter having the largest influence on aSIV is anomalous surface air temperature. This occurs during the cooling months and averages 4-39% of aSAT contribution to aSIV in the Central Arctic, 9-16% along the NWP, and 11-25% along the NSR. Results also suggest that atmospheric forcing alone does not explain all of aSIV.

THIS PAGE INTENTIONALLY LEFT BLANK

TABLE OF CONTENTS

I. INTRODUCTION....1
A. IMPORTANCE OF ARCTIC SEA ICE DECLINE RESEARCH....1
B. RELEVANCE TO THE DEPARTMENT OF DEFENSE....5
C. CURRENT STATE OF RESEARCH ON ARCTIC SEA ICE VARIABILITY....10

II. DESCRIPTION OF DATA AND METHODOLGY....19
A. DESCRIPTION OF NAVAL POSTGRADUATE SCHOOL (NPS) 1/12 DEGREE PAN-ARCTIC COUPLED ICE-OCEAN MODEL....19
B. DESCRIPTION OF EUROPEAN CENTRE FOR MEDIUM-RANGE WEATHER FORECASTS (ECMWF) REANALYSIS-15 AND EUROPEAN CENTRE FOR MEDIUM-RANGE WEATHER FORECASTS OPERATIONAL PRODUCTS....20
C. METHODOLOGY....21

III. RESULTS....25
A. MONTHLY ATMOSPHERIC FORCING AVERAGE OVER THE NAVAL POSTGRADUATE SCHOOL MODEL DOMAIN....25
1. Surface Air Temperature....26
2. Downward Shortwave Flux....33
3. Downward Longwave Flux....40
B. ANOMALOUS SEA ICE VOLUME, THICKNESS, AND AREA VARIABILITY IN THE CENTRAL ARCTIC (1979–2004)....47
C. ANOMALOUS SEA ICE VOLUME, THICKNESS, AND AREA VARIABILITY IN THE CENTRAL ARCTIC (1979–1991)....50
D. ANOMALOUS SEA ICE VOLUME, THICKNESS, AND AREA VARIABILITY IN THE CENTRAL ARCTIC (1992–2004)....54
E. ANOMALOUS SEA ICE VOLUME, THICKNESS, AND AREA VARIABILITY ALONG THE NORTHWEST PASSAGE (1979–2004)....56
F. ANOMALOUS SEA ICE VOLUME, THICKNESS, AND AREA VARIABILITY ALONG THE NORTHERN SEA ROUTE (1979–2004)....58
G. SUMMARY OF ATMOSPHERIC CONTRIBUTION TO ANOMALOUS SEA ICE VOLUME VARIABILITY IN THE CENTRAL ARCTIC (1979–2004)....60

IV. DISCUSSION OF RESULTS....63
A. SEA ICE VARIABILITY....63
B. COMPARISON WITH PREVIOUS STUDIES....65
1. Similarities with Previous Studies....65
2. Contrasts with Previous Studies....66
C. ANOMALOUS SEA ICE THICKNESS VARIABILITY....69

D. SEASONAL ANOMALOUS SURFACE AIR TEMPERATURE CONTRIBUTION TO SEA ICE VARIABILITY 70
E. NORTHWEST PASSAGE AND THE NORTHERN SEA ROUTE 70

V. CONCLUSIONS 73
A. AVERAGE ANOMALOUS ATMOSPHERIC FORCING CONTRIBUTION TO ANOMALOUS SEA ICE VARIABILITY 73
B. THE MISSING LINK 74
C. DEPARTMENT OF DEFENSE PARTNERSHIPS 76

VI. RECOMMENDATIONS FOR FUTURE ARCTIC CLIMATE RESEARCH 77

APPENDIX A: DAY CONVERSION AND LOCATION POSITION 79

APPENDIX B: ANOMALOUS SEA ICE VARIABILITY IN THE CENTRAL ARCTIC (1979–2004) 81
A. ANOMALOUS SEA ICE VOLUME VARIABILITY 81
B. ANOMALOUS SEA ICE THICKNESS VARIABILITY 85
C. ANOMALOUS SEA ICE AREA VARIABILITY 88

APPENDIX C: ANOMALOUS SEA ICE VARIABILITY IN THE CENTRAL ARCTIC (1979–1991) 93
A. ANOMALOUS SEA ICE VOLUME VARIABILITY 93
B. ANOMALOUS SEA ICE THICKNESS VARIABILITY 96
C. ANOMALOUS SEA ICE AREA VARIABILITY 99

APPENDIX D: ANOMALOUS SEA ICE VARIABILITY IN THE CENTRAL ARCTIC (1992–2004) 103
A. ANOMALOUS SEA ICE VOLUME VARIABILITY 103
B. ANOMALOUS SEA ICE THICKNESS VARIABILITY 106
C. ANOMALOUS SEA ICE AREA VARIABILITY 109

APPENDIX E: ANOMALOUS SEA ICE VARIABILITY ALONG THE NORTHWEST PASSAGE (1979–2004) 113
A. ANOMALOUS SEA ICE VOLUME VARIABILITY 113
B. ANOMALOUS SEA ICE THICKNESS VARIABILITY 116
C. ANOMALOUS SEA ICE AREA VARIABILITY 119

APPENDIX F: ANOMALOUS SEA ICE VARIABILITY ALONG THE NORTHERN SEA ROUTE (1979–2004) 123
A. ANOMALOUS SEA ICE VOLUME VARIABILITY 123
B. ANOMALOUS SEA ICE THICKNESS VARIABILITY 126
C. ANOMALOUS SEA ICE AREA VARIABILITY 129

APPENDIX G: SUMMARY OF ATMOSPHERIC CONTRIBUTION TO ANOMALOUS SEA ICE VOLUME VARIABILITY IN THE CENTRAL ARCTIC 133
A. 1979-2004 134
B. 1979-1991 137
C. 1992-2004 140

APPENDIX H: SUMMARY OF ATMOSPHERIC CONTRIBUTION TO ANOMALOUS SEA ICE THICKNESS IN THE CENTRAL ARCTIC.....143
A. 1979-2004.....144
B. 1979-1991.....147
C. 1992-2004.....150

APPENDIX I: SUMMARY OF ATMOSPHERIC CONTRIBUTION TO ANOMALOUS SEA ICE AREA VARIABILITY IN THE CENTRAL ARCTIC.....153
A. 1979-2004.....154
B. 1979-1991.....157
C. 1992-2004.....160

LIST OF REFERENCES.....163

INITIAL DISTRIBUTION LIST.....169

THIS PAGE INTENTIONALLY LEFT BLANK

LIST OF FIGURES

Figure 1. Arctic Geography and Topography [From Hassol 2004]. 2
Figure 2. The Positive (left) and Negative Phases (right) of the Arctic Oscillation (From Mitchell 2004).....11
Figure 3. Isochrone maps depicting the number of years required for ice to exit the Arctic region through Fram Strait during a positive phase of the AO (left) and during a negative phase of the AO (right) (From Rigor et al. 2002). 12
Figure 4. Time series of the winter (November-March) Arctic Oscillation Index from 1951-2004 show the positive and negative episodic behavior of the Arctic Oscillation [From Overland and Wang 2005]. 13
Figure 5. Time series of the Northern Hemisphere sea ice extent anomalies from 1979-2004 show a linear trend, contrary to the episodic behavior of the Arctic Oscillation Index (From Overland and Wang 2005). 14
Figure 6. NPS 1/12 Degree Pan-Arctic Coupled Ice-Ocean Model Domain (From Maslowski et al. 2004).....20
Figure 7. Map of Arctic region highlighting the seas analyzed in Francis et al. (2005), the North Pole and the Canadian Arctic Archipelago (white); locations along the Northwest Passage (orange); locations along the Northern Sea Route (violet).....21
Figure 8. Monthly Mean SAT: Month 1 (top) and Month 2 (bottom) 27
Figure 9. Monthly Mean SAT: Month 3 (top) and Month 4 (bottom) 28
Figure 10. Monthly Mean SAT: Month 5 (top) and Month 6 (bottom) 29
Figure 11. Monthly Mean SAT: Month 7 (top) and Month 8 (bottom) 30
Figure 12. Monthly Mean SAT: Month 9 (top) and Month 10 (bottom) 31
Figure 13. Monthly Mean SAT: Month 11 (top) and Month 12 (bottom) 32
Figure 14. Monthly Mean SWF: Month 1 (top) and Month 2 (bottom) 34
Figure 15. Monthly Mean SWF: Month 3 (top) and Month 4 (bottom) 35
Figure 16. Monthly Mean SWF: Month 5 (top) and Month 6 (bottom) 36
Figure 17. Monthly Mean SWF: Month 7 (top) and Month 8 (bottom) 37
Figure 18. Monthly Mean SWF: Month 9 (top) and Month 10 (bottom) 38
Figure 19. Monthly Mean SWF: Month 11 (top) and Month 12 (bottom) 39
Figure 20. Monthly Mean LWF: Month 1 (top) and Month 2 (bottom) 41
Figure 21. Monthly Mean LWF: Month 3 (top) and Month 4 (bottom) 42
Figure 22. Monthly Mean LWF: Month 5 (top) and Month 6 (bottom) 43
Figure 23. Monthly Mean LWF: Month 7 (top) and Month 8 (bottom) 44
Figure 24. Monthly Mean LWF: Month 9 (top) and Month 10 (bottom) 45
Figure 25. Monthly Mean LWF: Month 11 (top) and Month 12 (bottom) 46
Figure 26. Anomalous Sea Ice Volume Variability—Beaufort Sea (1979–2004).....47
Figure 27. Anomalous Sea Ice Thickness Variability—Beaufort Sea (1979–2004) 48
Figure 28. Anomalous Sea Ice Area Variability—Beaufort Sea (1979–2004).....48
Figure 29. Anomalous Sea Ice Volume Variability—North Pole (1979–1991) 50
Figure 30. Anomalous Sea Ice Volume Variability—Canadian Arctic Archipelago (1979–1991).....51

Figure 31. Anomalous Sea Ice Thickness Variability—North Pole (1979–1991).....51
Figure 32. Anomalous Sea Ice Thickness Variability—Canadian Arctic Archipelago (1979–1991).....52
Figure 33. Anomalous Sea Ice Area Variability—North Pole (1979–1991).....53
Figure 34. Anomalous Sea Ice Area Variability—Canadian Arctic Archipelago (1979–1991).....53
Figure 35. Anomalous Sea Ice Volume Variability—North Pole (1992–2004).....54
Figure 36. Anomalous Sea Ice Thickness Variability—North Pole (1992–2004).....55
Figure 37. Anomalous Sea Ice Area Variability—North Pole (1992–2004).....56
Figure 38. Anomalous Sea Ice Volume Variability—Cape Bathurst Polynya (1979–2004).....57
Figure 39. Anomalous Sea Ice Thickness Variability—Cape Bathurst Polynya (1979–2004).....57
Figure 40. Anomalous Sea Ice Area Variability—Cape Bathurst Polynya (1979–2004).....58
Figure 41. Anomalous Sea Ice Volume Variability—Bering Sea (1979–2004).....59
Figure 42. Anomalous Sea Ice Thickness Variability—Bering Sea (1979–2004).....59
Figure 43. Anomalous Sea Ice Area Variability—Bering Sea (1979–2004).....60
Figure 44. Average (green), Warming Months Minimum-Maximum Range (red), and Cooling Months Minimum-Maximum Range (blue) of aSAT Contribution to aVOLv (top) and Timing of Warming (red) and Cooling (blue) Minimum and Maximum (bottom)—Central Arctic (1979–2004).....62
Figure 45. Per grid cell (PGC) Mean Annual Sea Ice Volume Cycle for the Central Arctic Locations: Barents Sea (SBRNT), Kara Sea (SKARA), Laptev Sea (SLPTV), E. Siberian Sea (SESBN), Chukchi Sea (SCHKI), Beaufort Sea (SBFRT), the North Pole (ONPLE), and the Canadian Arctic Archipelago (OCAAW).....63
Figure 46. PGC Mean Annual Sea Ice Thickness Cycle for the Central Arctic Locations: SBRNT, SKARA, SLPTV, SESBN, SCHKI, SBFRT, ONPLE, and OCAAW.....64
Figure 47. PGC Mean Annual Sea Ice Concentration (Area) for the Central Arctic Locations: SBRNT, SKARA, SLPTV, SESBN, SCHKI, SBFRT, ONPLE, and OCAAW.....64
Figure 48. Time series of the winter (January-March) Arctic Oscillation Index from 1899-2002 show the positive and negative episodic behavior of the Arctic Oscillation. This AO Index time series is similar to that of Figure 4, but with AO indices from 1899 to 2002 instead of 1951 to 2004 (From Mitchell 2004).....67
Figure 49. Per grid cell (PGC) Mean Annual Sea Ice Volume Cycle for the Bering Sea.....75
Figure 50. Modeled annual climatological heat fluxes to the North and East (blue), to the South and West (red), and net heat flux (black) through northern Bering Sea sections: BS (Bering Strait), AS (Anadyr Strait), SS (Shpanberg Strait), AC (Anadyr Current), SL (St. Lawrence Island).

Monthly means are calculated from a 23-year time series (1979–2001) (From Clement et al. 2005). 75
Figure 51. Anomalous Sea Ice Volume Variability—Barents Sea (1979-2004) 81
Figure 52. Anomalous Sea Ice Volume Variability—Kara Sea (1979-2004) 81
Figure 53. Anomalous Sea Ice Volume Variability—Laptev Sea (1979-2004) 82
Figure 54. Anomalous Sea Ice Volume Variability—E. Siberian Sea (1979-2004) 82
Figure 55. Anomalous Sea Ice Volume Variability—Chukchi Sea (1979-2004) 83
Figure 56. Anomalous Sea Ice Volume Variability—Beaufort Sea (1979-2004) (same as Figure 26) 83
Figure 57. Anomalous Sea Ice Volume Variability—North Pole (1979-2004) 84
Figure 58. Anomalous Sea Ice Volume Variability—Canadian Arctic Archipelago (1979-2004) 84
Figure 59. Anomalous Sea Ice Thickness Variability—Barents Sea (1979-2004) 85
Figure 60. Anomalous Sea Ice Thickness Variability—Kara Sea (1979-2004) 85
Figure 61. Anomalous Sea Ice Thickness Variability—Laptev Sea (1979-2004) 86
Figure 62. Anomalous Sea Ice Thickness Variability—E. Siberian Sea (1979-2004) 86
Figure 63. Anomalous Sea Ice Thickness Variability—Chukchi Sea (1979-2004) 86
Figure 64. Anomalous Sea Ice Thickness Variability—Beaufort Sea (1979-2004) (same as Figure 27) 87
Figure 65. Anomalous Sea Ice Thickness Variability—North Pole (1979-2004) 87
Figure 66. Anomalous Sea Ice Thickness Variability—Canadian Arctic Archipelago (1979-2004) 88
Figure 67. Anomalous Sea Ice Area Variability—Barents Sea (1979-2004) 88
Figure 68. Anomalous Sea Ice Area Variability—Kara Sea (1979-2004) 89
Figure 69. Anomalous Sea Ice Area Variability—Laptev Sea (1979-2004) 89
Figure 70. Anomalous Sea Ice Area Variability—E. Siberian Sea (1979-2004) 89
Figure 71. Anomalous Sea Ice Area Variability—Chukchi Sea (1979-2004) 90
Figure 72. Anomalous Sea Ice Area Variability—Beaufort Sea (1979-2004) (same as Figure 28) 90
Figure 73. Anomalous Sea Ice Area Variability—North Pole (1979-2004) 91
Figure 74. Anomalous Sea Ice Area Variability—Canadian Arctic Archipelago (1979-2004) 91
Figure 75. Anomalous Sea Ice Volume Variability—Barents Sea (1979-1991) 93
Figure 76. Anomalous Sea Ice Volume Variability—Kara Sea (1979-1991) 93
Figure 77. Anomalous Sea Ice Volume Variability—Laptev Sea (1979–1991) 94
Figure 78. Anomalous Sea Ice Volume Variability—E. Siberian Sea (1979–1991) 94
Figure 79. Anomalous Sea Ice Volume Variability—Chukchi Sea (1979–1991) 94
Figure 80. Anomalous Sea Ice Volume Variability—Beaufort Sea (1979-1991) 95
Figure 81. Anomalous Sea Ice Volume Variability—North Pole (1979-1991) (same as Figure 29) 95
Figure 82. Anomalous Sea Ice Volume Variability—Canadian Arctic Archipelago (1979-1991) (same as Figure 30) 95
Figure 83. Anomalous Sea Ice Thickness Variability—Barents Sea (1979-1991) 96
Figure 84. Anomalous Sea Ice Thickness Variability—Kara Sea (1979-1991) 96
Figure 85. Anomalous Sea Ice Thickness Variability—Laptev Sea (1979-1991) 97

Figure 86. Anomalous Sea Ice Thickness Variability—E. Siberian Sea (1979-1991) 97
Figure 87. Anomalous Sea Ice Thickness Variability—Chukchi Sea (1979-1991).....97
Figure 88. Anomalous Sea Ice Thickness Variability—Beaufort Sea (1979-1991).....98
Figure 89. Anomalous Sea Ice Thickness Variability—North Pole (1979-1991) (same as Figure 31).....98
Figure 90. Anomalous Sea Ice Thickness Variability—Canadian Arctic Archipelago (1979-1991) (same as Figure 32).....98
Figure 91. Anomalous Sea Ice Area Variability—Barents Sea (1979-1991) 99
Figure 92. Anomalous Sea Ice Area Variability—Kara Sea (1979-1991).....99
Figure 93. Anomalous Sea Ice Area Variability—Laptev Sea (1979-1991) 100
Figure 94. Anomalous Sea Ice Area Variability—E. Siberian Sea (1979-1991).....100
Figure 95. Anomalous Sea Ice Area Variability—Chukchi Sea (1979-1991).....100
Figure 96. Anomalous Sea Ice Area Variability—Beaufort Sea (1979-1991).....101
Figure 97. Anomalous Sea Ice Area Variability—North Pole (1979-1991) (same as Figure 33).....101
Figure 98. Anomalous Sea Ice Area Variability—Canadian Arctic Archipelago (1979-1991) (same as Figure 34).....102
Figure 99. Anomalous Sea Ice Volume Variability—Barents Sea (1992-2004) 103
Figure 100. Anomalous Sea Ice Volume Variability—Kara Sea (1992-2004).....103
Figure 101. Anomalous Sea Ice Volume Variability—Laptev Sea (1992-2004) 104
Figure 102. Anomalous Sea Ice Volume Variability—E. Siberian Sea (1992-2004).....104
Figure 103. Anomalous Sea Ice Volume Variability—Chukchi Sea (1992-2004).....104
Figure 104. Anomalous Sea Ice Volume Variability—Beaufort Sea (1992-2004) 105
Figure 105. Anomalous Sea Ice Volume Variability—North Pole (1992-2004) (same as Figure 35) 105
Figure 106. Anomalous Sea Ice Volume Variability—Canadian Arctic Archipelago (1992-2004).....106
Figure 107. Anomalous Sea Ice Thickness Variability—Barents Sea (1992-2004).....106
Figure 108. Anomalous Sea Ice Thickness Variability—Kara Sea (1992-2004) 107
Figure 109. Anomalous Sea Ice Thickness Variability—Laptev Sea (1992-2004).....107
Figure 110. Anomalous Sea Ice Thickness Variability—E. Siberian Sea (1992-2004) ...107
Figure 111. Anomalous Sea Ice Thickness Variability—Chukchi Sea (1992-2004).....108
Figure 112. Anomalous Sea Ice Thickness Variability—Beaufort Sea (1992-2004).....108
Figure 113. Anomalous Sea Ice Thickness Variability—North Pole (1992-2004) (same as Figure 36).....108
Figure 114. Anomalous Sea Ice Thickness Variability—Canadian Arctic Archipelago (1992-2004).....109
Figure 115. Anomalous Sea Ice Area Variability—Barents Sea (1992-2004) 109
Figure 116. Anomalous Sea Ice Area Variability—Kara Sea (1992-2004).....110
Figure 117. Anomalous Sea Ice Area Variability—Laptev Sea (1992-2004) 110
Figure 118. Anomalous Sea Ice Area Variability—E. Siberian Sea (1992-2004).....110
Figure 119. Anomalous Sea Ice Area Variability—Chukchi Sea (1992-2004).....111
Figure 120. Anomalous Sea Ice Area Variability—Beaufort Sea (1992-2004).....111
Figure 121. Anomalous Sea Ice Area Variability—North Pole (1992-2004) (same as Figure 37).....111

Figure 122. Anomalous Sea Ice Area Variability—Canadian Arctic Archipelago (1992-2004).....112
Figure 123. Anomalous Sea Ice Volume Variability—Cape Bathurst Polynya (1979-2004) (same as Figure 38).....113
Figure 124. Anomalous Sea Ice Volume Variability—Amundsen Gulf (1979-2004).....113
Figure 125. Anomalous Sea Ice Volume Variability—Coronation Gulf (1979-2004).....114
Figure 126. Anomalous Sea Ice Volume Variability—Queen Maud Gulf (1979-2004) ..114
Figure 127. Anomalous Sea Ice Volume Variability—Lancaster Sound (1979-2004) 114
Figure 128. Anomalous Sea Ice Volume Variability—North Water Polynya (1979-2004).....115
Figure 129. Anomalous Sea Ice Volume Variability—Baffin Bay (1979-2004).....115
Figure 130. Anomalous Sea Ice Volume Variability—Davis Strait (1979-2004) 115
Figure 131. Anomalous Sea Ice Thickness Variability—Cape Bathurst Polynya (1979-2004) (same as Figure 39).....116
Figure 132. Anomalous Sea Ice Thickness Variability—Amundsen Gulf (1979-2004) ..116
Figure 133. Anomalous Sea Ice Thickness Variability—Coronation Gulf (1979-2004)..117
Figure 134. Anomalous Sea Ice Thickness Variability—Queen Maud Gulf (1979-2004).....117
Figure 135. Anomalous Sea Ice Thickness Variability—Lancaster Sound (1979-2004) .117
Figure 136. Anomalous Sea Ice Thickness Variability—North Water Polynya (1979-2004).....118
Figure 137. Anomalous Sea Ice Thickness Variability—Baffin Bay (1979-2004) 118
Figure 138. Anomalous Sea Ice Thickness Variability—Davis Strait (1979-2004).....118
Figure 139. Anomalous Sea Ice Area Variability—Cape Bathurst Polynya (1979-2004) (same as Figure 40).....119
Figure 140. Anomalous Sea Ice Area Variability—Amundsen Gulf (1979-2004).....119
Figure 141. Anomalous Sea Ice Area Variability—Coronation Gulf (1979-2004).....120
Figure 142. Anomalous Sea Ice Area Variability—Queen Maud Gulf (1979-2004) 120
Figure 143. Anomalous Sea Ice Area Variability—Lancaster Sound (1979-2004).....120
Figure 144. Anomalous Sea Ice Area Variability—North Water Polynya (1979-2004) ..121
Figure 145. Anomalous Sea Ice Area Variability—Baffin Bay (1979-2004).....121
Figure 146. Anomalous Sea Ice Area Variability—Davis Strait (1979-2004) 121
Figure 147. Anomalous Sea Ice Volume Variability—Bering Sea (1979-2004) (same as Figure 41) 123
Figure 148. Anomalous Sea Ice Volume Variability—Inner E. Siberian Sea (1979-2004).....123
Figure 149. Anomalous Sea Ice Volume Variability—New Siberian Islands (1979-2004).....124
Figure 150. Anomalous Sea Ice Volume Variability—Severnaya Zemlya (1979-2004) .124
Figure 151. Anomalous Sea Ice Volume Variability—Inner Kara Sea (1979-2004) 124
Figure 152. Anomalous Sea Ice Volume Variability—Inner Barents Sea (1979-2004)...125
Figure 153. Anomalous Sea Ice Volume Variability—White Sea (1979-2004).....125
Figure 154. Anomalous Sea Ice Thickness Variability—Bering Sea (1979-2004) (same as Figure 42) 126

Figure 155. Anomalous Sea Ice Thickness Variability—Inner E. Siberian Sea (1979-2004).....126
Figure 156. Anomalous Sea Ice Thickness Variability—New Siberian Islands (1979-2004).....127
Figure 157. Anomalous Sea Ice Thickness Variability—Severnaya Zemlya (1979-2004).....127
Figure 158. Anomalous Sea Ice Thickness Variability—Inner Kara Sea (1979-2004)....127
Figure 159. Anomalous Sea Ice Thickness Variability—Inner Barents Sea (1979-2004).....128
Figure 160. Anomalous Sea Ice Thickness Variability—White Sea (1979-2004) 128
Figure 161. Anomalous Sea Ice Area Variability—Bering Sea (1979-2004) (same as Figure 43).....129
Figure 162. Anomalous Sea Ice Area Variability—Inner E. Siberian Sea (1979-2004) ..129
Figure 163. Anomalous Sea Ice Area Variability—New Siberian Islands (1979-2004) ..130
Figure 164. Anomalous Sea Ice Area Variability—Severnaya Zemlya (1979-2004) 130
Figure 165. Anomalous Sea Ice Area Variability—Inner Kara Sea (1979-2004) 130
Figure 166. Anomalous Sea Ice Area Variability—Inner Barents Sea (1979-2004).....131
Figure 167. Anomalous Sea Ice Area Variability—White Sea (1979-2004).....131
Figure 168. Average (green), Warming Months Minimum-Maximum Range (red), and Cooling Months Minimum-Maximum Range (blue) of aSAT Contribution to aVOLv (top) and Timing of Warming (red) and Cooling (blue) Minimum and Maximum (bottom)—Central Arctic (1979–2004) (same as Figure 44).....134
Figure 169. Average (green), Warming Months Minimum-Maximum Range (red), and Cooling Months Minimum-Maximum Range (blue) of aSWF Contribution to aVOLv (top) and Timing of Warming (red) and Cooling (blue) Minimum and Maximum (bottom)—Central Arctic (1979–2004).....135
Figure 170. Average (green), Warming Months Minimum-Maximum Range (red), and Cooling Months Minimum-Maximum Range (blue) of aLWF Contribution to aVOLv (top) and Timing of Warming (red) and Cooling (blue) Minimum and Maximum (bottom)—Central Arctic (1979–2004).....136
Figure 171. Average (green), Warming Months Minimum-Maximum Range (red), and Cooling Months Minimum-Maximum Range (blue) of aSAT Contribution to aVOLv (top) and Timing of Warming (red) and Cooling (blue) Minimum and Maximum (bottom)—Central Arctic (1979–1991).....137
Figure 172. Average (green), Warming Months Minimum-Maximum Range (red), and Cooling Months Minimum-Maximum Range (blue) of aSWF Contribution to aVOLv (top) and Timing of Warming (red) and Cooling (blue) Minimum and Maximum (bottom)—Central Arctic (1979–1991).....138
Figure 173. Average (green), Warming Months Minimum-Maximum Range (red), and Cooling Months Minimum-Maximum Range (blue) of aLWF Contribution to aVOLv (top) and Timing of Warming (red) and Cooling (blue) Minimum and Maximum (bottom)—Central Arctic (1979–1991).....139
Figure 174. Average (green), Warming Months Minimum-Maximum Range (red), and Cooling Months Minimum-Maximum Range (blue) of aSAT Contribution

to aVOLv (top) and Timing of Warming (red) and Cooling (blue) Minimum and Maximum (bottom)—Central Arctic (1992–2004).....140
Figure 175. Average (green), Warming Months Minimum-Maximum Range (red), and Cooling Months Minimum-Maximum Range (blue) of aSWF Contribution to aVOLv (top) and Timing of Warming (red) and Cooling (blue) Minimum and Maximum (bottom)—Central Arctic (1992–2004).....141
Figure 176. Average (green), Warming Months Minimum-Maximum Range (red), and Cooling Months Minimum-Maximum Range (blue) of aLWF Contribution to aVOLv (top) and Timing of Warming (red) and Cooling (blue) Minimum and Maximum (bottom)—Central Arctic (1992–2004).....142
Figure 177. Average (green), Warming Months Minimum-Maximum Range (red), and Cooling Months Minimum-Maximum Range (blue) of aSAT Contribution to aTHKv (top) and Timing of Warming (red) and Cooling (blue) Minimum and Maximum (bottom)—Central Arctic (1979–2004).....144
Figure 178. (Top) Average (green), Warming Months Minimum-Maximum Range (red), and Cooling Months Minimum-Maximum Range (blue) of aSWF Contribution to aTHKv (top) and Timing of Warming (red) and Cooling (blue) Minimum and Maximum (bottom)—Central Arctic (1979–2004) 145
Figure 179. Average (green), Warming Months Minimum-Maximum Range (red), and Cooling Months Minimum-Maximum Range (blue) of aLWF Contribution to aTHKv (top) and Timing of Warming (red) and Cooling (blue) Minimum and Maximum (bottom)—Central Arctic (1979–2004).....146
Figure 180. Average (green), Warming Months Minimum-Maximum Range (red), and Cooling Months Minimum-Maximum Range (blue) of aSAT Contribution to aTHKv (top) and Timing of Warming (red) and Cooling (blue) Minimum and Maximum (bottom)—Central Arctic (1979–1991).....147
Figure 181. Average (green), Warming Months Minimum-Maximum Range (red), and Cooling Months Minimum-Maximum Range (blue) of aSWF Contribution to aTHKv (top) and Timing of Warming (red) and Cooling (blue) Minimum and Maximum (bottom)—Central Arctic (1979–1991).....148
Figure 182. Average (green), Warming Months Minimum-Maximum Range (red), and Cooling Months Minimum-Maximum Range (blue) of aLWF Contribution to aTHKv (top) and Timing of Warming (red) and Cooling (blue) Minimum and Maximum (bottom)—Central Arctic (1979–1991).....149
Figure 183. Average (green), Warming Months Minimum-Maximum Range (red), and Cooling Months Minimum-Maximum Range (blue) of aSAT Contribution to aTHKv (top) and Timing of Warming (red) and Cooling (blue) Minimum and Maximum (bottom)—Central Arctic (1992–2004).....150
Figure 184. Average (green), Warming Months Minimum-Maximum Range (red), and Cooling Months Minimum-Maximum Range (blue) of aSWF Contribution to aTHKv (top) and Timing of Warming (red) and Cooling (blue) Minimum and Maximum (bottom)—Central Arctic (1992–2004).....151
Figure 185. Average (green), Warming Months Minimum-Maximum Range (red), and Cooling Months Minimum-Maximum Range (blue) of aLWF Contribution

to aTHKv (top) and Timing of Warming (red) and Cooling (blue) Minimum and Maximum (bottom)—Central Arctic (1992–2004).....152
Figure 186. Average (green), Warming Months Minimum-Maximum Range (red), and Cooling Months Minimum-Maximum Range (blue) of aSAT Contribution to aARAv (top) and Timing of Warming (red) and Cooling (blue) Minimum and Maximum (bottom)—Central Arctic (1979–2004).....154
Figure 187. Average (green), Warming Months Minimum-Maximum Range (red), and Cooling Months Minimum-Maximum Range (blue) of aSWF Contribution to aARAv (top) and Timing of Warming (red) and Cooling (blue) Minimum and Maximum (bottom)—Central Arctic (1979–2004).....155
Figure 188. Average (green), Warming Months Minimum-Maximum Range (red), and Cooling Months Minimum-Maximum Range (blue) of aLWF Contribution to aARAv (top) and Timing of Warming (red) and Cooling (blue) Minimum and Maximum (bottom)—Central Arctic (1979–2004).....156
Figure 189. Average (green), Warming Months Minimum-Maximum Range (red), and Cooling Months Minimum-Maximum Range (blue) of aSAT Contribution to aARAv (top) and Timing of Warming (red) and Cooling (blue) Minimum and Maximum (bottom)—Central Arctic (1979–1991).....157
Figure 190. Average (green), Warming Months Minimum-Maximum Range (red), and Cooling Months Minimum-Maximum Range (blue) of aSWF Contribution to aARAv (top) and Timing of Warming (red) and Cooling (blue) Minimum and Maximum (bottom)—Central Arctic (1979–1991).....158
Figure 191. Average (green), Warming Months Minimum-Maximum Range (red), and Cooling Months Minimum-Maximum Range (blue) of aLWF Contribution to aARAv (top) and Timing of Warming (red) and Cooling (blue) Minimum and Maximum (bottom)—Central Arctic (1979–1991).....159
Figure 192. Average (green), Warming Months Minimum-Maximum Range (red), and Cooling Months Minimum-Maximum Range (blue) of aSAT Contribution to aARAv (top) and Timing of Warming (red) and Cooling (blue) Minimum and Maximum (bottom)—Central Arctic (1992–2004).....160
Figure 193. Average (green), Warming Months Minimum-Maximum Range (red), and Cooling Months Minimum-Maximum Range (blue) of aSWF Contribution to aARAv (top) and Timing of Warming (red) and Cooling (blue) Minimum and Maximum (bottom)—Central Arctic (1992–2004).....161
Figure 194. Average (green), Warming Months Minimum-Maximum Range (red), and Cooling Months Minimum-Maximum Range (blue) of aLWF Contribution to aARAv (top) and Timing of Warming (red) and Cooling (blue) Minimum and Maximum (bottom)—Central Arctic (1992–2004).....162

LIST OF TABLES

Table 1. Conversion from Julian days to months with near equal number of days. Days with a remainder of 0.4–0.6 days are shared between the preceding and subsequent months. 79
Table 2. Latitude, longitude, and NPS Model grid points of all locations of interest within the Central Arctic, the Northwest Passage and the Northern Sea Route. 80

THIS PAGE INTENTIONALLY LEFT BLANK

LIST OF ACRONYMS AND ABBREVIATIONS

ADVa	Advective Sensible Heat Anomaly
AO	Arctic Oscillation
aARAv	Anomalous Sea Ice Area Variability
AC	Anadyr Current
AFFOR	Air Force Forces
aLWF	Anomalous Longwave Flux
AO	Arctic Oscillation
AR4	Fourth Assessment (IPCC)
ARFOR	Army Forces
AS	Anadyr Strait
aSAT	Anomalous Surface Air Temperature
aSIV	Anomalous Sea Ice Variability
aSWF	Anomalous Shortwave Flux
aTHE	Anomalous Wind Direction
aTHKv	Anomalous Sea Ice Thickness Variability
aUWD	Anomalous Zonal Wind
aVOLv	Anomalous Sea Ice Volume Variability
aVWD	Anomalous Meridional Wind
aWDS	Anomalous Wind Speed
aWSC	Anomalous Wind Stress Curl
aXST	Anomalous Zonal Stress
aYST	Anomalous Meridional Stress
BS	Bering Strait

CH_4	Methane
CNA	Center for Naval Analyses
CO_2	Carbon Dioxide
DLFa	Downwelling Longwave Flux Anomaly
DoD	Department of Defense
ECMWF	European Centre for Medium-Range Weather Forecasts
GHG	Greenhouse Gases
HSPD	Homeland Security Presidential Directive
IPCC	Intergovernmental Panel on Climate Change
LWF	Longwave Flux
MARFOR	Marine Corps Forces
METOC	Meteorological and Oceanographic
MIA	Annual-Maximum Ice-Retreat Anomaly
MR	Meteorology Department, Naval Postgraduate School
N_2O	Nitrous Oxide
NAM	Northern Annular Mode
NAME	Naval Postgraduate School Modeling Effort
NAO	North Atlantic Oscillation
NAVFOR	Navy Forces
NPS	Naval Postgraduate School
NSPD	National Security Presidential Directive
NSR	Northern Sea Route
NWP	Northwest Passage
OC	Oceanography Department, Naval Postgraduate School
OCAAW	Canadian Arctic Archipelago

ONPLE	North Pole
OPNAV	Office of the Chief of Naval Operations
PGC	Per Grid Cell
SAT	Surface Air Temperature
SBFRT	Beaufort Sea
SBRNT	Barents Sea
SCHKI	Chukchi Sea
SESBN	E. Siberian Sea
SKARA	Kara Sea
SL	St. Lawrence Island
SLP	Sea Level Pressure
SLPTV	Laptev Sea
SS	Shpanberg Strait
SSM/I	Special Sensor Microwave/Imager
SSMR	Scanning Multichannel Microwave Radiometer
SST	Sea Surface Temperature
SWF	Shortwave Flux
THE	Wind Direction
USAF	United States Air Force
USN	United States Navy
USS	United States Ship
UWD	Zonal Wind
UWDa	Zonal Wind Anomaly
VWD	Meridional Wind
VWDa	Meridional Wind Anomaly

WDS	Wind Speed
WSC	Wind Stress Curl

ACKNOWLEDGMENTS

The thesis before you is the result of the hard work and diligence of many and to these I offer my heartfelt gratitude:

OPNAV N-84 for their generous support in funding my participation and poster presentation at the 3rd Symposium on the Impacts of an Ice-Diminishing Arctic on Naval and Maritime Operations at the U.S. Naval Academy.

Research Associates and NPS PhD Candidates: **Mark Orzech** (OC) for converting the red in MATLAB Command Window into working programs. >> disp('Thank you!'); **Jaclyn C. Kinney** (OC) for obtaining data, and providing me with hard-to-find articles and helpful advice throughout the research process.

Department Chairs, Professors and the METOC Program Officer: **Philip A. Durkee** (MR), **Mary L. Batteen** (OC), and **Wendell Nuss** (MR) for allowing me to embark on this METOC MS journey; **Patrick A. Harr** (MR) for his direction with partial correlation coefficients analyses; **Peter Guest** (MR) for his help with understanding the surface air temperature and dew point relationship in the Arctic region; and **Lieutenant Commander Victoria L. Taber** (USN), the METOC Program Officer, for her encouragement and strategic academic planning.

Professor Wieslaw Maslowski (OC) for taking me under his wing, sharing his passion for Arctic climate research, and teaching me the importance of seeing the Arctic climate from both atmospheric and oceanic aspects.

Commander Rebecca E. Stone (USN) for exploring thesis topics with me, securing funding, and for her guidance and professional mentorship. CDR Stone has been the keystone throughout this entire NPS METOC MS journey, and for her time and energy I am most grateful.

My classmates who shared their unique academic gifts and talents, and brought thoughtful and creative discussions that made this NPS MS journey a successful and colorful one.

Last, but not least, my family: **My mother** who teaches me perseverance, and **my father** who encouraged graduate education; and **my nieces, Elisabeth and Grace**, for their enthusiasm, inquisitiveness, and thoughtfulness about the Arctic region. For them, may every living creature from the polar bears to the penguins and all that dwell in between forever have their natural habitat, and may only the appropriate natural resources be tapped.

THIS PAGE INTENTIONALLY LEFT BLANK

I. INTRODUCTION

A. IMPORTANCE OF ARCTIC SEA ICE DECLINE RESEARCH

The pristine Arctic is quickly fading (Figure 1). The build-up of carbon dioxide has increased by 35% since the industrial revolution, and the areal sea ice is depleting more in the recent years than ever recorded with a record minimum in 2007 (Intergovernmental Panel on Climate Change [IPCC] 2007). The once-fabled Northwest Passage (NWP) and the Northern Sea Route (NSR), that remained impenetrable to 400 years of exploration, now happens to be navigable (Delaney 2004; CNA 2009). Alaska, sold in 1856 for a mere $7.2 million, is now estimated to have the densest concentration of undiscovered oil and natural gas within the Arctic region (Bird et al. 2008; U.S. Department of State n.d.). Thus, the Arctic that was once deemed of little economic or military importance has now become the primary zone of territorial contention in the Northern Hemisphere.

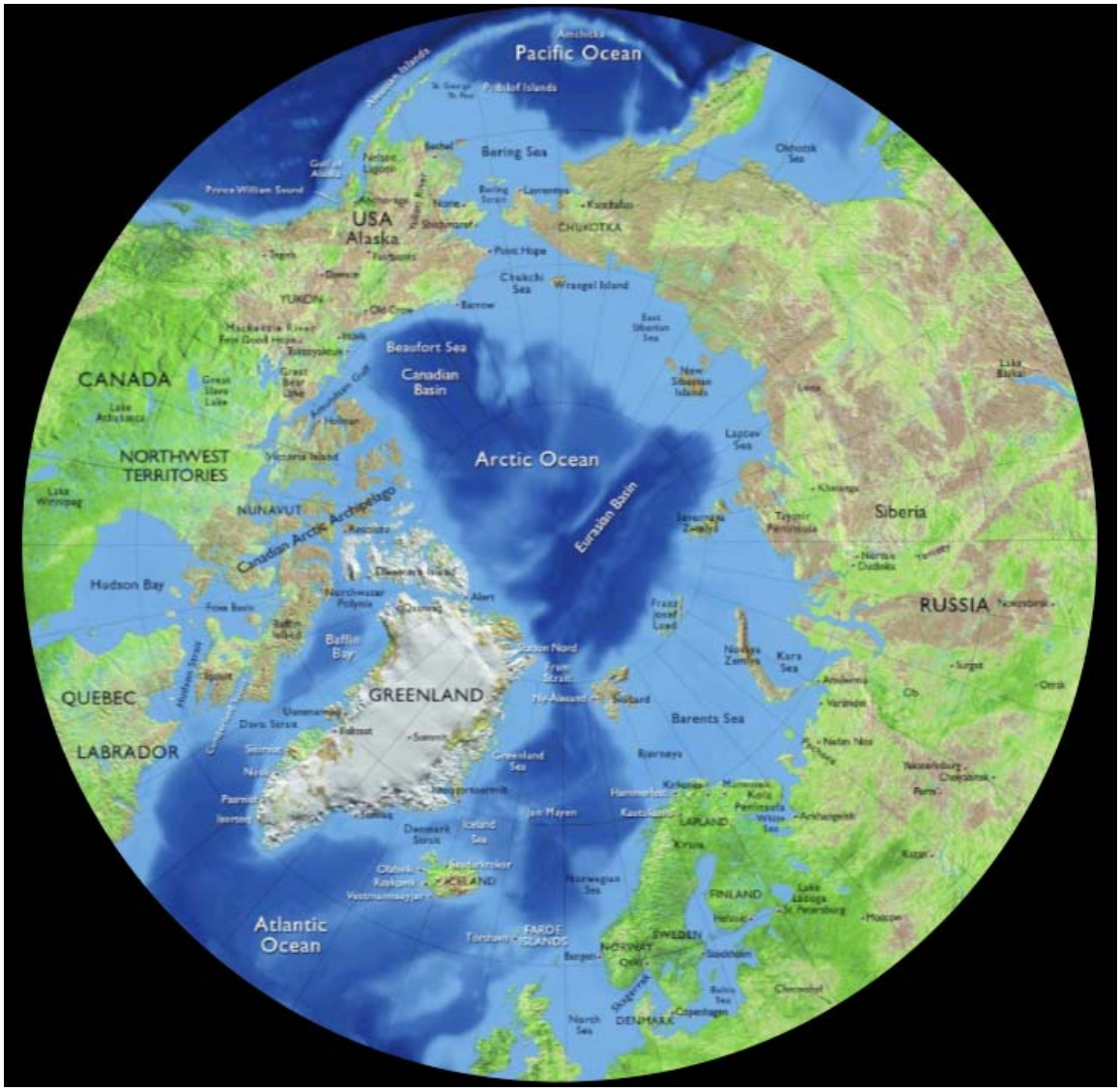

Figure 1. Arctic Geography and Topography [From Hassol 2004].

At the same time, the surface air temperature (SAT) in the Arctic has been climbing. SAT trends have steadily increased since 1910, with the greatest acceleration beginning in the 1970s (IPCC 2007). In 2007 autumn temperatures reached a record 5°C higher than average with 2008 following close behind at 4°C above average (Richter-Menge et al. 2008). Global climate models predict a continual Arctic SAT increase with greater interannual variability throughout the next century (Hassol 2004).

Escalating fossil fuels use, increasing agricultural production, and generation of long-lasting halocarbons may have a direct link to global and Arctic warming. Human

development in transport, commerce and energy produces greenhouse gases (GHG) such as carbon dioxide (CO_2), methane (CH_4), nitrous oxide (N_2O), and halocarbons. CO_2 alone accounts for an overwhelming 75% of GHG released into the atmosphere (IPCC, 2007). GHG allow only some infrared radiation to exit from the Earth's surface into space, leaving the trapped infrared radiation to increase the tropospheric temperatures. In turn, tropospheric water vapor increases, which further boosts the GHG effect (water vapor is also a GHG). Skeptics of anthropogenic global warming may point to solar radiation as a natural cause; however, solar irradiance has increased by only +0.12 W/m^2, just 7% of the total (natural and anthropogenic) radiative forcing increase of 1.6 W/m^2 since 1750 (IPCC 2007).

The results of Arctic warming are unforgiving to both the Earth's ecosystems and the climate. Warming upsets plant and animal ecosystems, and increases the likelihood of weather and precipitation extremes. The Northern Hemisphere treeline is projected to progress northward, following the warming projection. Siberian studies have shown the presence of trees across the northern most edge of the Russian Arctic during the last warming event 8000–9000 years ago (Hassol 2004). The thicker vegetation found further northward only worsens Arctic warming as it fuels the positive vegetation-albedo effect similar to that of Kellog's ice-albedo effect (Sturm et al. 2005). Substituting thick vegetation for snow reduces albedo such that earth absorbs a greater amount of solar radiation, which further exposes the amount of vegetation (Sturm et al. 2005). Solar heating can also provide ideal temperatures for greater vegetation growth. Animals dependent on sea ice for shelter and food such as polar bears, seabirds, walruses and seals will have to adapt to new open ocean or face a probability (20–30%) for extinction (Hassol 2004). Significant changes to weather events have been observed in the last 50 years. While there is some uncertainty, the number of cold days has decreased while the number of heat waves has increased (IPCC 2007). Warming temperatures may cause heavier precipitation in some areas while causing drought in others (IPCC 2007). 2008 proved to be a record-setting year with 41 gigatons more precipitation when compared to the 1971–2001 standard normal period of precipitation over Greenland (Richter-Menge and Overland 2009).

Beyond the ecosystems and weather, the impacts of a warmer Arctic cascade into sea level and global ocean circulation changes, as well as changes in sea ice extent and thickness (Hassol 2004). Greater glacial melting and anomalously large amounts of river runoff from Alaska and Greenland into the Arctic Ocean in the summer months is expected to raise the sea level 10–90 cm within the next century (Hassol 2004), raising concerns for coastal erosion and damage. Those most susceptible to sea level increases are the coastal communities, including naval military bases such as Diego Garcia, which sits just four meters above sea level (Military Sealift Command n.d.). Furthermore, because the freshwater inflow into the Arctic decreases the salinity of the Greenland-Norwegian and the Labrador Seas, the North Atlantic Deep Water formation may lag, slowing the thermohaline circulation (Hassol 2004; Broecker 1999). Slowing of the global ocean system that conveys warm water from the tropics to the polar region could mean warmer tropical summers and colder European winters, as well as a buildup of carbon dioxide concentration in the North Atlantic (Hassol 2004). This GHG buildup essentially completes the freshwater-SAT amplifying cycle. Finally, caught in another self-amplifying cycle are sea ice extent (area) and sea ice thickness. Thick ice and snow have high albedo (0.5–0.9), which reflects a majority of incoming solar radiation, keeping the Arctic cold year round (National Snow and Ice Data Center n.d.). If a perturbation such as an altered export of ice related to the circulation of the Arctic Oscillation causes ice melt, open ocean with much lower albedo (0.06–0.07) is left behind to absorb almost all of the incoming solar radiation, which further increases ocean temperature and melts even more ice (National Snow and Ice Data Center n.d.; Curry et al. 1995). Multiyear ice packs are not exempt from this ice-albedo positive feedback cycle. The development of leads and melt ponds, which have low albedo, can also alter ice thickness (Curry et al. 1995). Analyses of both ice extent and ice thickness are important because sea ice volume is dependent on both of these parameters. Recent satellite altimetry shows a 0.6 m/year decrease in overall sea ice thickness occurred between 2004 and 2008, indicating a reduction in total sea ice volume (Richter-Menge and Overland 2009).

A smaller areal extent of ice can be expected in a warming Arctic. However, the decline in Arctic sea ice extent is accelerating faster than all the Intergovernmental Panel

on Climate Change Fourth Assessment (IPCC AR4) predictions (Stroeve et al. 2007). In 2005, the Arctic sea ice extent registered as the fourth lowest (including 2009) since the availability of the earliest Arctic sea ice satellite images in 1979. In 2008, the Arctic sea ice extent was 34% less than the 1979–2000 mean sea ice extent. The largest decrease in sea ice extent was in the summer of 2007, when the Arctic lost 39% more sea ice than the 1979–2000 mean sea ice extent (CNA 2009). At this accelerated rate of sea ice decrease, the Arctic may see seasonally ice-free conditions within the next 30 years (Wang and Overland 2009), or perhaps even within the next decade as W. Maslowski (personal communication) warns.

Even with such a wide range of forecasts there are countries anticipating an imminent seasonally ice-free Arctic. The Arctic holds a future that boasts potential in oil and natural gas resources, transportation, and commerce possibilities. The United States Geological Survey estimates approximately 90 billion barrels of oil, 1,669 trillion cubic feet of natural gas, and 44 billion barrels of natural gas liquids are within the Arctic region (Bird et al. 2008). This amounts to about 22% of the world's remaining undiscovered oil and gas deposits (CNA 2009; Borgerson 2008). In 2008, both the NWP and the NSR became fully navigable (Braithwaite 2009). Use of the NWP as a shipping route would save 9,000 nautical miles (20% of current distance) between Seattle and Rotterdam; use of the NSR would save 11,200 nautical miles (40% of current distance) between Rotterdam and Yokohama. A commercial transportation shortcut has the potential of evolving into an alternate route for domestic and foreign military operations (Borgerson 2008). Moreover, the Alaskan Arctic coastline of the seemingly valueless piece of land Russia sold the United States in 1856 actually has the densest amount of untapped oil and natural resources within the Arctic Circle. The Alaskan Arctic coastline has at least 27 billion barrels of oil and more than 100 trillion cubic feet of natural gas (Bird et al. 2008; Borgerson 2008).

B. RELEVANCE TO THE DEPARTMENT OF DEFENSE

Russia is eager to use the Arctic to bolster international respect and is determined to claim what she deems is rightfully hers. That which stands in her way will be "met

with military actions" such that "no one will take [Russia's] Arctic" (Andres 2009). In 2001 Russia submitted a claim to the United Nations Convention on the Law of the Seas for 1.2 million km^2 of Arctic seabed that includes the North Pole (CNA 2009). Despite the United Nations' rejection of this request, Russia used icebreakers and submarines to plant the Russian flag on the ocean floor of the North Pole in 2007. Russian military presence ensued in 2007 and 2008 with bombers carrying out test cruise missile launches, increased naval presence in Svalbard, missile submarines sailing from the Barents Sea to the Pacific Ocean and a mock bombing run on Norway's northern command center (CNA 2009).

Russia's more aggressive behavior in the recent years reaffirms the resources at stake in the Arctic region and only heightens the uneasiness between the Arctic countries. Russia's actions also raise issues of sovereignty, fair access to these untapped resources between Arctic nations, and national security of the United States (Gove 2009).

Former President George W. Bush signed the National Security Presidential Directive 66 (NSPD-66)/Homeland Security Presidential Directive 25 (HSPD-25), the United States Arctic Region Policy, into effect on 9 January 2009. This Directive calls the United States to meet national security and homeland security interests that include missile defense and early warning, deployment of sea and air systems for strategic sealift, strategic deterrence, maritime presence, and maritime security operations, as well as ensuring freedom of navigation and overflight. Moreover, the United States is to exercise authority in accordance with lawful claims of the United States sovereignty the rights over natural resources such as oil, natural gas, minerals and living marine species for economic and energy security. In the defense of all these interests, NSPD–66 also directs the United States to execute maritime mobility of her Armed Forces worldwide.

Thus far, however, the scope of the United States' presence in and knowledge of the Arctic, and capabilities to operate therein are considerably limited compared to the NSPD–66 requirements. Currently, there is no U.S. presence north of the Bering Strait, and United States Coast Guard air patrol flights are limited to two weeks each summer. Ships located north of 74°N are not detectable with the current Automatic Identification System (CNA 2009). Furthermore, the United States lacks advanced operational

experience in ice and high latitudes, forecasting Arctic-specific temperatures, icing, and weather. In the U.S. arsenal is a collection of outdated and sparse charting of the Arctic region. Perhaps the most obvious limitation is the lack of icebreakers capable for extended Arctic missions. The only ship capable of operating in the Arctic's heavy ice, *USS Healy*, belongs to the United States Coast Guard (Gove 2009) and is over 10 years old. The ship superstructures and sensors that are in the United States Navy are not ice-strengthened and are sensitive to icing and low temperatures (Titley 2009).

Arctic-bordering countries are not wasting any time in exercising sovereignty of their coastline, and are preparing to protect what they believe is their rightful territory. As part of the *Canada First Defence Strategy*, Canada has the capability for extended Arctic operations with two icebreakers, six to eight Arctic Offshore Patrol Ships, a deepwater docking and refueling facility in Nanisivik, expansion of military presence in the North, establishment of the Arctic Training Center in Resolute, and enhanced surveillance through the use of unmanned aerial vehicles and satellite program. Canada also holds regular exercises in preparation for oil spills and maritime safety incidents (CNA 2009). In 2006, Canada renamed the NWP as Canadian Internal Waters (VanderKlippe 2006), asserting the right to deny others from using a large portion of the NWP. Although Canada does not yet have adequate means to physically enforce this territorial claim, the reference change does show her resolve and intent to protect what she deems is rightfully hers (VanderKlippe 2006). Denmark now has year-round presence around Greenland, operating her four ice-strengthened frigates, and two new Arctic offshore patrol vessels in surveillance, fisheries enforcement, and search and rescue missions. Denmark's missions also include collaboration with Sweden, Russia and Canada, and both Demark and Russia are looking to claim the seabed in the vicinity of the North Pole. Norway has instituted a High North Strategy, whose mission is to protect the environment, sustainably develop, and project sovereignty in the northern waters (CNA 2009). Denmark and Canada both want rights to Hans Island, which lies within the Canadian Arctic Archipelago. While this island is very small and unpopulated, it may be a key access point to the NWP (Bishop Allen Academy Model United Nations Conference 2009).

Not to be left out of the potential goldmine of oil, natural gas, and commerce possibilities, non-Arctic countries are weighing in with their capabilities. The Chinese Arctic and Antarctic Administration has joined seven other countries in conducting oceanographic, meteorological, biological, and geological research on the Svalbard Islands using their icebreaker. South Korea is building double-acting, ice-breaking tankers used in Russian oil fields. Both of these countries, along with Japan, are interested in the savings the NSR may be able to provide. The European Union has taken interest in maritime safety and the environmental impacts inevitable to increased sea traffic (CNA 2009).

Amongst the Arctic nations, United States, Canada, Russia, Norway, Denmark, Sweden, Finland, and Iceland, as well as non-Arctic nations, China, Japan, South Korea and the European Union are equally ready to preserve their rights to the resources in the Arctic region. The United States [must] aggressively lead the effort to tackle climate change by assembling partnerships and building trust and cooperation" (Ackerman 2008). In addition to multilateral cooperation, it would be wise for the United States to strengthen the special relationship between the United States and Canada and continue to develop bilateral agreement with Canada on the usage of the NWP (Borgerson 2009).

The United States needs an accurate projection of Arctic ice conditions in order to lead the world in Arctic sovereignty, fair resource access, and security (Titley 2009). A forecast that hypothesizes an ice-free Arctic too soon wastes resources and manpower, and a forecast that hypothesizes an ice-free Arctic too late can contribute to Arctic and national security mission failure (Titley 2009). For an accurate timeline and to predict the future state of the Arctic Ocean, the United States must understand the scientific cause of Arctic sea ice decline (The White House Council on Environmental Quality Interagency Ocean Policy Task Force 2009). As we join multinational efforts that are deemed to be in the best interest of the United States, we must be able to act based on both sound science and logistical competency.

The operational ramifications of the increasing Arctic SAT cannot be ignored. Increased temperatures result in increased saturation vapor pressure; the air's ability to hold moisture would increase. This, in turn, could cause more icing on aircraft and ship

superstructures, and degrade weapon systems (Gove 2009; Whelan 2007). Vessel icing is particularly hazardous to smaller boats and ships as they can become completely disabled and sink (Guest 2001). River and glacial runoff due to warmer Arctic temperatures also decreases the salinity of the ocean, changing its acoustic properties (Whelan 2007). The reduction of sea ice extent renders the surface of the ocean more open to noise-generating effects due to wind waves, ice floe collisions, and precipitation. Additionally, because the ice within the ocean acts as a noise sink, the reduction of sea ice thickness alters ambient noise levels on ships' communication system (Whelan 2007). Although sea ice can hinder deep-water operations, it also serves as a cover for submarines. With the loss of sea ice comes the loss of this natural shelter from enemy detection (Whelan 2007).

The potential forecast for a seasonally ice-free Arctic within the next decade (Maslowski private communication) is a wake-up call. Updates to maritime assets and personnel training in time for the United States to fulfill the missions outlined in NSPD-66 are estimated to cost hundreds of millions of dollars (CNA 2009). To be the best prepared nation for the challenges that lie ahead with Arctic warming means for the United States to no longer treat the Arctic as a stepchild, but to take advantage of the potentially few years remaining to readying for effects of a seasonally ice-free Arctic.

To protect and defend the right of the United States and other nations to move freely on the Arctic Ocean may seem like a daunting task for the United States Navy, especially with insufficiently trained personnel and capable equipment. Fortunately, this task does not rest on the shoulders of the United States Navy alone. As a nation, the United States wages war and maintains peace using all instruments of national power to achieve national strategy objectives (Department of Defense 2008a). This means that the U.S. military shares the workload of Arctic defense and early warning, deployment of sea and air systems, strategic deterrence, air and maritime presence, and ensuring freedom of navigation and overflight between the Navy Forces (NAVFOR), Army Forces (ARFOR), Marine Corps Forces (MARFOR), and Air Force Forces (AFFOR). Sharing the duty between branches of the military ensures savings of time and money, and reduces duplication of effort.

The United States Air Force and United States Army have operated within the Air-Land Battle Concept since the Cold War. In this joint environment, both Services are efficiently conducting overlapping missions such as air-ground support and integrating ground-attack aircraft, attack helicopters and artillery. In late 2009, in an effort to be ready to defend against actors with rapid militarization and advancing threats, Defense Secretary Robert Gates directed the United States Navy and the United States Air Force to form the Air-Sea Battle Concept (Defense News 2009). A joint Navy-Air Force effort will fill in any gaps the separate Services would otherwise have.

In meteorological and oceanographic (METOC) operations, all services collect, analyze, and predict in the environment that is their specialty, and in a combined effort, integrate their products from the air and the sea and give the Joint Forces Commander one clear picture of the weather that is timely, accurate, relevant, and consistent (Department of Defense 2008b). Joint METOC operations are critical to a commander's awareness of the operational environment and his ability to exploit that awareness to gain an advantage across the range of military operations. Properly applied, joint METOC operations can provide our air, land, maritime, space, and special operations forces with a significant, even decisive, advantage over their enemies (Department of Defense, 2008b).

C. CURRENT STATE OF RESEARCH ON ARCTIC SEA ICE VARIABILITY

"The ice goes where the wind blows," a Russian saying, may not be too far from the truth. Thompson and Wallace (1998) coined the term "Arctic Oscillation" (AO) to describe the first mode of variability of Northern Hemisphere winter sea level pressure (SLP) based on an empirical orthogonal function analysis of three "centers of action": North Pacific at the location of the Aleutian Low; North Atlantic at the location of the Azores Island off of the coast of Spain; and between Greenland and Iceland where the Icelandic Low is centered. This atmospheric circulation plays a role in determining speed and direction of the wind and ice. (Note the North Atlantic Oscillation (NAO) is similar to that of the AO, or the Northern Annular Mode (NAM), in that the NAO hones in on

SLP variability between the North Atlantic and the area of the Icelandic Low centers of action. Due to this similarity many NAO research findings can also apply to the AO.)

The AO oscillates (Figure 2) between positive and negative phases on time scales ranging from weeks to decades (Maslowski 2009). A deep Icelandic Low as well as strong Siberian High and Azores High pressure centers define the positive phase of the AO. During this phase, the temperatures over Canada and Greenland (western Arctic) are anomalously cold and winds are anomalously strong while the temperatures over Scandinavia and Europe (eastern Arctic) are warmer and winds are weaker than average (Serreze and Barry 2005). (Note the positive phase of the AO is also known as the "warm phase" or the "cyclonic phase," and its strength is quantified by a positive AO Index). During a negative, or "cold, anticyclonic phase of the AO (quantified by a negative AO Index), temperature and wind patterns reverse between the eastern and western Arctic regions as the Icelandic Low fills and North Pacific and North Atlantic High pressure centers strengthen.

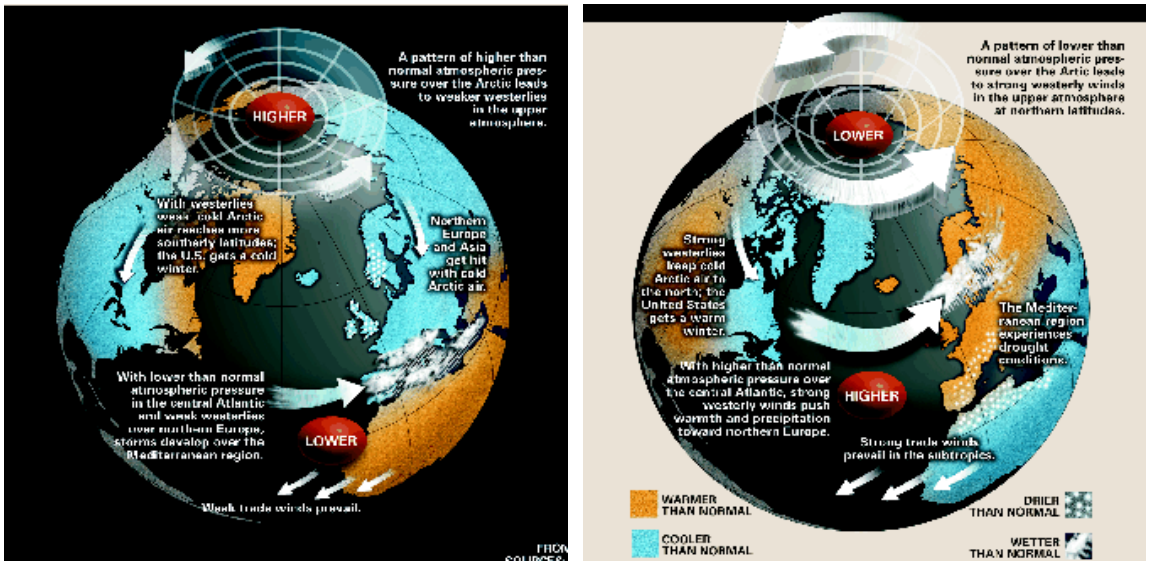

Figure 2. The Positive (left) and Negative Phases (right) of the Arctic Oscillation (From Mitchell 2004).

Cyclone frequency and moisture advection vary with the two phases of the AO. Serreze and Barry (2005) state that a stronger low pressure influence over the Arctic region during a positive phase of the AO increases the lateral moisture advection from the

lower latitudes over the Nordic Seas. The moisture from the lower latitudes drawn by the deep cyclonic activity fuels the formation of more and deeper cyclones. Precipitation under this phase increases over Norwegian-Greenland Seas and parts of central Eurasia and Alaska (Thompson and Wallace 2000). During a negative AO phase, cyclone tracks shift to zonal or equatorward (Serreze and Barry 2005).

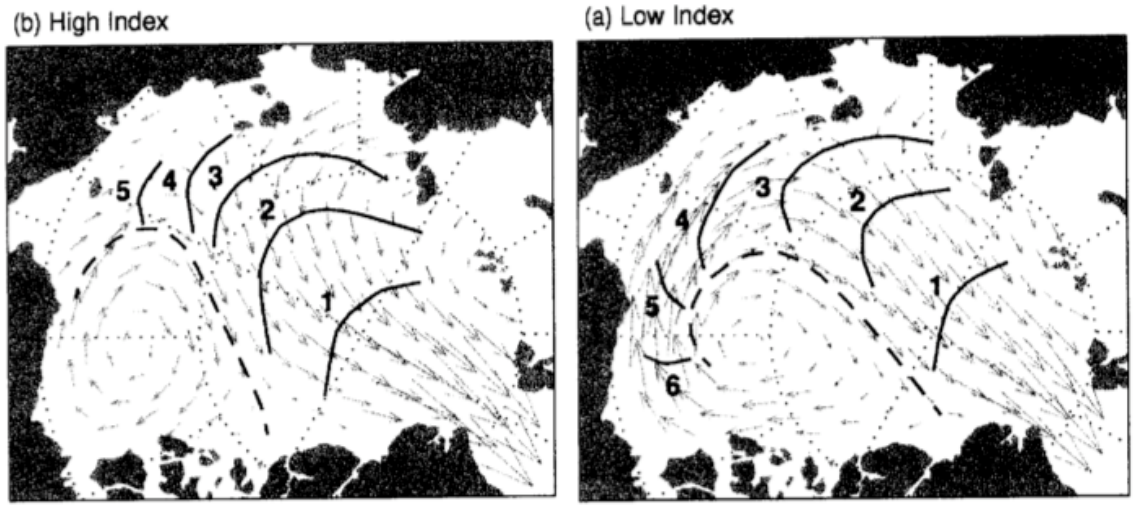

Figure 3. Isochrone maps depicting the number of years required for ice to exit the Arctic region through Fram Strait during a positive phase of the AO (left) and during a negative phase of the AO (right) (From Rigor et al. 2002).

Rigor et al. (2002) determined that the changes in the AO match the changes in sea ice motion, which can impact the sea ice extent and sea ice thickness distribution. The climatological average winter position of Arctic high pressure lies over the Beaufort Sea region. The anticyclonic (convergent) Beaufort Gyre creates thick, multiyear ice as the gyre allows ice to recirculate, deform and ridge. Ice is exported from the Arctic to the lower latitudes via the Fram Strait. In the summer, a weakened high pressure dominates the Beaufort Sea and the low over the Eastern Arctic expands and deepens toward the center of the Arctic. In part, because of this low pressure strength and position change, less ice is exported in the summer than in the winter. During a positive AO phase, an anomalous cyclonic circulation increases over most of the Arctic Ocean region, increasing the divergence in the central and Eastern Arctic sea ice, and decreasing the convergence of the sea ice within the Beaufort Sea. The Beaufort Gyre reduces in size and strength, lowering the residence time thick ice has within this gyre (Figure 3). At the same time, the excess divergence pulls ice away from E.

Siberian and Laptev Seas, forming leads and cracks within the ice. With temperatures near freezing, ice easily reforms, but only as thin ice. This thin ice has a short residence time and is quickly exported through the Fram Strait.

This could be the end to the sea ice variability mystery might if the AO completely explained the variability in SLP or if the AO was the sole answer to the thinning of the sea ice. However, the AO only explains 52% of SLP variability and only through the 1990s (Rigor et al. 2002).

Overland and Wang (2005) provide further evidence that the AO is not the only answer to the sea ice variability. They find a paradoxical relationship between the AO and the indicators of Arctic climate change: While the AO is episodic in behavior (the AO has returned to neutral and negative values since its high index maximum in 1990 as depicted in Figure 4), summer sea ice extent (Figure 5), spring SAT, cloud cover, and shifts in vegetation and other ecosystems seems to be on a linear track for the past two and a half decades. Overland and Wang (2005) suggest possible reasons for the continual linear trend of Arctic climate change indicators are heat advection via persistently strong SLP gradients or an Arctic response to external forcing involving connections through the stratosphere.

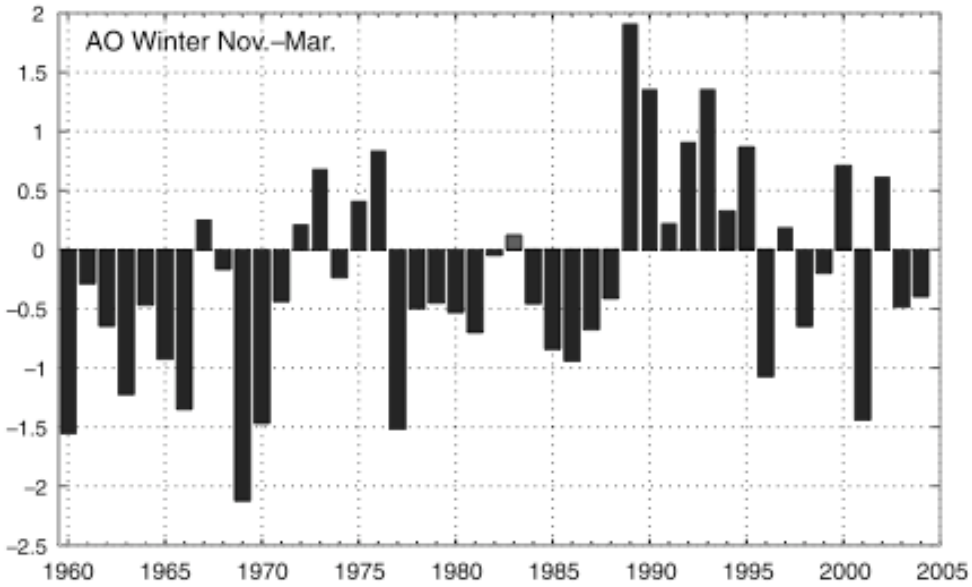

Figure 4. Time series of the winter (November-March) Arctic Oscillation Index from 1951-2004 show the positive and negative episodic behavior of the Arctic Oscillation [From Overland and Wang 2005].

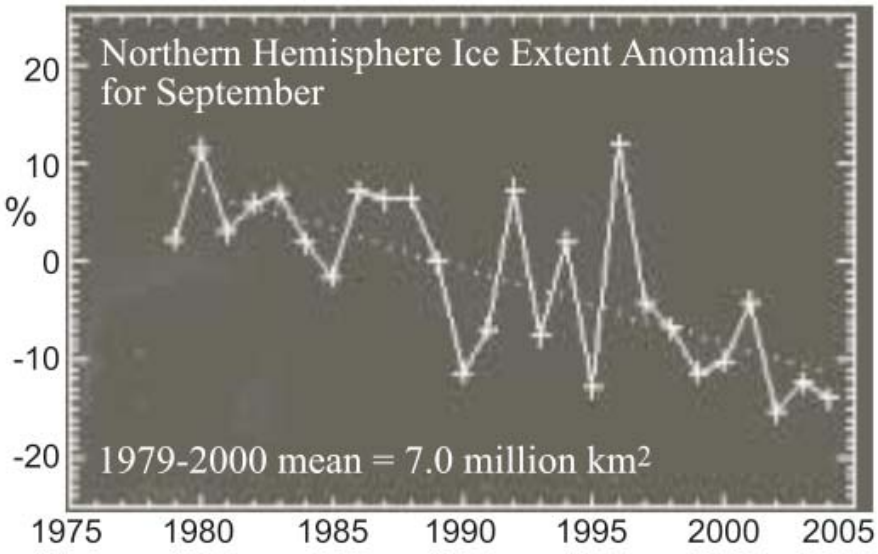

Figure 5. Time series of the Northern Hemisphere sea ice extent anomalies from 1979-2004 show a linear trend, contrary to the episodic behavior of the Arctic Oscillation Index (From Overland and Wang 2005).

Other possible explanations in sea ice variability could be related to atmospheric forcing due to wind and SAT. Ogi and Wallace (2007) found that between 1979 and 2006, years with low sea ice extent in the summer tend to be under anticyclonic circulation. Under this circulation pattern, anomalous easterly winds reside over the marginal seas (outlying seas of the Arctic Ocean such as the Laptev, E. Siberian, and Kara Seas). These easterly wind anomalies create an Ekman divergence, thereby thinning the sea ice in these vulnerable areas. Ogi and Wallace (2007) also found that SAT anomalies are the greatest in marginal sea ice, regions that are most variable during the summer time and define sea ice extent. Ogi and Wallace's (2007) findings are similar to that of Rothrock et al. (2003), who showed an overall ice thickness maximum in the Arctic in 1965–1966 during the same time the Arctic mean annual temperature was approximately 2ºC below normal and the NAO index was strongly negative (anomalous anticyclonic circulation). By modeling climatological seasonal cycles of temperature, dew point, scalar wind, cloudiness, precipitation and monthly means of wind stresses (NCEP Reanalysis data 1955–1995) on a coupled ocean-sea ice model (horizontal resolution of 1ºx1º), Köberle and Gerdes (2003) showed wind and thermal forcing both influence sea ice extent. Over this period the weight of thermal forcing was greater than

that of wind forcing as sea ice volume variability and thermal forcing had a correlation of 0.63. In Wang and Overland's (2009) analysis of six global climate models used in IPCC AR4's sea ice extent projections from 1950–2100, sea ice extent had already decreased to 4.6 million km^2, a threshold that reduces general Arctic sea ice thickness down to 2.5 m. With the increasing ice-albedo effect due to a greater area of open ocean, recent warming, and changes in wind-driven sea ice drifts, an accelerated forecast for an ice-free Arctic summer within 30 years is warranted (Wang and Overland 2009). SAT anomalies and winds are credited with the Bering Sea progressing toward an earlier spring transition (Stabeno and Overland 2001). Under normal circumstances northerly winds are over Kamchatka and westerly winds over the southern Bering Sea. When the Bering Sea transitions to spring earlier winds are southerly and southeasterly over Kamchatka and the southern Bering Sea (Stabeno and Overland 2001).

Using partial correlation coefficients, Francis et al. (2005) calculated the influence of downwelling longwave flux anomaly (DLFa), zonal wind anomaly (UWDa), meridional wind anomaly (VWDa), and advective sensible heat anomaly (ADVa) jointly explain of annual-maximum ice retreat anomaly (MIA), i.e., meridional ice-edge position anomaly, for six selected seas: Barents, Kara, Laptev, E. Siberian, Chukchi, and Beaufort Seas. The 26-year data set ranges from 1979–2004. Calculations are shown for 0, 10, 25, 50, and 80 days between atmospheric forcing and MIA. Maximum sea ice retreat anomaly is calculated using National Aeronautics and Space Administration Bootstrap Algorithm from the National Snow and Ice Data Center and subtracting a 26-year mean maximum distance. DLFa, UWDa, VWDa, and ADVa are all calculated using products derived from Television Infrared Observation Satellite Operational Vertical Sounder. Francis et al. (2005) finds that DLFa explains up to 50% of MIA variability. The dominance of DLFa's influence on MIA may be due to the increased precipitable water, cloud amount and SAT. UWDa, VWDa, and ADVa are found to have a weak overall influence on MIA variability. UWDa and VWDa do not explain as much of MIA as expected, suggesting that thermodynamic forcing may be the main driver for MIA rather than mechanical forcing (Francis et al. 2005).

In their following study, Francis and Hunter's (2006) find that by replacing lag days with accumulated days, DLFa explains an even greater percentage of MIA variability across all seas and time periods. Additionally, Francis and Hunter split the 26-year period into two periods: 1979–1991 and 1992–2004 to further investigate the cause of MIA in the Barents and Chukchi Seas (Francis and Hunter 2006). The results reveal details masked by the large influence of DLFa over the entire 26-year period. MIA in the Barents Sea is heavily influenced by DLFa and VWDa in the first period while MIA is heavily influence by ADVa and very little DLFa in the second half of the data period (Francis and Hunter 2006). The Chukchi Sea MIA shows VWDa explains nearly 70% of the MIA in the first period and ADVa and DLFa in the second period (Francis and Hunter 2006).

While atmospheric forcing is generally accepted as the culprit for the Arctic sea ice decline, it may underestimate the role the ocean has on the sea ice variability (Maslowski et al. 2000). The ocean is home to currents, eddies and other mesoscale features that have the ability to mix and convey heat, which can cause sea ice to melt at the bottom. Sea ice thickness is often overlooked due to data limitations but may be more critical to characterize the condition of Arctic sea ice than sea ice area or extent. One reason why the ocean's influence is often not quantitatively considered may be that the horizontal resolution of global climate models (on the order of hundreds of km), commonly used in Arctic climate studies, do not possess the fine resolution necessary to resolve critical mesoscale features in the polar ocean. Deser and Teng (2008) compare the SLP pattern of the AO to sea ice extent variability for two seasons: Winter (February, March, and April) and summer (August, September, and October) for two periods: 1979–1993 and 1993–2007. The winter SLP pattern closely resembles that of the positive phase of the AO. The summer SLP pattern, however, seems to be inconsistent with atmospheric forcing. Deser and Teng (2008) suggest that their findings "imply that other factors are responsible for the residual winter sea ice [extent] decline, for example enhanced ocean heat storage and transport."

Advancements in ice-ocean models are being made. By comparing 18-km and 9-km coupled ice-ocean models, Maslowski and Lipscomb (2003) find that the more

realistic ocean currents, water mass properties, and ice edge position in the finer horizontal resolution model produces improvements in ice deformation, drift fields, polynyas, ice edge position, and sea ice concentration and thickness. By using the same 9-km coupled ice-ocean model, Maslowski et al. (2004) find the Barents Sea branch of the Norwegian Atlantic Current to be a more significant source of mass, heat and salt into the central Arctic Ocean than the Fram Strait branch than previously thought. This could facilitate an increase in the frequency of storms reaching higher latitudes (Maslowski et al. 2004). Because the Rossby radius of deformation, which defines the size of oceanic eddies, decreases with increasing latitude, models with even finer resolution are needed to resolve these high latitude features (Maslowski et al. 2008). One such example of this ultra high-resolution model is the NPS coupled ice-ocean model with 1/48º horizontal resolution (approximately 2.36 km), which resolves many more mesoscale eddies in the western Arctic (Maslowski 2009).

Accurately modeling oceanic mesoscale features is important because of their contribution to the large-scale circulation and processes in the ocean, which have the potential to influence the Arctic sea ice variability. Sea ice thickness helps determine the ice strength, which in turn can dictate the motion of sea ice due to atmospheric and oceanic forcing. For example, warm core eddies drive oceanic advection and anticyclonic eddies can entrain oceanic heat into the mixed layer (Maslowski 2009). This heat, which is otherwise absent or underrepresented in global climate models, plays a role in the sea ice variability and may be another reason why the Arctic sea ice is melting faster than previously forecast.

Much of the research on the Arctic sea ice state thus far have used lower resolution global climate models, atmospheric parameters that are aggregates of fundamental quantities (referred to as “second order” atmospheric parameters in this research), and atmospheric forcing and sea ice response from two different sources. In this research, a one-system approach is used where the sea ice response is the direct result of the atmospheric forcing input into the coupled ice-ocean mesoscale model. This research also uses fundamental atmospheric parameters in examining the relationship between atmospheric forcing to sea ice variability. The purpose of this research is to

quantify how much atmospheric forcing parameters (e.g., wind) explain sea ice variability in the Barents, Kara, Laptev, E. Siberian, Chukchi, Beaufort Seas, the North Pole and the western side of the Canadian Arctic Archipelago, and various points along the NWP and NSR.

This thesis is organized into the following: Chapter II describes the data and methodology used in this research; Chapter III presents results; and Chapter IV discusses how the results of our study work toward quantifying the influence of atmospheric forcing on Arctic sea ice variability; Chapter V summarizes the conclusions; and Chapter VI presents recommendations for future Arctic climate research.

II. DESCRIPTION OF DATA AND METHODOLGY

A. DESCRIPTION OF NAVAL POSTGRADUATE SCHOOL (NPS) 1/12 DEGREE PAN-ARCTIC COUPLED ICE-OCEAN MODEL

The Naval Postgraduate School (NPS) pan-Arctic coupled ice-ocean model (also referred to as NAME for *N*aval Postgraduate School *A*rctic *M*odeling *E*ffort or the NPS Model) is configured on a rotated spherical coordinate grid and has a horizontal resolution of 1/12 degree (approximately 9 km) covering 1280 x 720 grid cells (Figure 6). This horizontal resolution of the NPS model allows for modeling of Arctic mesoscale features down to approximately 36 km (four grid points) including oceanic eddies. This model has 45 z-coordinate levels with 11 layers in the upper 100 m and 19 layers in the upper 500 m. This detailed vertical resolution accurately represents the Arctic continental shelves and slopes. Its bathymetry is based on the 2.5-km resolution International Bathymetric Chart of the Arctic Ocean digital bathymetry data set. The NPS model includes all major inflow and outflow areas of the Arctic Ocean and all of the seasonally ice-covered seas in the Northern Hemisphere, including the Sea of Japan, Sea of Okhotsk, sub-Arctic North Pacific and North Atlantic Oceans, the Arctic Ocean, the Canadian Arctic Archipelago, and the Nordic Seas. Extension of model domain to the mid-latitudes minimizes the influence of lateral boundaries in the central Arctic (Maslowski et al. 2004). More information about the NPS model can be found in Maslowski et al. (2004) and Maslowski and Lipscomb (2003).

The NPS coupled ice-ocean model is forced with atmospheric parameters from the ECMWF Reanalysis-15 data set. These parameters were interpolated from the Reanalysis data set grid of 2.5º x 2.5º to the NPS model grid. The atmospheric forcing fields include 2-m temperature, 10-m zonal and meridional wind speeds and wind stresses, and longwave and shortwave radiation.

The NPS model output data set used in this research consists of daily snapshot files from 1 January 1979 to 10 November 2004 with 12 and 22 January missing from the 2003 data set and the following days missing from the 2004 data set: 8 May, 10–12 May,

14–22 May, 24–31 May, and 2–3 June. Sea ice parameters included sea ice area (concentration) and sea ice thickness as well as sea ice volume, which is the product of area and thickness. Although lack of sea ice thickness data was a limitation in Francis et al. (2005) and Francis and Hunter (2006), the full visibility of the output from this one-system model allows us to employ both thickness and volume to render a more complete picture of sea ice variability.

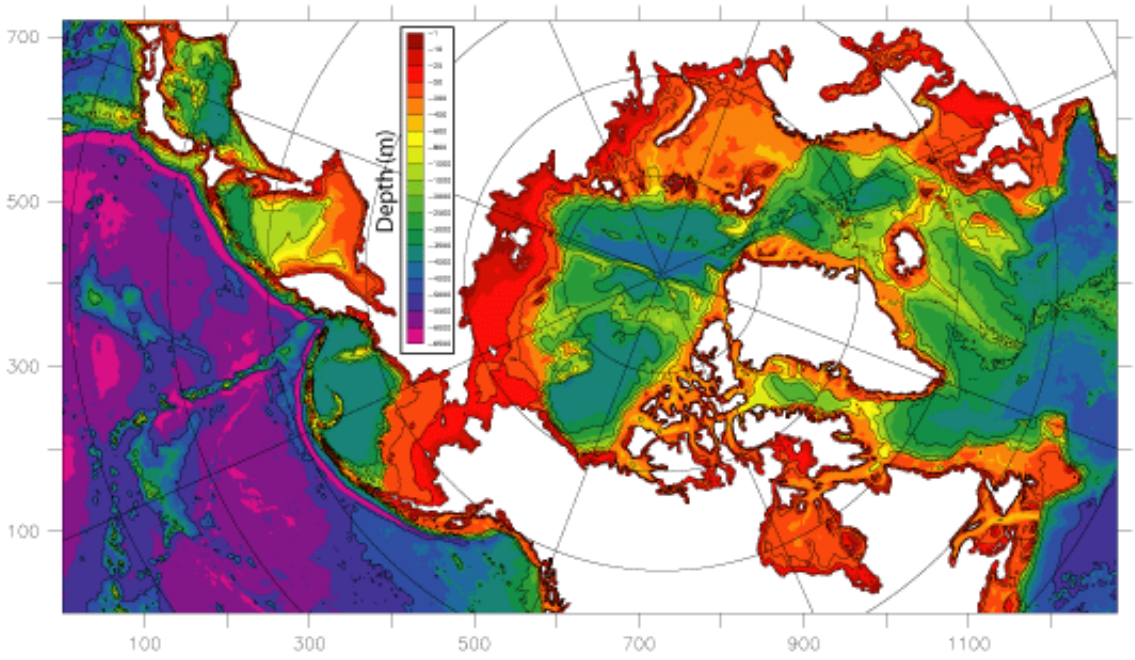

Figure 6. NPS 1/12 Degree Pan-Arctic Coupled Ice-Ocean Model Domain (From Maslowski et al. 2004).

B. DESCRIPTION OF EUROPEAN CENTRE FOR MEDIUM-RANGE WEATHER FORECASTS (ECMWF) REANALYSIS-15 AND EUROPEAN CENTRE FOR MEDIUM-RANGE WEATHER FORECASTS OPERATIONAL PRODUCTS

The NPS model is forced with atmospheric forcing parameters from the European Centre for Medium-Range Weather Forecasts (ECMWF) model data. The atmospheric fields from January 1979 through February 1994 are from the ECMWF Reanalysis-15 data set. The atmospheric fields from March 1994 thru 10 November 2004 are from ECWMF Operational Products. Atmospheric data from 1 January 1979 through 1

December 1999 have a coarser resolution (2.5º x 2.5º) than data from 1 January 2000 through 10 November 2004 (1.125º x 1.125º). The ECMWF data is interpolated onto the NPS model grid. Rather than daily snapshots, each daily ECMWF atmospheric forcing file is the average of four, six-hourly analyses. Data missing from the NPS model output are intentionally excluded from the atmospheric analysis to maintain data consistency. Atmospheric forcing parameters examined are 2-m temperature, shortwave and longwave flux, 10-m zonal and meridional wind and stresses. More information regarding ECMWF Reanalysis-15 and Operational Products can be found at http://badc.nerc.ac.uk/data/ecmwf-era/ and http://badc.nerc.ac.uk/data/ecmwf-op/.

C. METHODOLOGY

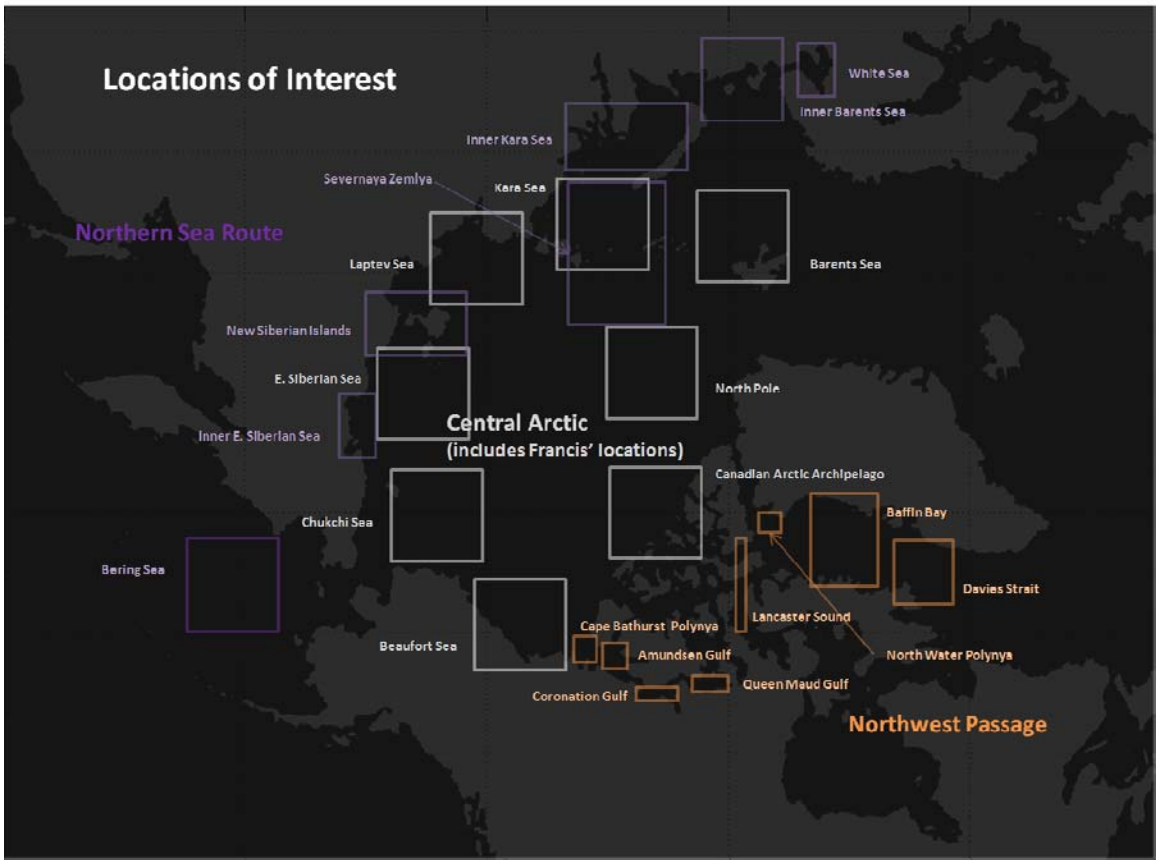

Figure 7. Map of Arctic region highlighting the seas analyzed in Francis et al. (2005), the North Pole and the Canadian Arctic Archipelago (white); locations along the Northwest Passage (orange); locations along the Northern Sea Route (violet).

Atmospheric forcing and sea ice variability data for 365 days for each year (assume neither data sets have leap years) are divided into 12 near-equal months (approximately 30.4 days per month) such that Months 1 and 2 include Day 31, Months 6 and 7 include Day 183, and Months 11 and 12 both include Day 335. Thus, these months are referred to as numbered months (i.e., Month 1, Month 2, etc.) rather than Gregorian months. Exact days in months are in Appendix A, Table 1. The mean value for each atmospheric forcing and sea ice parameter is calculated for each location shown in Figure 7. Monthly averages are then demeaned to become anomalies of each atmospheric forcing and sea ice parameter. Anomalies of atmospheric and ice parameters are used to investigate the relation of the variability from the mean. This is completed for each location. Exact NPS Model grid points used are listed on Table 2 of Appendix A.

Partial covariances calculated between anomalies of the atmospheric forcing parameters and anomalies of sea ice variability parameters explain the amount of anomalous sea ice area variability (aARAv), anomalous sea ice thickness variability (aTHKv) or anomalous sea ice volume variability (aVOLv) by each atmospheric forcing parameter. Atmospheric forcing parameters are anomalies of 2-m temperature, which serves as anomalous SAT (aSAT), downward shortwave flux (aSWF), downward longwave flux (aLWF), 10-m zonal wind (aUWD), 10-m meridional wind (aVWD), zonal component of stress (aXST), and meridional component of stress (aYST) as well as wind speed (aWDS), wind direction (aTHE), and wind stress curl (aWSC), which are calculated. Partial correlation coefficients are used since the predictors (atmospheric forcing parameters) are interdependent. Partial covariance (Bernstein et al. 1988) is

$$\left[\frac{N\sum_{i=1}^{N} r_{x,i}, r_{y,i} - \sum_{i=1}^{N} r_{x,i} \sum r_{y,i}}{\sqrt{N\sum_{i=1}^{N} r_{x,i}^2 - \left(\sum_{i=1}^{N} r_{x,i} \right)^2} \sqrt{N\sum_{i=1}^{N} r_{y,i}^2 - \left(\sum_{i=1}^{N} r_{y,i} \right)^2}} \right]^2, \qquad (1)$$

where N is the sample number, which in our case is 311 (12 months in the years 1979–2003 and 11 months in 2004). Singling out one atmospheric forcing parameter and one sea ice parameter, $r_{y,i}$ is the residual calculated from standard multiple regression

analysis between the singled out sea ice parameter and all other atmospheric forcing, and $r_{x,i}$ is the residual between the singled out atmospheric forcing and all other atmospheric forcing parameters. Wind speed (WDS) equals

$$\sqrt{u^2 + v^2}, \qquad (2)$$

where u is UWD v is VWD. Wind direction (THE) equals

$$\tan^{-1}\left(\frac{u}{v}\right), \qquad (3)$$

where u is UWD v is VWD. Wind stress curl (WSC), $\nabla \times \vec{\tau}$, equals

$$\frac{\partial \tau_y}{\partial x} - \frac{\partial \tau_x}{\partial y}, \qquad (4)$$

where τ_y is the meridional component of the stress vector $\vec{\tau}$, τ_x is the zonal component of the stress vector, $\vec{\tau}$; and ∂x and ∂y are the distance between two NPS Model grid points (approximately 9260 meters).

Because most of the sea ice variability during the summer ice extent occurs along the marginal seas, we focus on the six locations, one in each of the following marginal seas: Barents, Kara, Laptev, E. Siberian, Chukchi, Bering and Beaufort Seas. These seas are the same as those Francis et al. (2005), and Francis and Hunter (2006) analyzed. Together with two additional locations, one at the North Pole and one at the Canadian Arctic Archipelago, these eight locations cover and are referred to as the Central Arctic in this research. Because NSPD-66 specifically names the Northwest Passage (NWP) and the Northern Sea Route (NSR), eight additional locations along NWP and seven additional locations along NSR are also investigated. The locations along NWP are the Chukchi and Beaufort Seas, Cape Bathurst Polynya, Amundsen Gulf, Coronation Gulf, Queen Maud Gulf, Lancaster Sound, North Water Polynya, Baffin Bay, and Davis Strait. The locations along NSR are the Bering and Chukchi Seas, Inner E. Siberian Sea, New Siberian Islands, Laptev Seas, Severnaya Zemlya, inner Kara Sea, inner Barents Sea, and White Sea. All latitude, latitude, and NPS model grid points are tabulated in Table 2 of

the Appendix A. The area of the Central Arctic locations in this research closely follows that of Francis and Hunter (2005, 2006) with each location occupying 77 x 77 (5929) NPS model grid cells (approximately 5.08 x 10^6 km^2). Atmospheric parameters are averaged over the 5929 grid points while the sea ice variability parameters are averaged only over the non-land grid points. Unlike the locations in the Central Arctic, the number of grid points for each of the NWP and NSR locations of interest is not standardized, but locally defined.

Thus far, research on sea ice variability has used difference sources for atmospheric forcing and sea ice variability parameters. The advantage of using an one-system approach as this research does with the NPS model sea ice variability output being the direct result of ECMWF atmospheric forcing input is that all the modeled dynamic and thermodynamic processes are accounted for entirely.

"Second order" atmospheric parameters are dependent on one or more fundamental atmospheric parameters. For example, DLFa is dependent on the temperature profile, water vapor distribution, and various cloud properties. Therefore, variation in second order atmospheric parameters can mask the source of change in the fundamental parameters. Using fundamental atmospheric parameters can provide more information on the effects basic atmospheric parameters can have on second order parameters. For example, positive DLFa may be due to increased SAT and/or changes in cloud type. However, if it is known that there is an increase in SAT, a positive DLFa may be expected.

This chapter discussed the sources of data and methodology for this research. The next chapter presents the results of the methodology.

III. RESULTS

In this chapter, an overview of atmospheric forcing used in the NPS Model and graphical results for partial correlations of each sea ice parameter with all atmospheric forcing parameters are presented. They are organized as follows: Section A presents plots of atmospheric forcing parameters; Section B presents plots for anomalous sea ice volume, thickness, and area, for each Central Arctic boxed region, over the entire time period 1979–2004. Section C presents plots for anomalous sea ice volume, thickness and, area for each Central Arctic boxed region, over the first half of the time period 1979–1991; Section D presents plots for anomalous sea ice volume, thickness, and area, for each Central Arctic boxed region, over the second part of the time period 1992–2004; and Sections E and F presents plots for anomalous sea ice volume, thickness, and area, for each Northwest Passage and Northern Sea Route boxed location, over the entire time period 1979–2004, respectively. Additionally, the graphics in Sections G summarizes the average, minimum, and maximum ranges of atmospheric contribution to anomalous sea ice volume and the timing of occurrence of these minimum and maximum ranges for the entire data period 1979–2004. Figures summarizing atmospheric contribution to aVOLv for data periods 1979–1991 and 1992–2004 as well as atmospheric contribution to aTHKv and aARAv for 1979–2004, 1979–1991, and 1992–2004 are located in Appendices G–I.

A. MONTHLY ATMOSPHERIC FORCING AVERAGE OVER THE NAVAL POSTGRADUATE SCHOOL MODEL DOMAIN

The inherent uniqueness of the Arctic atmosphere stems directly from its position on the earth. This high latitudinal locality provides the Arctic with oscillating days and nights but with a pattern quite different from that of the mid-latitudes. The Arctic is subject to winters without daylight (polar nights) and summers without darkness (polar days). This seasonal heating and cooling impacts the temperature and the amount of shortwave and longwave radiation within the Arctic.

1. Surface Air Temperature

Plotted below (Figures 8–13) are the average monthly 2-m temperatures (SAT) from ECMWF Renanalysis-15 (January 1979-February 1994) and Operational products (March 1994–November 2004). The ECMWF data are interpolated onto the model 9-km domain, which covers 1280 x 720 grid cells.

The SAT ranges between -45C and 30C throughout the year. In the winter months, the lowest SAT is over Siberia, Canada and Greenland with -35C to -25C over the Arctic Ocean. In the summer months, with long polar days, SAT increases above 0°C over land (with the exception of Greenland) with the Arctic Ocean hovering near 0°C.

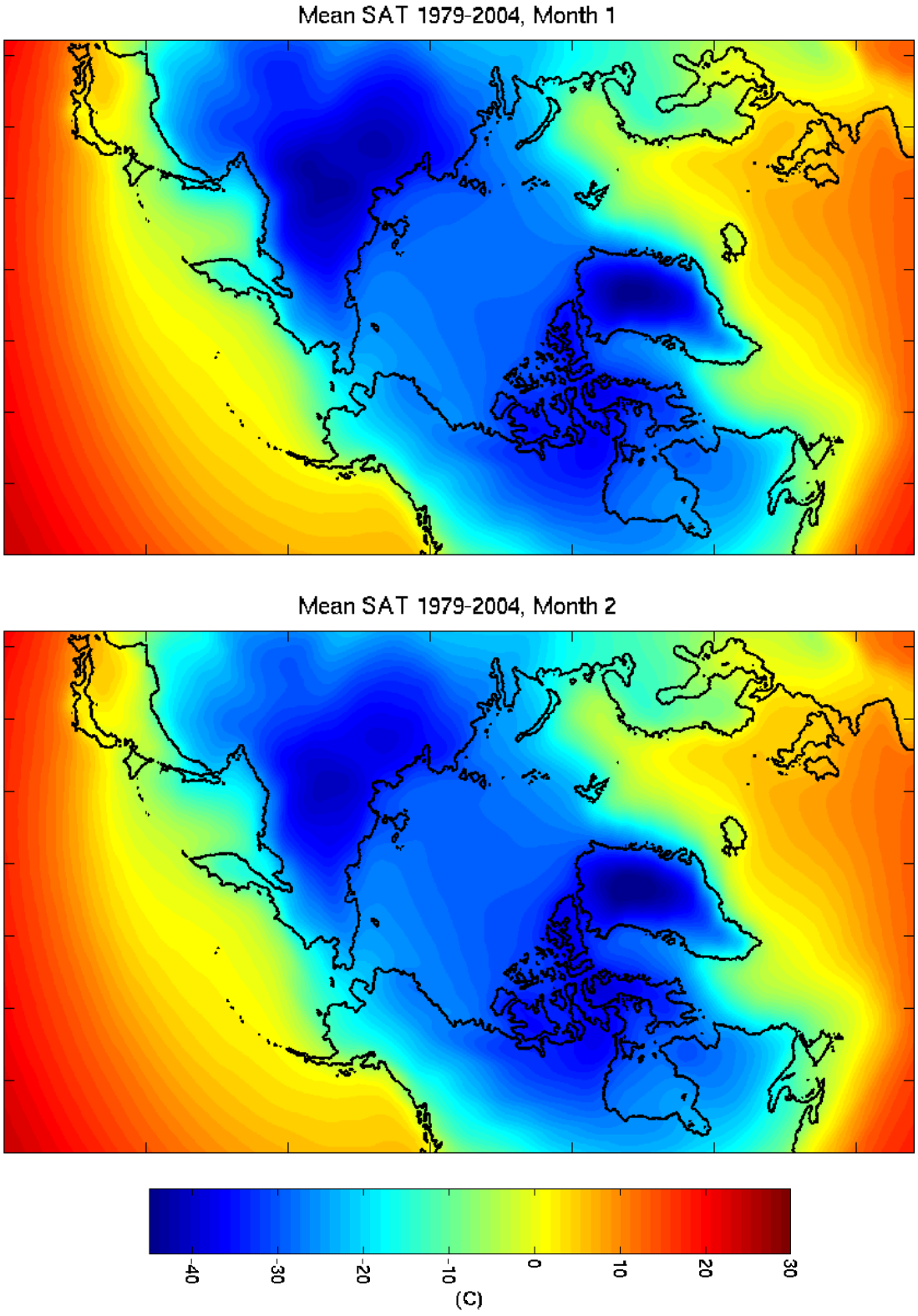

Figure 8. Monthly Mean SAT: Month 1 (top) and Month 2 (bottom)

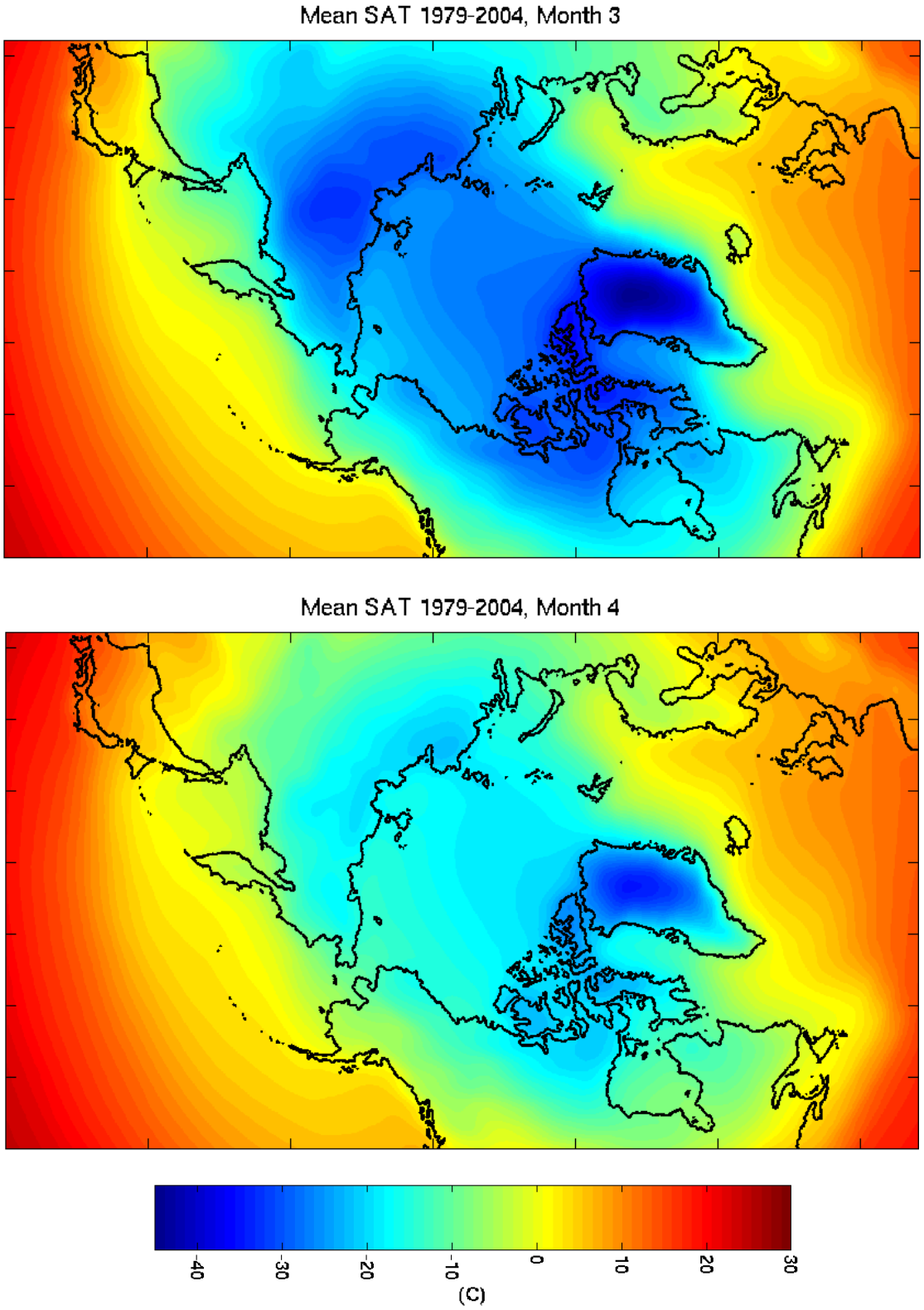

Figure 9. Monthly Mean SAT: Month 3 (top) and Month 4 (bottom)

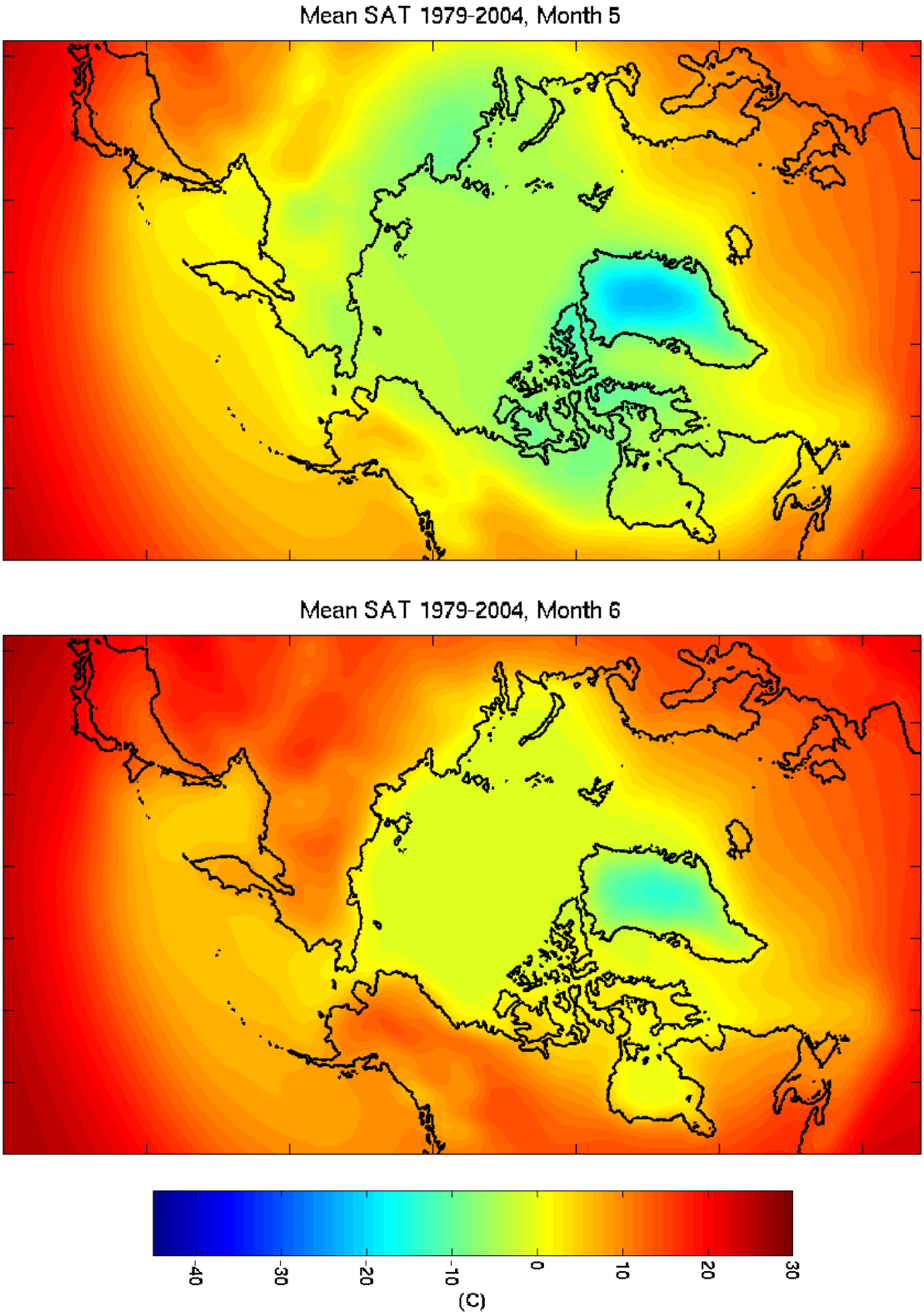

Figure 10. Monthly Mean SAT: Month 5 (top) and Month 6 (bottom)

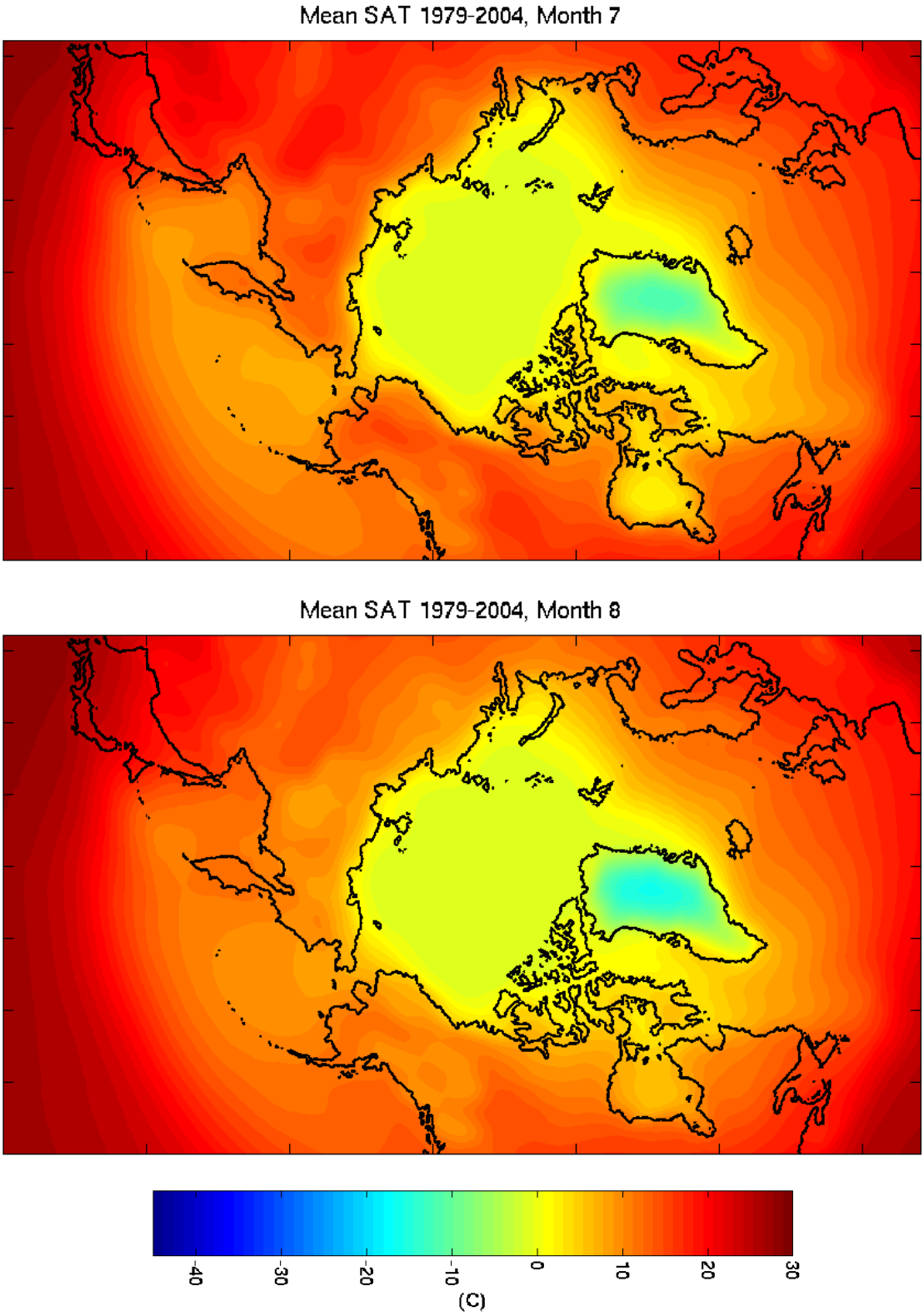

Figure 11. Monthly Mean SAT: Month 7 (top) and Month 8 (bottom)

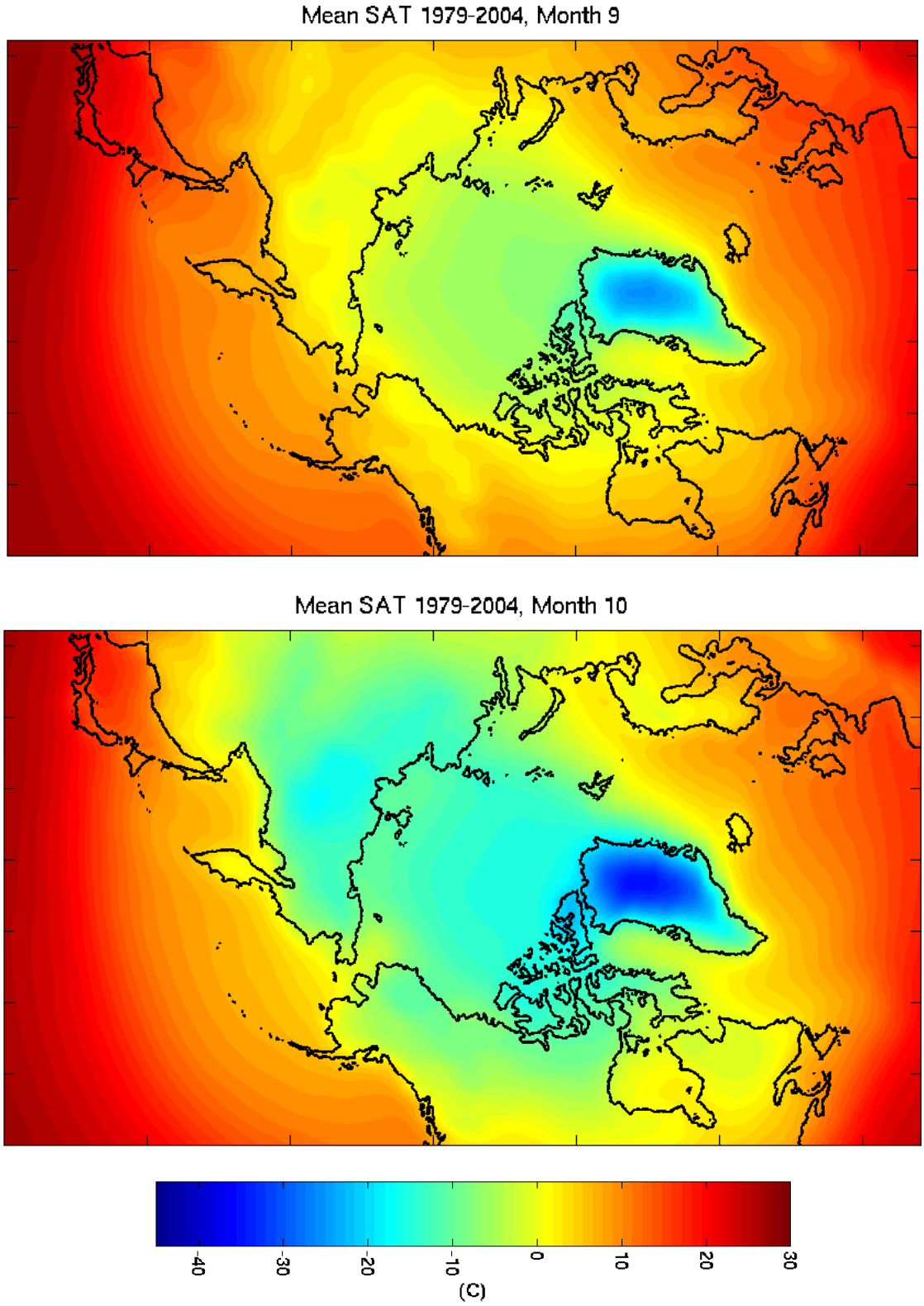

Figure 12. Monthly Mean SAT: Month 9 (top) and Month 10 (bottom)

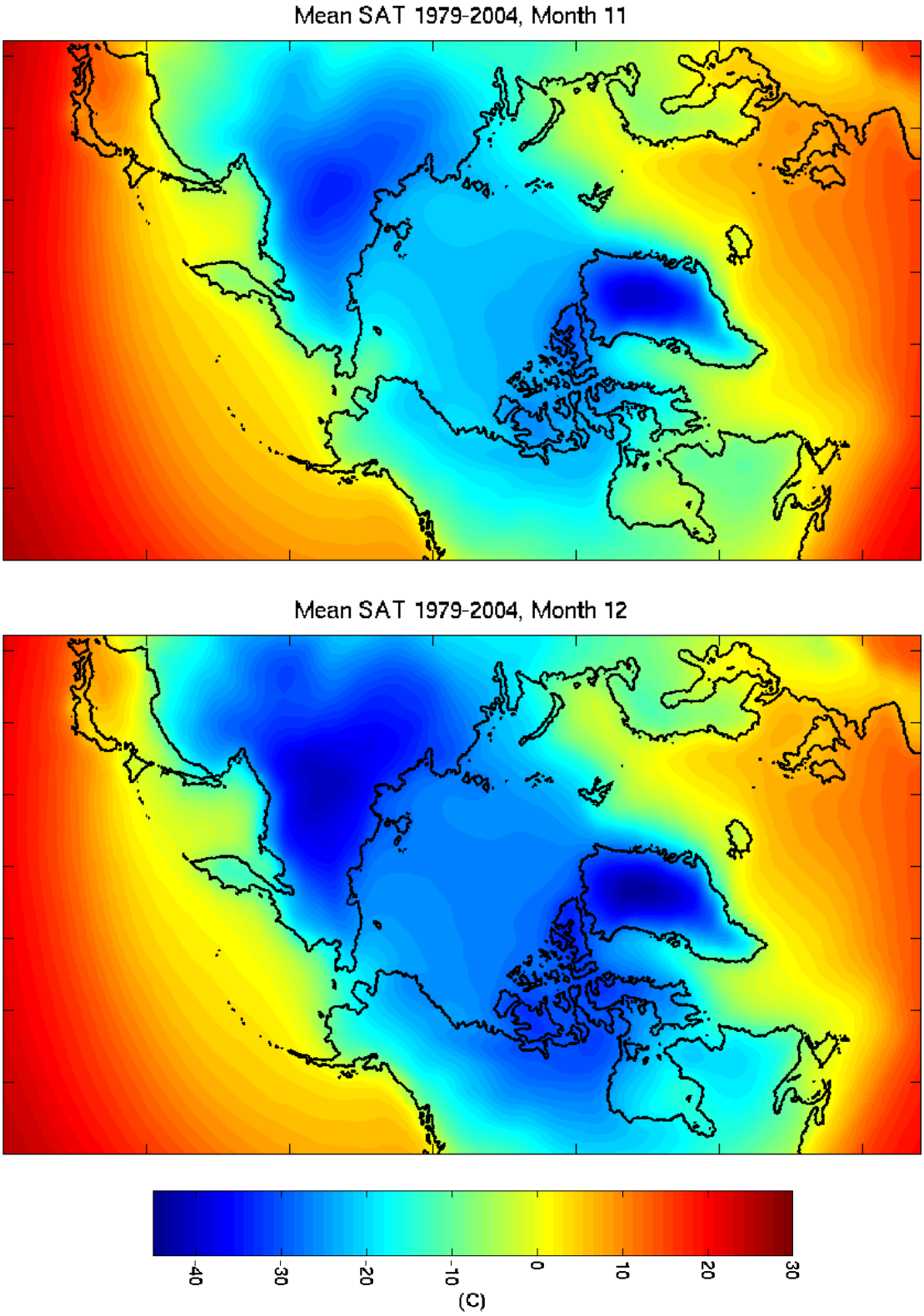

Figure 13. Monthly Mean SAT: Month 11 (top) and Month 12 (bottom)

2. Downward Shortwave Flux

Plotted below (Figures 14–19) are the average monthly downward shortwave flux (SWF) from ECMWF Renanalysis-15 (January 1979–February 1994) and Operational products (March 1994–November 2004). The ECMWF data are interpolated onto the model 9-km grid, which covers 1280 x 720 grid cells.

The amount of SWF, the solar radiation from the sun, ranges between 0 Ws/m^2 and 350 Ws/ m^2 throughout the year. From the warming months to the cooling months, SWF decreases toward the North Pole. During polar days in the late spring and early summer time, maximum SWF is over Greenland followed by the Chukchi and Beaufort Sea areas.

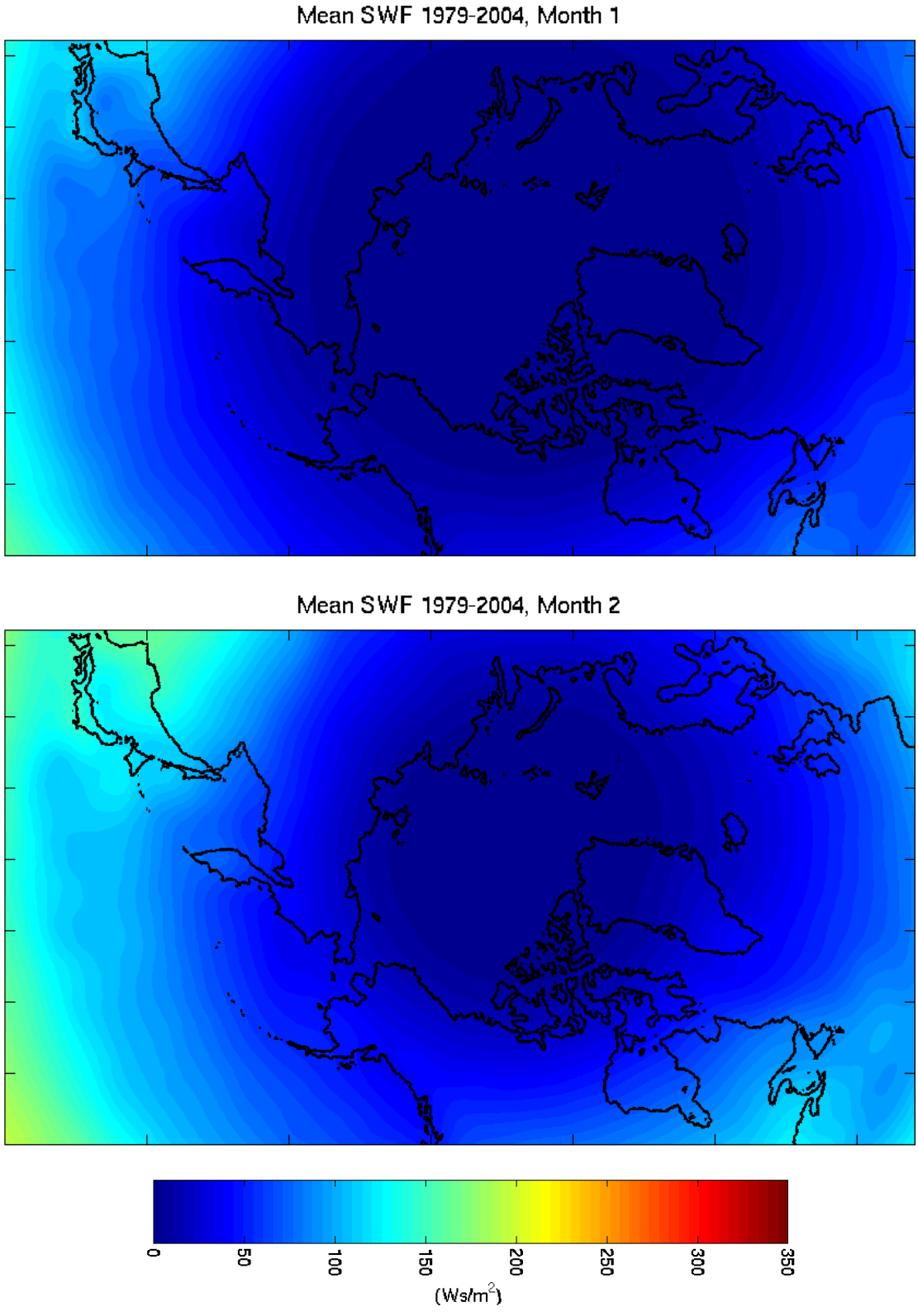

Figure 14. Monthly Mean SWF: Month 1 (top) and Month 2 (bottom)

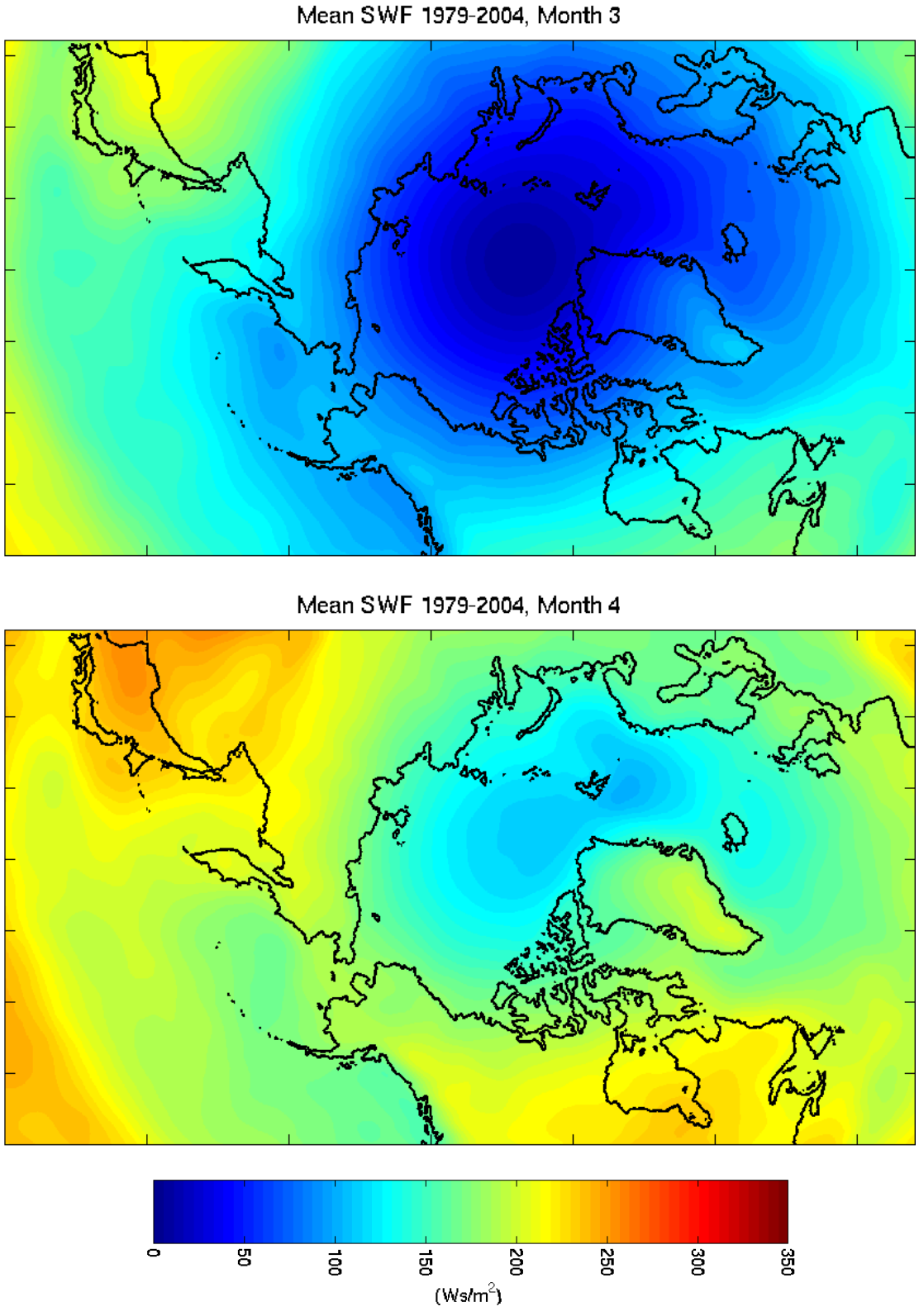

Figure 15. Monthly Mean SWF: Month 3 (top) and Month 4 (bottom)

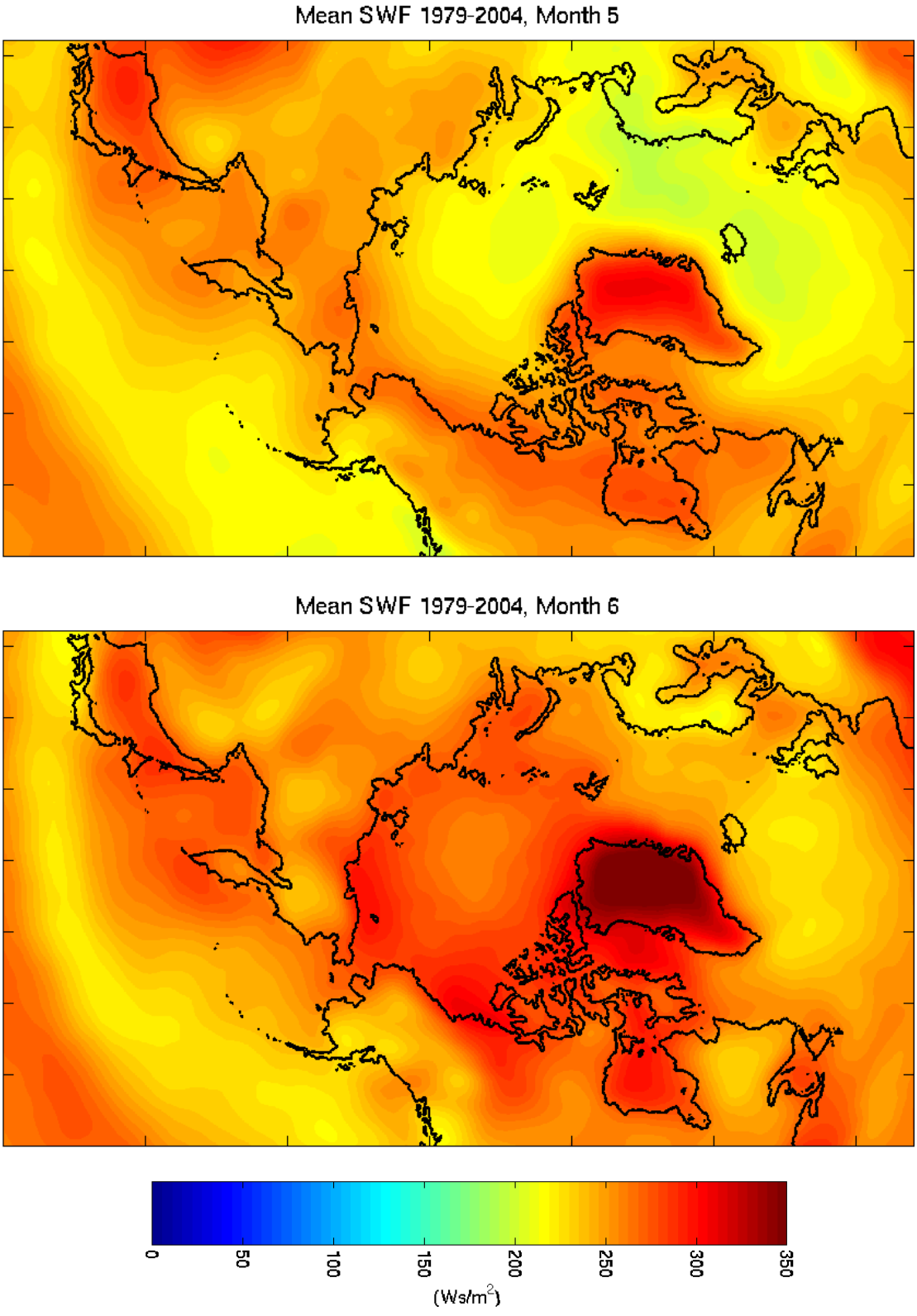

Figure 16. Monthly Mean SWF: Month 5 (top) and Month 6 (bottom)

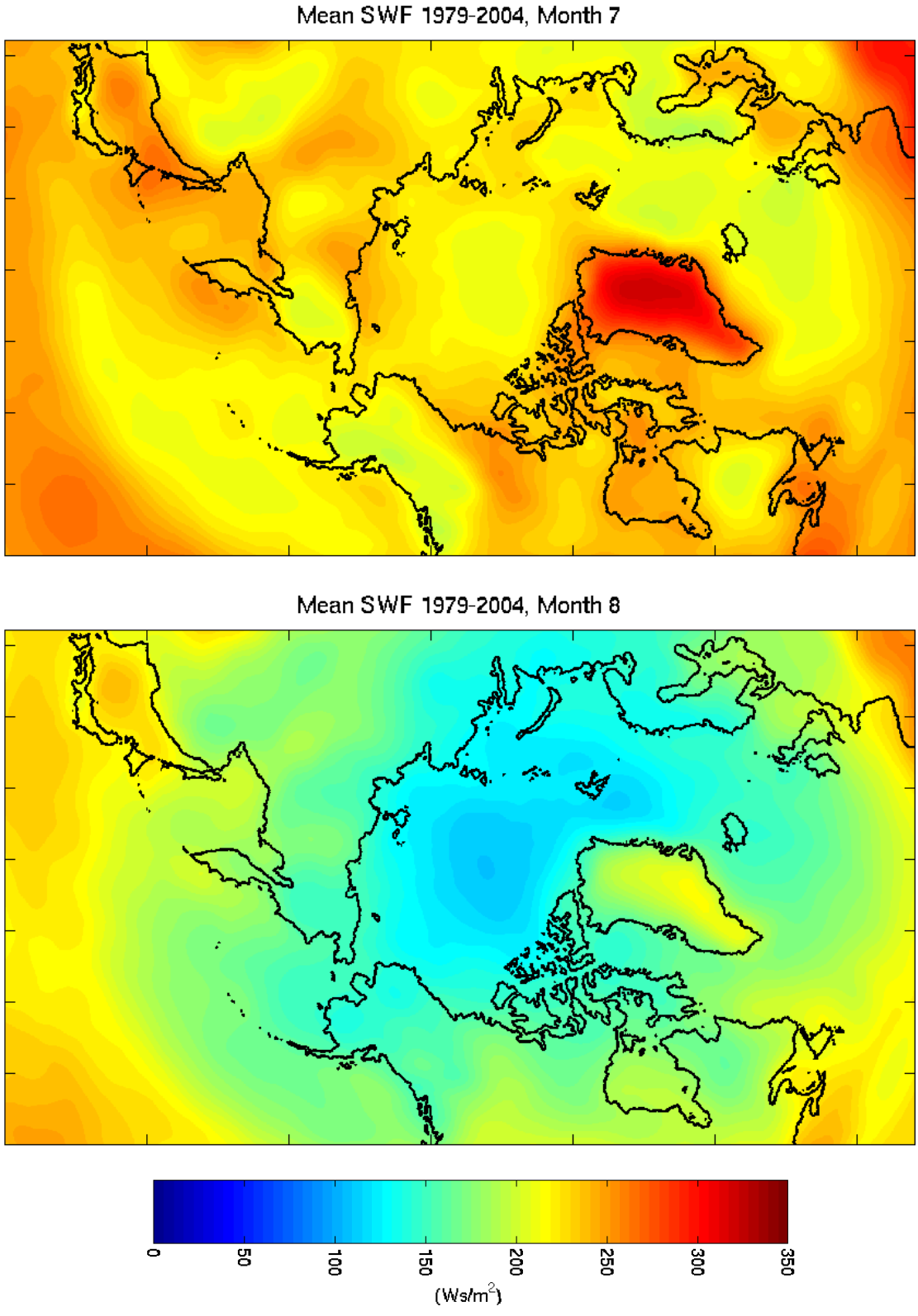

Figure 17. Monthly Mean SWF: Month 7 (top) and Month 8 (bottom)

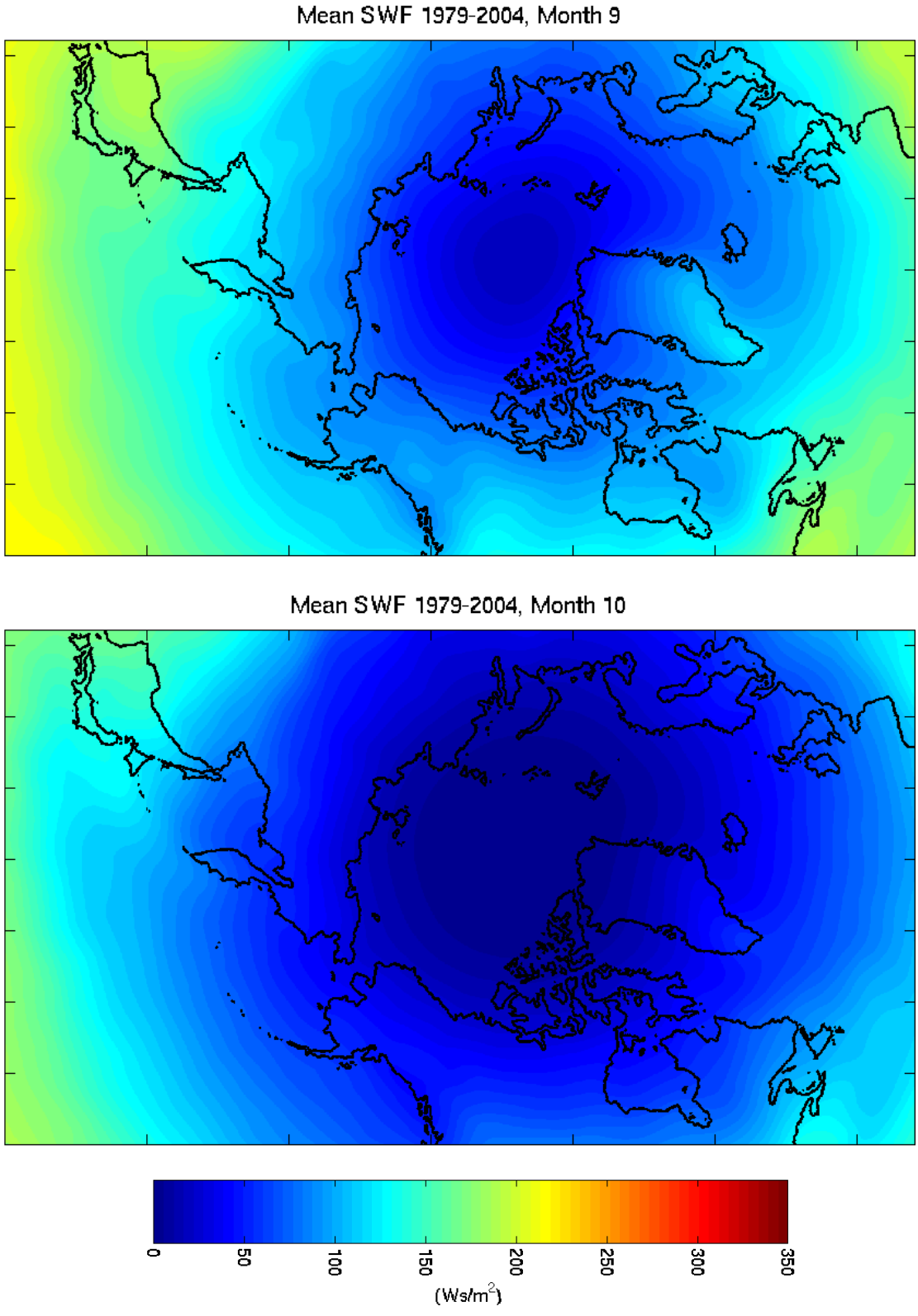

Figure 18. Monthly Mean SWF: Month 9 (top) and Month 10 (bottom)

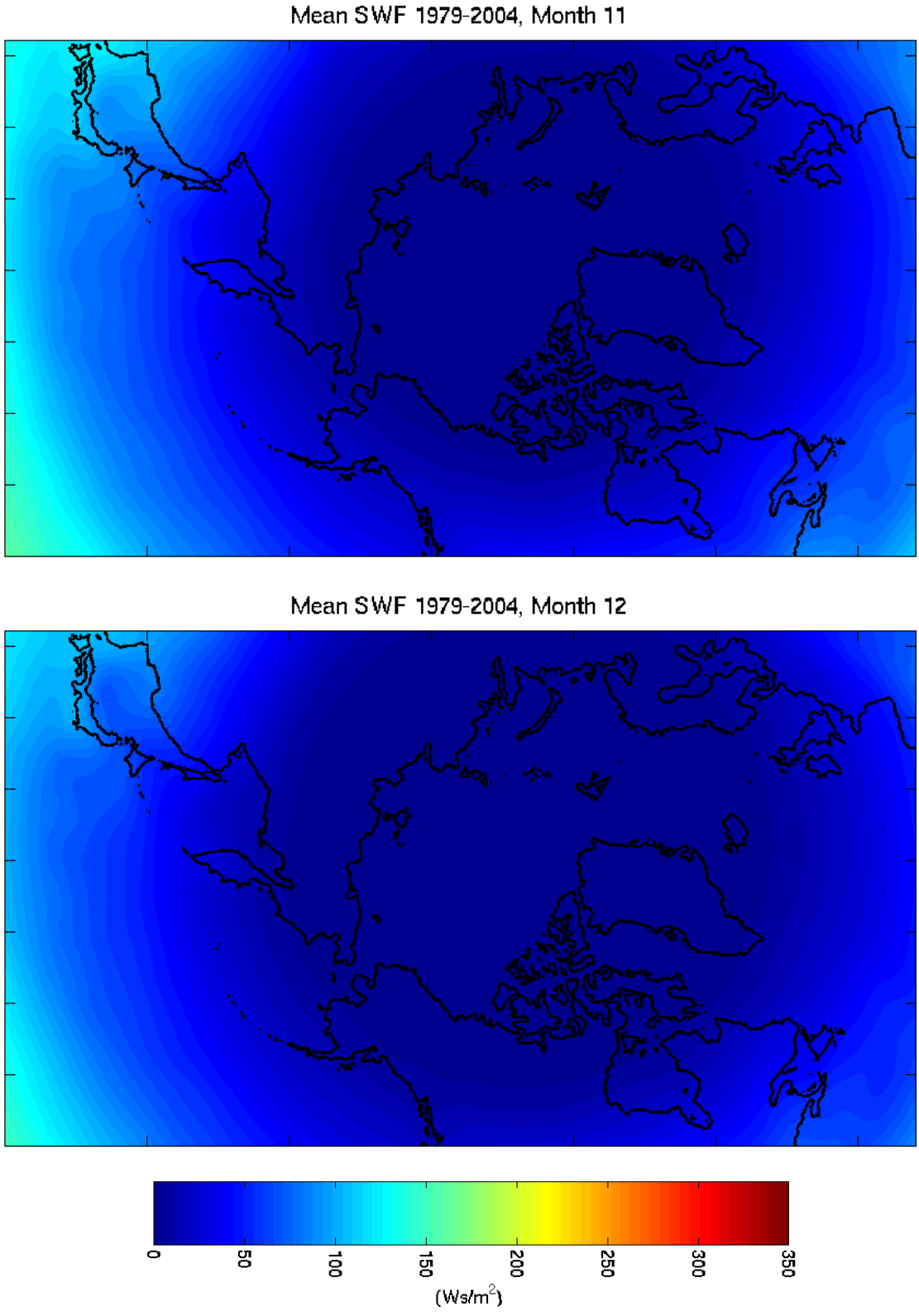

Figure 19. Monthly Mean SWF: Month 11 (top) and Month 12 (bottom)

3. Downward Longwave Flux

Plotted below (Figures 20–25) are the average monthly downward longwave flux from ECMWF Renanalysis-15 (January 1979–February 1994) and Operational products (March 1994–November 2004). The ECMWF data are interpolated onto the model 9-km grid, which covers 1280 x 720 grid cells.

The amount of LWF, the thermal radiation from the bottom of clouds, ranges from 100 Ws/ m^2 to 450 Ws/ m^2. In the non-summer months, clouds keep the Arctic warm (Schweiger, 2008). Thus, the spatial and temporal pattern largely resembles that of the SAT.

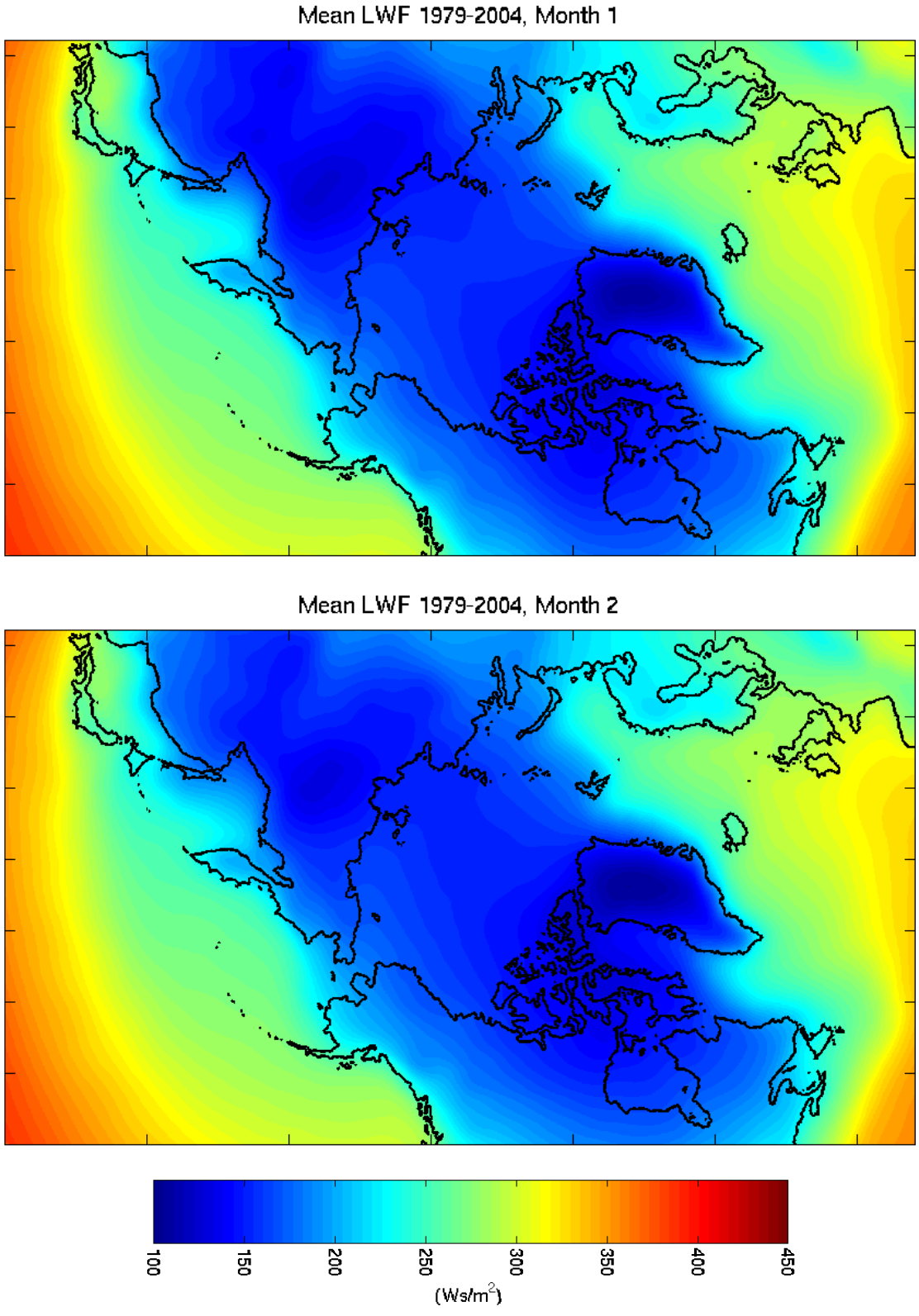

Figure 20. Monthly Mean LWF: Month 1 (top) and Month 2 (bottom)

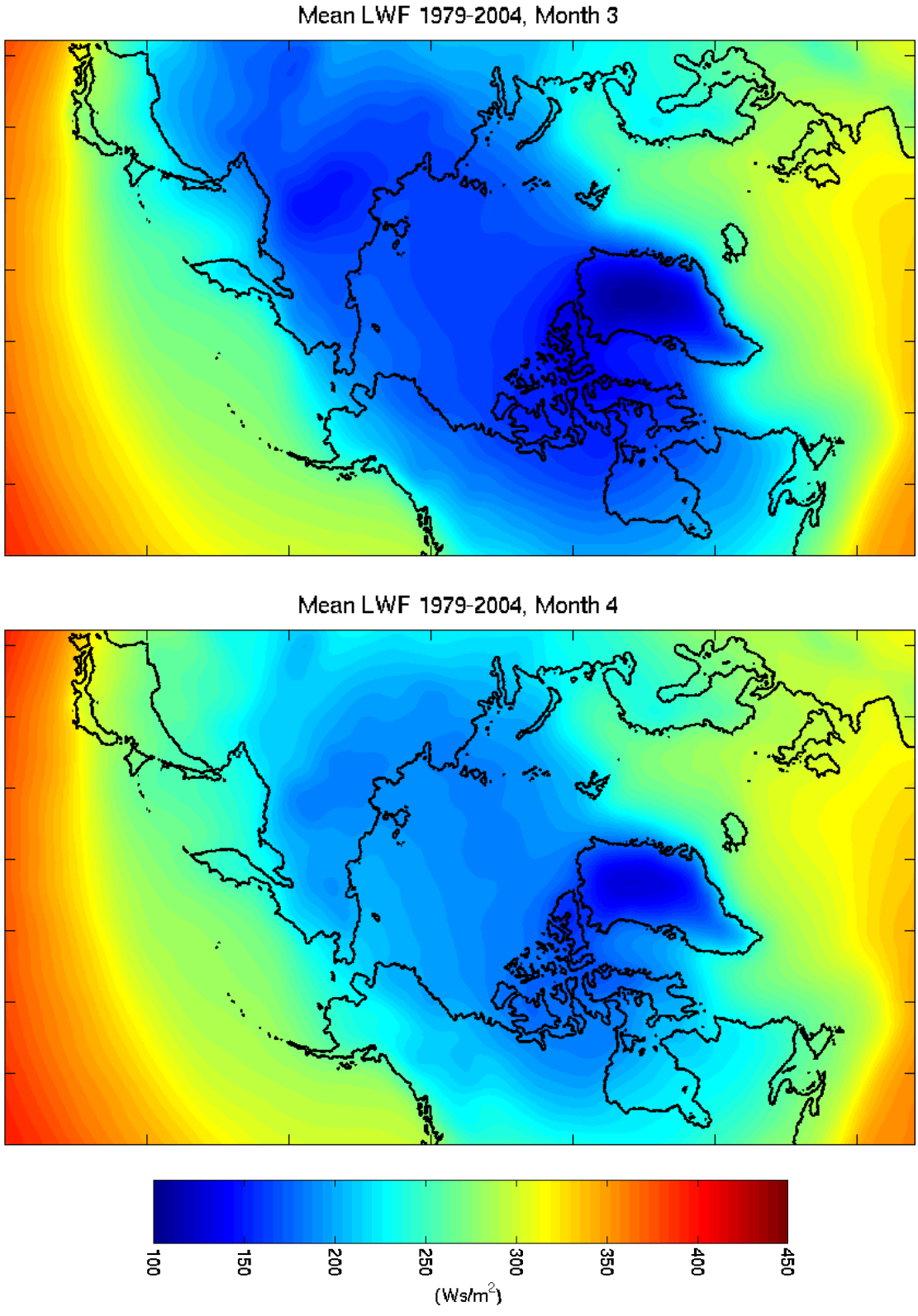

Figure 21. Monthly Mean LWF: Month 3 (top) and Month 4 (bottom)

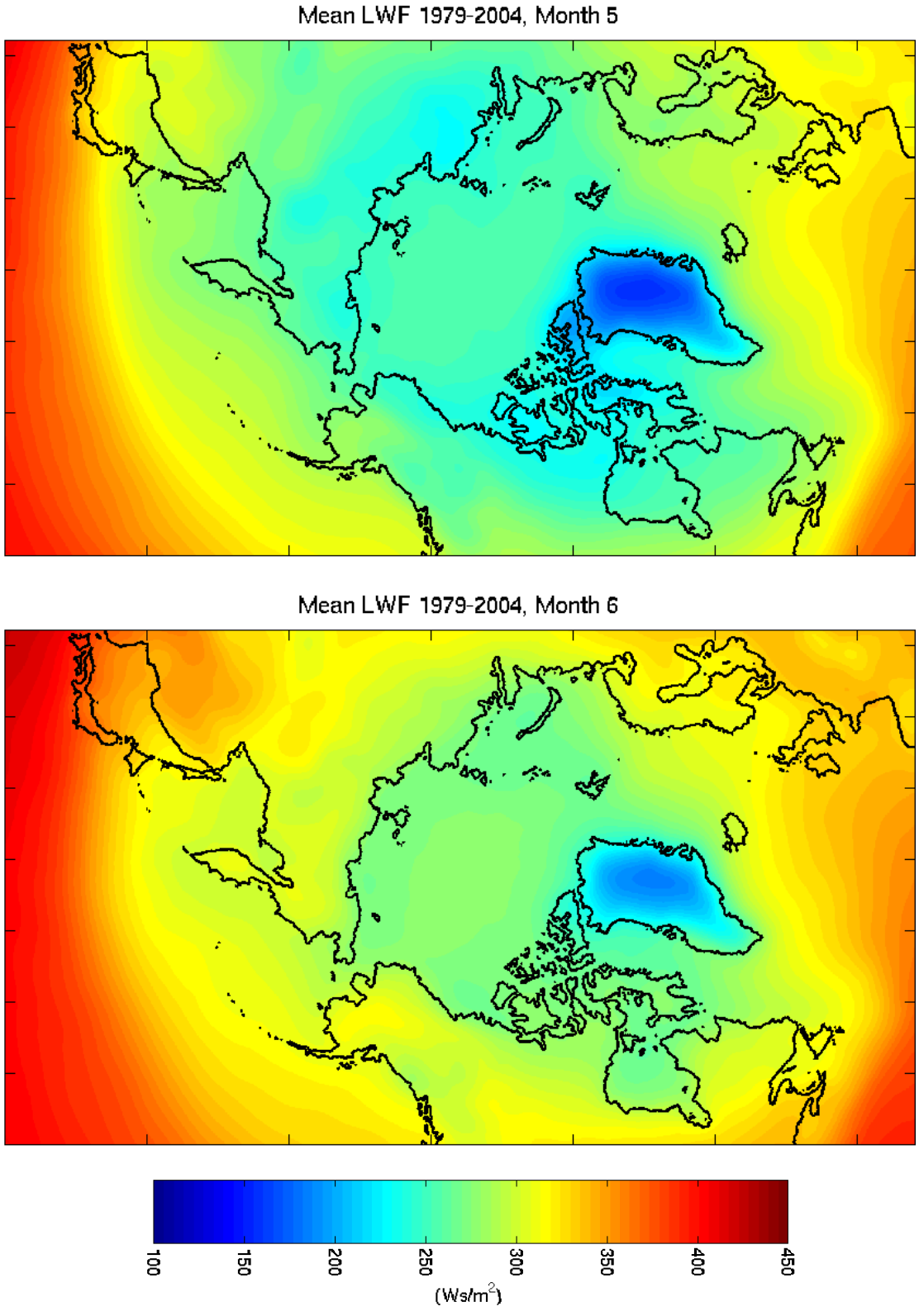

Figure 22. Monthly Mean LWF: Month 5 (top) and Month 6 (bottom)

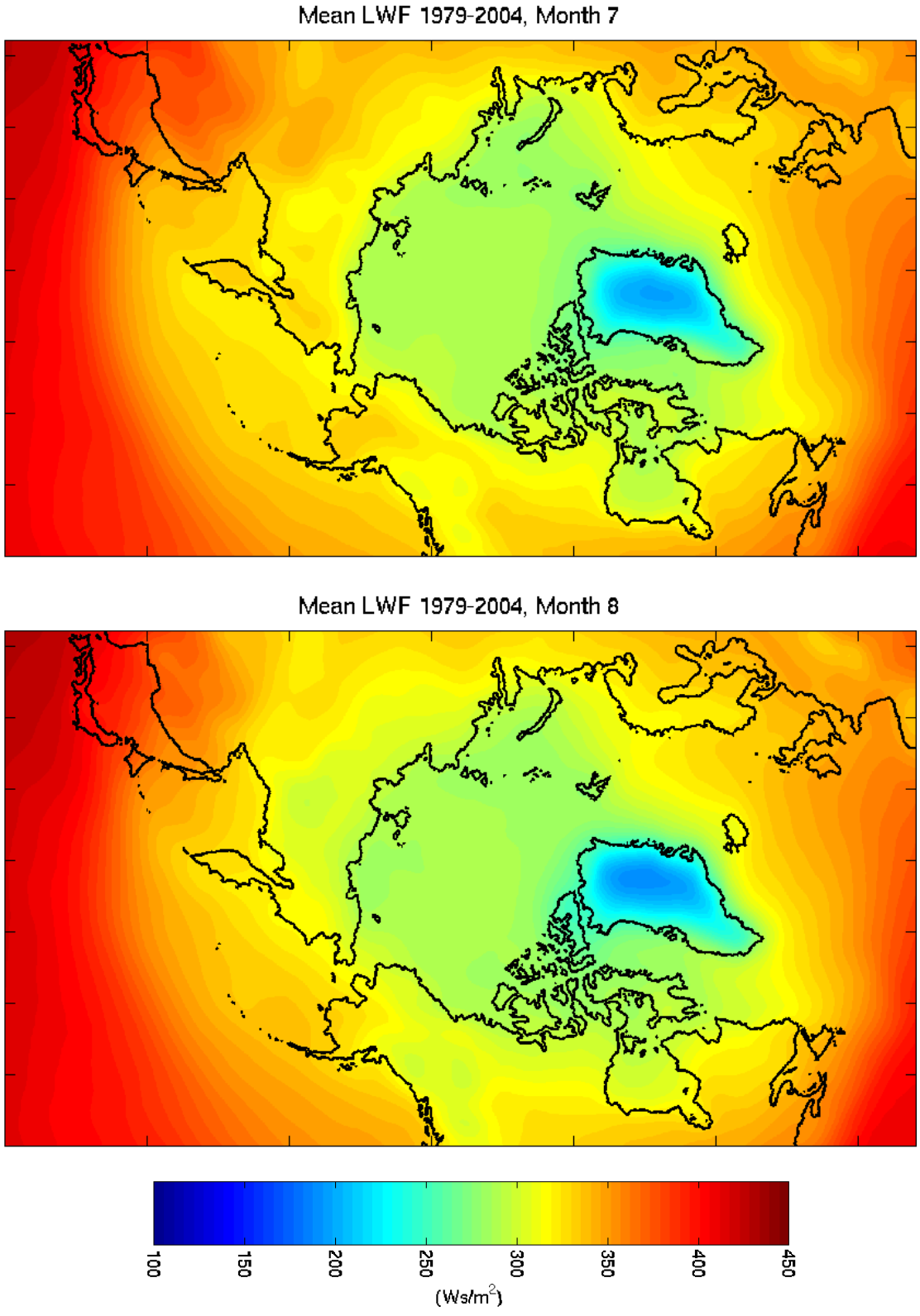

Figure 23. Monthly Mean LWF: Month 7 (top) and Month 8 (bottom)

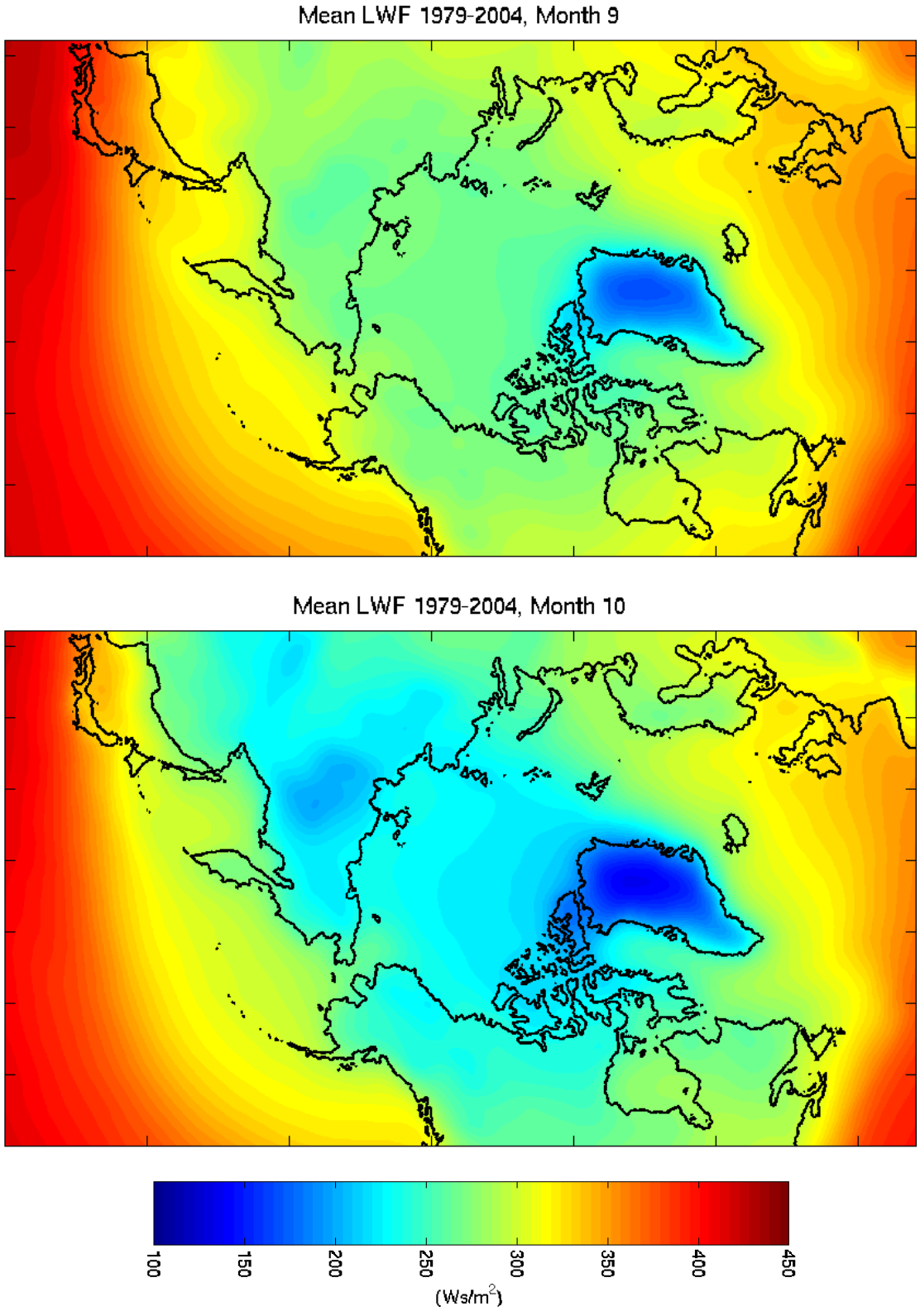

Figure 24. Monthly Mean LWF: Month 9 (top) and Month 10 (bottom)

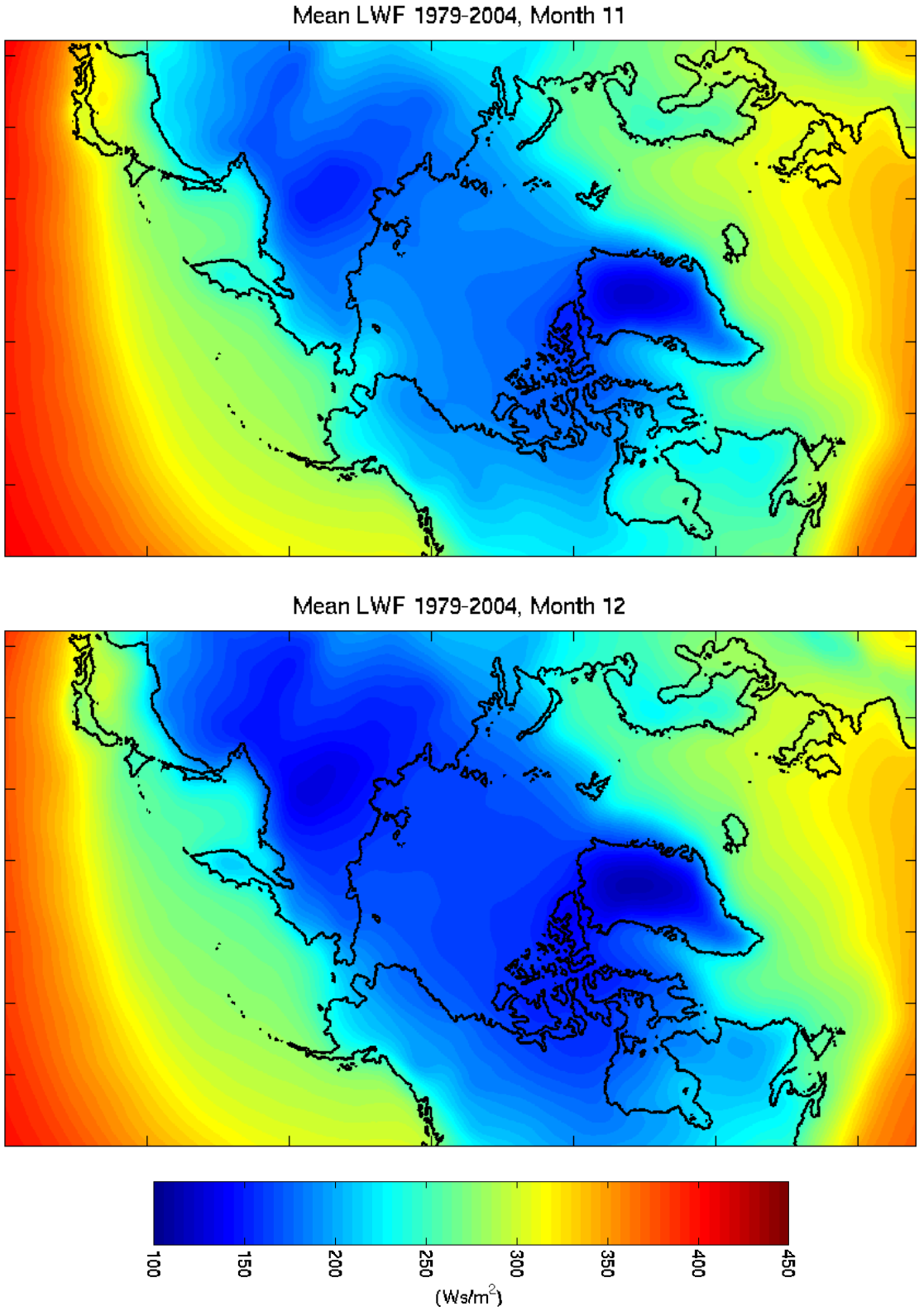

Figure 25. Monthly Mean LWF: Month 11 (top) and Month 12 (bottom)

B. ANOMALOUS SEA ICE VOLUME, THICKNESS, AND AREA VARIABILITY IN THE CENTRAL ARCTIC (1979–2004)

Figures 26–28 below and Appendix B depict the amount of anomalous sea ice volume variability (aVOLv), anomalous thickness variability (aTHKv), and anomalous area variability (aARAv) accounted for by each atmospheric parameter used in the NPS Model for the entire data period 1979–2004. The atmospheric parameters are labeled along the x-axis. Partial covariance of sea the ice parameter explained by each atmospheric forcing parameter is determined by the partial correlation method described in Chapter II and indicated by the percentage along the y-axis. Each monthly atmospheric contribution to sea ice variability is ordered from the left to the right with the darkest-colored bar being Month 1 and the lightest-colored bar being Month 12. Months 4–9 are referred to as the warming months and Months 10–3 are referred to as the cooling months.

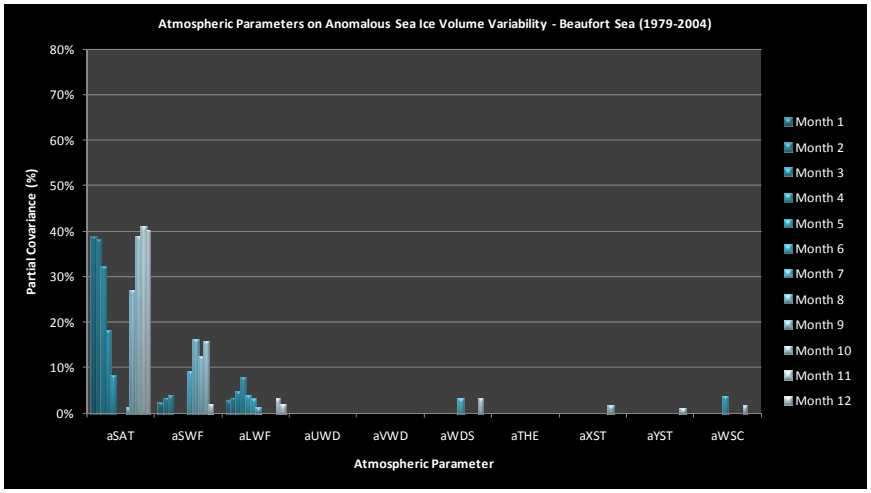

Figure 26. Anomalous Sea Ice Volume Variability—Beaufort Sea (1979–2004)

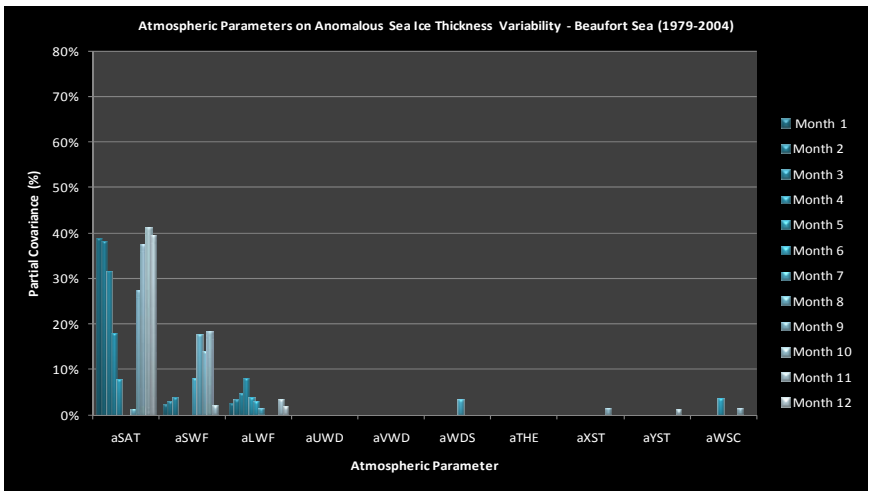

Figure 27. Anomalous Sea Ice Thickness Variability—Beaufort Sea (1979–2004)

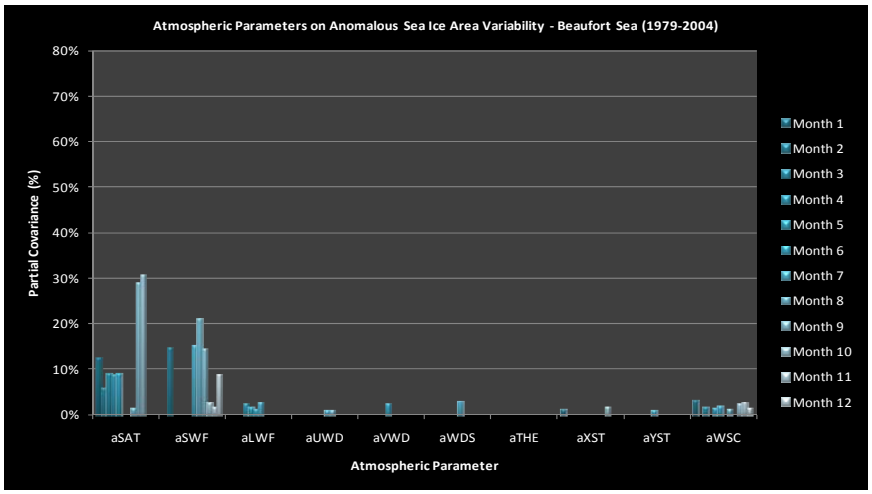

Figure 28. Anomalous Sea Ice Area Variability—Beaufort Sea (1979–2004)

Figures 26–28 above show that from 1979–2004 aSAT, aSWF, and aLWF explain the largest amount of aVOLv, aTHKv, and aARAv in the Beaufort Sea. Similar patterns are seen for other regions, figures for which are found in Appendix B. The contributions from zonal and meridional winds and stresses are negligible.

In the annual average context, aSAT explains 24–39% of aVOLv in the Central Arctic regions, with the maximum partial covariance of 58% of aVOLv at the North Pole during the cooling months. aSWF and aLWF, the atmospheric forcing parameters that explain the next largest amount of aVOLv, explain 3–6% and 0–9% of annual average

aVOLv, respectively. At 23%, aSWF's largest contribution to aVOLv in the E. Siberian Sea is less than half of maximum aSAT's influence on aVOLv in the North Pole.

Figure 27 and similar figures in Appendix B show the amounts of aTHKv the atmospheric forcing parameters explain closely resemble that of aVOLv. In the annual average context, aSAT explains 23–39% of aTHKv in the Central Arctic, with a maximum partial covariance of 59% of aTHKv at the North Pole in the cooling months. aSWF and aLWF contribution to aTHKv match that of aVOLv at 3–6% and 0–9%, respectively.

Anomalous zonal and meridional winds and stresses as well as aWSC explain less than 5% of aVOLv and aTHKv. This may be due to a lag period between atmospheric wind and sea ice response. Rigor and Wallace (2004) found that ice responds to atmospheric wind and stresses after a period of days to weeks. Köberle and Gerdes (2003) found wind stresses significantly contribute to the decadal variability of Arctic sea ice volume. Still, Barry et al. (1993) reported that due to high variation in winds, wind forcing on ice tends to cancel out.

The aSAT, aSWF, and aLWF patterns seen in aVOLv and aTHKv are also seen in the aARAv during 1979–2004 (Figure 28 above and Figures 67–74 in Appendix B). However, the annual average amount of variability that aSAT and aSWF account for of aARAv is decreased up to 30%. In the North Pole and Canadian Arctic Archipelago regions, aARAv responds to the increase of the aLWF-aSWF-aSAT as seen before with aVOLv and aTHKv, and aSWF remains dominant in explaining aARAv in the E. Siberian, Chukchi, and Beaufort Seas, at the North Pole and at the Canadian Arctic Archipelago. At no location, however, does aLWF account for more aARAv than aSWF or aSAT. In order to better understand the temporal change in atmospheric forcing of sea ice the following two sections (C and D) show results for the first and second half of the entire data period, similar to the split done by Francis and Hunter (2006).

C. ANOMALOUS SEA ICE VOLUME, THICKNESS, AND AREA VARIABILITY IN THE CENTRAL ARCTIC (1979–1991)

Figures 29–32 below and Figures 75–98 in Appendix B depict the amount of anomalous sea ice volume variability (aVOLv), anomalous sea ice thickness variability (aTHKv), and anomalous sea ice area variability (aARAv) accounted for by each atmospheric parameter used in the NPS Model for the data period 1979–1991. The atmospheric parameters are labeled along the x-axis. Partial covariance of sea ice parameter explained by each atmospheric forcing parameter is determined by the partial correlation method described in Chapter II and indicated by the percentage along the y-axis. Each monthly atmospheric contribution to aVOLv is ordered from the left to the right with the darkest-colored bar being Month 1 and the lightest-colored bar being Month 12. Months 4–9 are referred to as the warming months and Months 10–3 are referred to as the cooling months.

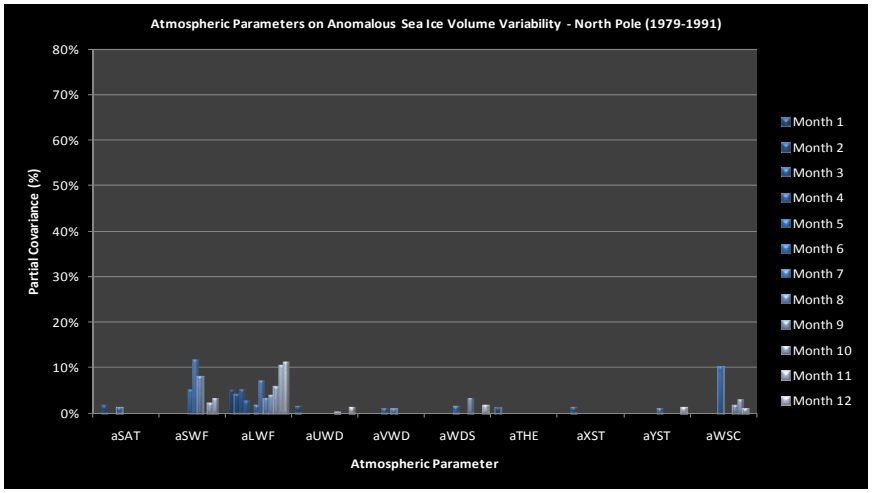

Figure 29. Anomalous Sea Ice Volume Variability—North Pole (1979–1991)

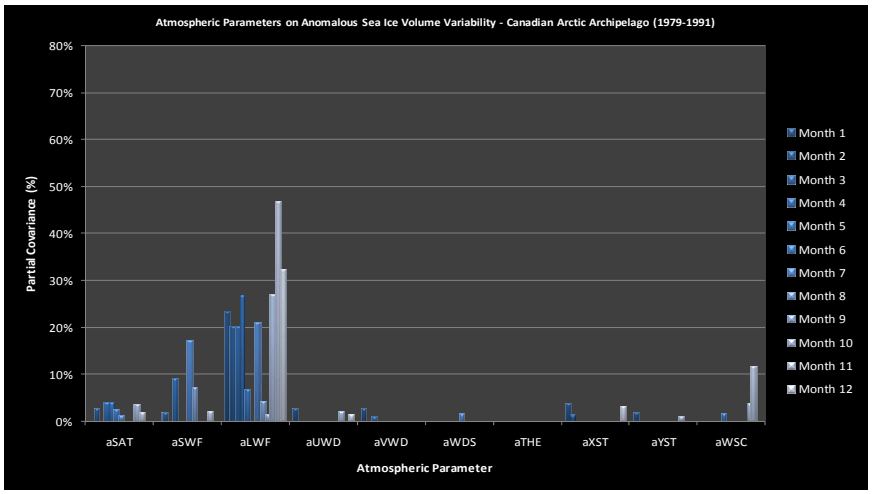

Figure 30. Anomalous Sea Ice Volume Variability—Canadian Arctic Archipelago (1979–1991)

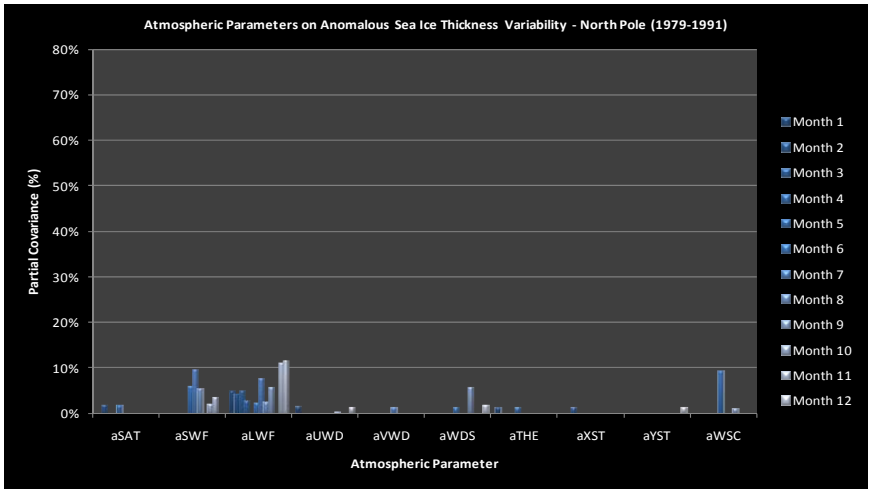

Figure 31. Anomalous Sea Ice Thickness Variability—North Pole (1979–1991)

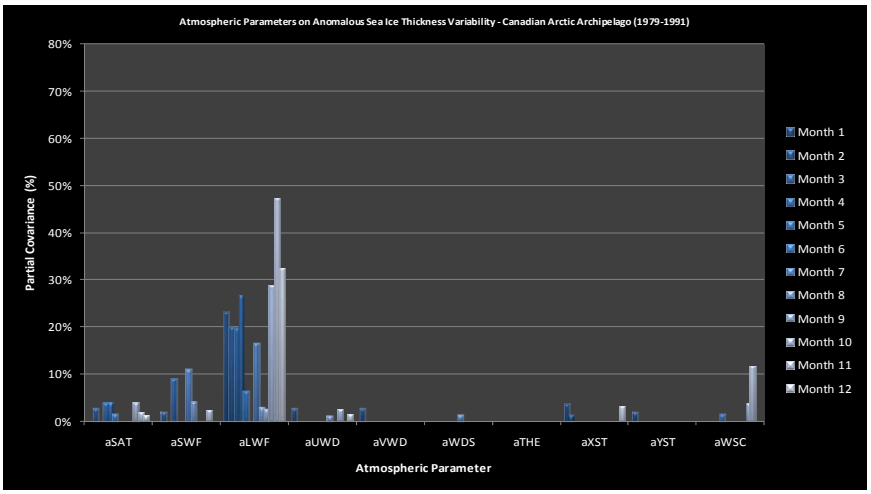

Figure 32. Anomalous Sea Ice Thickness Variability—Canadian Arctic Archipelago (1979–1991)

As shown in Figures 29–30 (and Figures 75–90 in Appendix C) the decreasing aSAT-aSWF-aLWF trend is not found in aVOLv nor aTHKv at the North Pole or Canadian Arctic Archipelago; more generally, it is not exhibited during the first 13 years of the data set. The annual aSAT partial covariance with aVOLv averages between 0–15%, while aSWF and aLWF partial covariance with aVOLv average 3–10% and 1–19%, respectively. Similarly, the annual aSAT portion of aTHKv averages between 0–12% with aSWF and aLWF portions of aTHKv averaging 2–11% and 1–19%, respectively. During this period aSWF contributes to more aVOLv than aSAT by 1–6% in the E. Siberian, Chukchi and Beaufort Seas, at the North Pole and the Canadian Archipelago; aLWF contributes to more aVOLv than aSWF by 1–16% in the Barents and Laptev Seas, at the North Pole and the Canadian Archipelago; and aLWF contributes to more aVOLv than aSAT by 5–17% at the North Pole and the Canadian Archipelago. Likewise, aSWF contributes to more aTHKv than aSAT by 2–7% in the E. Siberian, Chukchi and Beaufort Seas and at the North Pole; aLWF contributes to more aTHKv than aSWF by 3–17% at the North Pole and Canadian Arctic Archipelago; and aLWF contributes to more aTHKv than aSAT by 1–17% in the Beaufort Sea, at the North Pole and Canadian Arctic Archipelago.

To generalize, aSAT generally explains a larger amount of aVOLv and aTHKv in Central Arctic during the cooling months when sea ice is forming than in the warming

months when sea ice is melting. aSWF and aLWF explain a larger amount of aVOLv and aTHKv during the warming months than the cooling months.

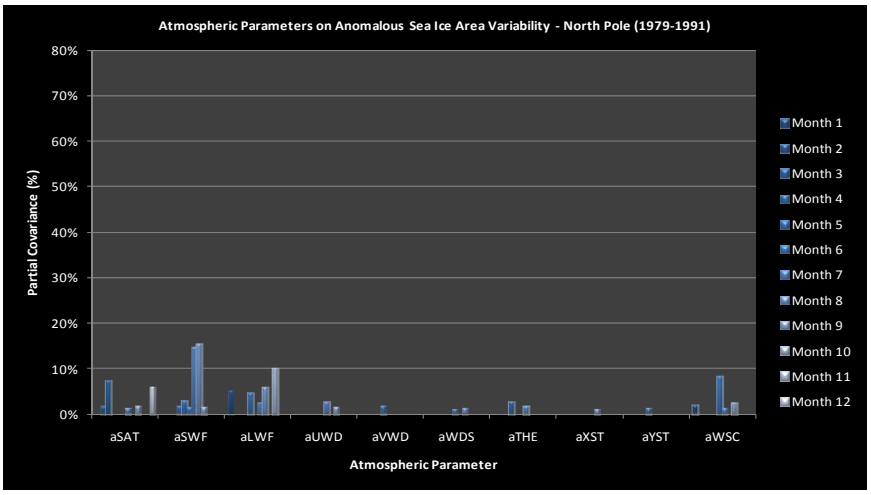

Figure 33. Anomalous Sea Ice Area Variability—North Pole (1979–1991)

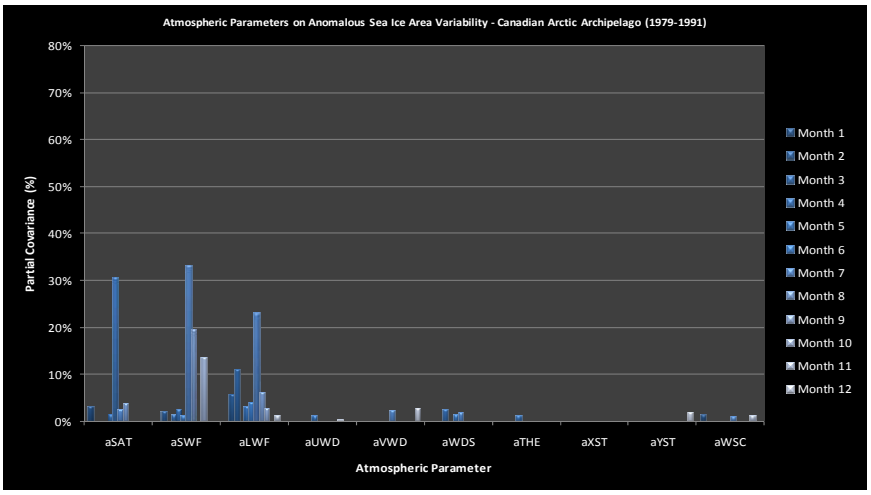

Figure 34. Anomalous Sea Ice Area Variability—Canadian Arctic Archipelago (1979–1991)

In Figures 33–34 above, aARAv in the North Pole and Canadian Arctic Archipelago during the first 13 years do not exhibit the decreasing aSAT-aSWF-aLWF contribution pattern to aARAv as it does in the entire 26-year data period. Figures 91–98 in Appendix C show similar trends in for other areas in the Central Arctic. For example, in the annual average context, aSWF contributes 2–5% more to aARAv than aSAT and 1–7% more to aLWF in the E. Siberian, Chukchi, and Beaufort Seas, at the North Pole and the Canadian Arctic Archipelago.

At varying strengths, aSAT generally explains a larger amount of aARAv in Central Arctic during the cooling months when sea ice is forming than in the warming months when sea ice is melting. aSWF and aLWF explain a larger amount of aVOLv and aTHKv during the warming months than the cooling months.

D. ANOMALOUS SEA ICE VOLUME, THICKNESS, AND AREA VARIABILITY IN THE CENTRAL ARCTIC (1992–2004)

Figures 35–37 below and Figures 99–122 in Appendix D depict the amount of anomalous sea ice volume variability (aVOLv), anomalous sea ice thickness variability (aTHKv), and anomalous sea ice area variability (aARAv) accounted for by each atmospheric parameter used in the NPS Model for the data period 1992–2004. The atmospheric parameters are labeled along the x-axis. Partial covariance of sea ice parameter explained by each atmospheric forcing parameter is determined by the partial correlation method described in Chapter II and indicated by the percentage along the y-axis. Each monthly atmospheric contribution to aVOLv is ordered from the left to the right with the darkest-colored bar being Month 1 and the lightest-colored bar being Month 12. Months 4–9 are referred to as the warming months and Months 10–3 are referred to as the cooling months.

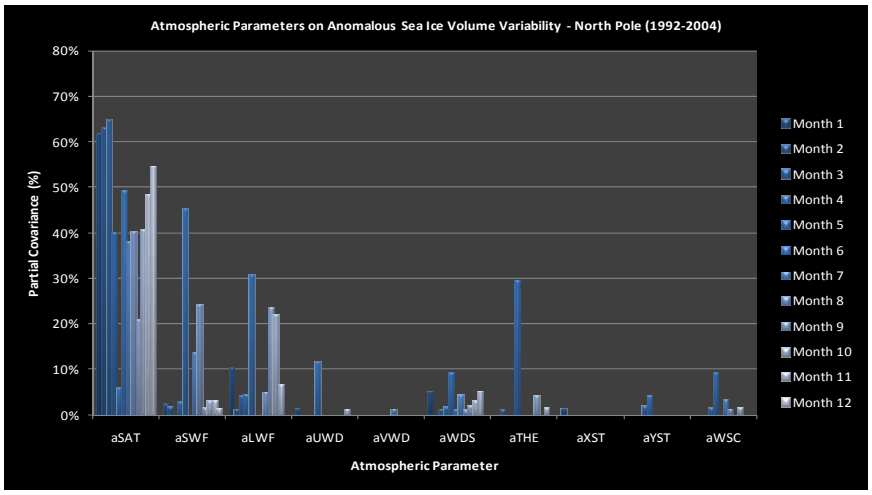

Figure 35. Anomalous Sea Ice Volume Variability—North Pole (1992–2004)

Figure 35 above shows that the trend of aVOLv being dominated by aSAT is magnified during 1992–2004. Figures 99–106 in Appendix D show similar patterns for

other regions. In these 13 years, aSAT explains 27–44% of aVOLv on annual average with a maximum as high as 65% of aVOLv at the North Pole. The annual average aSWF contribution to aVOLv increases to 1–5% over the previous 13 years, and the annual average aLWF contribution to aVOLv increases 1–4% over the previous 13 years.

During both warming and cooling months, aSAT explains the most aVOLv, followed by aSWF. aLWF's contribution to aVOLv is greater in the cooling months than in the warming months in the Barents and Kara Seas, at the North Pole and Canadian Arctic Archipelago. aLWF's contribution to aVOL is greater in the warming months than in the cooling months in the Laptev, E. Siberian, Chukchi, and Beaufort Seas.

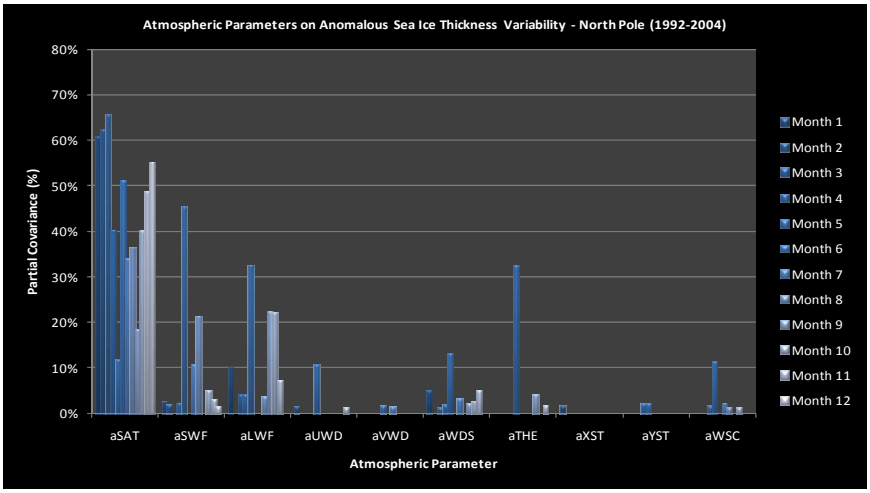

Figure 36. Anomalous Sea Ice Thickness Variability—North Pole (1992–2004)

In Figure 35–36 above and Figures 99–114 in Appendix D, atmospheric contribution to aTHKv is similar to that of aVOLv during 1992–2004. aTHKv due to aSAT contribution is magnified during 1992–2004. In these 13 years, aSAT explains 27–44% of aVOLv on annual average with a maximum as high as 66% of aVOLv at the North Pole.

During both warming and cooling months, aSAT explains the most aVOLv, followed by aSWF. aLWF's contribution to aVOLv is greater in the cooling months than in the warming months in the Barents and Kara Seas, at the North Pole and Canadian Arctic Archipelago. aLWF's contribution to aVOL is greater in the warming months than in the cooling months in the Laptev, E. Siberian, Chukchi, and Beaufort Seas.

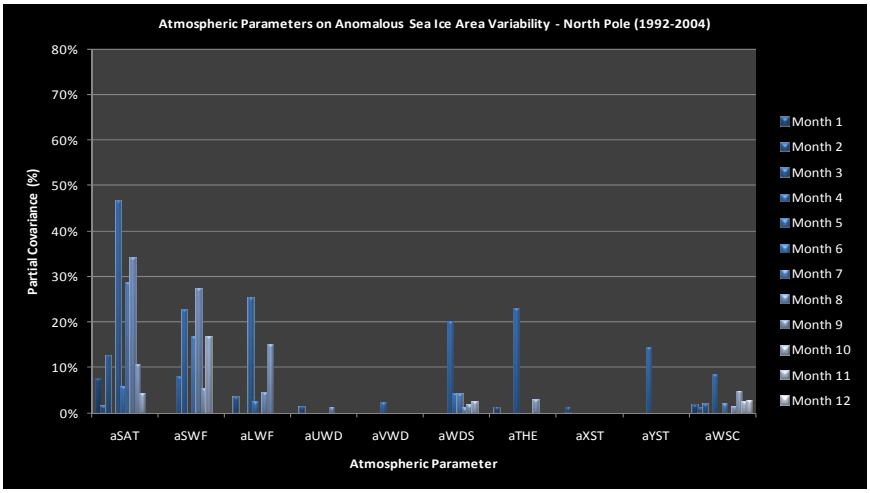

Figure 37. Anomalous Sea Ice Area Variability—North Pole (1992–2004)

In Figure 37 above and Figures 115–122 in Appendix D, aSAT, aSWF and aLWF's contribution to aARAv during the 1992–2004 period continues to show the dominance of aSAT on aARAv. In the annual average context, aSAT explains 4–31%, aSWF explains 4–10%, and aLWF explains 1–4% of aARAv.

Warming air temperature can be more influential on slowing and accelerating the freezing of sea ice; aSAT contribution to aARAv during the cooling months is larger than atmospheric contribution to aARAv during the warming months. aSAT contributes 13–57%, aSWF contributes 3–31%, and aLWF contributes 1–10% to aARAv during the cooling months. aSAT contributes 9–46%, aSWF contributes 16–34%, and aLWF contributes 4–32% to aARAv during the warming months.

E. ANOMALOUS SEA ICE VOLUME, THICKNESS, AND AREA VARIABILITY ALONG THE NORTHWEST PASSAGE (1979–2004)

Understanding the strategic and economic importance of the Arctic region, Former President George W. Bush signed the National/Homeland Presidential Security Directive-66/25 into effect in January of 2009. These directives outline defense strategies for the Arctic region, specifically naming the Northwest Passage and the Northern Sea Route. The following are sea ice variability studies for locations along these two coastal routes.

Figures 38–40 below (and Figures 123–146 in Appendix E) depict the amount of anomalous sea ice volume variability (aVOLv), anomalous sea ice thickness variability (aTHKv), and anomalous sea ice area variability (aARAv) accounted for by each atmospheric parameter used in the NPS Model for the entire data period 1979–2004. The atmospheric parameters are labeled along the x-axis. Partial covariance of each sea ice parameter with each atmospheric forcing parameter is determined by the partial correlation method described in Chapter II and indicated by the percentage along the y-axis. Each monthly atmospheric contribution to aVOLv is ordered from the left to the right with the darkest-colored bar being Month 1 and the lightest-colored bar being Month 12. Months 4–9 are referred to as the warming months and Months 10–3 are referred to as the cooling months.

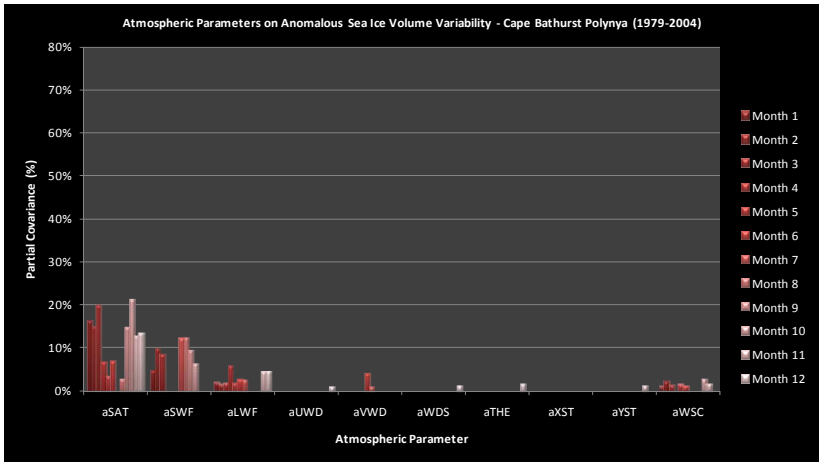

Figure 38. Anomalous Sea Ice Volume Variability—Cape Bathurst Polynya (1979–2004)

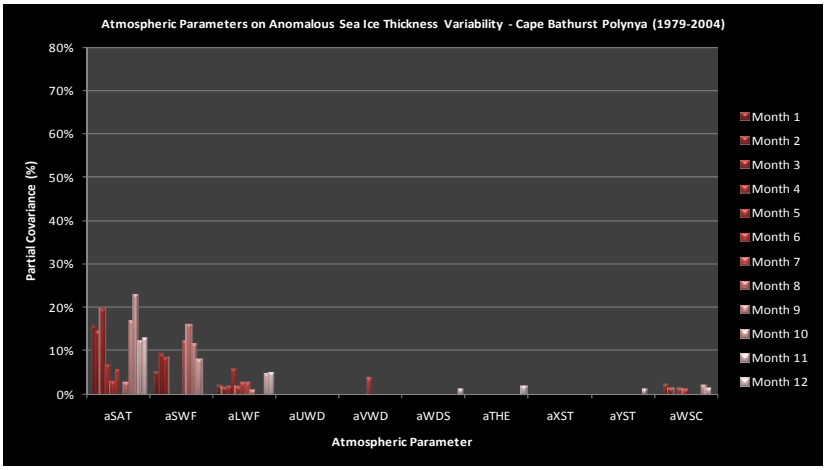

Figure 39. Anomalous Sea Ice Thickness Variability—Cape Bathurst Polynya (1979–2004)

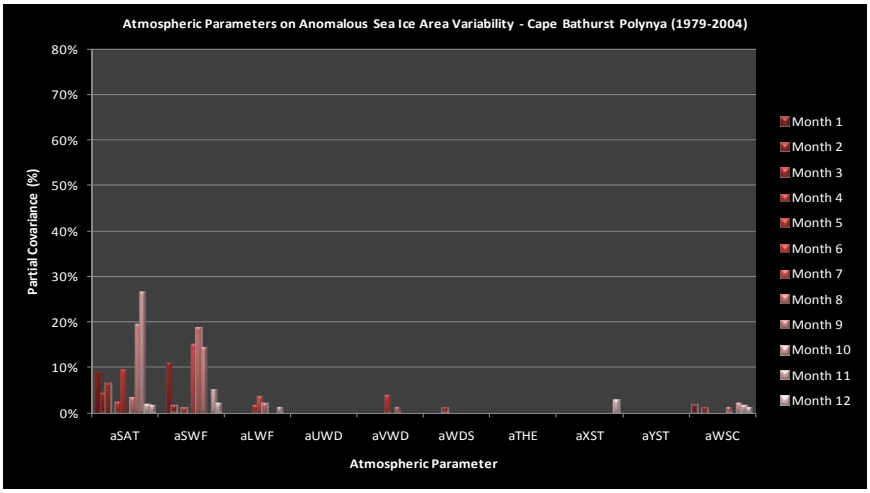

Figure 40. Anomalous Sea Ice Area Variability—Cape Bathurst Polynya (1979–2004)

The Cape Bathurst Polynya, and the other locations along the NWP, with exceptions of the Amundsen, Coronation, and Queen Maud Gulfs, have atmospheric contributions to aVOLv, aTHKv, and aARAv that exhibit similar decreasing aSAT-aSWF-aLWF trend to that shown in the Central Arctic locations. Winds and wind stresses continue to explain less than 2% of aSIV at all the NWP locations.

The amount of influence atmospheric forcing has on sea ice variability is lower along the NWP than in the Central Arctic. aSAT explains 9–16%, aSWF explains 2–18%, and aLWF explains 1–8% of aVOLv. aSAT explains 9–15%, aSWF explains 2–20%, and aLWF explains 1–8% of aTHKv. aSAT explains 4–12%, aSWF explains 1–11%, and aLWF explains 1–4% of aARAv.

F. ANOMALOUS SEA ICE VOLUME, THICKNESS, AND AREA VARIABILITY ALONG THE NORTHERN SEA ROUTE (1979–2004)

Figures 41–43 below and Figures 147–167 in Appendix F depict the amount of anomalous sea ice volume variability (aVOLv), anomalous sea ice thickness variability (aTHKv), and anomalous sea ice area variability (aARAv) accounted for by each atmospheric parameter used in the NPS Model for the entire data period 1979–2004. The atmospheric parameters are labeled along the x-axis. Partial covariance of sea ice parameter explained by each atmospheric forcing parameter is determined by the partial correlation method described in Chapter II and indicated by the percentage along the y-

axis. Each monthly atmospheric contribution to aVOLv is ordered from the left to the right with the darkest-colored bar being Month 1 and the lightest-colored bar being Month 12. Months 4–9 are referred to as the warming months and Months 10–3 are referred to as the cooling months.

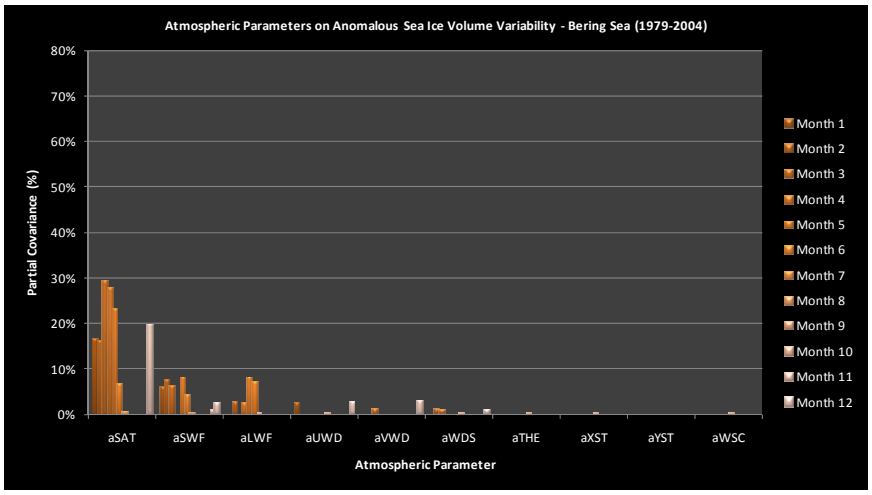

Figure 41. Anomalous Sea Ice Volume Variability—Bering Sea (1979–2004)

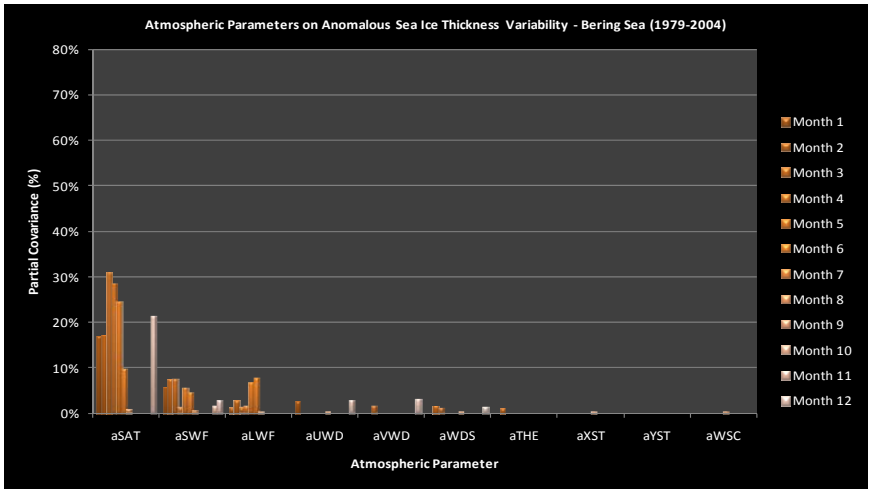

Figure 42. Anomalous Sea Ice Thickness Variability—Bering Sea (1979–2004)

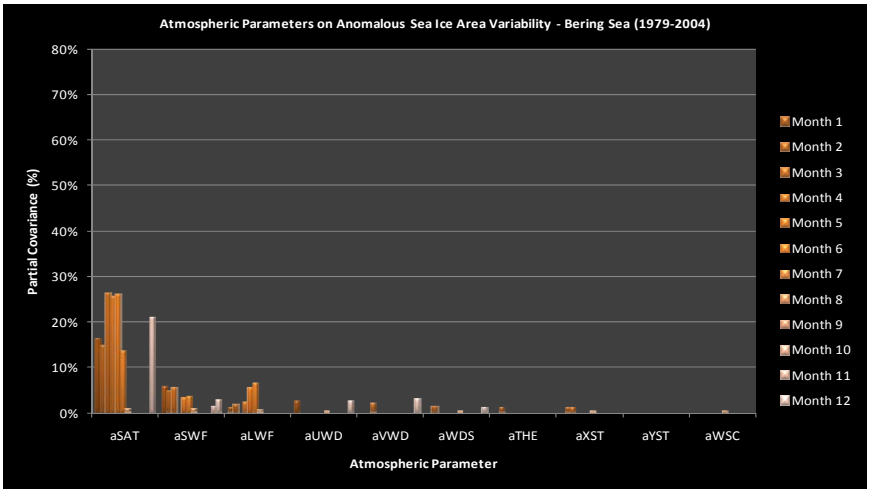

Figure 43. Anomalous Sea Ice Area Variability—Bering Sea (1979–2004)

The atmospheric contribution to aVOLv, aTHKv, and aARA in the Bering Sea, and locations along the NSR, exhibit the decreasing aSAT-aSWF-aLWF trend shown in that of the Central Arctic locations. Winds and wind stresses continue to explain less than 2% at all the NWP locations.

The amount of influence the atmospheric forcing has on sea ice variability is lower along the NSR than in the Central Arctic. aSAT explains 11–25%, aSWF explains 5–12%, and aLWF explains 1% of aVOLv. aSAT explains 12–25%, aSWF explains 5–12%, and aLWF explains 1% of aTHKv. aSAT explains 2–11%, aSWF explains 3–9%, and aLWF explains 1–2% of aARAv.

G. SUMMARY OF ATMOSPHERIC CONTRIBUTION TO ANOMALOUS SEA ICE VOLUME VARIABILITY IN THE CENTRAL ARCTIC (1979–2004)

Figure 44, as well as the figures in Appendices G through I, provides summaries of the average, minimum, and maximum percentage of aSAT, aSWF, and aLWF contribute to aVOLv in the Central Arctic as well as their month(s) of occurrence. This is done for 1979–2004; the first half of the data period, 1979–1991; and the second half of the data period, 1992–2004, for aVOLv (Appendix G), aTHKv (Appendix H), and aARAv (Appendix I).

Two images make up each of the summary figures. In both images, each square outlines a location in the Central Arctic. In the top image, each outlined location has a column of three numbers: the first number, the range in red, denotes the range of atmospheric forcing contribution to aVOLv during the warming months. The second number, in green, denotes the annual average of atmospheric forcing contribution to aVOLv. The third number, in blue, denotes the range of atmospheric forcing contribution to aVOLv during the cooling months. In the bottom image, each outlined location contains the warming and cooling months' maximum and minimum atmospheric forcing contributions to aVOLv along with their specific month(s) of occurrence. These figures show a compact comparison of the results from Appendices B-F.

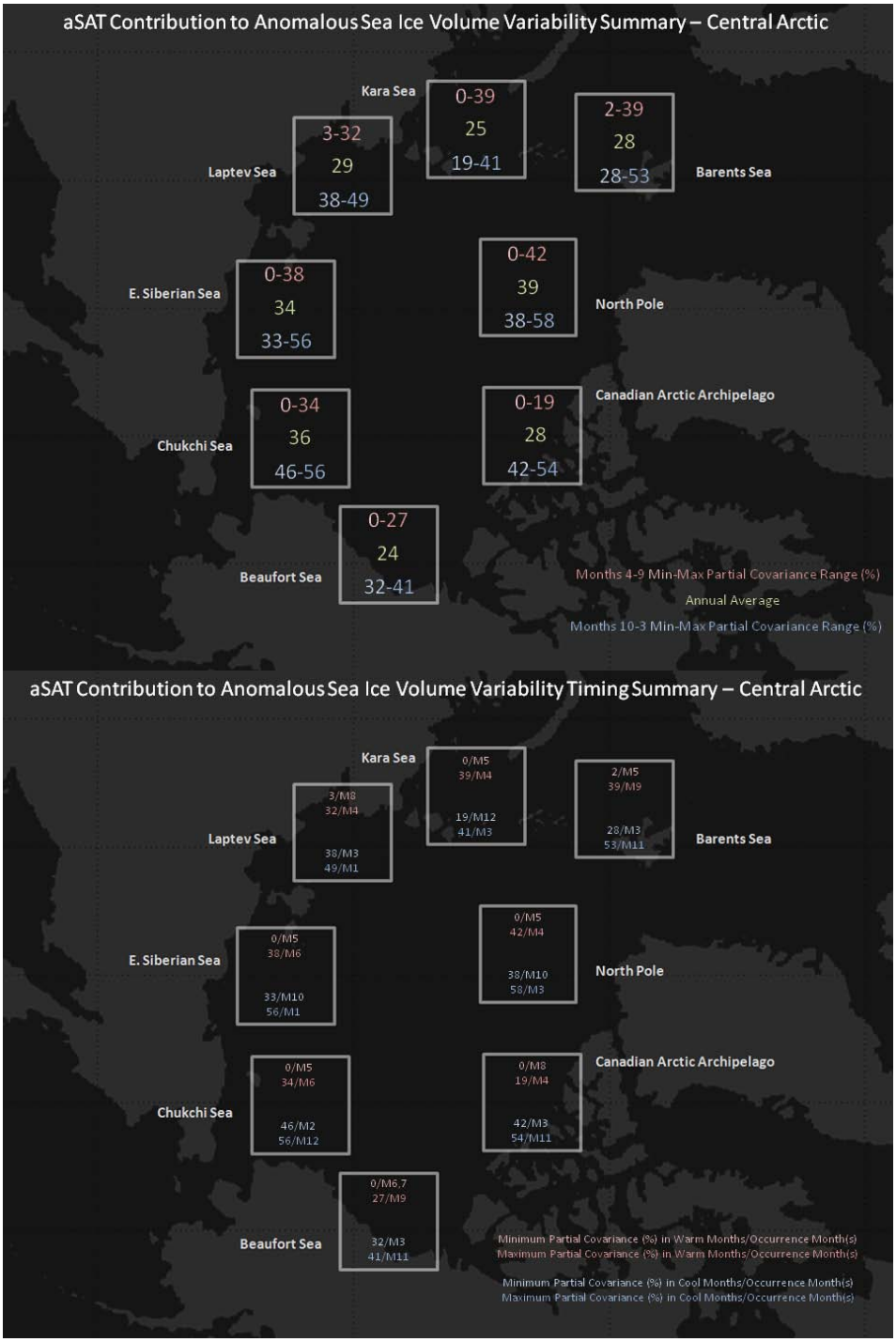

Figure 44. Average (green), Warming Months Minimum-Maximum Range (red), and Cooling Months Minimum-Maximum Range (blue) of aSAT Contribution to aVOLv (top) and Timing of Warming (red) and Cooling (blue) Minimum and Maximum (bottom)—Central Arctic (1979–2004)

IV. DISCUSSION OF RESULTS

A. SEA ICE VARIABILITY

The annual cycle of sea ice volume and thickness resembles a sinusoid where the maximum occurs in the late winter and the minimum occurs in the late summer (Figures 45-46). The annual cycle of sea ice area is slightly different in that the areal concentration of ice remains close to 100% with a dip in concentration during the summer. In the outer locations of the Arctic region such as the Barents Sea, the sinusoid representing thickness and volume flattens in the summer and the fall. Sea ice concentration loses its "V" shape and resembles a curve similar to volume and thickness due to the low or lack of sea ice concentration in the Barents Sea during summer (Figure 47).

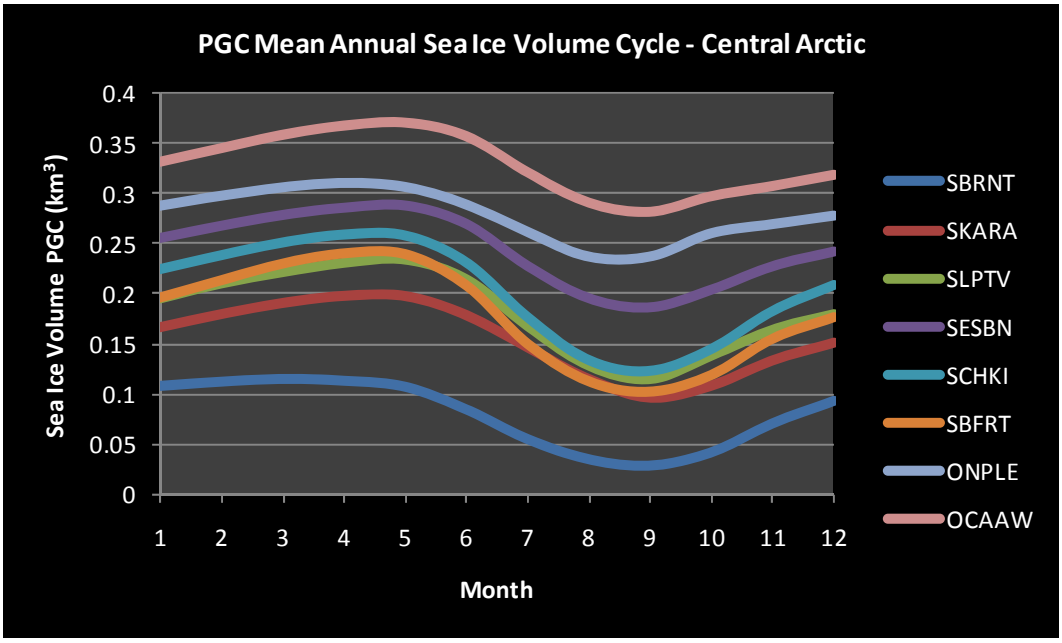

Figure 45. Per grid cell (PGC) Mean Annual Sea Ice Volume Cycle for the Central Arctic Locations: Barents Sea (SBRNT), Kara Sea (SKARA), Laptev Sea (SLPTV), E. Siberian Sea (SESBN), Chukchi Sea (SCHKI), Beaufort Sea (SBFRT), the North Pole (ONPLE), and the Canadian Arctic Archipelago (OCAAW)

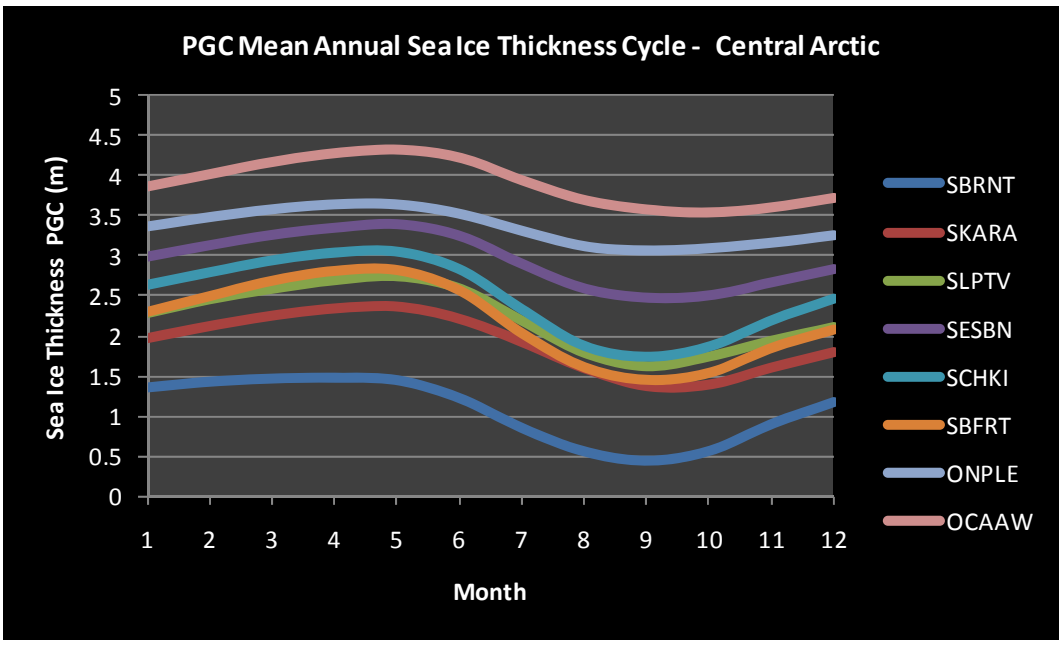

Figure 46. PGC Mean Annual Sea Ice Thickness Cycle for the Central Arctic Locations: SBRNT, SKARA, SLPTV, SESBN, SCHKI, SBFRT, ONPLE, and OCAAW.

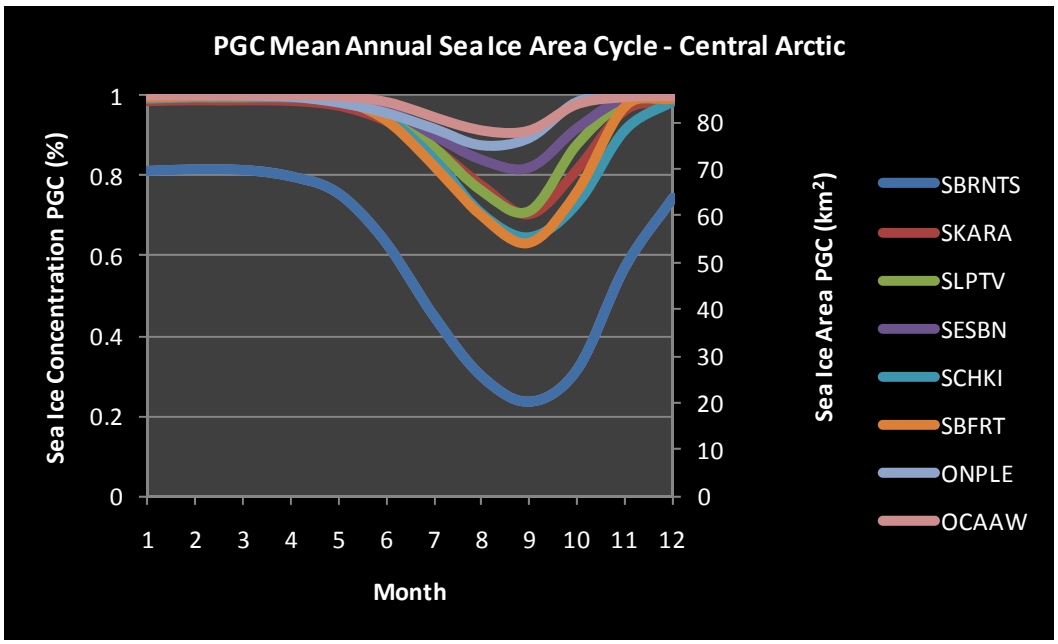

Figure 47. PGC Mean Annual Sea Ice Concentration (Area) for the Central Arctic Locations: SBRNT, SKARA, SLPTV, SESBN, SCHKI, SBFRT, ONPLE, and OCAAW.

Sea ice distribution in the Arctic generally houses the thickest sea ice near the center of the Arctic and at the Canadian Arctic Archipelago (Figure 46).

B. COMPARISON WITH PREVIOUS STUDIES

1. Similarities with Previous Studies

The dominant partial covariances resulting from the analysis of ECMWF atmospheric forcing and NPS model aARAv are in general agreement with the findings of Francis et al. (2005), who studied variances derived from zonal wind anomaly (UWDa), meridional wind anomaly (VWDa), downwelling longwave flux anomaly (DLFa), heat advection anomaly (ADVa) and the annual maximum ice retreat anomaly (MIA) up to and including 25-day lag period. Francis et al. (2005) reports the dominance of DLFa, ADVa and VWDa in explaining MIA. While not immediately obvious, DLFa and ADVa explanation of MIA corresponds well to dominant aSAT trend discussed above, because aSAT drives both the calculation of DLFa and ADVa (Francis, 1994; Francis, 1997).

Positive aSAT provides the thermal energy necessary to break the hydrogen bonds within ice to form liquid water. During the warming months the melting of ice edges creates open water, which has a lower albedo, and allows for increased shortwave radiation absorption into the ocean mixed layer at the edge of the sea ice of within leads. This increases lateral melting of ice, closing the ice-albedo positive feedback cycle (Zhang, 2000). One of the reasons that aSWF is not as influential during the melting season may be that the absorption of shortwave radiation slightly below the surface of the ice can actually increase the sea ice equilibrium thickness. This is because there is a variable amount of net shortwave radiation absorbed into brine pockets of the ice, which shortchanges the amount of energy available for melting the surface of the ice (Maykut and Untersteiner 1971; and Barry et al. 1993). Positive aSAT also can increase the saturation vapor pressure, the amount of water vapor air can hold, potentially resulting in increased cloud cover (Miller 2007). Stratus clouds warm the Arctic in the non-summer months, thereby closing the aLWF-aSAT positive feedback loop (Schweiger 2008). An

increase in stratus clouds can also point to more shortwave radiation reflected back into the atmosphere, supporting a decrease in aSWF.

Francis and Hunter (2006) split the 26 years of data into two equal periods and analyze the accumulation of atmospheric forcing on the Barents and Chukchi Seas. During the first half of the data period, 1979–1991, atmospheric forcing integration up to 25 days showed DLFa and VWDa were dominant in accounting for MIA in both Seas. DLFa explained 50% of MIA in the Barents Sea. DLFa explained 20% of MIA in the Chukchi Sea. During the second half of the data period, 1992–2004, ADVa accounted for 20–30% and DLFa accounted for 10–20% of MIA in the Barents Sea, ADVa accounted for 20% and DLFa accounted for 20–40% of MIA in the Chukchi Sea. Like Francis and Hunter (2006), the results from this thesis research confirm the significance of aSAT during both of these periods (Figures 51-74, and Figures 99-122).

2. Contrasts with Previous Studies

Although the results of Francis et al. (2005), and Francis and Hunter (2006), and this research found similar results for DLFa and aSAT, the research results here differ in significant ways from these studies. In our one-system study, wind components do not have strong correlations with aARAv from 1979-2004 or 1979–1991, time periods during which both Francis et al. (2005), and Francis and Hunter (2006) report MIA due to VWDa. In Francis' calculations, VWDa is expected to play a large role in the meridional ice edge position anomaly as the ice edge retreats parallel to the meridional wind. During 1992–2004, our analyses show that the average winds and stresses that account for aARAv peak up to 47% in Month 5 (average remain at less than 5% as previously discussed) while Francis and Hunter (2006) find that winds do not play a role in MIA. Sea ice in our one-system approach, during the latter 13 years, is more vulnerable to the effects of wind and wind stresses. This is shown by the significant increase in contribution from wind and wind stresses to aARAv. The highest contributions for this period are: aUWD, which explains 47% of aARAv in the Laptev Sea (Figure 117); aVWD, which explains 12% of aARAv in the Laptev Sea (Figure 117); aWDS, which explains 14–20% of aARAv in the Kara (Figure 116), Laptev (Figure 117), Chukchi (Figure 119) and Beaufort Seas (Figure 120), and at the North Pole (Figure 121); aTHE, which

explains 16–31% of aARAv in the Laptev (Figure 117), E. Siberian (Figure 118) and Beaufort Seas (Figure 120), and at the North Pole (Figure 121) ; aXST, which explains 47% of aARAv in the Laptev Sea (Figure 117); aYST, which explains 10–14% of aARAv in the Laptev (Figure 117) and Chukchi Seas (Figure 119), and at the North Pole (Figures 121); and aWSC, which explains 11–22% of aARAv in the Chukchi (Figure 119) and Beaufort Seas (Figures 120). A possible factor in the higher contribution of wind and stress forcing to account for aARAv during 1992–2004 is the positive AO Index period during the winters of 1989–1995. In particular, in response to a highly positive (cyclonic) AO phase, or in the case of 1989–1990 the most positive AO index since 1899 (Figure 48), the Transpolar Drift shifts cyclonically from a path that extends from the Laptev Sea to the Fram Strait to one that extends from the Chukchi and E. Siberian Seas to the Fram Strait (Figure 3). With this cyclonic shift, thick ice from the Beaufort, Chukchi, E. Siberian and Laptev basins can be exported out via the Fram Strait. In its place is thin first year ice is formed, especially over the E. Siberian and Laptev Seas (Rigor et al. 2002; Belchansky 2004). The increasingly cyclonic pattern over the Arctic Ocean also forces divergence of the sea ice, forming open leads during winter and enhancing sensible heat flux from the ocean beneath. At the same time, the anticyclonic Beaufort Gyre is weakened, rendering less convergence, and thus less ridged sea ice (Rigor et al. 2002). Also following a positive AO phase in the winter is a melt season lengthened by 2–3 weeks during the following summer (Belchansky 2004; Hu et al. 2002).

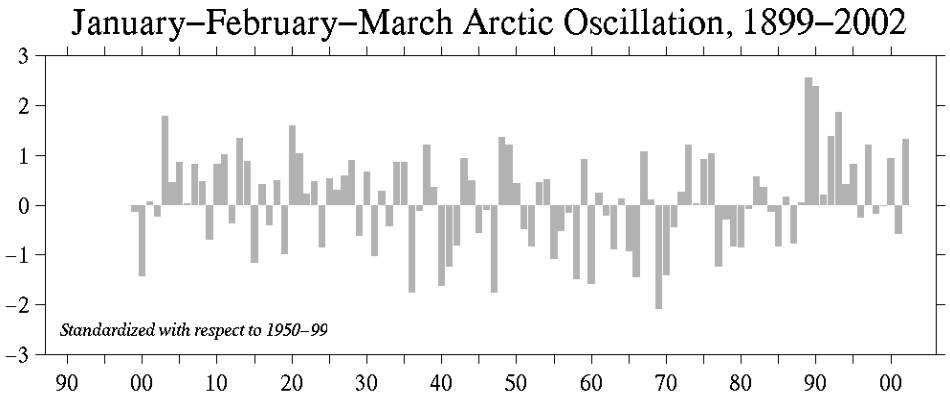

Figure 48. Time series of the winter (January-March) Arctic Oscillation Index from 1899-2002 show the positive and negative episodic behavior of the Arctic Oscillation. This AO Index time series is similar to that of Figure 4, but with AO indices from 1899 to 2002 instead of 1951 to 2004 (From Mitchell 2004).

The combination of thick ice export, thin ice formation, and a longer melt season results in an overall weakened state of Arctic sea ice as defined by the following empirical equation,

$$P = P^{*} h e^{-C(1-a_i)}, \qquad (5)$$

which relates the strength of sea ice to the thickness of the thinnest fraction of sea ice, where P is strength of sea ice, P^{*} and C are empirical constants, h is the thickness of the thinnest fraction of ice within a unit area, and a_i is the total fraction of ice coverage within that area (Hibler 1979). Thus, in the years following the 1989–1995 positive AO phase, the weaker ice was more vulnerable to winds and stresses. It is by this reasoning that aTHKv from the same period show peaks in atmospheric wind and stress forcing: aUWD contributes 11–14% of aTHKv in the Laptev Sea (Figure 109) and at the North Pole (Figure 113); aWDS contributes 13–37% of aTHKv in the Kara (Figure 1087), Chukchi (Figure 109) and Beaufort Seas (Figure 110), and at the North Pole (Figure 111) and Canadian Arctic Archipelago (Figure 114); aTHE contributes 24–32% of aTHKv in the Laptev Sea (Figure 109) and at the North Pole (Figure 113); aXST contributes 15% of aTHKv in the Beaufort Sea (Figure 112); aYST contributes 15% of aTHKv at the North Pole (Figure 113); and aWSC contributes 11-24% of aTHKv in the Beaufort Sea (Figure 112) and at the North Pole (Figure 113).

Additionally, the highly cyclonic pattern due to a positive AO phase decreases the overall thickness of the tropospheric column, which can allow for more upward vertical motion. With adequate moisture in the atmosphere, cloud cover can increase. This, in turn, increases aLWF and warming over the Arctic Ocean (Liu 2007). The increased amount of leads and thinner sea ice causes the overall ice cover to be more responsive to the atmospheric forcing (i.e., warming conditions) in the second half of the analyzed time period. This is possibly the reason why the results in this thesis show that aSAT contributes 9–17% more aARAv in this latter period.

Francis and Hunter (2006), on the other hand, showed that the atmospheric account of MIA was larger from 1979–1991 than from 1992–2004. This contradictory result of magnitude of atmospheric forcing between the two periods along with the wind

accountability of aARAv and MIA are two differences between Francis et al. (2005), Francis and Hunter (2006), and the results of this thesis. Some explanations for these differences may involve differences in calculating sea ice variability parameter and differing data sources. This research calculates aARAv in terms of total area anomaly whereas Francis et al. (2005), and Francis and Hunter (2006) calculate areal sea ice as meridional ice retreat anomaly, a fraction of aARAv. Moreover, MIA for each of the 400-km radius area Francis and colleagues examine is calculated using a Scanning Multichannel Microwave Radiometer (SMMR) and Special Sensor Microwave/Imager (SSM/I) data, whereas aARAv for each 55 by 55 grid point sea is calculated from the NPS model output. One of the major differences between these two data sets is the melt pond coverage during the summer, which influences estimates of ice concentration in satellite data, but is not an issue in the NPS Model output.

C. ANOMALOUS SEA ICE THICKNESS VARIABILITY

Although thickness and volume incorporate the vertical dimension in contrast to the lateral dimensions accounted for in ice area and extent, and thus more fully account for thermodynamic processes, the results of aTHKv are similar that of aVOLv. SAT can melt the surface of the ice, reducing sea ice thickness. Warming of SAT also warms the sea surface temperatures (SST) and the ocean mixed layer in the summer. This, in turn, helps melt ice from the bottom. aLWF enhances the warming of the SAT via the aLWF-aSAT feedback loop described above (Miller 2007). SWF, when absorbed through thin ice and open ocean during the warm months, can warm the upper ocean and contribute to sea ice melt from the bottom of the ice. The bottom melting of sea ice becomes increasingly more evident as ice thins (Perovich et al. 2008; Stephens n.d.). The positive AO episode during 1989–1995 are followed by the export of thick ice from the Beaufort, Chukchi, E. Siberian, and Laptev basins are exported out from the central Arctic via the Fram Strait. Left in its place is newly formed thin ice, which injects more salt into the ocean, increasing the buoyancy flux and deepening the mixed layer (Hu et al. 2002). A deepened mixed layer with positive temperatures can aid in the melting of sea ice below the surface of the ocean.

D. SEASONAL ANOMALOUS SURFACE AIR TEMPERATURE CONTRIBUTION TO SEA ICE VARIABILITY

In the 26-year data set and the two, 13-year data sets, at no location does aSAT contribute to anomalous sea ice variability more in the warming months than in the cooling months. Locations that exhibit a temporal trend show that aSAT contributes more in the cooling than in the warming months. For example, in the Central Arctic this seasonal contribution difference between the warming and cooling months is approximately 20%. From 1979–2004, aSAT explains up to 39% of aVOLv in the warming months and up to 58% of aVOLv in the cooling months (Figure 168). From 1979–1991, aSAT explains up to 22% of aVOLv during the warming months and up to 45% during the cooling months (Figure 171). From 1992–2004, aSAT explains up to 52% of aVOLv in the warming months and up to 65% of aVOLv in the cooling months (Figure 174). This indicates that the aSAT explain 10–25% more of sea ice growth (cooling months) than of sea ice decline (warming months). This temporal trend is most evident in the analysis of aVOLv and aTHKv than in the analysis of aARAv.

E. NORTHWEST PASSAGE AND THE NORTHERN SEA ROUTE

Locations along the NWP generally follow the increasing aLWF-aSWF-aSAT trend of the Central Arctic Seas. A few locations where aSWF explains more aVOLv and aTHKv than aLWF but less than aSAT are the Amundsen, Coronation and Queen Maud Gulfs (Figure 124-126). Warming temperatures can lead to a decrease of low level clouds, but an increase in midlevel clouds, which can decrease SWF. This may explain why aSWF account for the more sea ice variability than aSAT or aLWF in the Amundsen, Coronation, and Queen Maud Gulfs (Miller 2007; Schweiger 2008).

Sea ice volume and thickness in the locations along the NSR are affected more by aSAT than the locations along NWP. Overall, atmospheric forcing parameters explain relatively small amount of aVOLv, aTHKv, and aARAv (approximately up to 30% in NWP and 40% in NSR) when comparing to partial covariances from the locations in the Central Arctic (nearly 70%). (Compare Figures 51-74 with Figures 123–146, and compare Figures 51-74 with Figures 147-167) This may mean that the locations in the

Central Arctic have more anomalous sea ice variability while the sea ice variability along NWP and NSR more closely match that of mean annual variability.

This chapter presented and analyzed results of various locations within the Arctic over the entire data period of 1979–2004 as well as over the first, 1979–1991, and the second half, 1992–2004, of this data period. Chapter V summarizes the main conclusions from these analyses, including percentages of anomalous sea ice variability attributed to various anomalous atmospheric forcing parameters.

THIS PAGE INTENTIONALLY LEFT BLANK

V. CONCLUSIONS

A. AVERAGE ANOMALOUS ATMOSPHERIC FORCING CONTRIBUTION TO ANOMALOUS SEA ICE VARIABILITY

Depending on the location within Central Arctic, from 1979–2004, aSAT can explain 4–39% of anomalous sea ice variability, aSWF can explain 2–7% of anomalous sea ice variability, and aLWF can explain 1–9% of anomalous sea ice variability. From 1992-2004, aSAT can explain an additional 3–15% of anomalous sea ice volume and thickness variability, and an additional 2–10% of anomalous sea ice area variability.

Along the NWP and NSR, from 1979–2004, aSAT can explain 11–25% of anomalous sea ice variability, aSWF can explain 1-20% of anomalous sea ice variability, and aLWF can explain 1–8% of anomalous sea ice variability.

Over all, the atmospheric forcing during the 26-year period, from 1979 to 2004, shows less atmospheric forcing contribution to sea ice variability than the atmospheric forcing during only the latter half of the data period. As described in Chapter I, Section C, the AO is a potentially influential atmospheric phenomenon whose occurrence may have spring-boarded the Arctic sea ice into perpetual decline, contributing to sea ice variability as previously discussed.

Whether or not the AO proves to be a strong indicator for characteristics of the atmospheric circulation that affect sea ice variability, atmospheric factors clearly do not tell the whole story; a piece of the Arctic sea ice variability puzzle remains missing. In this research as well as in Francis et al. (2005) and Francis and Hunter (2006), the maximum amount of sea ice variability explained by atmospheric parameters is approximately 80%, and the typical amounts are significantly less (approximately 20-60%). During the first 13 years, the atmospheric influence on of sea ice variability was lower than that of the latter 13 years. During the same first 13 years, with lower atmospheric influence, there were generally positive anomalous sea ice volume, thickness and area growth. During the second 13 years, with stronger atmospheric influence there were negative sea ice volume anomalies, and thickness and area decreases. Excluding

the effects of time lag (not looking at winds and wind stresses), aSAT, aSWF, and aLWF explain more of anomalous sea ice growth (i.e., rapid ice formation in early winter) than sea ice decline (i.e., melting season anomalies). This is further supported by the greater atmospheric contribution to anomalous sea ice variability during the cooling months, which is when ice grows in volume. Second, the temporal and spatial variation between the atmospheric parameters that account for aTHKv is almost identical to that of aVOLv. The dynamics and thermodynamics of aTHKv inherently involve the ocean. These results support Deser and Teng's (2008) conclusion that "the long-term retreat of Arctic sea ice since 1979 in all seasons is due to factors other than wind-driven atmospheric thermal advection."

B. THE MISSING LINK

Oceanic contribution to sea ice variability may have already been evident in our analyses. Anomalous sea ice decreases during the melting season are not predominantly the result of anomalous atmospheric forcing. The Barents, Bering, inner Barents, and White Seas all show similar atmospheric contribution to aVOLv, aTHKv and aARAv. This indicates that there may be a limit to the influence atmospheric forcing has on the sea ice despite the different dimensions between thickness and area. Not coincidentally, these seas are located in regions readily receptive to warmer waters. The Barents Sea is located at the opening of the Barents Sea Opening where the North Cape Current and the Norwegian Atlantic Current flow northward and then eastward from the Atlantic Ocean. Francis and Hunter (2007) showed that approximately 20–25% of MIA in the Barents Sea is explained by SST. The North Cape Current continues its journey toward the inner Barents and White Seas, where these locations are ice-free in Months 8 and 9 and in Months 7–10, respectively. The Bering Sea, which is ice-free in Months 8-10 (Figure 49.), has the highest amount of heat flux in August as shown in Figure 50 (Clement et al. 2005).

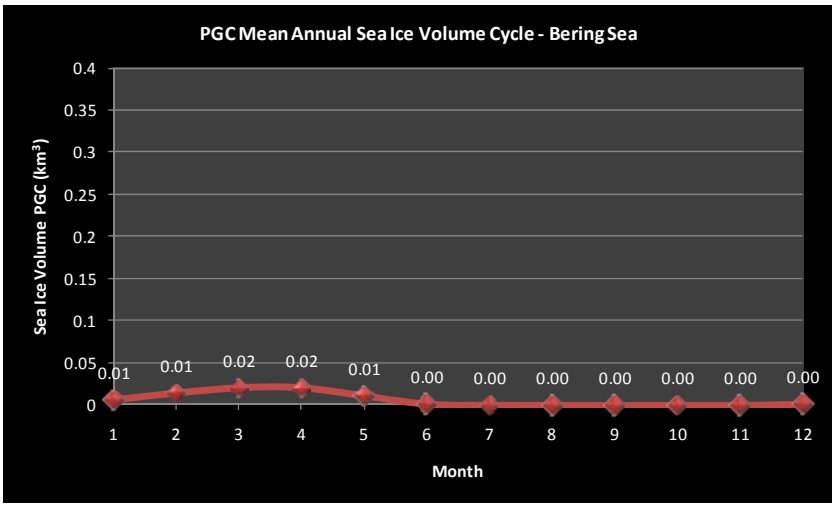

Figure 49. Per grid cell (PGC) Mean Annual Sea Ice Volume Cycle for the Bering Sea

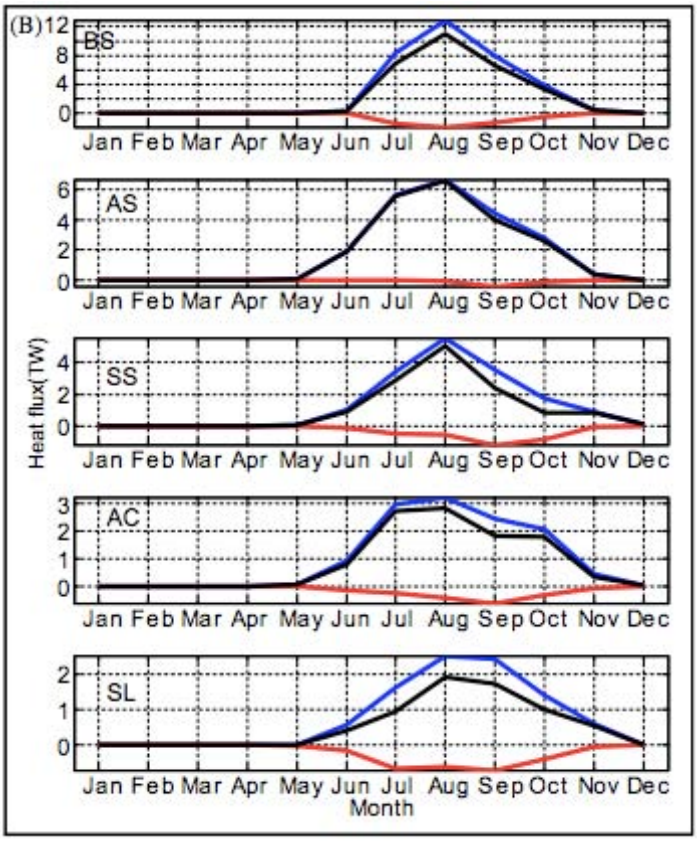

Figure 50. Modeled annual climatological heat fluxes to the North and East (blue), to the South and West (red), and net heat flux (black) through northern Bering Sea sections: BS (Bering Strait), AS (Anadyr Strait), SS (Shpanberg Strait), AC (Anadyr Current), SL (St. Lawrence Island). Monthly means are calculated from a 23-year time series (1979–2001) (From Clement et al. 2005).

Despite the differences in results between this thesis and Francis et al. (2005) and Francis and Hunter (2006), analyzing the atmospheric forcing and sea ice variability parameters from the NPS model is another step toward understanding the science behind the variability of Arctic sea ice and information superiority.

C. DEPARTMENT OF DEFENSE PARTNERSHIPS

Along with scientific advancements the Department of Defense (DoD) is actively working toward optimizing the Air-Sea Battle Concept. The Air-Sea Battle Concept was put in the Quadrennial Defense Review with the intent to foster a close partnership between the Air Force and Navy at the tactical level in order to maximize efficiency and resources (Rolfsen 2010). Since the inception of the Air-Sea Battle Concept in November 2009, logistics, transportation, and engineering needs of the Air Force and Navy have been centralized at Joint Base Charleston (Bowles 2010).

The DoD is engaged in forging strong multinational relations. In November 2009, the highest-ranking U.S. Air Force enlisted leader met with his counterpart in the Canadian Air Force to start an enlisted professional military education partnership (Stump 2009). In February 2010, the United States Air Forces' 5th Air Force initiated an exchange program with Japan Air Self Defense Force with the goal of learning about each others' jobs and cultures (Ramon 2010). In the same month, the Air Education Training Command hosted the Commander of the Royal Netherlands Air Force to discuss training possibilities such as the Euro-Northern Alliance Treaty Organization Joint Jet Pilot Training program with the Dutch and to share training philosophies (Richeson 2010). Partnerships with key Arctic allies like Canada and the Netherlands are critical to any future U.S. endeavors in the Arctic region.

VI. RECOMMENDATIONS FOR FUTURE ARCTIC CLIMATE RESEARCH

Just as the interests of the U.S. require collaboration among all the Uniformed Services, advancement in modeling technologies for the Arctic climate system requires the mutual commitment of both atmospheric and oceanographic research communities. Each brings unique and undoubtedly necessary expertise for successful climate research and prediction.

Recommendations for future Arctic research are in line with the U.S. Navy Arctic Roadmap (Task Force Climate Change 2009), Joint Publication 3–59: Meteorological and Oceanographic Operations (Department of Defense 2008b), and the Air-Sea Battle Concept:

- Improve model representation of Arctic sea ice and oceanic processes to advance predictive skill and predictability in order to better prepare for and address DoD requirements.
- Design and test new parameterizations for fully coupled air-ice-ocean models.
- Incorporate data from advanced technologies such as buoys and autonomous vehicles for model validation studies and real-time operational model data assimilation.

THIS PAGE INTENTIONALLY LEFT BLANK

APPENDIX A: DAY CONVERSION AND LOCATION POSITION

Table 1. Conversion from Julian days to months with near equal number of days. Days with a remainder of 0.4–0.6 days are shared between the preceding and subsequent months.

Year	Month 1	Month 2	Month 3	Month 4	Month 5	Month 6	Month 7	Month 8	Month 9	Month 10	Month 11	Month 12	First Day of Following Year
	1	31.41666667	61.83333333	92.25	122.6666667	153.0833333	183.5	213.9166667	244.3333333	274.75	305.1666667	335.5833333	366
1979	1:31	31:61	62:91	92:122	123:152	153:183	183:213	214:243	244:274	275:304	305:335	335:365	
	366	396.4166667	426.8333333	457.25	487.6666667	518.0833333	548.5	578.9166667	609.3333333	639.75	670.1666667	700.5833333	731
1980	366:396	396:426	427:456	457:487	488:517	518:548	548:578	579:608	609:639	640:669	670:700	700:730	
	731	761.4166667	791.8333333	822.25	852.6666667	883.0833333	913.5	943.9166667	974.3333333	1004.75	1035.166667	1065.583333	1096
1981	731:761	761:791	792:821	822:852	853:882	883:913	913:943	944:973	974:1004	1005:1034	1035:1065	1065:1095	
	1096	1126.416667	1156.833333	1187.25	1217.666667	1248.083333	1278.5	1308.916667	1339.333333	1369.75	1400.166667	1430.583333	1461
1982	1096:1126	1126:1156	1157:1186	1187:1217	1218:1247	1248:1278	1278:1308	1309:1338	1339:1369	1370:1399	1400:1430	1430:1460	
	1461	1491.416667	1521.833333	1552.25	1582.666667	1613.083333	1643.5	1673.916667	1704.333333	1734.75	1765.166667	1795.583333	1826
1983	1461:1491	1491:1521	1522:1551	1552:1582	1583:1612	1613:1643	1643:1673	1674:1703	1704:1734	1735:1764	1765:1795	1795:1825	
	1826	1856.416667	1886.833333	1917.25	1947.666667	1978.083333	2008.5	2038.916667	2069.333333	2099.75	2130.166667	2160.583333	2191
1984	1826:1856	1856:1886	1887:1916	1917:1947	1948:1977	1978:2008	2008:2038	2039:2068	2069:2099	2100:2129	2130:2160	2160:2190	
	2191	2221.416667	2251.833333	2282.25	2312.666667	2343.083333	2373.5	2403.916667	2434.333333	2464.75	2495.166667	2525.583333	2556
1985	2191:2221	2221:2251	2252:2281	2282:2312	2313:2342	2343:2373	2373:2403	2404:2433	2434:2464	2465:2494	2495:2525	2525:2555	
	2556	2586.416667	2616.833333	2647.25	2677.666667	2708.083333	2738.5	2768.916667	2799.333333	2829.75	2860.166667	2890.583333	2921
1986	2556:2586	2586:2616	2617:2646	2547:2677	2678:2707	2708:2738	2738:2768	2769:2798	2799:2829	2830:2859	2860:2890	2890:2920	
	2921	2951.416667	2981.833333	3012.25	3042.666667	3073.083333	3103.5	3133.916667	3164.333333	3194.75	3225.166667	3255.583333	3286
1987	2921:2951	2951:2981	2982:3011	3012:3042	3043:3072	3073:3103	3103:3133	3134:3163	3164:3194	3195:3224	3225:3255	3255:3285	
	3286	3316.416667	3346.833333	3377.25	3407.666667	3438.083333	3468.5	3498.916667	3529.333333	3559.75	3590.166667	3620.583333	3651
1988	3286:3316	3316:2246	3347:3376	3377:3407	3408:3437	3438:3468	3468:3498	3499:3528	3529:3559	3560:3589	3590:3620	3620:2650	
	3651	3681.416667	3711.833333	3742.25	3772.666667	3803.083333	3833.5	3863.916667	3894.333333	3924.75	3955.166667	3985.583333	4016
1989	3651:3681	3681:3711	3712:3741	3742:3772	3773:3802	3803:3833	3833:3863	3864:3893	3894:3924	3925:3954	3955:3985	3985:4015	
	4016	4046.416667	4076.833333	4107.25	4137.666667	4168.083333	4198.5	4228.916667	4259.333333	4289.75	4320.166667	4350.583333	4381
1990	4016:4046	4046:4076	4077:4106	4107:4137	4138:4167	4168:4198	4198:4228	4229:4258	4259:4289	4290:4319	4320:4350	4350:4381	
	4381	4411.416667	4441.833333	4472.25	4502.666667	4533.083333	4563.5	4593.916667	4624.333333	4654.75	4685.166667	4715.583333	4746
1991	4381:4411	4411:4441	4442:4471	4472:4502	4503:4532	4533:4563	4563:4593	4594:4623	4624:4654	4655:4684	4685:4715	4715:4746	
	4746	4776.416667	4806.833333	4837.25	4867.666667	4898.083333	4928.5	4958.916667	4989.333333	5019.75	5050.166667	5080.583333	5111
1992	4746:4776	4776:4806	4807:4836	4837:4867	4868:4897	4898:4928	4828:4958	4959:4988	4989:5019	5020:5049	5050:5080	5080:5110	
	5111	5141.416667	5171.833333	5202.25	5232.666667	5263.083333	5293.5	5323.916667	5354.333333	5384.75	5415.166667	5445.583333	5476
1993	5111:5141	5141:5171	5171:5201	5202:5232	5233:5262	5263:5293	5293:5323	5324:5353	5354:5384	5385:5414	5415:5445	5445:5475	
	5476	5506.416667	5536.833333	5567.25	5597.666667	5628.083333	5658.5	5688.916667	5719.333333	5749.75	5780.166667	5810.583333	5841
1994	5476:5506	5506:5536	5537:5566	5567:5597	5598:5627	5628:5658	5658:5688	5689:5718	5719:5749	5750:5779	5780:5810	5810:5840	
	5841	5871.416667	5901.833333	5932.25	5962.666667	5993.083333	6023.5	6053.916667	6084.333333	6114.75	6145.166667	6175.583333	6206
1995	5841:5871	5871:5901	5902:5931	5932:5962	5963:5992	5993:6023	6023:6053	6054:6083	6084:6114	6115:6144	6145:6175	6175:6205	
	6206	6236.416667	6266.833333	6297.25	6327.666667	6358.083333	6388.5	6418.916667	6449.333333	6479.75	6510.166667	6540.583333	6571
1996	6206:6236	6236:6266	6267:6296	6297:6327	6328:6357	6358:6388	6388:6418	6419:6448	6449:6479	6480:6509	6510:6540	6540:6570	
	6571	6601.416667	6631.833333	6662.25	6692.666667	6723.083333	6753.5	6783.916667	6814.333333	6844.75	6875.166667	6905.583333	6936
1997	6571:6601	6601:6631	6632:6661	6662:6692	6693:6722	6723:6753	6753:6783	6784:6813	6814:6844	6845:6874	6875:6905	6905:6936	
	6936	6966.416667	6996.833333	7027.25	7057.666667	7088.083333	7118.5	7148.916667	7179.333333	7209.75	7240.166667	7270.583333	7301
1998	6936:6966	6966:6996	6997:7026	7027:7057	7058:7087	7088:7118	7118:7148	7149:7178	7179:7209	7210:7239	7240:7270	7270:7300	
	7301	7331.416667	7361.833333	7392.25	7422.666667	7453.083333	7483.5	7513.916667	7544.333333	7574.75	7605.166667	7635.583333	7666
1999	7301:7331	7331:7361	7362:7391	7392:7422	7423:7452	7453:7483	7483:7513	7514:7543	7544:7574	7575:7604	7605:7635	7635:7665	
	7666	7696.416667	7726.833333	7757.25	7787.666667	7818.083333	7848.5	7878.916667	7909.333333	7939.75	7970.166667	8000.583333	8031
2000	7666:7696	7696:7726	7727:7756	7757:7787	7788:7817	7818:7848	7848:7878	7879:7908	7909:7939	7940:7969	7970:8000	8000:8030	
	8031	8061.416667	8091.833333	8122.25	8152.666667	8183.083333	8213.5	8243.916667	8274.333333	8304.75	8335.166667	8365.583333	8396
2001	8031:8061	8061:8091	8092:8121	8122:8152	8153:8182	8183:8213	8213:8243	8244:8273	8274:8304	8305:8334	8335:8365	8365:8395	
	8396	8426.416667	8456.833333	8487.25	8517.666667	8548.083333	8578.5	8608.916667	8639.333333	8669.75	8700.166667	8730.583333	8761
2002	8396:8426	8426:8456	8457:8486	8487:8517	8518:8547	8548:8578	8578:8608	8609:8638	8639:8669	8670:8669	8700:8730	8730:8760	
	8761	8791.416667	8821.833333	8852.25	8882.666667	8913.083333	8943.5	8973.916667	9004.333333	9034.75	9065.166667	9095.583333	9126
2003	8761:8791	8791:8821	8822:8851	8852:8882	8883:8912	8913:8943	8943:8973	8974:9003	9004:9034	9035:9064	9065:9095	9095:9125	
	9126	9156.416667	9186.833333	9217.25	9247.666667	9278.083333	9308.5	9338.916667	9369.333333	9399.75	9430.166667	9460.583333	9491
2004	9126:9156	9156:9186	9187:9216	9217:9247	9248:9277	9278:9308	9308:9338	9339:9368	9369:9399	9400:9429	9430:9460	9460:9490	

Table 2. Latitude, longitude, and NPS Model grid points of all locations of interest within the Central Arctic, the Northwest Passage and the Northern Sea Route.

				Latitude, Longitude and NPS Model Grid Points of Each Location in the Central Arctic, Northwest Passage, and Northern Sea Route												
				Latitude (y) and Longitude (x)								NPS Model Grid Points X		NPS Model Grid Points Y		# of non-land grid cells
		Locations of Interest	Abbrev.	x-left	y-top	x-left	y-bottom	x-right	y-top	x-right	y-bottom	left	right	bottom	top	
	1	**Central Arctic**														
1	1-1	Barents Sea	SBRNT	49.13	76.50	35.25	82.34	27.57	73.51	8.71	77.82	775	851	491	567	5295
2	1-2	Kara Sea	SKARA	88.86	74.99	103.88	80.50	63.93	76.16	62.19	82.48	658	734	502	578	5575
3	1-3	Laptev Sea	SLPTV	117.78	71.54	136.68	74.63	101.58	75.96	124.10	80.38	554	630	473	549	4661
4	1-4	E. Siberian Sea	SESBN	149.46	71.71	169.17	71.34	146.01	77.98	175.76	77.43	510	586	361	437	5861
5	1-5	Chukchi Sea	SCHKI	176.16	71.62	192.29	68.60	186.12	77.38	205.24	73.28	521	597	260	336	5873
6	1-6	Beaufort Sea	SBFRT	206.43	71.95	216.41	66.71	225.63	75.16	231.69	69.10	590	666	169	245	4178
7	1-7	North Pole	ONPLE	100.62	85.75	205.54	86.28	17.78	84.75	300.12	85.17	699	775	378	454	5929
8	1-8	Canadian Arctic Archipelago	OCAAW	226.64	83.46	236.17	77.31	280.05	82.56	264.43	76.82	702	778	262	338	5307
9	1-9	Svalbard	TSVBD	37.34	81.83	17.10	84.80	17.56	79.20	358.91	81.22	775	825	453	498	2250
	2	**Northwest Passage**														
5	*1-5*	*(Chukchi Sea)*														
6	*1-6*	*(Beaufort Sea)*														
10	2-1	Cape Bathurst Polyna	PCPBH	231.65	71.51	232.83	69.89	236.24	71.82	237.05	70.18	673	691	177	197	386
11	2-2	Amundsen Gulf	NADMG	237.76	71.39	238.47	69.66	242.89	71.56	243.16	69.81	696	716	170	191	421
12	2-3	Coronation Gulf	NCRNG	245.11	68.58	245.14	67.66	252.66	68.44	252.39	67.53	724	758	144	155	338
13	2-4	Queen Maud Gulf	NQMDG	255.61	69.04	255.14	67.97	262.19	68.48	261.42	67.44	770	800	151	164	359
14	2-5	Lancaster Sound	NLSTR	276.2	77.08	266.38	71.33	278.69	76.73	268.27	71.09	806	814	202	278	522
15	2-6	North Water Polyna	PNWTR	286.93	77.54	283.22	76.50	291.50	76.56	287.72	75.60	826	843	283	299	289
16	2-7	Baffin Bay	NBFNB	301.28	75.81	284.98	71.45	309.67	71.78	294.57	68.21	868	924	239	315	2065
17	2-8	Davis Strait	CDVST	303.33	69.31	294.03	66.57	308.55	65.77	299.92	63.40	937	986	224	278	2379
	3	**Northern Sea Route**														
18	3-1	Bering Sea	NBRGS	175.62	56.74	185.18	54.11	180.07	62.62	190.99	59.48	352	428	202	278	5929
5	*1-5*	*(Chukchi Sea)*														
19	3-2	Inner E. Siberian Sea	RIESS	158.75	69.14	171.00	68.43	159.14	71.72	173.01	70.92	478	509	345	400	1250
20	3-3	New Siberian Islands	RNSBI	138.7	70.10	151.24	70.93	129.91	76.55	148.53	77.81	500	583	431	483	2844
3	*1-3*	*(Laptev Sea)*														
21	3-4	Severnaya Zemlaya	TSVZM	86.4	75.42	120.20	83.73	59.05	76.23	41.56	85.97	667	748	456	576	9687
22	3-5	Inner Kara Sea	RIKAR	81.21	70.31	85.82	74.76	56.29	70.72	53.22	75.30	666	767	584	640	4289
23	3-6	Inner Barents Sea	RIBRS	55.98	66.05	52.79	71.77	43.54	64.48	37.22	69.75	778	845	625	695	2737
24	3-7	White Sea	RWHTS	40.86	64.50	36.95	67.69	36.14	63.38	31.80	66.42	858	887	646	689	646

Note 1: The four polar stereographic points are the corner points, which make up the rectangular area of each of the Locations of Interest. The Edge Coordinates corresponds to the specific NPS model domain grid point.

Note 2: Longitudinal coordinates (x-left and x-right) start with 0° at the Prime Meridian and rotate positively east to west.

APPENDIX B: ANOMALOUS SEA ICE VARIABILITY IN THE CENTRAL ARCTIC (1979–2004)

A. ANOMALOUS SEA ICE VOLUME VARIABILITY

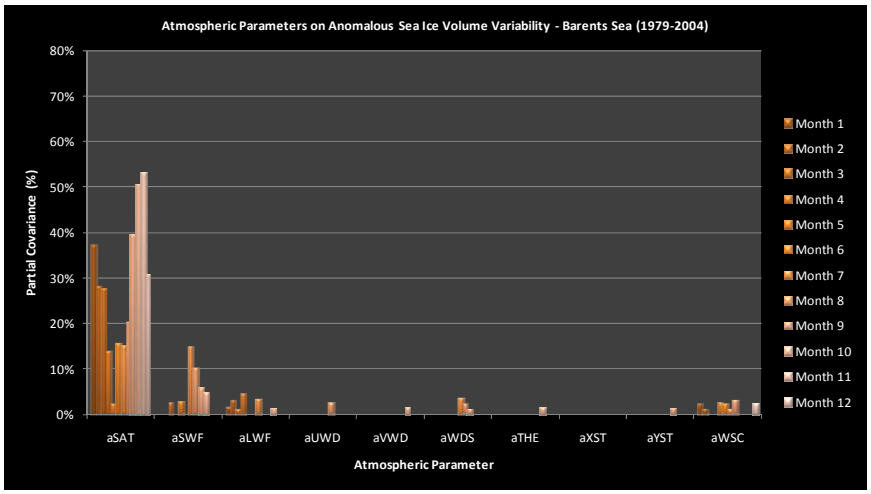

Figure 51. Anomalous Sea Ice Volume Variability—Barents Sea (1979-2004)

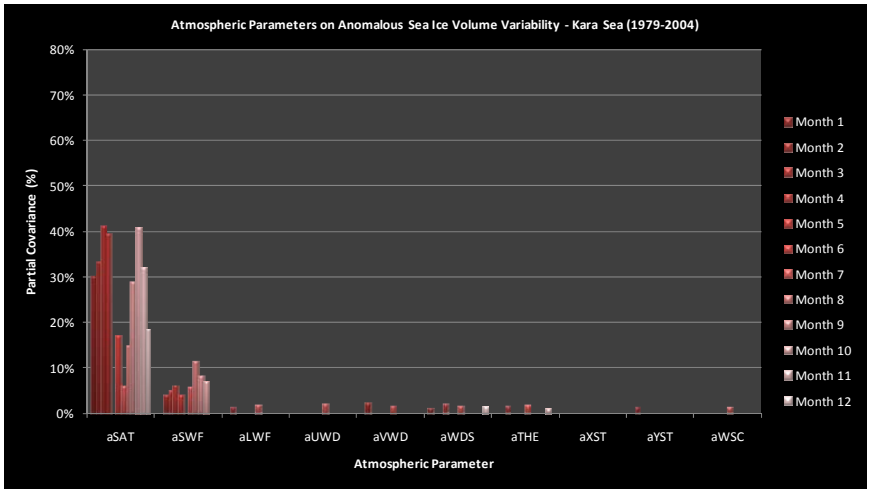

Figure 52. Anomalous Sea Ice Volume Variability—Kara Sea (1979-2004)

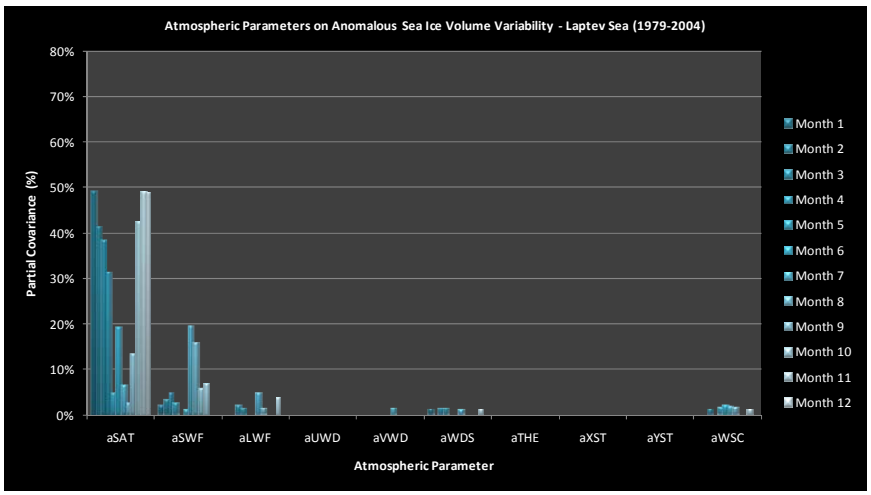

Figure 53. Anomalous Sea Ice Volume Variability—Laptev Sea (1979-2004)

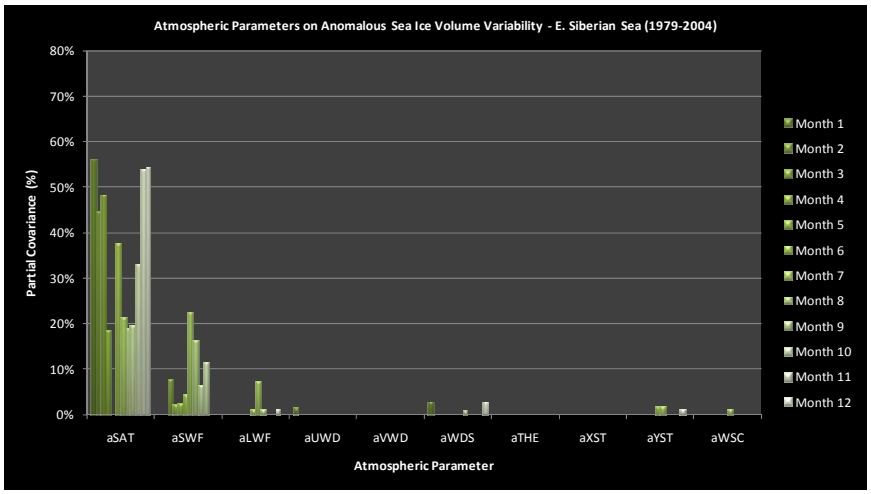

Figure 54. Anomalous Sea Ice Volume Variability—E. Siberian Sea (1979-2004)

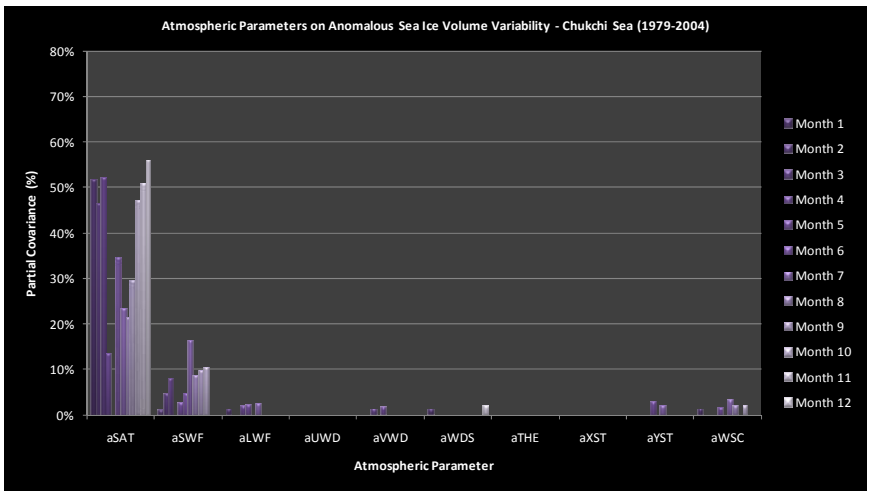

Figure 55. Anomalous Sea Ice Volume Variability—Chukchi Sea (1979-2004)

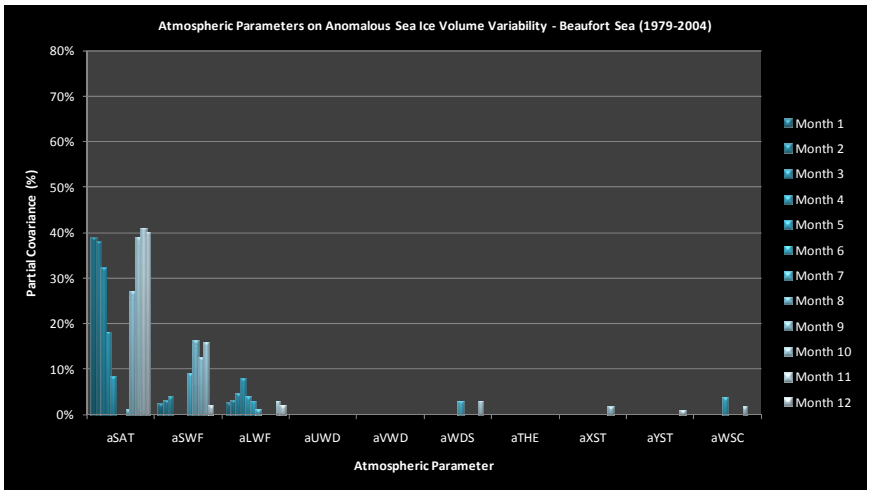

Figure 56. Anomalous Sea Ice Volume Variability—Beaufort Sea (1979-2004) (same as Figure 26)

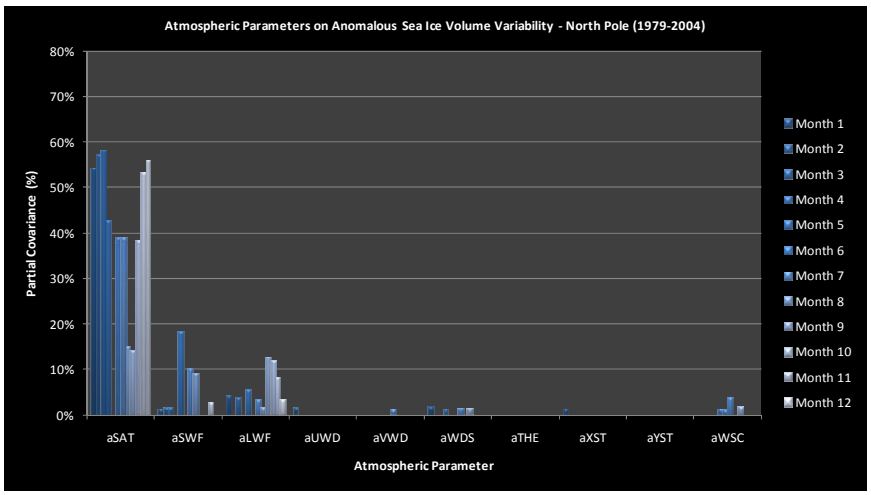

Figure 57. Anomalous Sea Ice Volume Variability—North Pole (1979-2004)

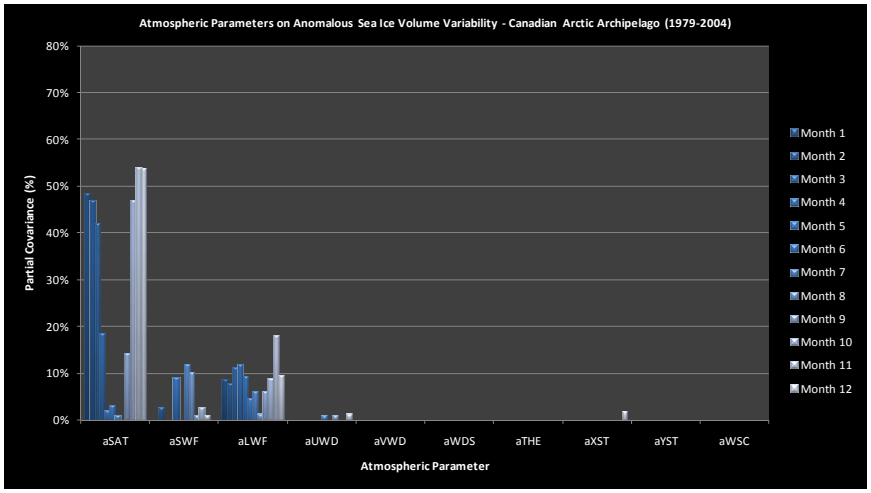

Figure 58. Anomalous Sea Ice Volume Variability—Canadian Arctic Archipelago (1979-2004)

B. ANOMALOUS SEA ICE THICKNESS VARIABILITY

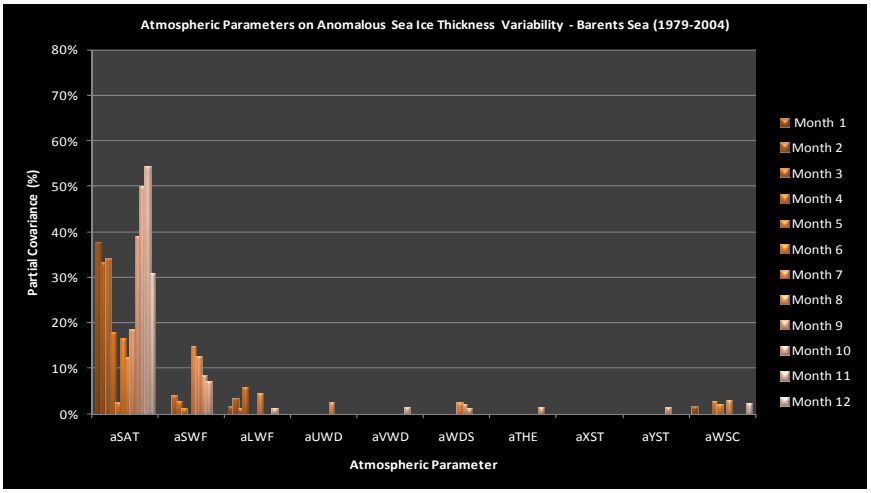

Figure 59. Anomalous Sea Ice Thickness Variability—Barents Sea (1979-2004)

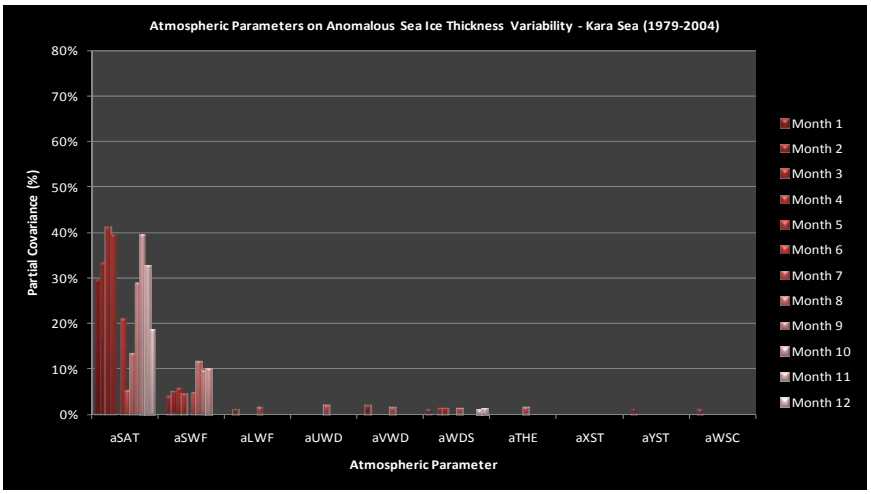

Figure 60. Anomalous Sea Ice Thickness Variability—Kara Sea (1979-2004)

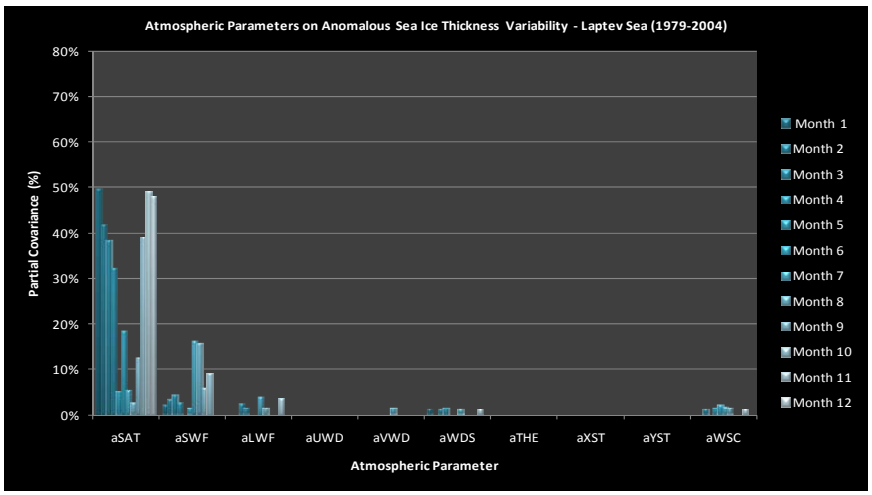

Figure 61. Anomalous Sea Ice Thickness Variability—Laptev Sea (1979-2004)

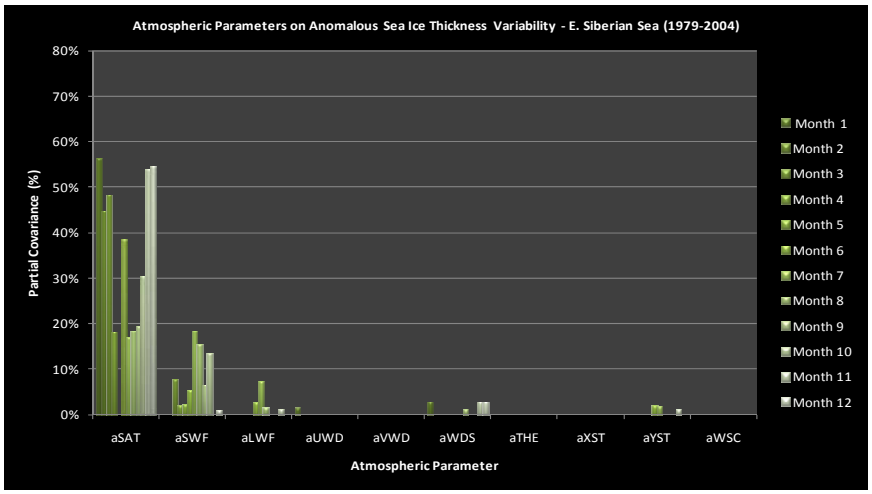

Figure 62. Anomalous Sea Ice Thickness Variability—E. Siberian Sea (1979-2004)

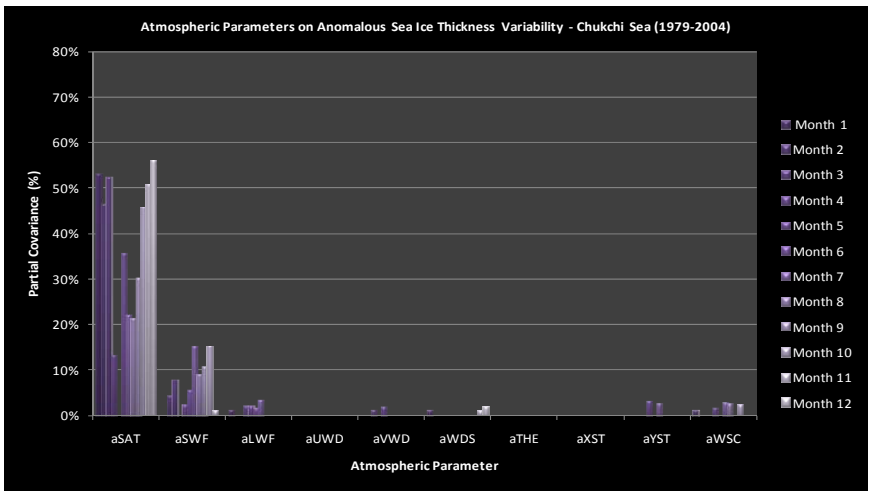

Figure 63. Anomalous Sea Ice Thickness Variability—Chukchi Sea (1979-2004)

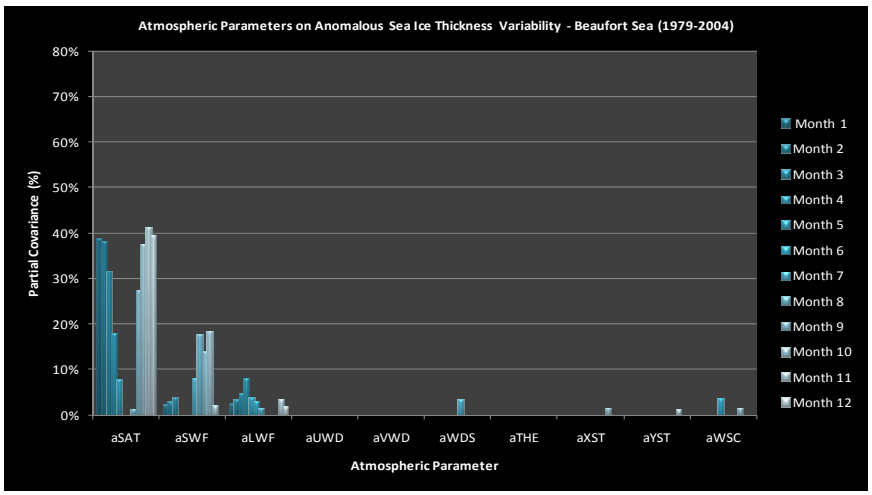

Figure 64. Anomalous Sea Ice Thickness Variability—Beaufort Sea (1979-2004) (same as Figure 27)

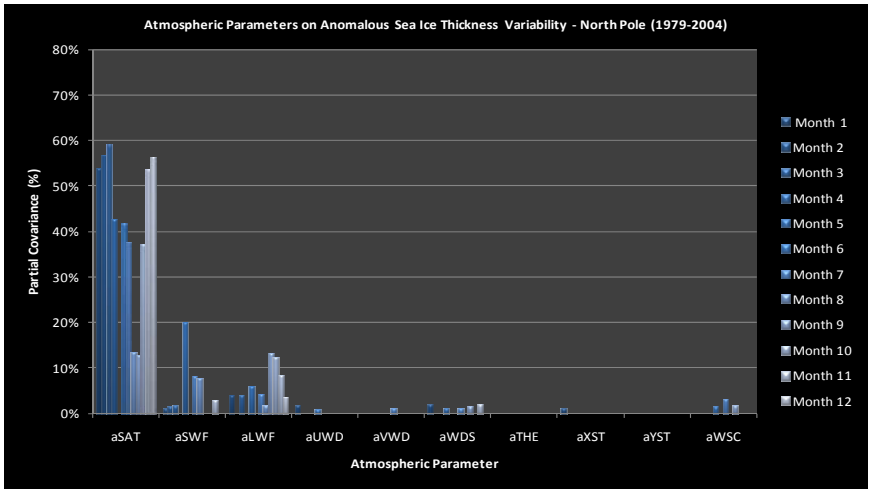

Figure 65. Anomalous Sea Ice Thickness Variability—North Pole (1979-2004)

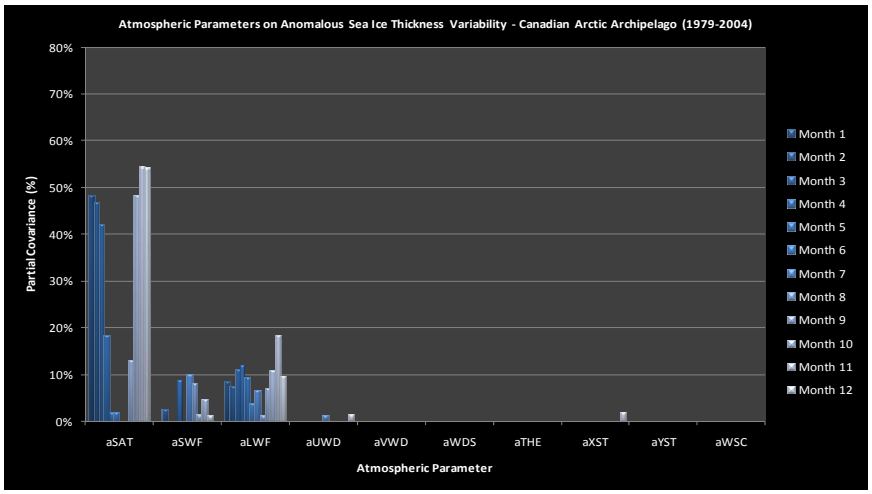

Figure 66. Anomalous Sea Ice Thickness Variability—Canadian Arctic Archipelago (1979-2004)

C. ANOMALOUS SEA ICE AREA VARIABILITY

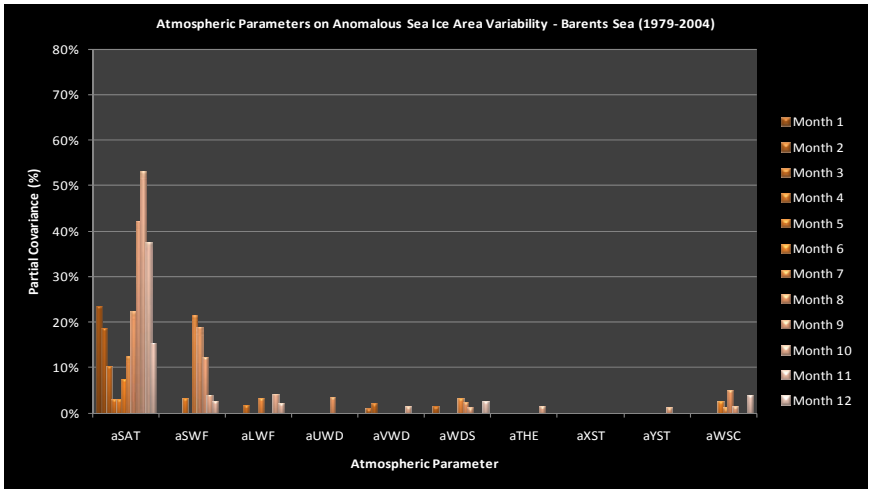

Figure 67. Anomalous Sea Ice Area Variability—Barents Sea (1979-2004)

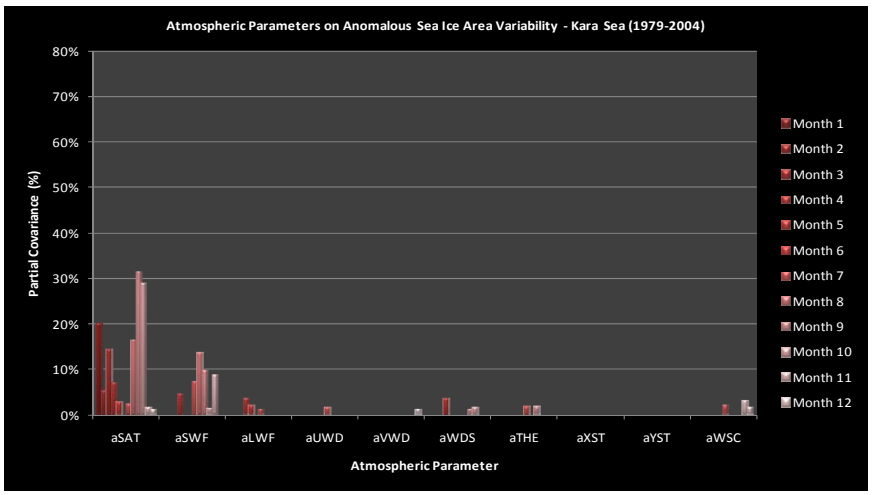

Figure 68. Anomalous Sea Ice Area Variability—Kara Sea (1979-2004)

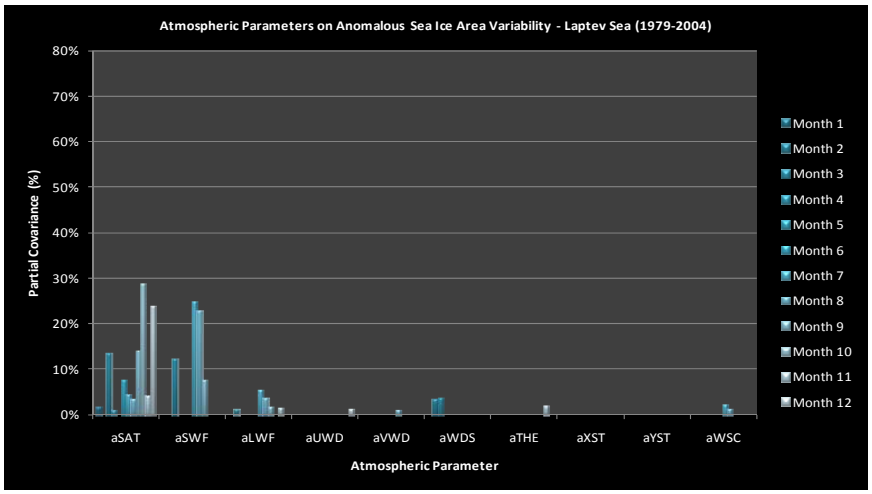

Figure 69. Anomalous Sea Ice Area Variability—Laptev Sea (1979-2004)

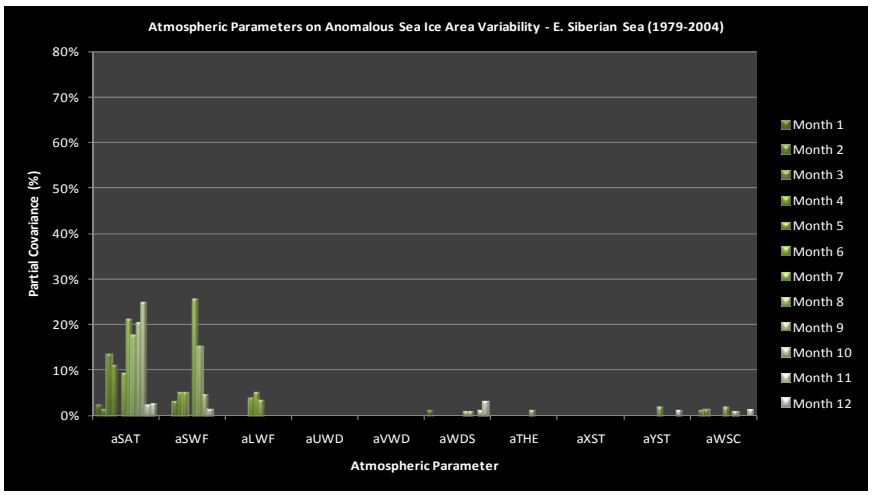

Figure 70. Anomalous Sea Ice Area Variability—E. Siberian Sea (1979-2004)

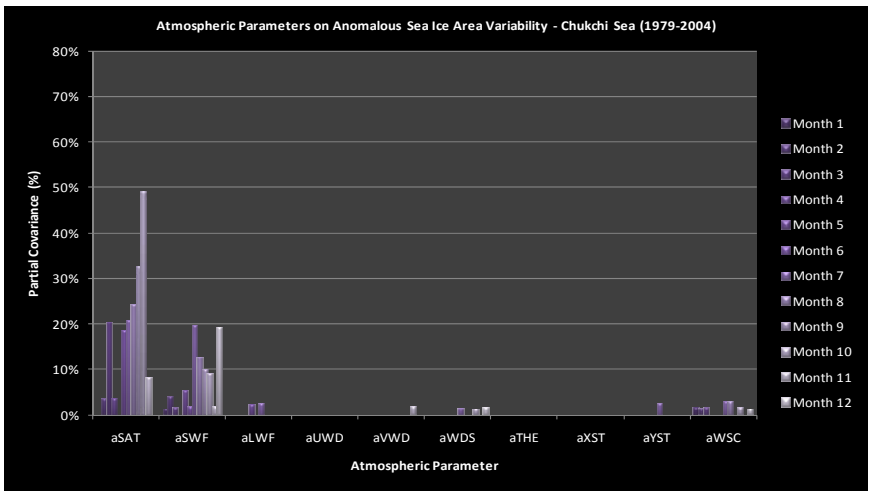

Figure 71. Anomalous Sea Ice Area Variability—Chukchi Sea (1979-2004)

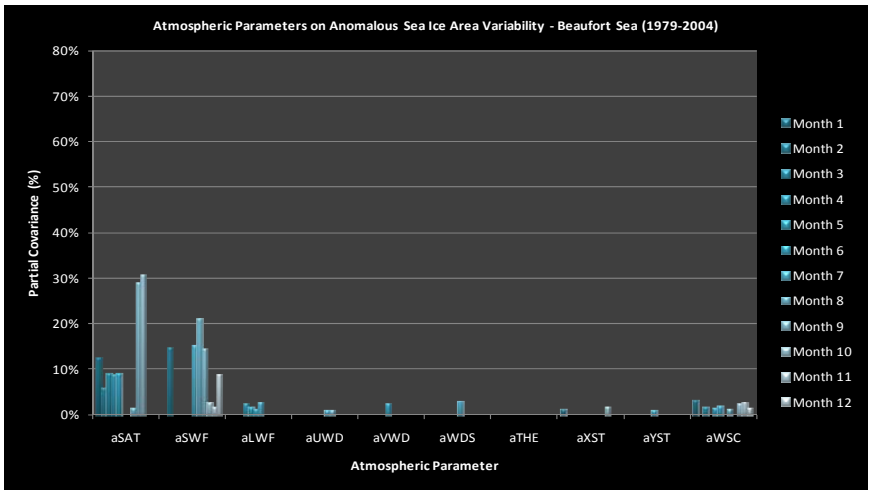

Figure 72. Anomalous Sea Ice Area Variability—Beaufort Sea (1979-2004) (same as Figure 28)

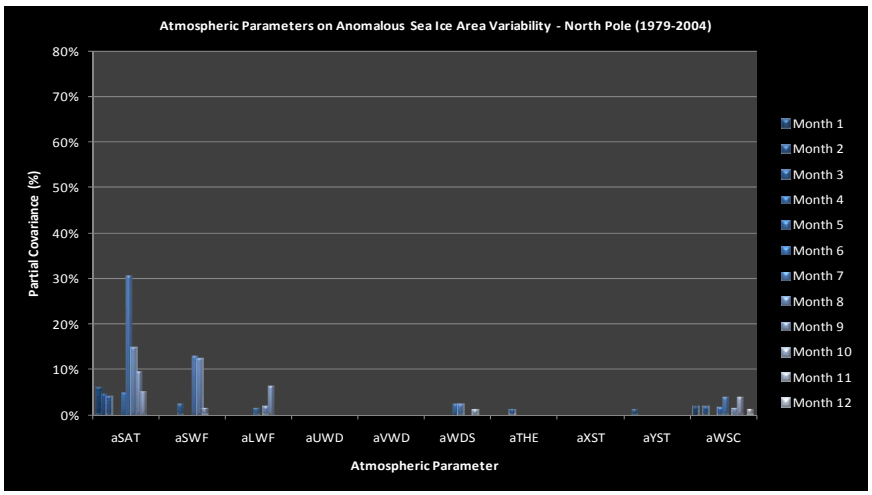

Figure 73. Anomalous Sea Ice Area Variability—North Pole (1979-2004)

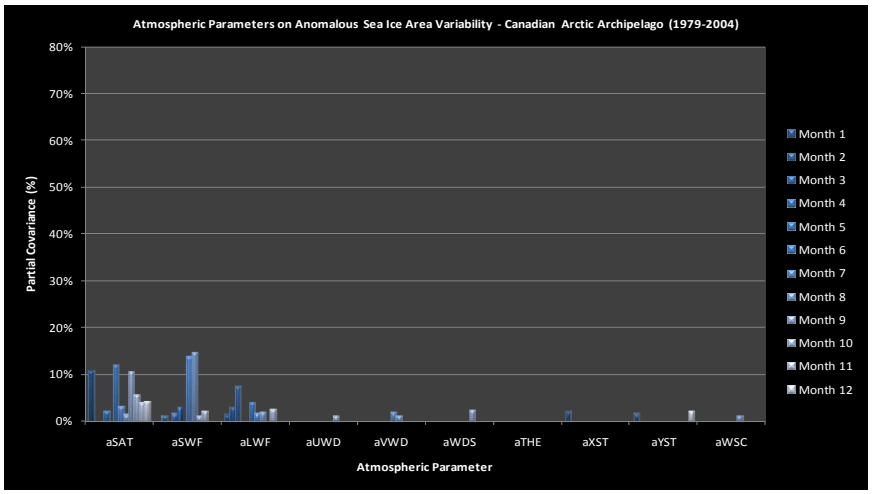

Figure 74. Anomalous Sea Ice Area Variability—Canadian Arctic Archipelago (1979-2004)

THIS PAGE INTENTIONALLY LEFT BLANK

APPENDIX C: ANOMALOUS SEA ICE VARIABILITY IN THE CENTRAL ARCTIC (1979–1991)

A. ANOMALOUS SEA ICE VOLUME VARIABILITY

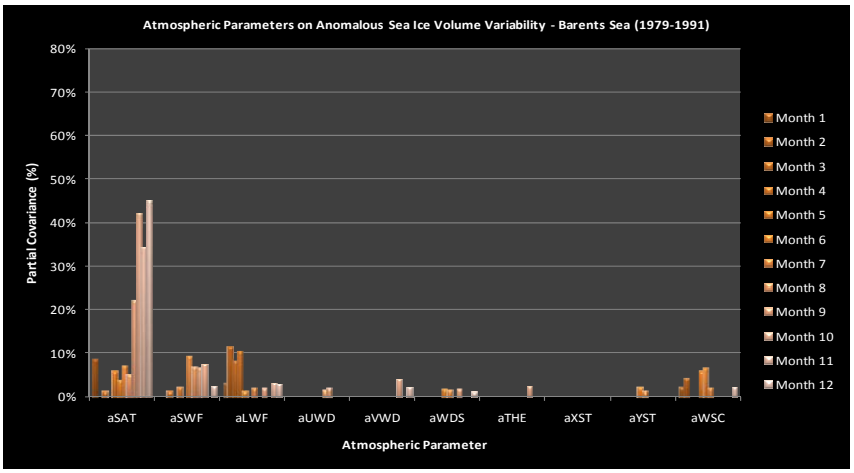

Figure 75. Anomalous Sea Ice Volume Variability—Barents Sea (1979-1991)

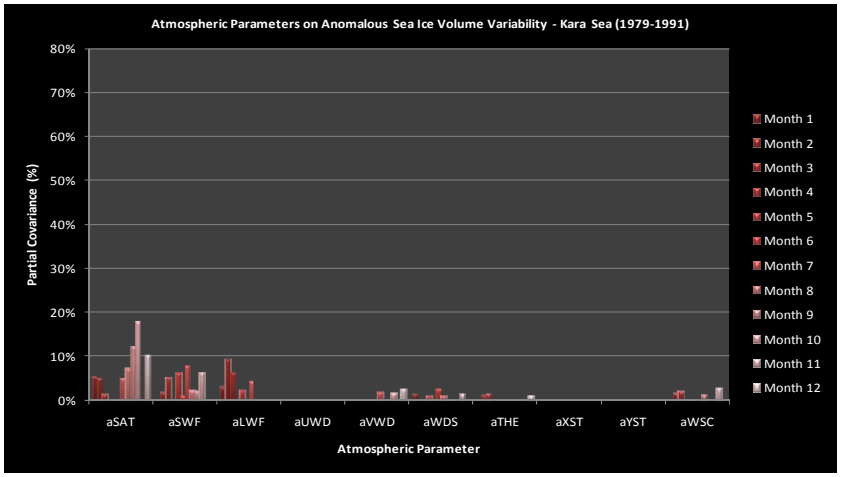

Figure 76. Anomalous Sea Ice Volume Variability—Kara Sea (1979-1991)

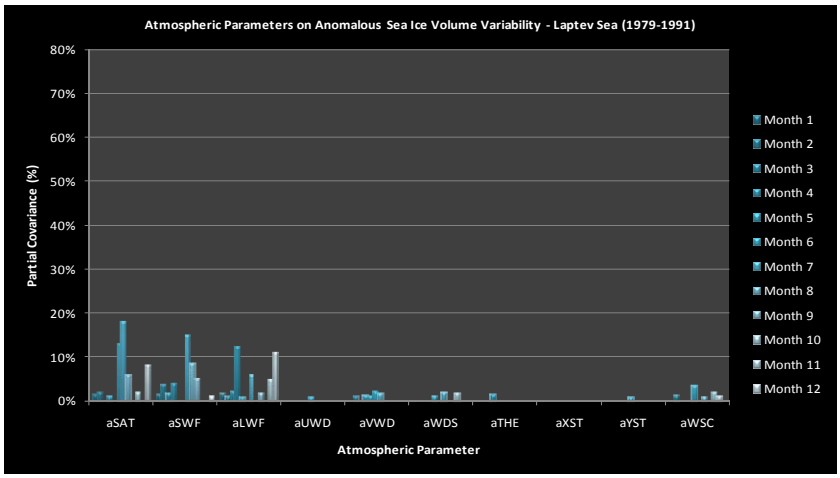

Figure 77. Anomalous Sea Ice Volume Variability—Laptev Sea (1979–1991)

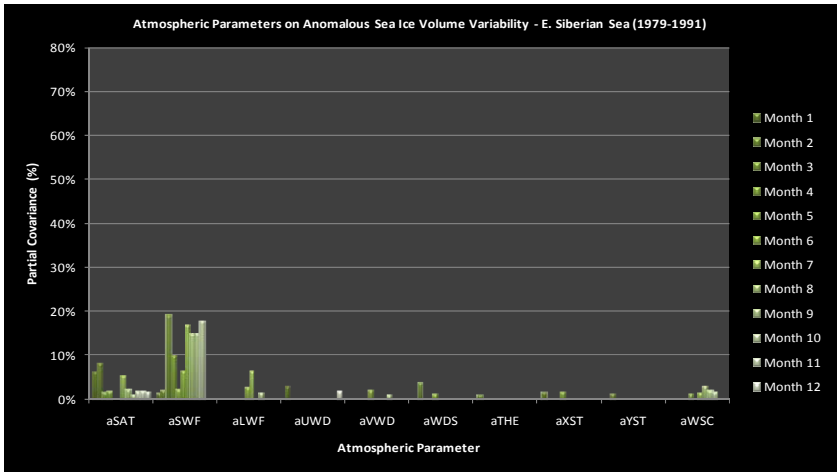

Figure 78. Anomalous Sea Ice Volume Variability—E. Siberian Sea (1979–1991)

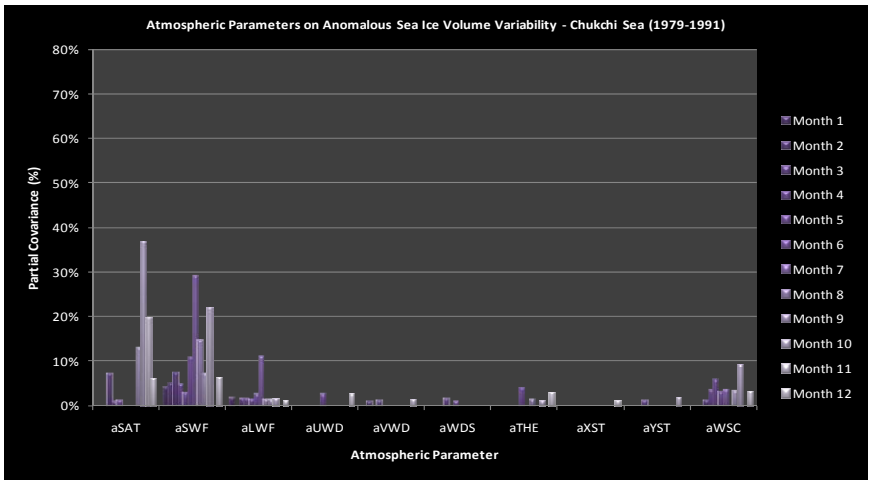

Figure 79. Anomalous Sea Ice Volume Variability—Chukchi Sea (1979–1991)

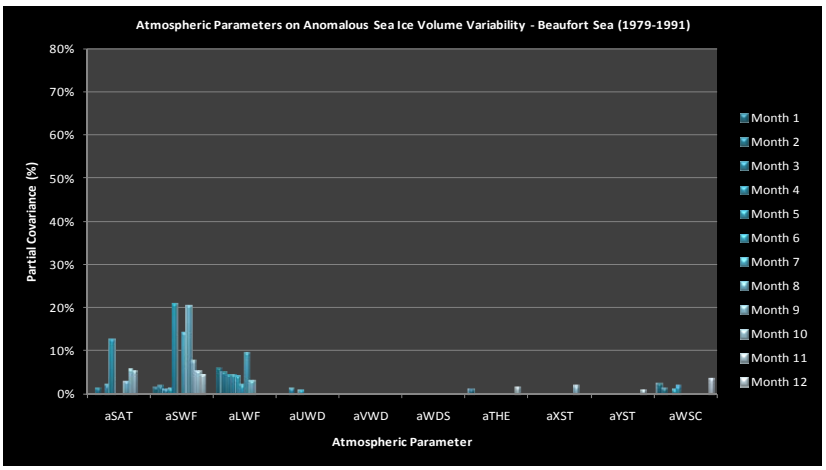

Figure 80. Anomalous Sea Ice Volume Variability—Beaufort Sea (1979-1991)

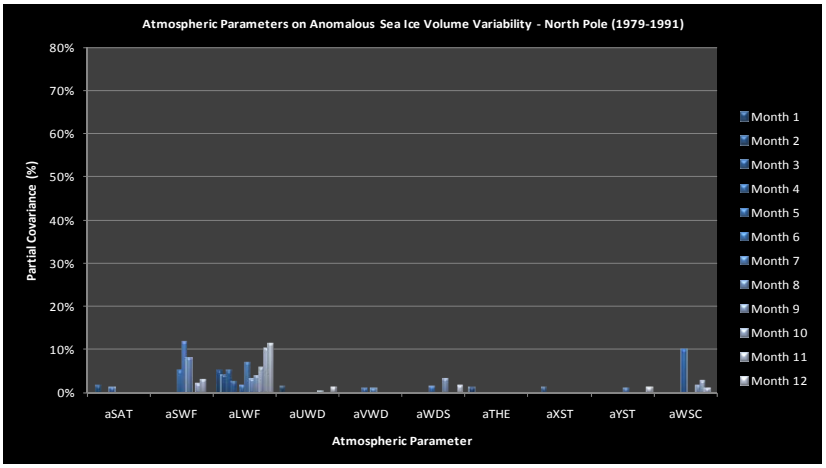

Figure 81. Anomalous Sea Ice Volume Variability—North Pole (1979-1991) (same as Figure 29)

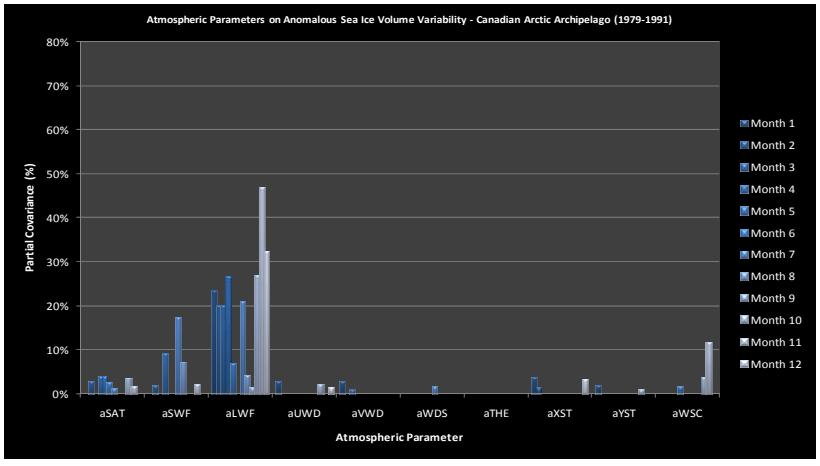

Figure 82. Anomalous Sea Ice Volume Variability—Canadian Arctic Archipelago (1979-1991) (same as Figure 30)

B. ANOMALOUS SEA ICE THICKNESS VARIABILITY

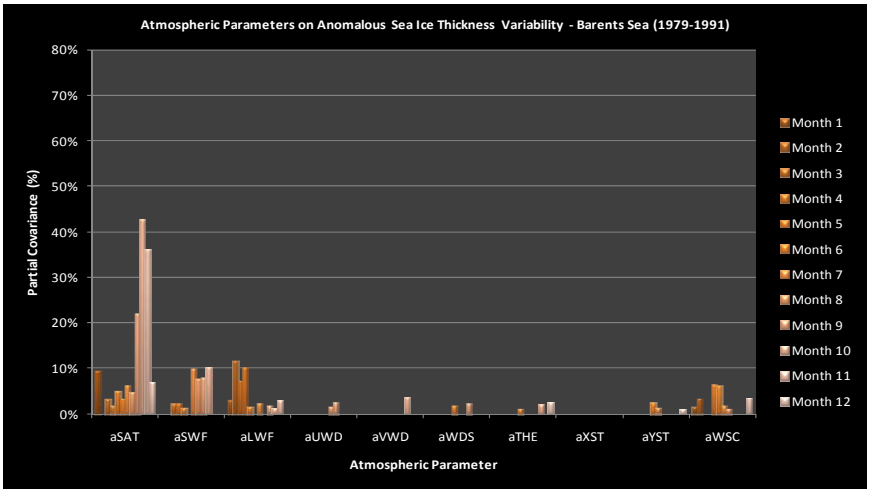

Figure 83. Anomalous Sea Ice Thickness Variability—Barents Sea (1979-1991)

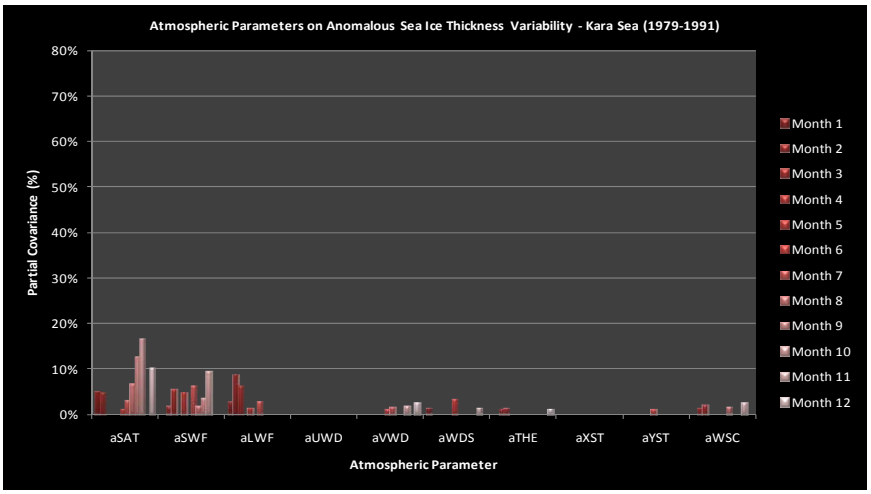

Figure 84. Anomalous Sea Ice Thickness Variability—Kara Sea (1979-1991)

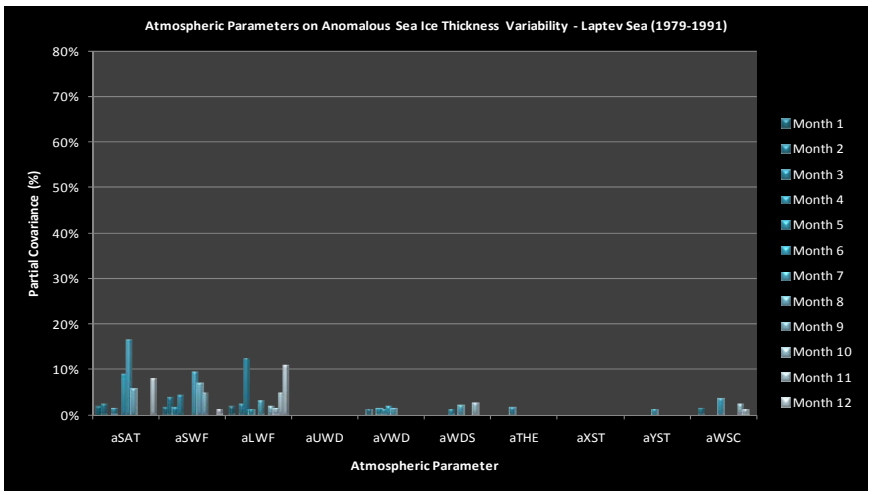

Figure 85. Anomalous Sea Ice Thickness Variability—Laptev Sea (1979-1991)

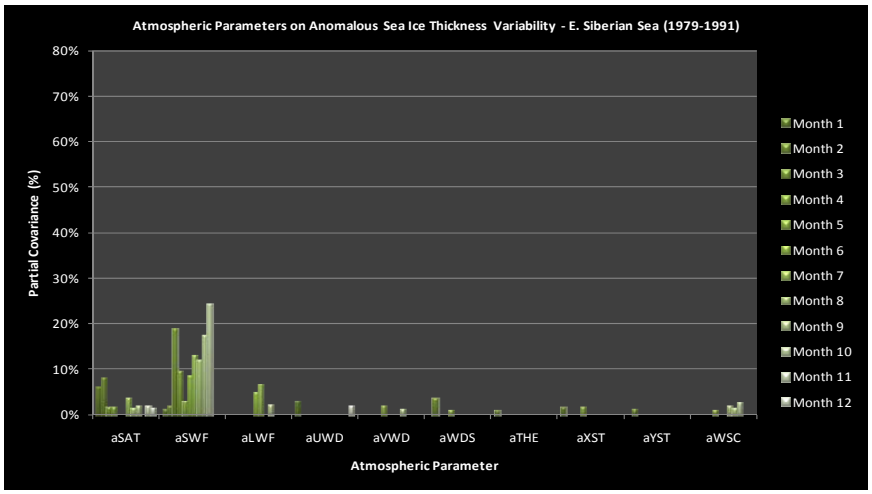

Figure 86. Anomalous Sea Ice Thickness Variability—E. Siberian Sea (1979-1991)

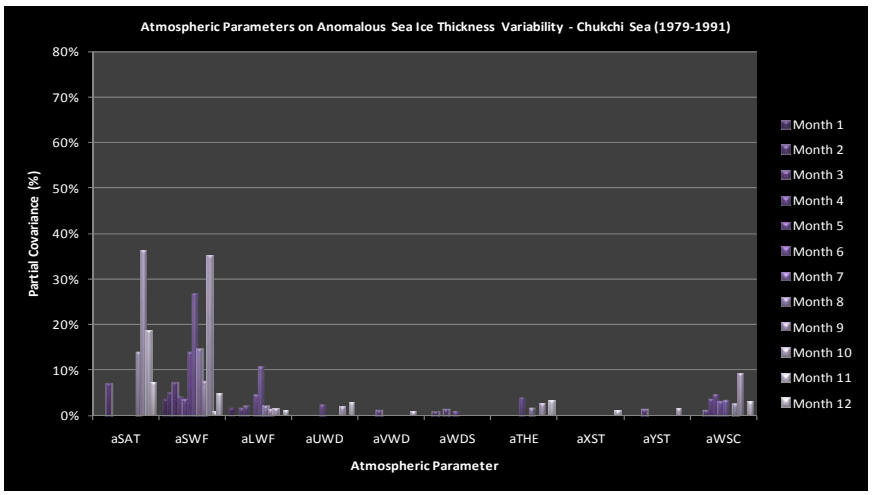

Figure 87. Anomalous Sea Ice Thickness Variability—Chukchi Sea (1979-1991)

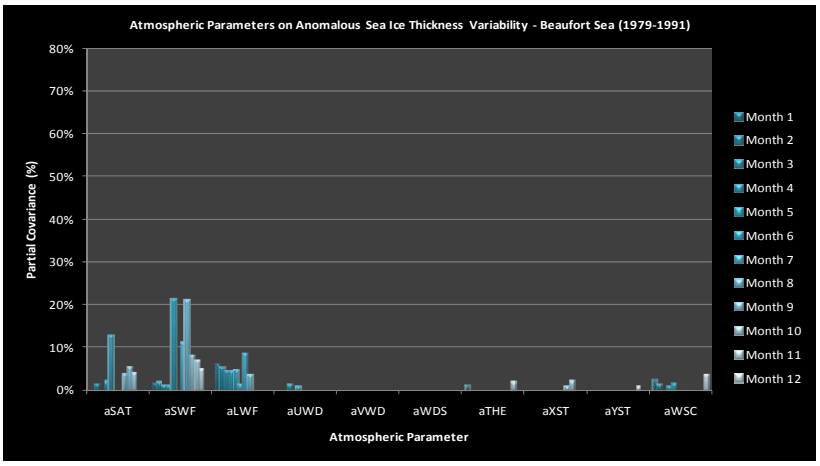

Figure 88. Anomalous Sea Ice Thickness Variability—Beaufort Sea (1979-1991)

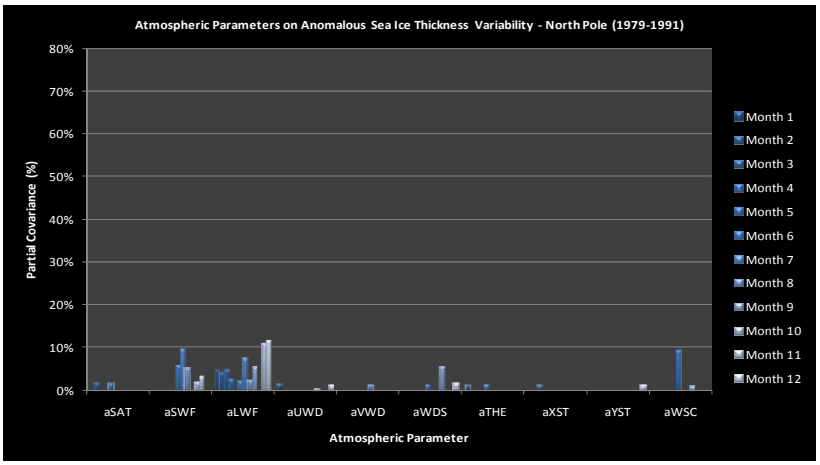

Figure 89. Anomalous Sea Ice Thickness Variability—North Pole (1979-1991) (same as Figure 31)

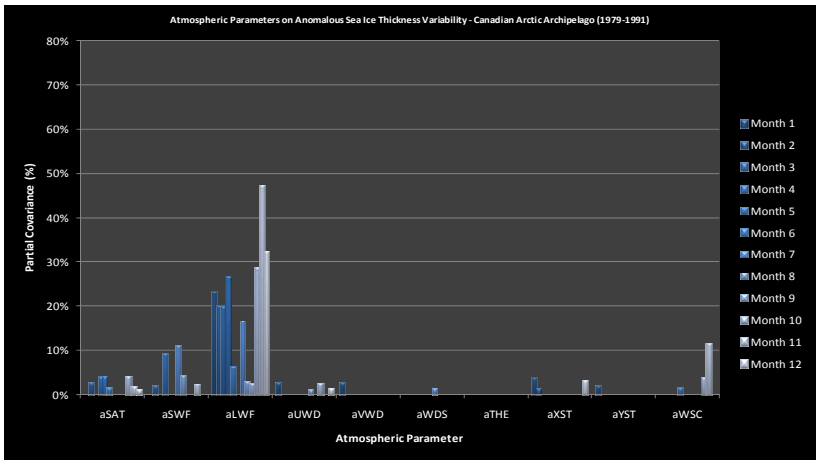

Figure 90. Anomalous Sea Ice Thickness Variability—Canadian Arctic Archipelago (1979-1991) (same as Figure 32)

C. ANOMALOUS SEA ICE AREA VARIABILITY

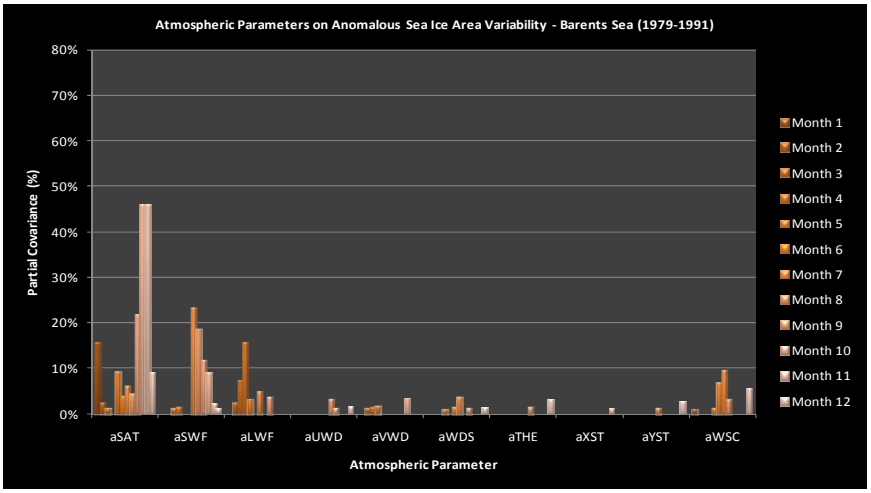

Figure 91. Anomalous Sea Ice Area Variability—Barents Sea (1979-1991)

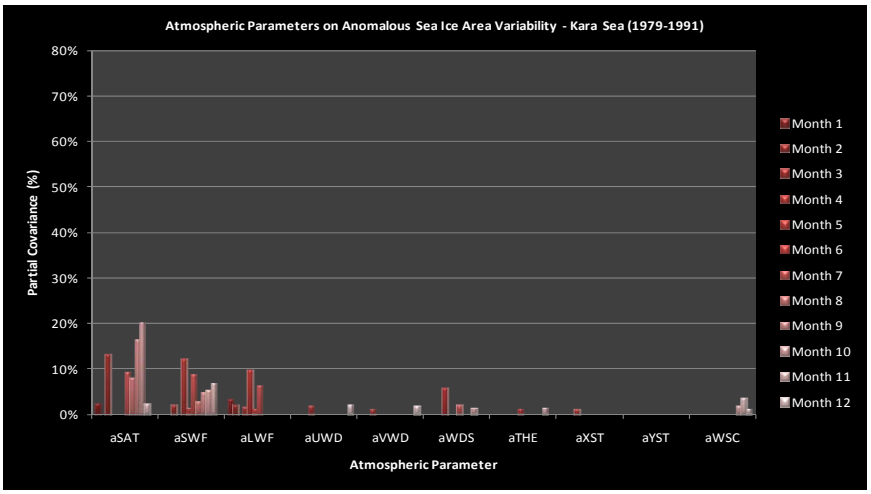

Figure 92. Anomalous Sea Ice Area Variability—Kara Sea (1979-1991)

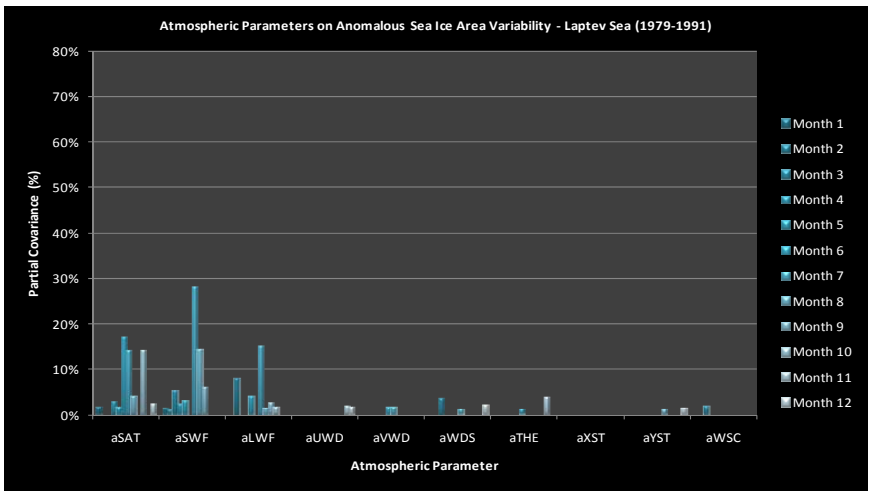

Figure 93. Anomalous Sea Ice Area Variability—Laptev Sea (1979-1991)

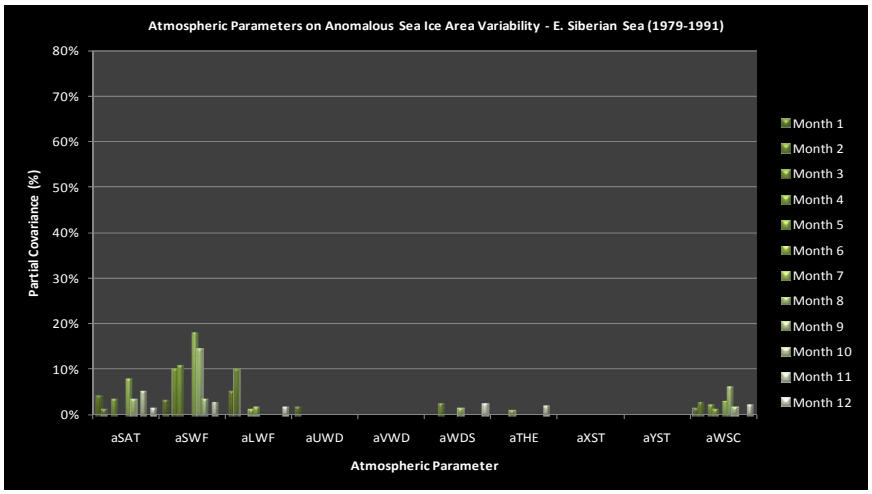

Figure 94. Anomalous Sea Ice Area Variability—E. Siberian Sea (1979-1991)

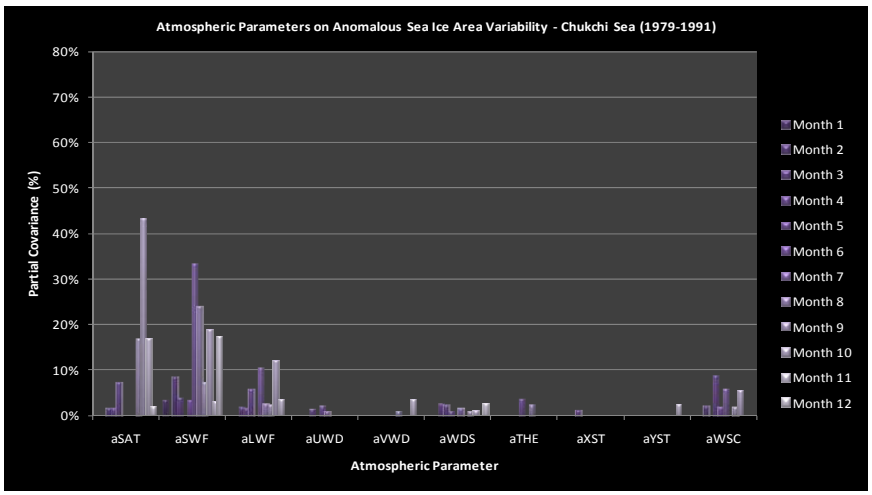

Figure 95. Anomalous Sea Ice Area Variability—Chukchi Sea (1979-1991)

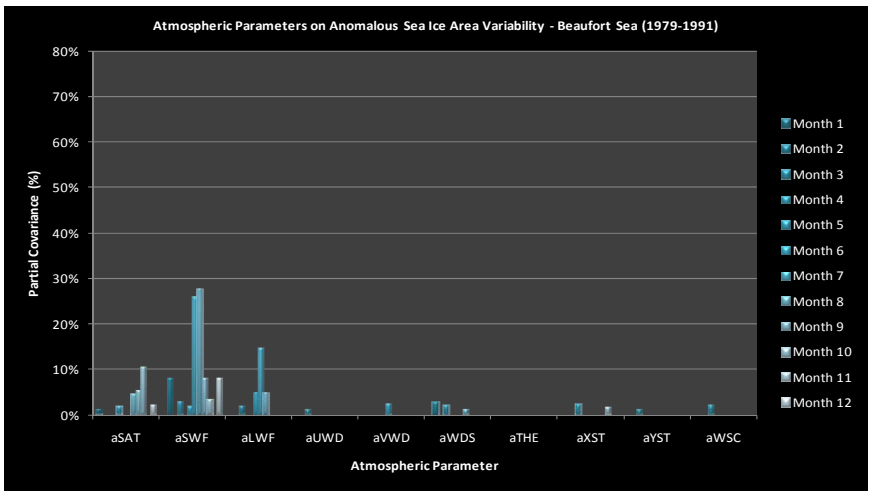

Figure 96. Anomalous Sea Ice Area Variability—Beaufort Sea (1979-1991)

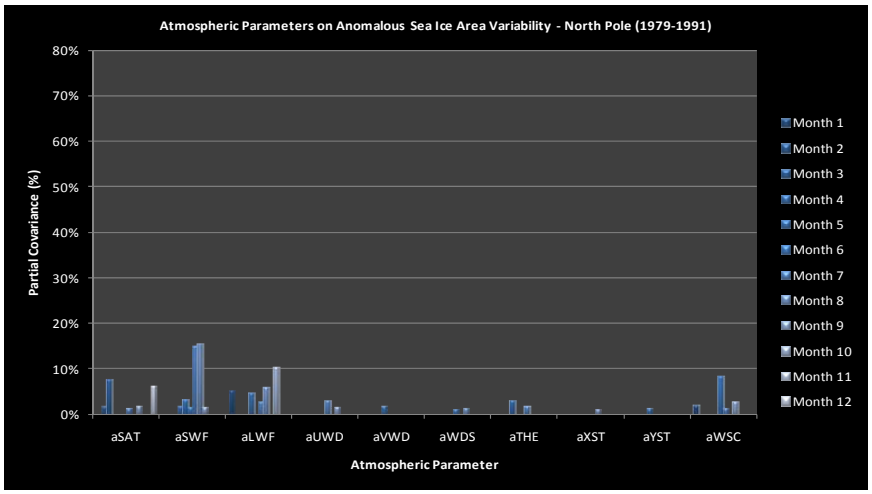

Figure 97. Anomalous Sea Ice Area Variability—North Pole (1979-1991) (same as Figure 33)

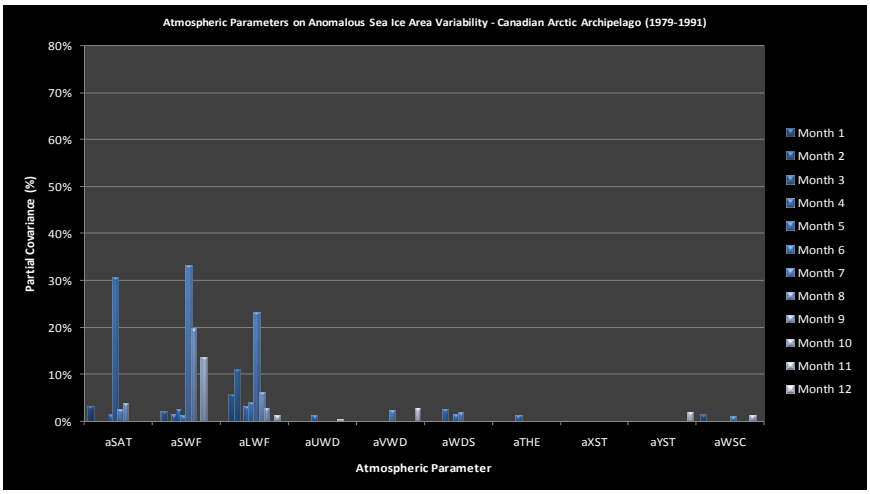

Figure 98. Anomalous Sea Ice Area Variability—Canadian Arctic Archipelago (1979-1991) (same as Figure 34)

APPENDIX D: ANOMALOUS SEA ICE VARIABILITY IN THE CENTRAL ARCTIC (1992–2004)

A. ANOMALOUS SEA ICE VOLUME VARIABILITY

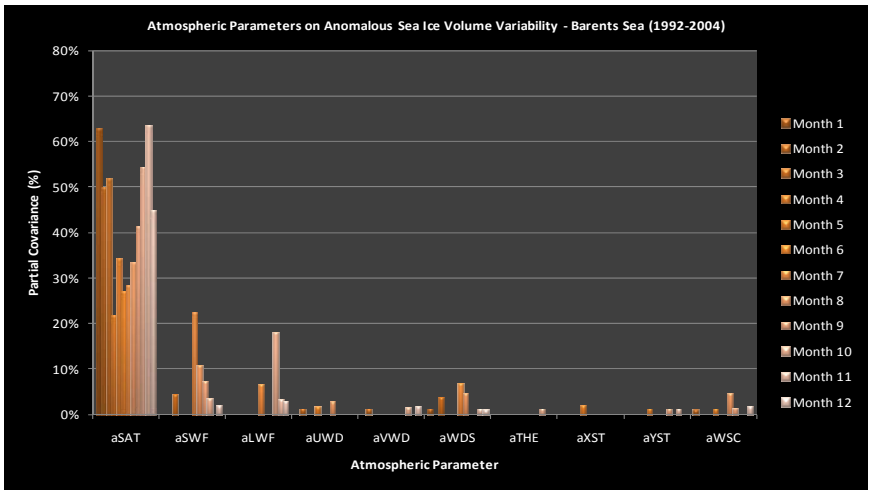

Figure 99. Anomalous Sea Ice Volume Variability—Barents Sea (1992-2004)

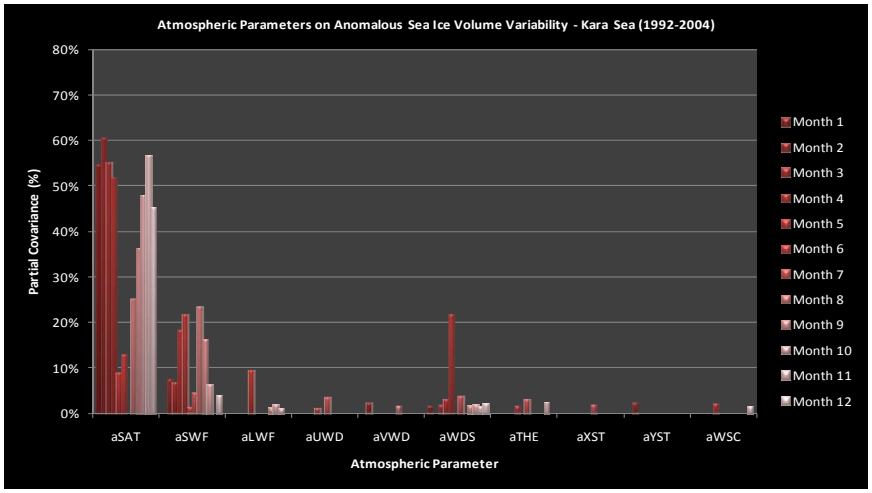

Figure 100. Anomalous Sea Ice Volume Variability—Kara Sea (1992-2004)

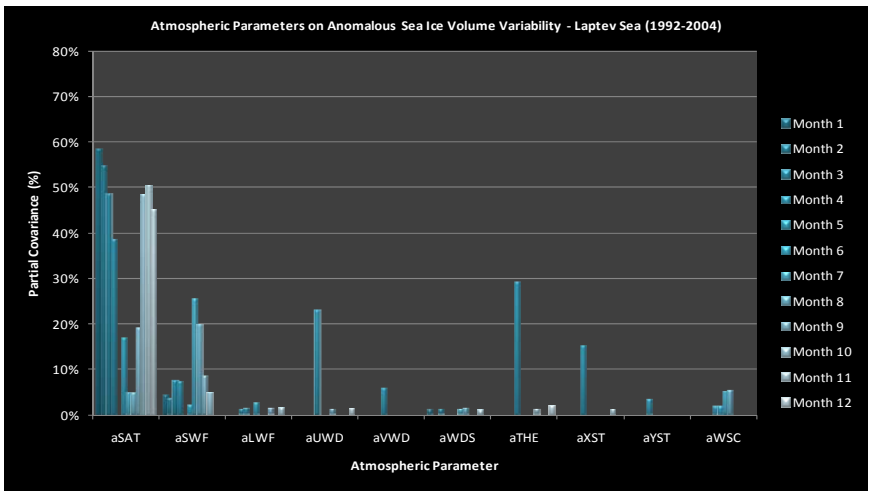

Figure 101. Anomalous Sea Ice Volume Variability—Laptev Sea (1992-2004)

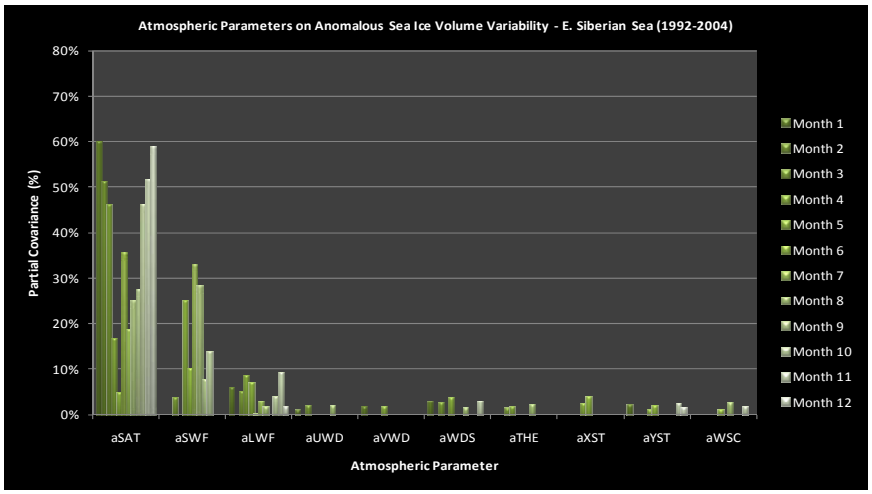

Figure 102. Anomalous Sea Ice Volume Variability—E. Siberian Sea (1992-2004)

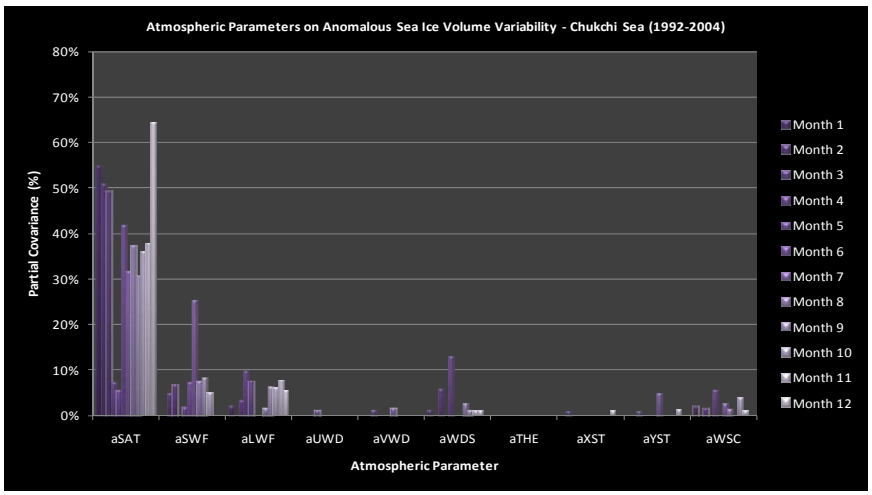

Figure 103. Anomalous Sea Ice Volume Variability—Chukchi Sea (1992-2004)

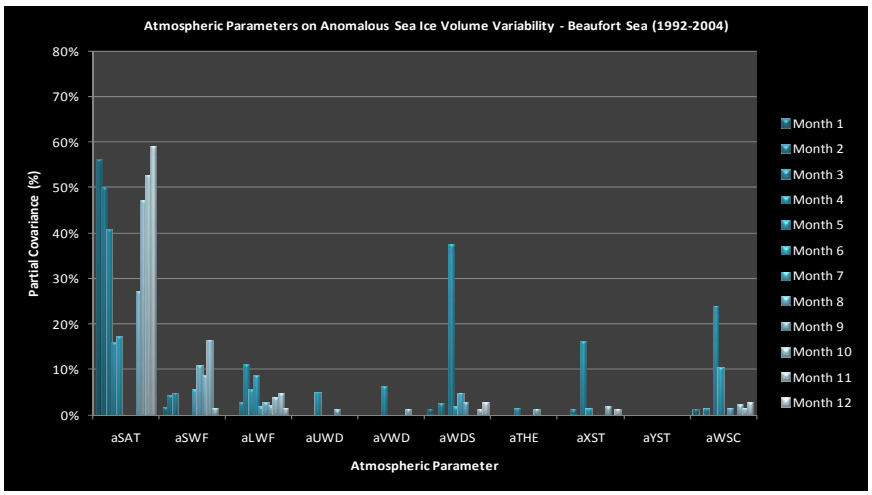

Figure 104. Anomalous Sea Ice Volume Variability—Beaufort Sea (1992-2004)

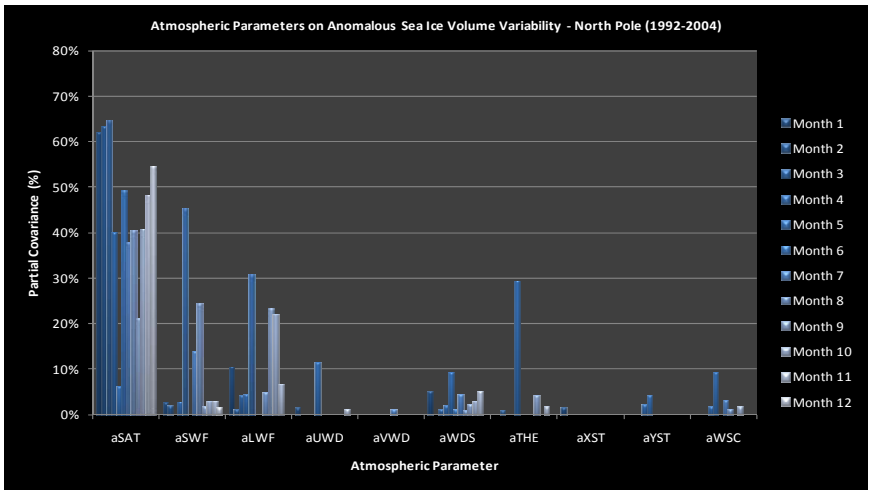

Figure 105. Anomalous Sea Ice Volume Variability—North Pole (1992-2004) (same as Figure 35)

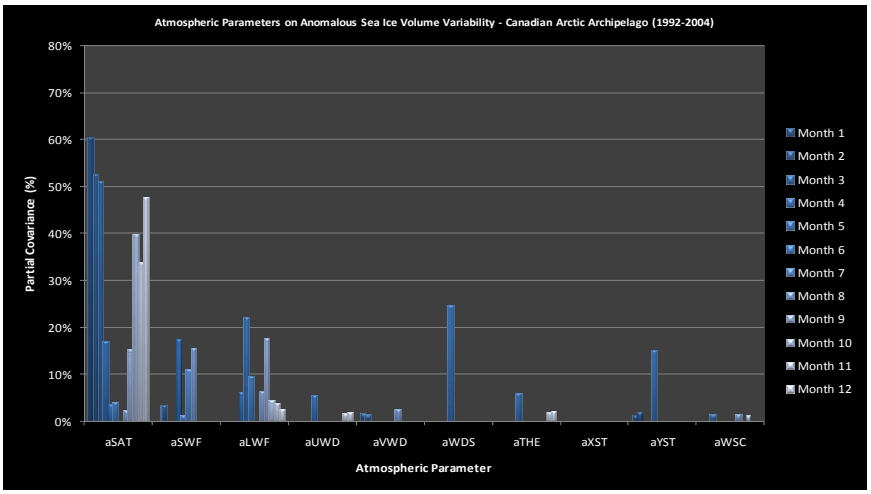

Figure 106. Anomalous Sea Ice Volume Variability—Canadian Arctic Archipelago (1992-2004)

B. ANOMALOUS SEA ICE THICKNESS VARIABILITY

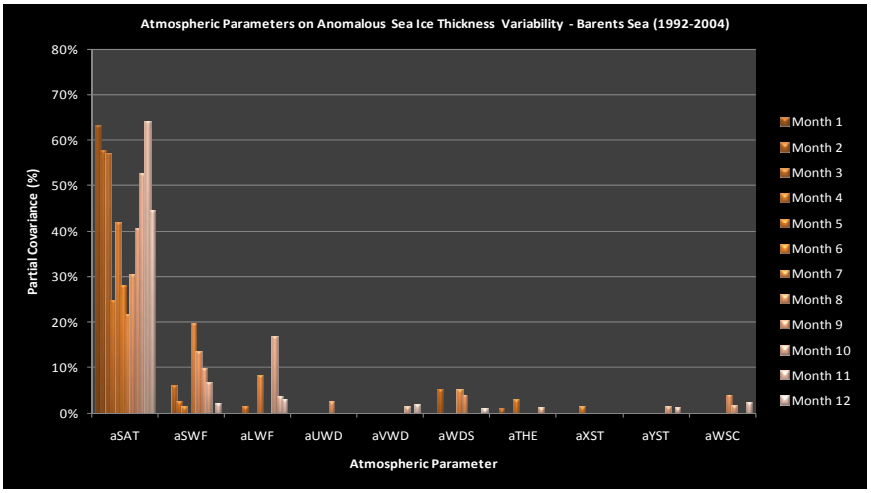

Figure 107. Anomalous Sea Ice Thickness Variability—Barents Sea (1992-2004)

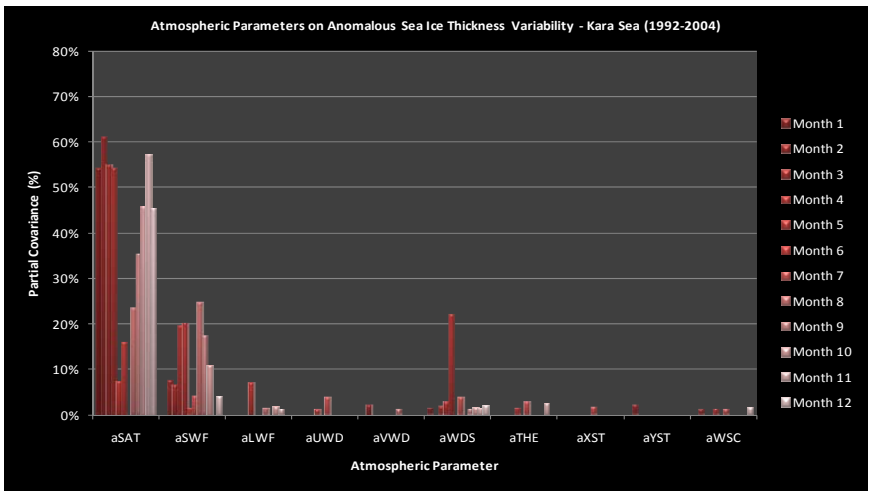

Figure 108. Anomalous Sea Ice Thickness Variability—Kara Sea (1992-2004)

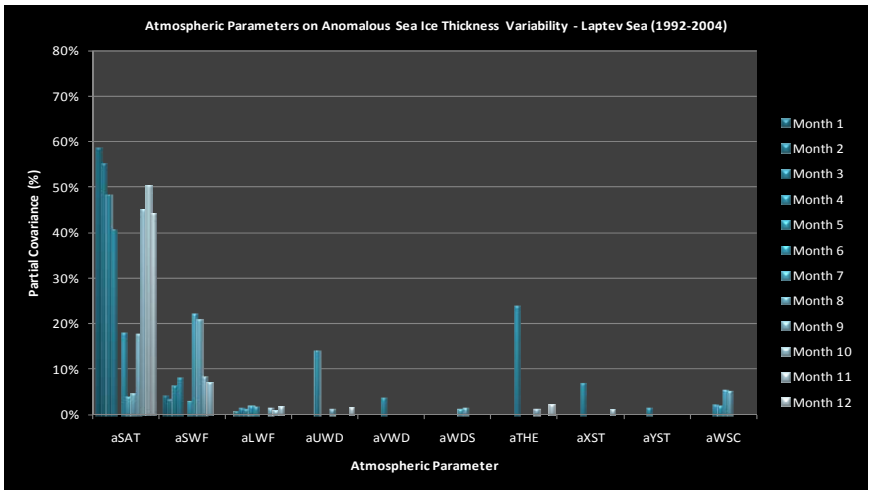

Figure 109. Anomalous Sea Ice Thickness Variability—Laptev Sea (1992-2004)

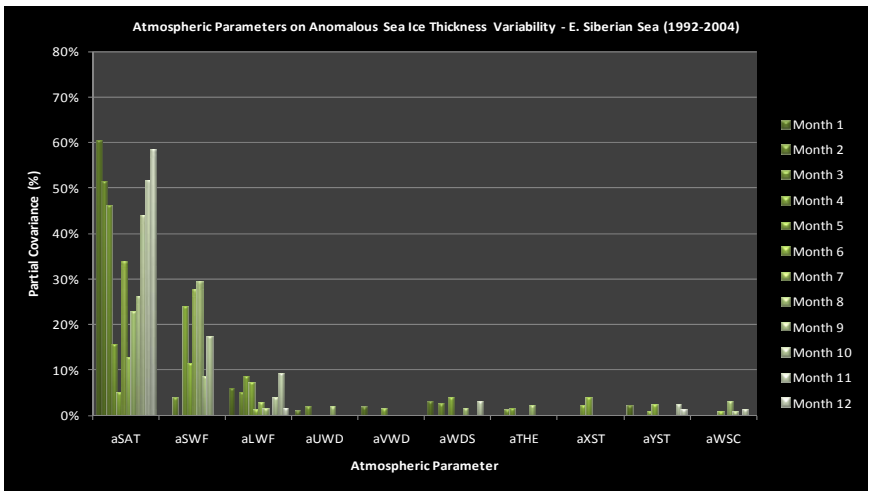

Figure 110. Anomalous Sea Ice Thickness Variability—E. Siberian Sea (1992-2004)

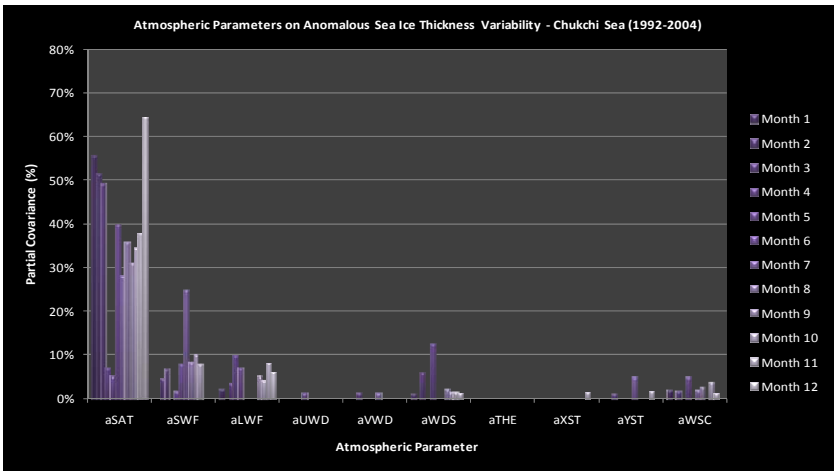

Figure 111. Anomalous Sea Ice Thickness Variability—Chukchi Sea (1992-2004)

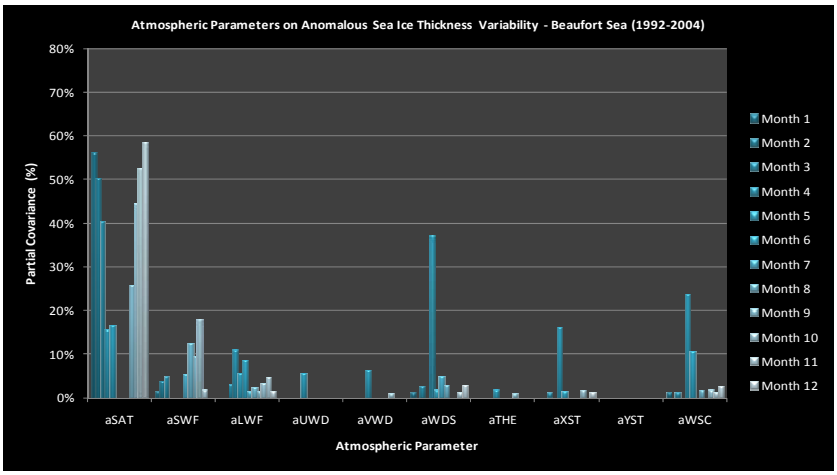

Figure 112. Anomalous Sea Ice Thickness Variability—Beaufort Sea (1992-2004)

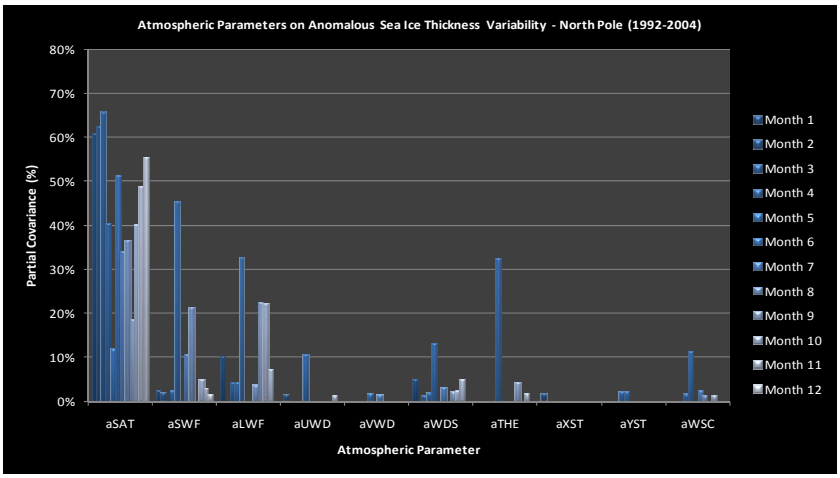

Figure 113. Anomalous Sea Ice Thickness Variability—North Pole (1992-2004) (same as Figure 36)

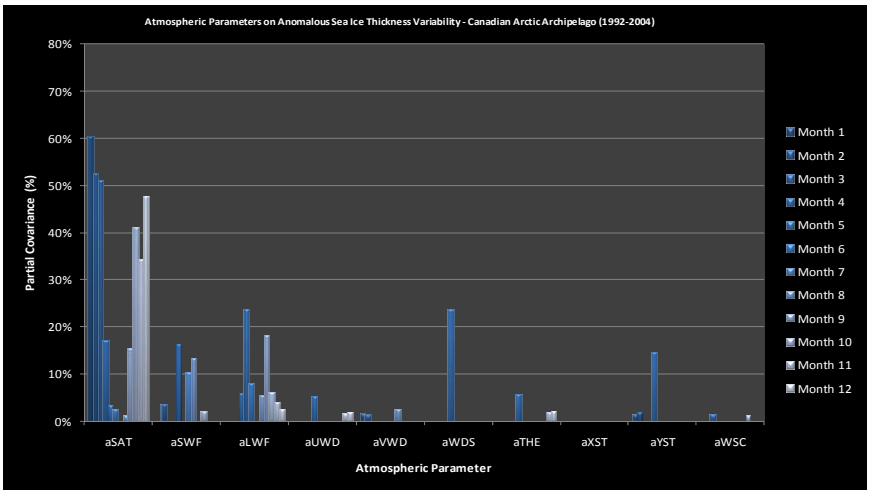

Figure 114. Anomalous Sea Ice Thickness Variability—Canadian Arctic Archipelago (1992-2004)

C. ANOMALOUS SEA ICE AREA VARIABILITY

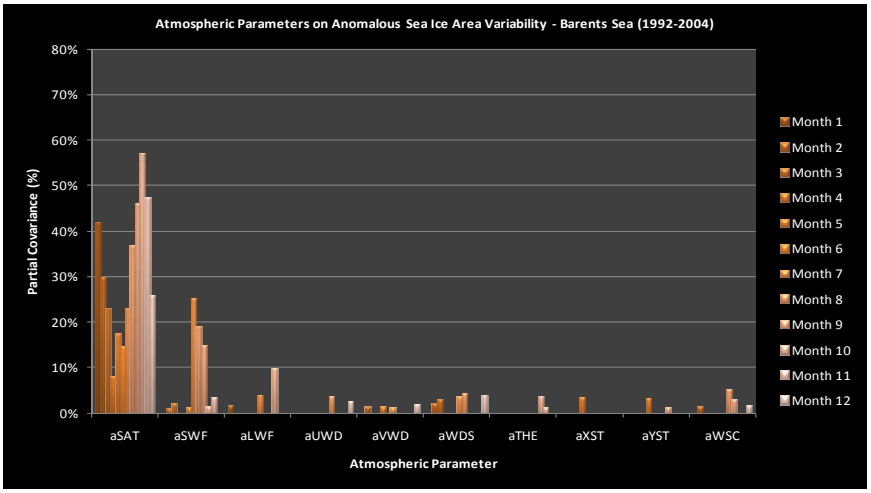

Figure 115. Anomalous Sea Ice Area Variability—Barents Sea (1992-2004)

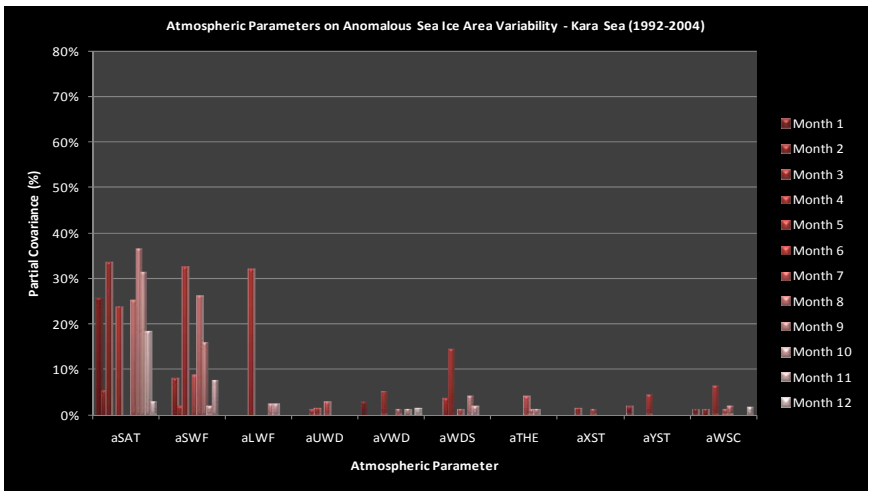

Figure 116. Anomalous Sea Ice Area Variability—Kara Sea (1992-2004)

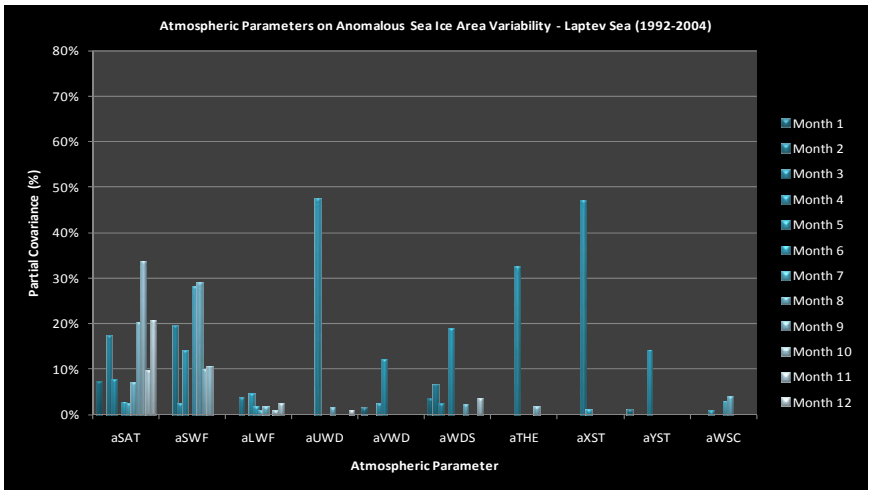

Figure 117. Anomalous Sea Ice Area Variability—Laptev Sea (1992-2004)

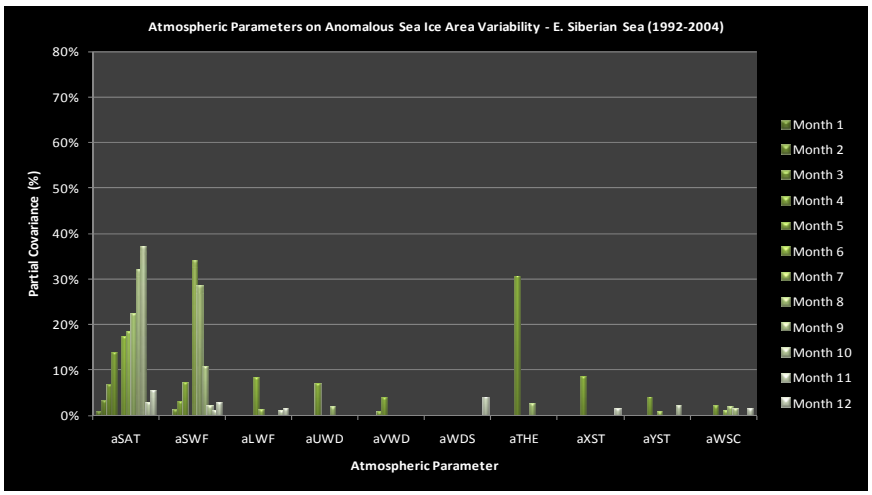

Figure 118. Anomalous Sea Ice Area Variability—E. Siberian Sea (1992-2004)

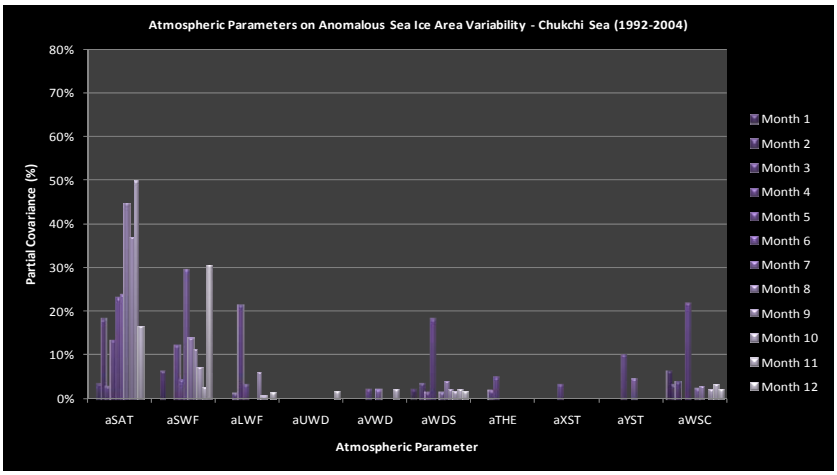

Figure 119. Anomalous Sea Ice Area Variability—Chukchi Sea (1992-2004)

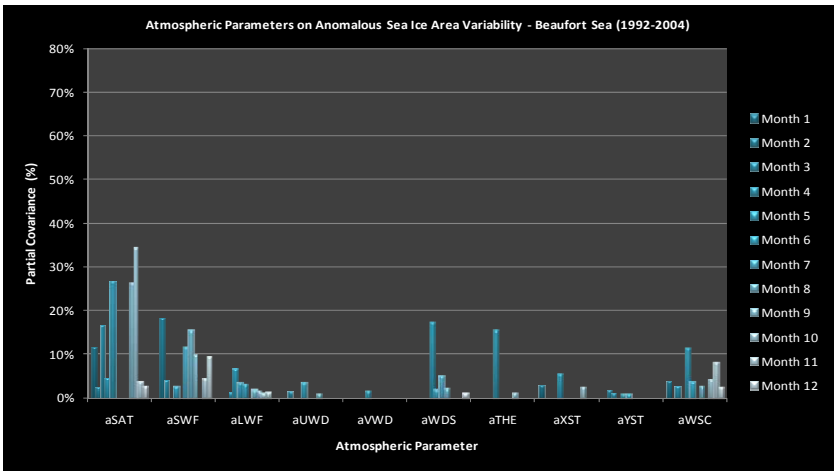

Figure 120. Anomalous Sea Ice Area Variability—Beaufort Sea (1992-2004)

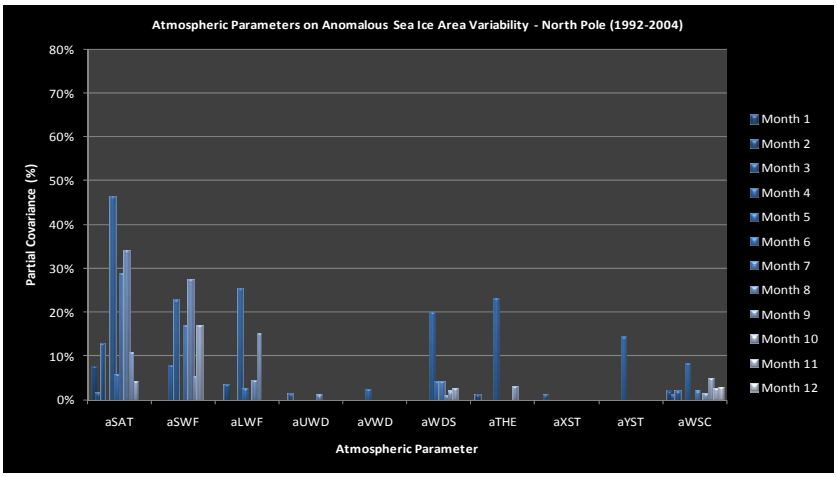

Figure 121. Anomalous Sea Ice Area Variability—North Pole (1992-2004) (same as Figure 37)

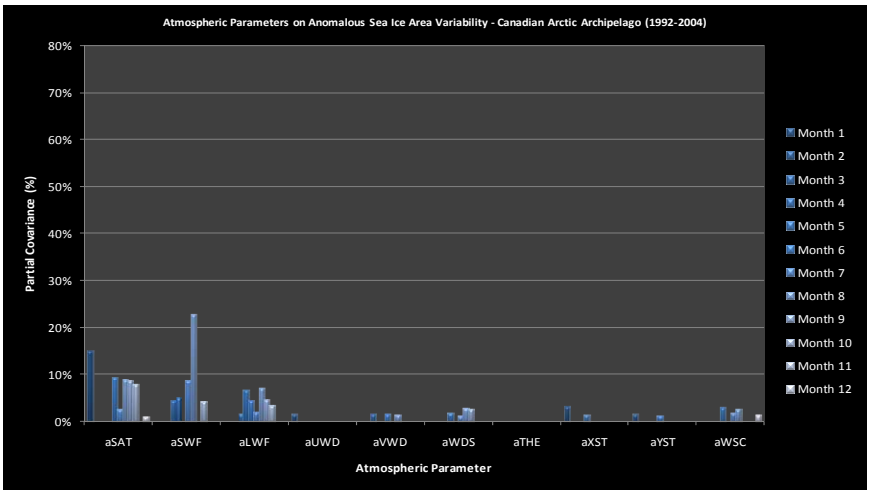

Figure 122. Anomalous Sea Ice Area Variability—Canadian Arctic Archipelago (1992-2004)

APPENDIX E: ANOMALOUS SEA ICE VARIABILITY ALONG THE NORTHWEST PASSAGE (1979–2004)

A. ANOMALOUS SEA ICE VOLUME VARIABILITY

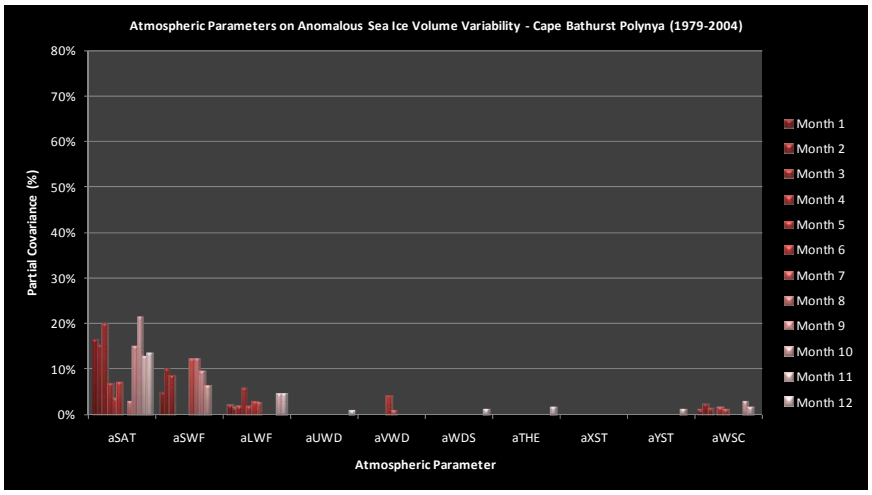

Figure 123. Anomalous Sea Ice Volume Variability—Cape Bathurst Polynya (1979-2004) (same as Figure 38)

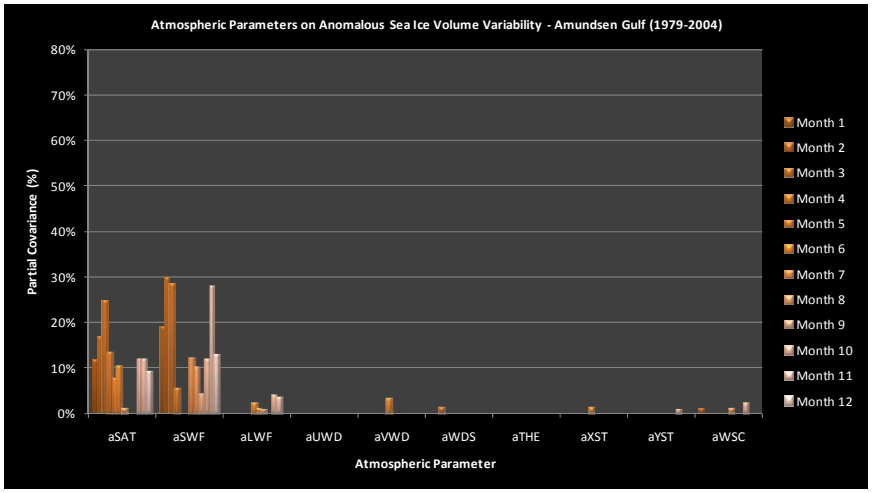

Figure 124. Anomalous Sea Ice Volume Variability—Amundsen Gulf (1979-2004)

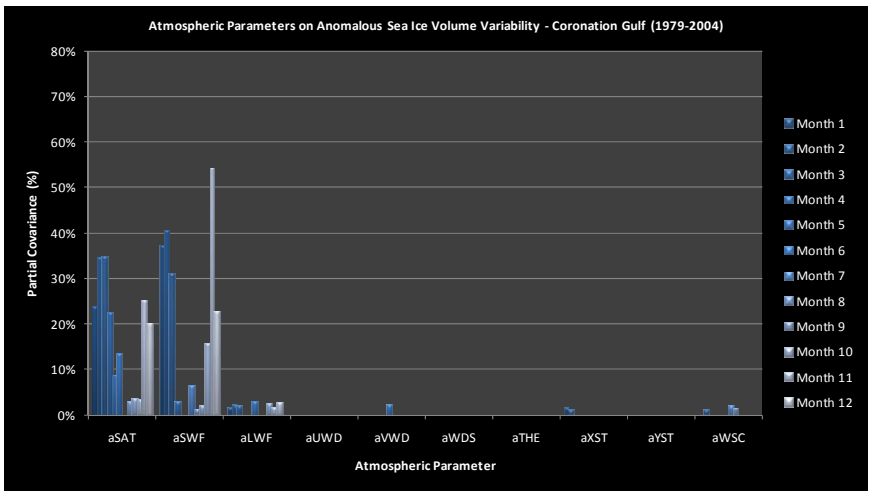

Figure 125. Anomalous Sea Ice Volume Variability—Coronation Gulf (1979-2004)

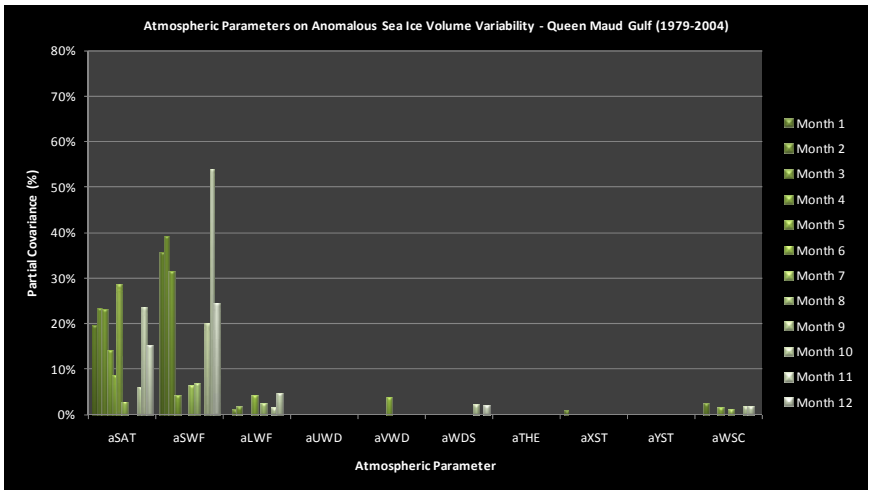

Figure 126. Anomalous Sea Ice Volume Variability—Queen Maud Gulf (1979-2004)

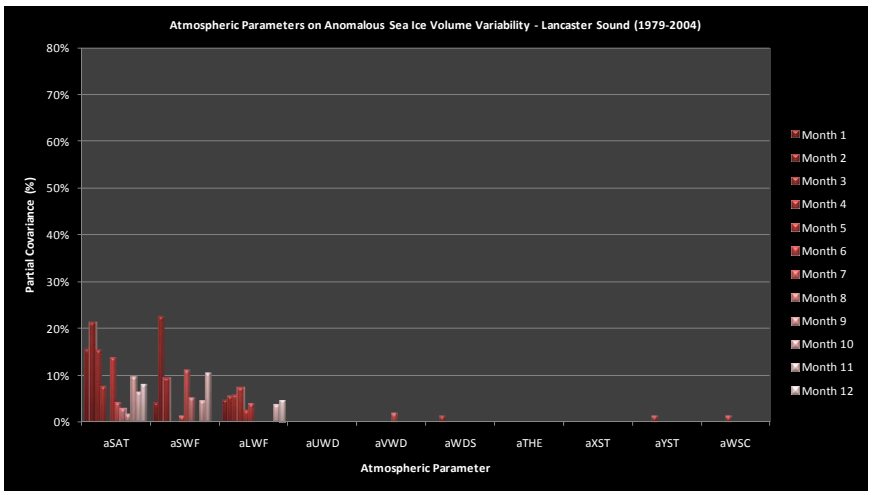

Figure 127. Anomalous Sea Ice Volume Variability—Lancaster Sound (1979-2004)

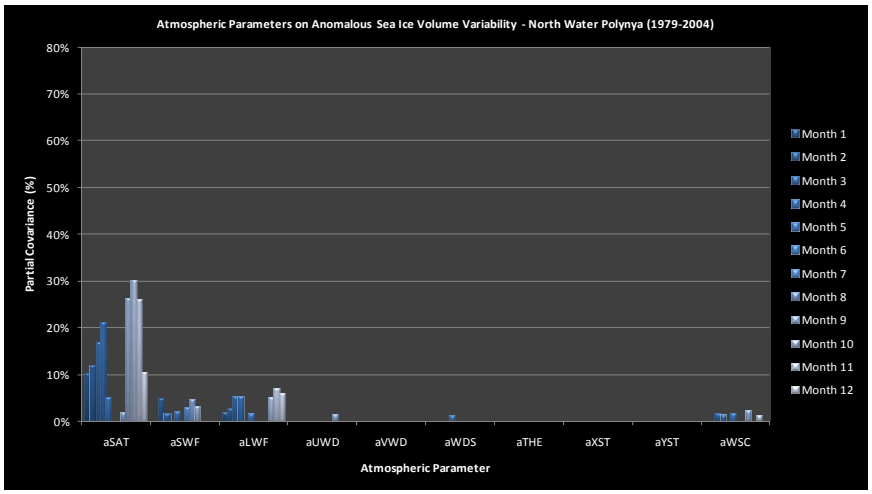

Figure 128. Anomalous Sea Ice Volume Variability—North Water Polynya (1979-2004)

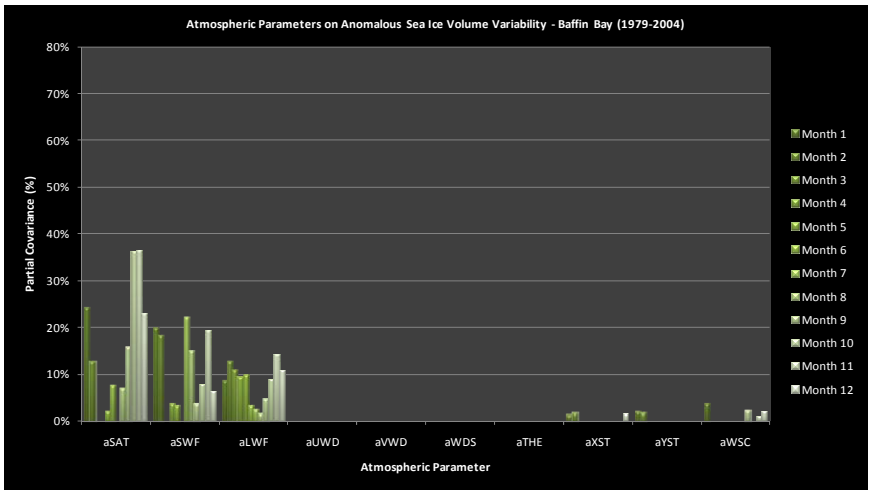

Figure 129. Anomalous Sea Ice Volume Variability—Baffin Bay (1979-2004)

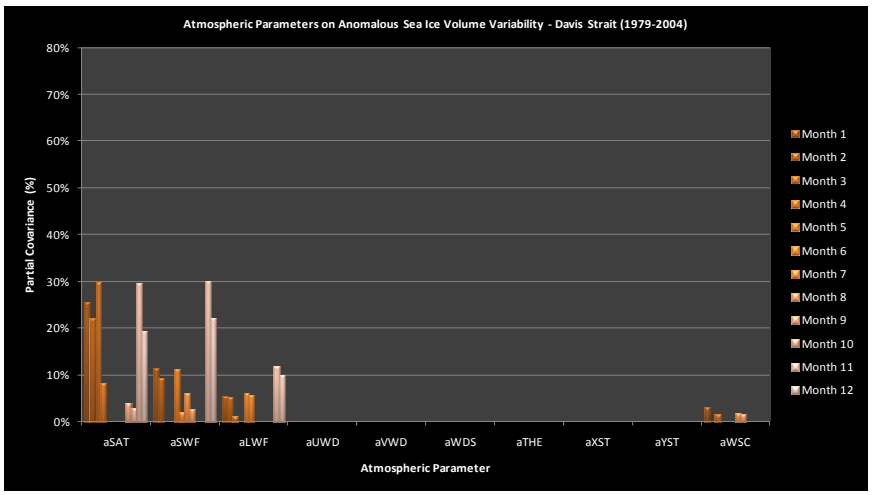

Figure 130. Anomalous Sea Ice Volume Variability—Davis Strait (1979-2004)

B. ANOMALOUS SEA ICE THICKNESS VARIABILITY

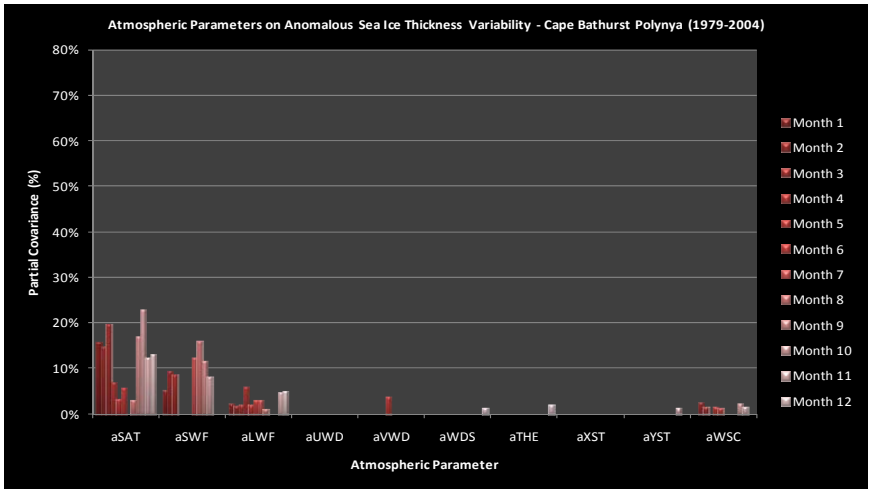

Figure 131. Anomalous Sea Ice Thickness Variability—Cape Bathurst Polynya (1979-2004) (same as Figure 39)

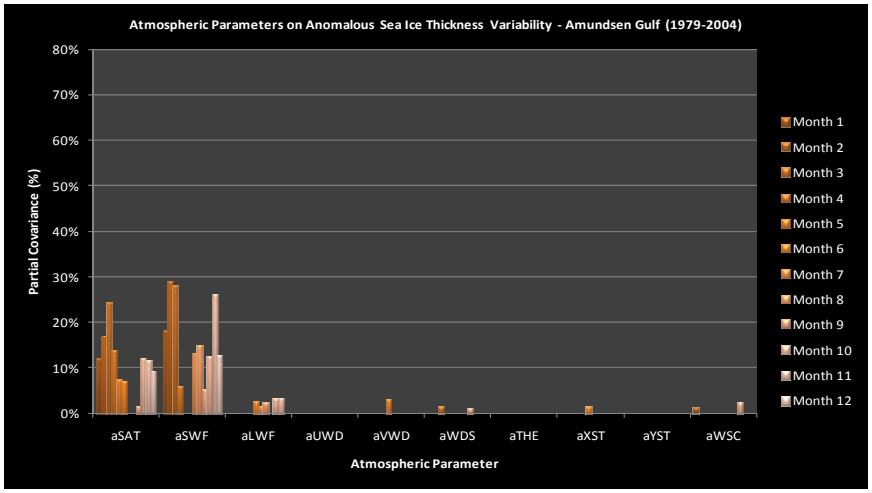

Figure 132. Anomalous Sea Ice Thickness Variability—Amundsen Gulf (1979-2004)

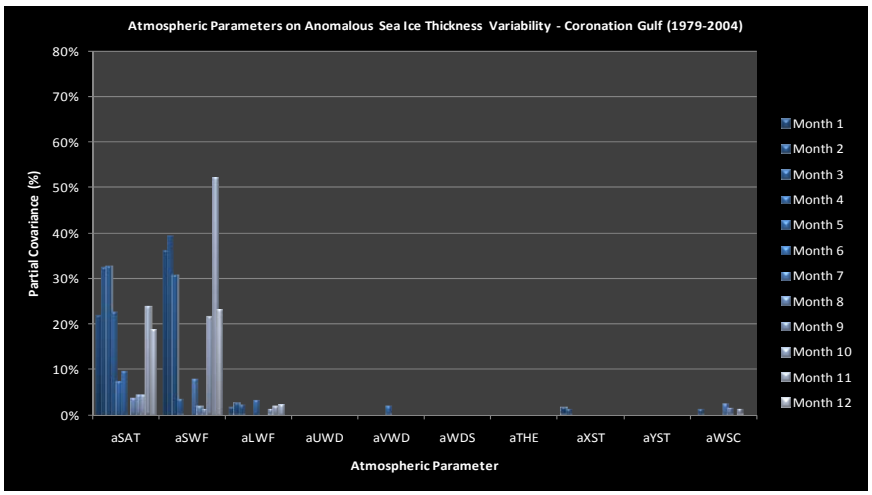

Figure 133. Anomalous Sea Ice Thickness Variability—Coronation Gulf (1979-2004)

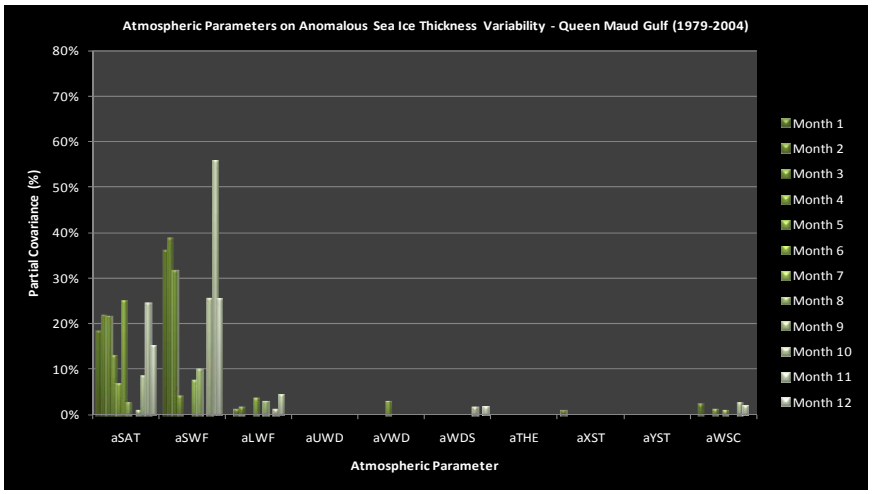

Figure 134. Anomalous Sea Ice Thickness Variability—Queen Maud Gulf (1979-2004)

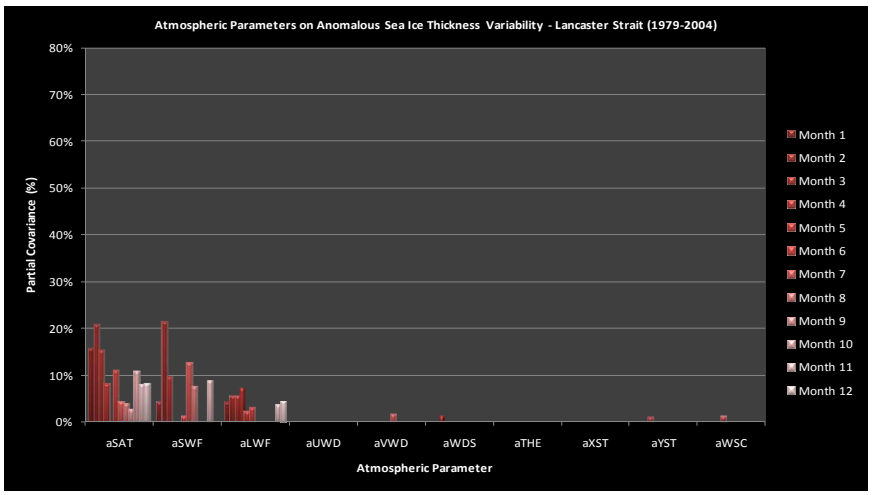

Figure 135. Anomalous Sea Ice Thickness Variability—Lancaster Sound (1979-2004)

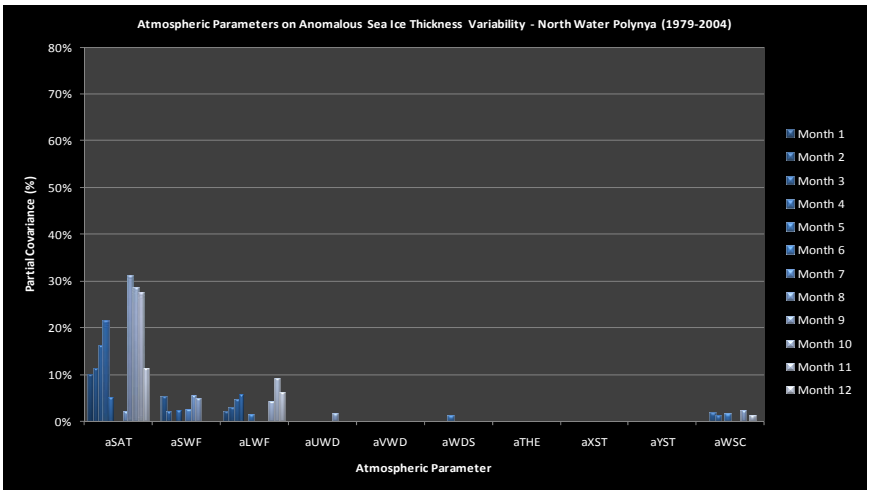

Figure 136. Anomalous Sea Ice Thickness Variability—North Water Polynya (1979-2004)

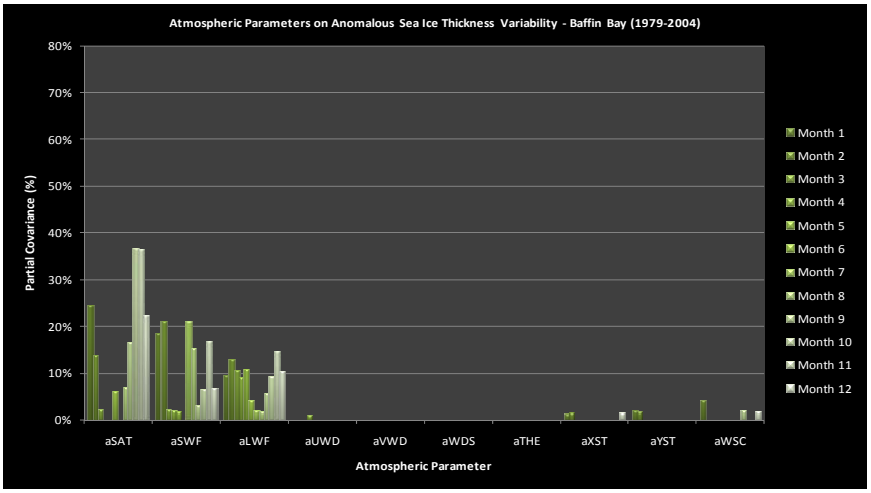

Figure 137. Anomalous Sea Ice Thickness Variability—Baffin Bay (1979-2004)

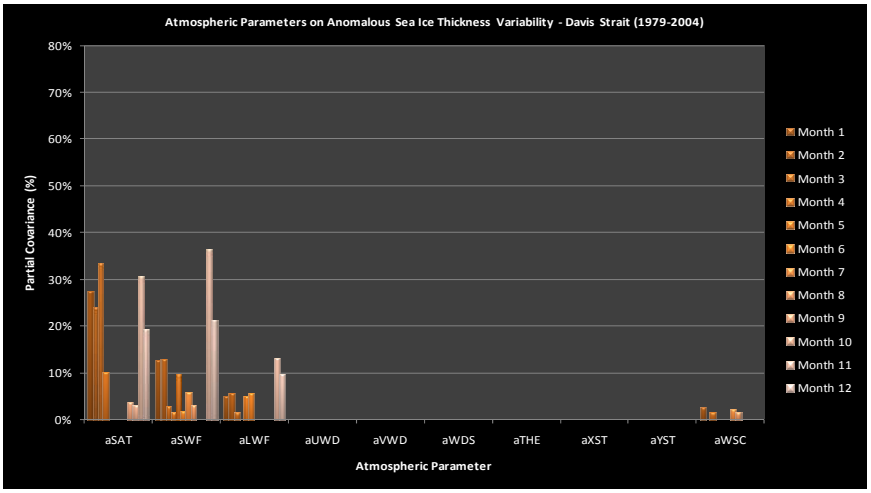

Figure 138. Anomalous Sea Ice Thickness Variability—Davis Strait (1979-2004)

C. ANOMALOUS SEA ICE AREA VARIABILITY

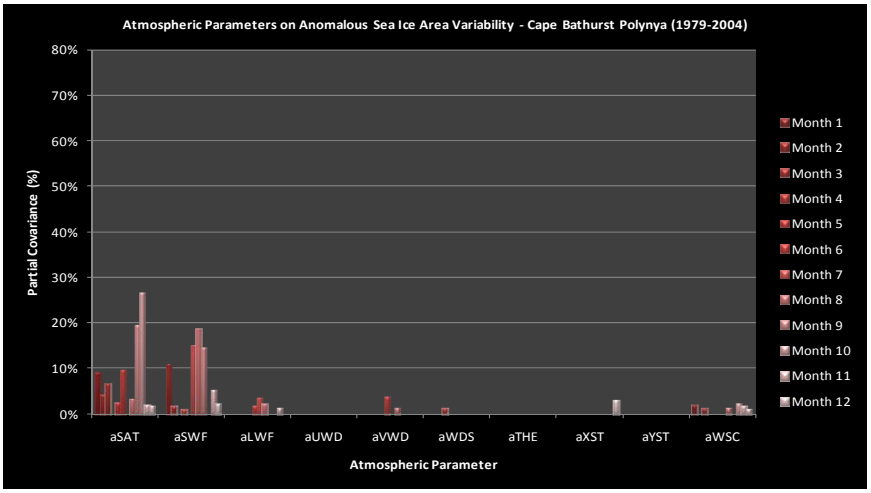

Figure 139. Anomalous Sea Ice Area Variability—Cape Bathurst Polynya (1979-2004) (same as Figure 40)

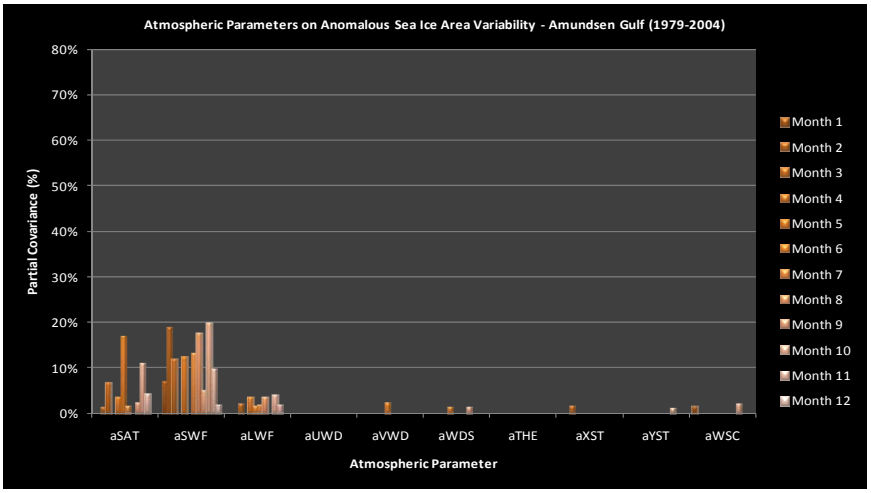

Figure 140. Anomalous Sea Ice Area Variability—Amundsen Gulf (1979-2004)

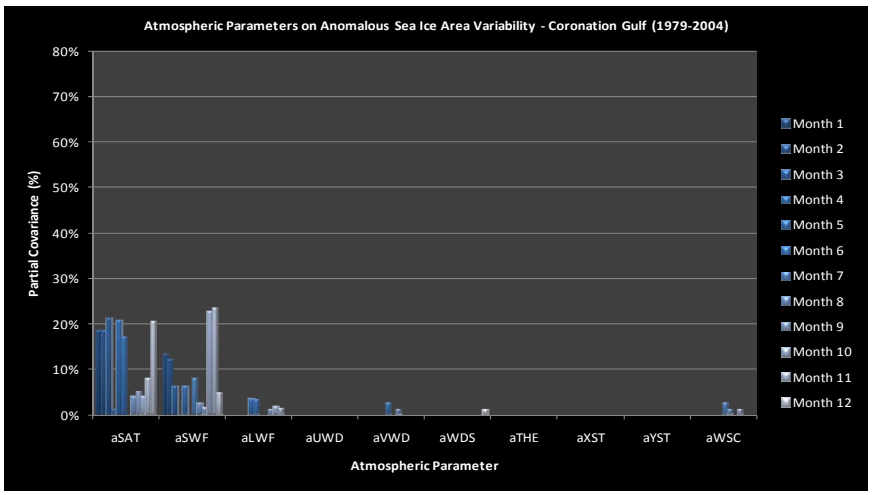

Figure 141. Anomalous Sea Ice Area Variability—Coronation Gulf (1979-2004)

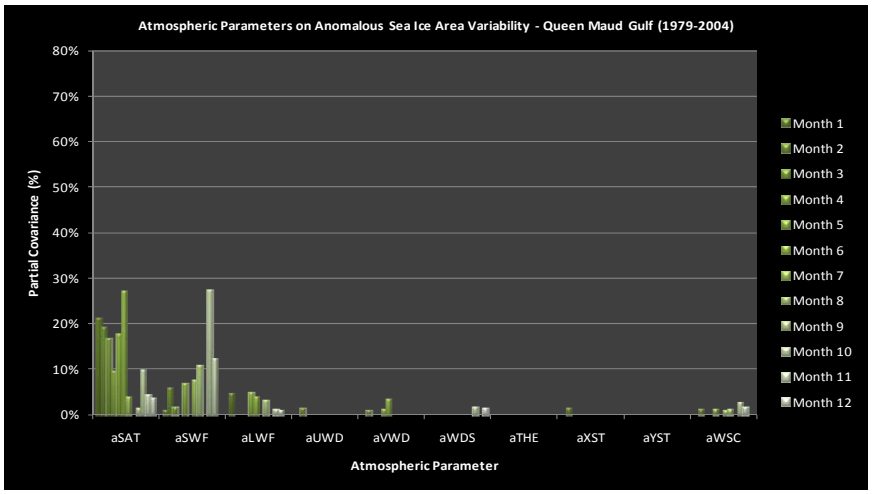

Figure 142. Anomalous Sea Ice Area Variability—Queen Maud Gulf (1979-2004)

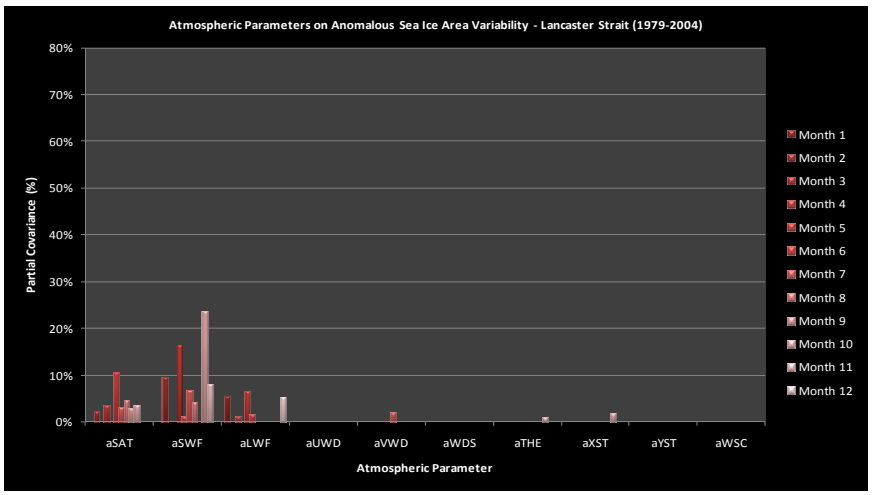

Figure 143. Anomalous Sea Ice Area Variability—Lancaster Sound (1979-2004)

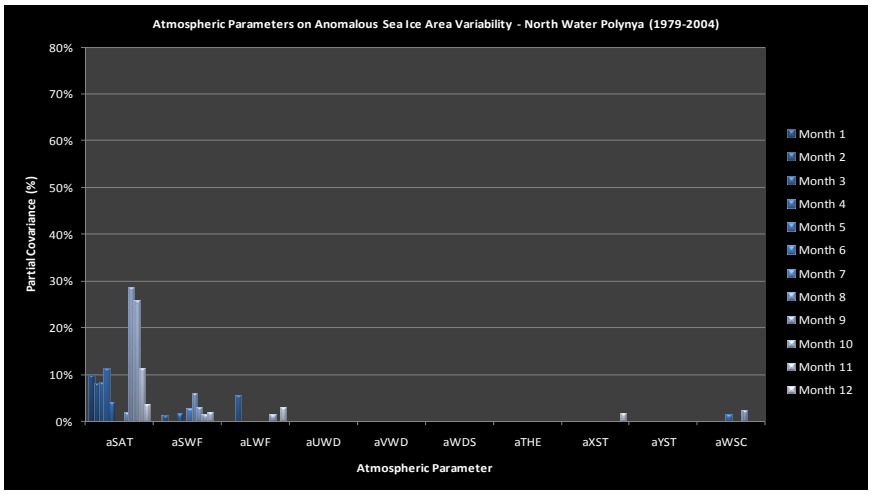

Figure 144. Anomalous Sea Ice Area Variability—North Water Polynya (1979-2004)

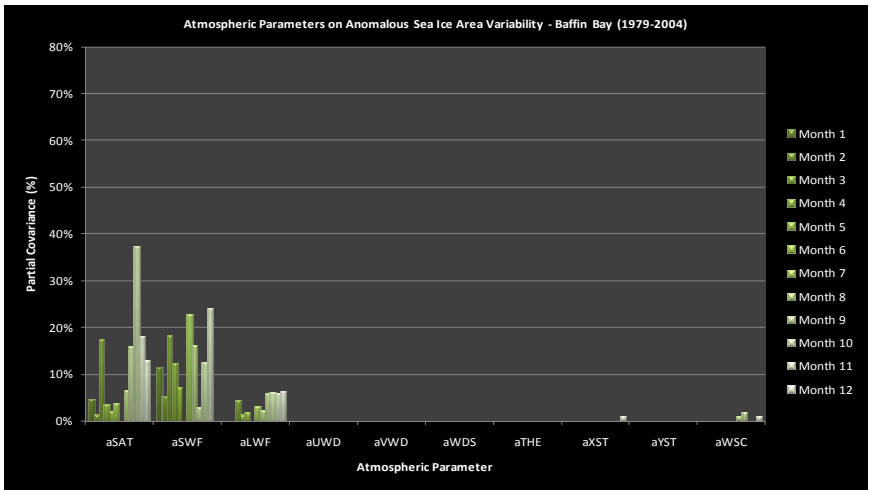

Figure 145. Anomalous Sea Ice Area Variability—Baffin Bay (1979-2004)

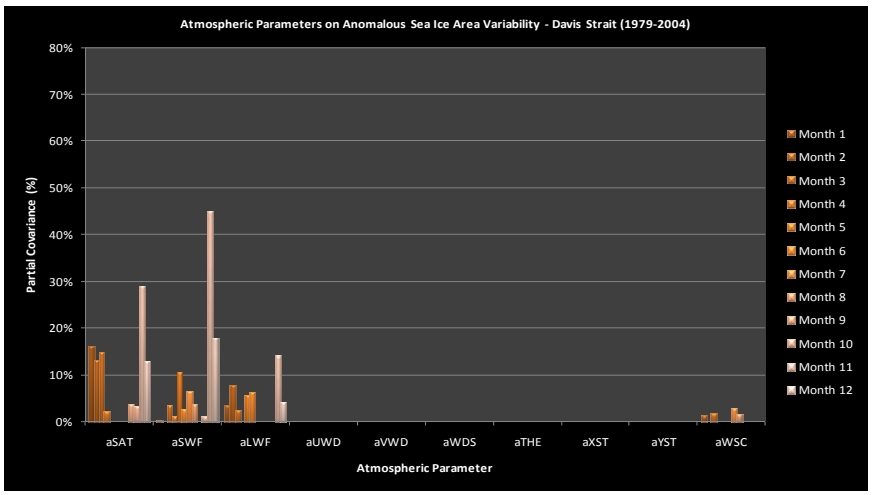

Figure 146. Anomalous Sea Ice Area Variability—Davis Strait (1979-2004)

THIS PAGE INTENTIONALLY LEFT BLANK

APPENDIX F: ANOMALOUS SEA ICE VARIABILITY ALONG THE NORTHERN SEA ROUTE (1979–2004)

A. ANOMALOUS SEA ICE VOLUME VARIABILITY

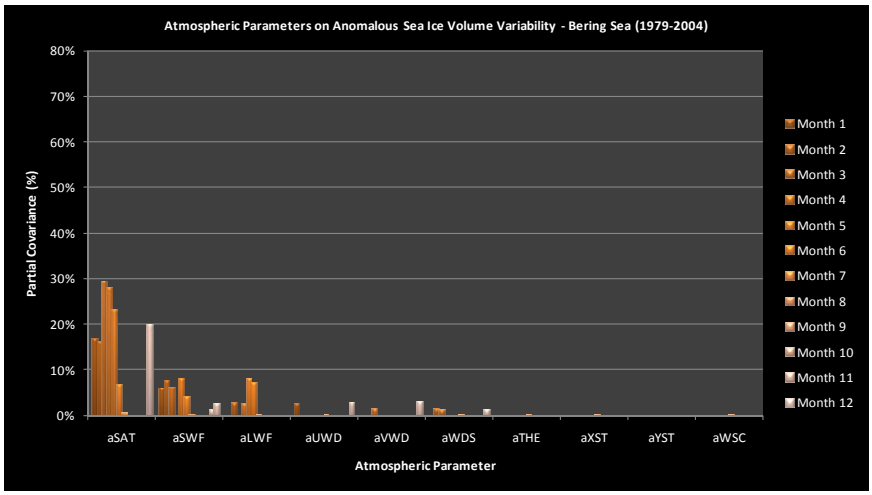

Figure 147. Anomalous Sea Ice Volume Variability—Bering Sea (1979-2004) (same as Figure 41)

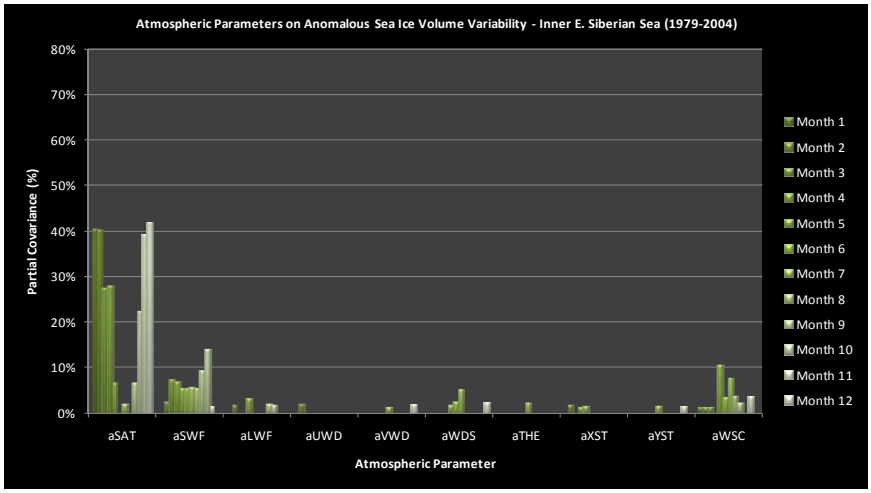

Figure 148. Anomalous Sea Ice Volume Variability—Inner E. Siberian Sea (1979-2004)

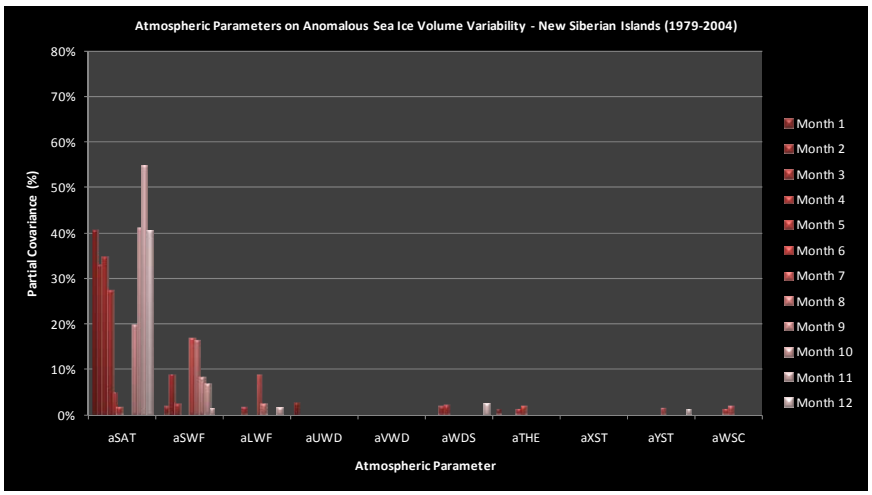

Figure 149. Anomalous Sea Ice Volume Variability—New Siberian Islands (1979-2004)

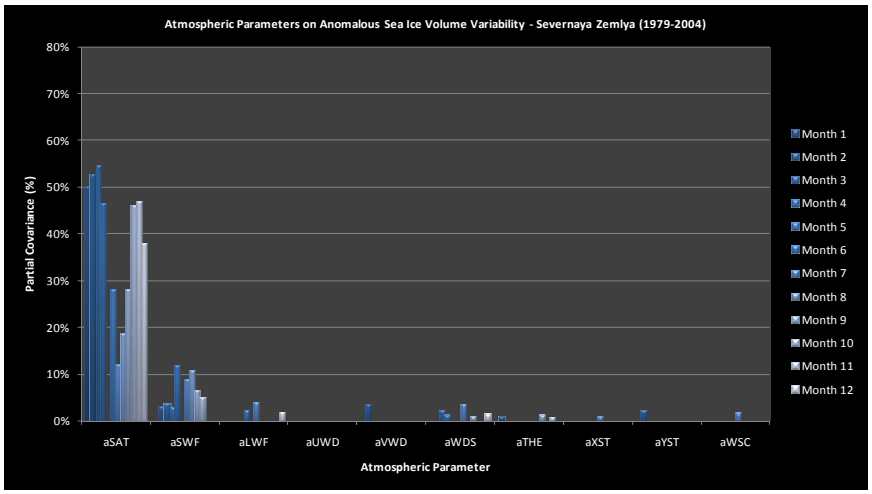

Figure 150. Anomalous Sea Ice Volume Variability—Severnaya Zemlya (1979-2004)

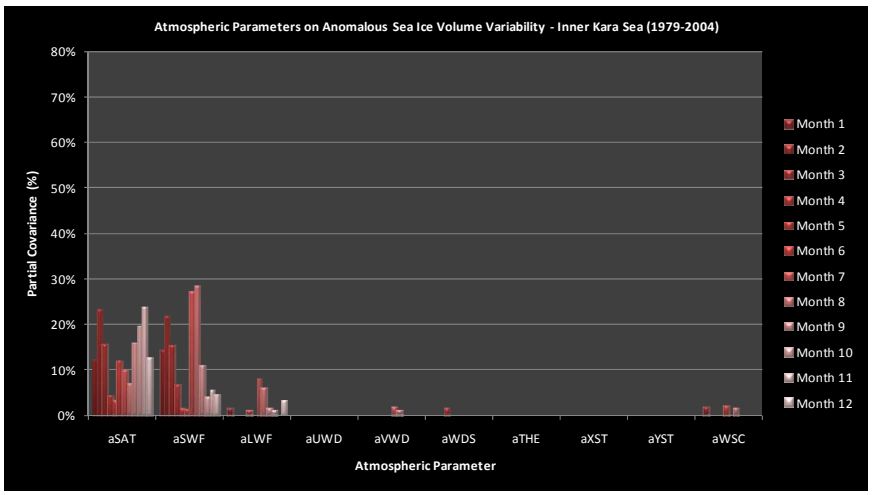

Figure 151. Anomalous Sea Ice Volume Variability—Inner Kara Sea (1979-2004)

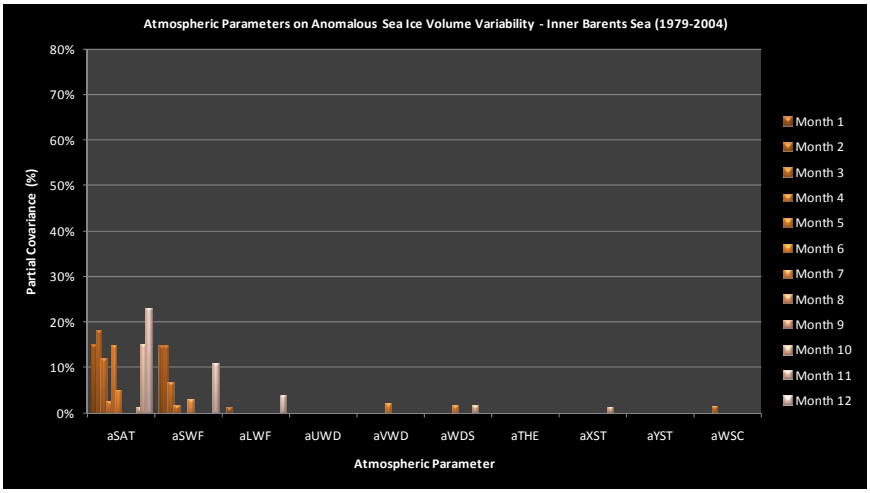

Figure 152. Anomalous Sea Ice Volume Variability—Inner Barents Sea (1979-2004)

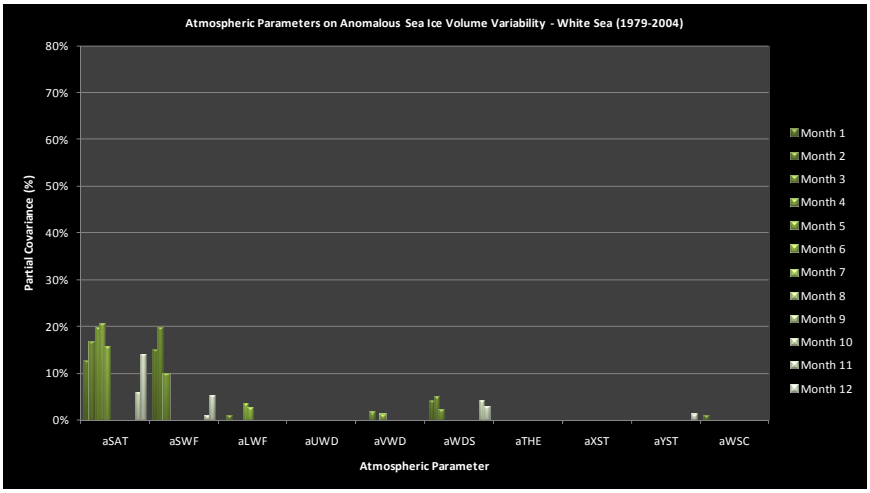

Figure 153. Anomalous Sea Ice Volume Variability—White Sea (1979-2004)

B. ANOMALOUS SEA ICE THICKNESS VARIABILITY

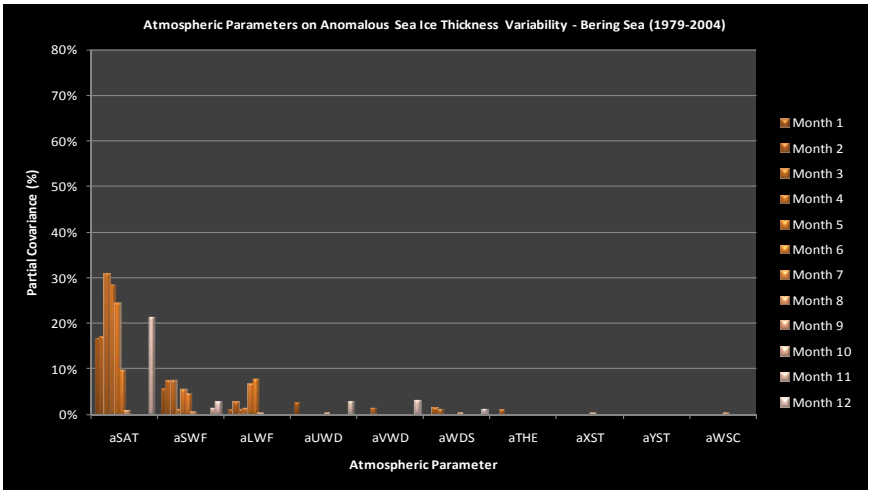

Figure 154. Anomalous Sea Ice Thickness Variability—Bering Sea (1979-2004) (same as Figure 42)

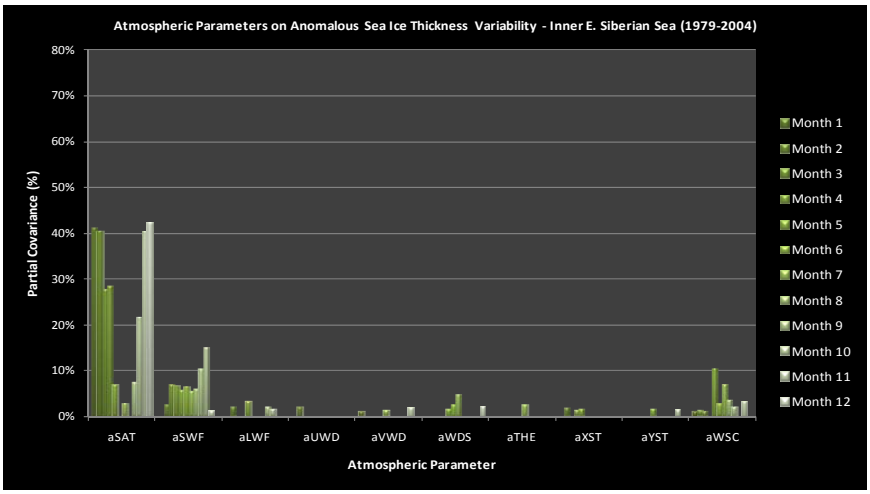

Figure 155. Anomalous Sea Ice Thickness Variability—Inner E. Siberian Sea (1979-2004)

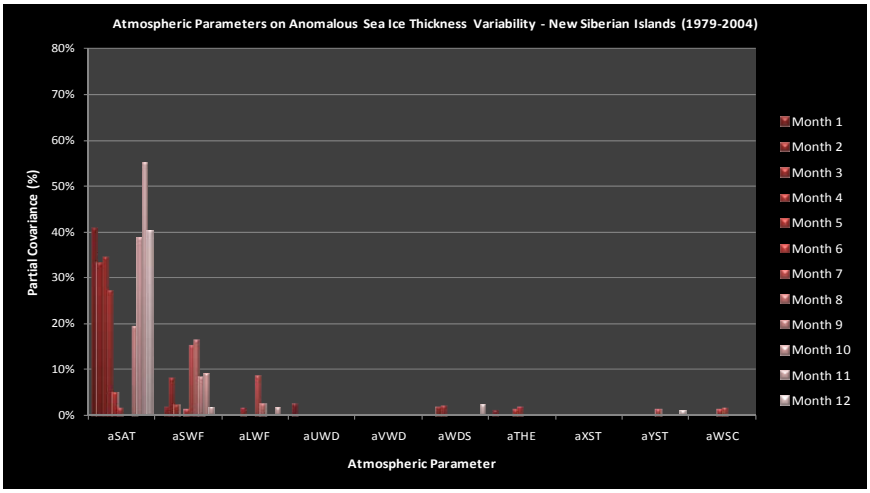

Figure 156. Anomalous Sea Ice Thickness Variability—New Siberian Islands (1979-2004)

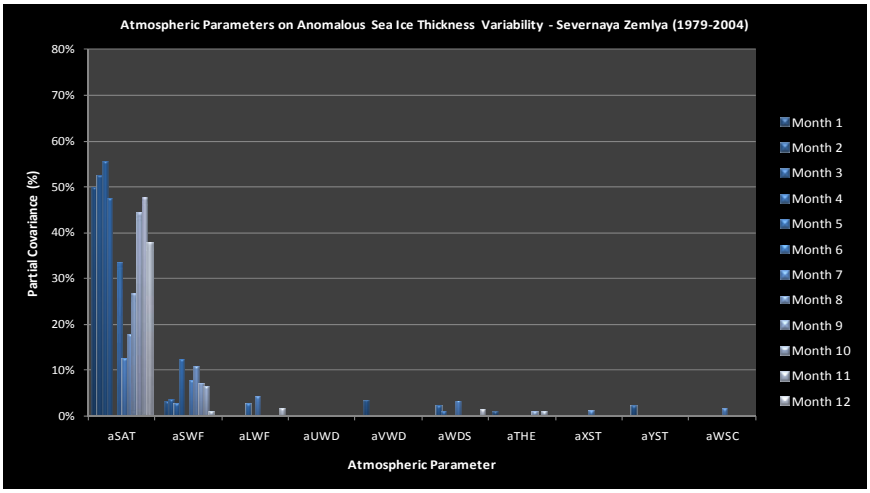

Figure 157. Anomalous Sea Ice Thickness Variability—Severnaya Zemlya (1979-2004)

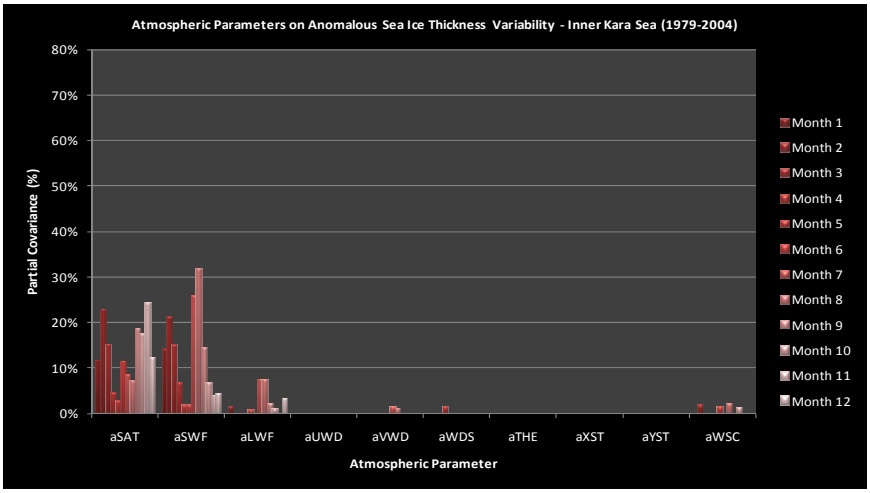

Figure 158. Anomalous Sea Ice Thickness Variability—Inner Kara Sea (1979-2004)

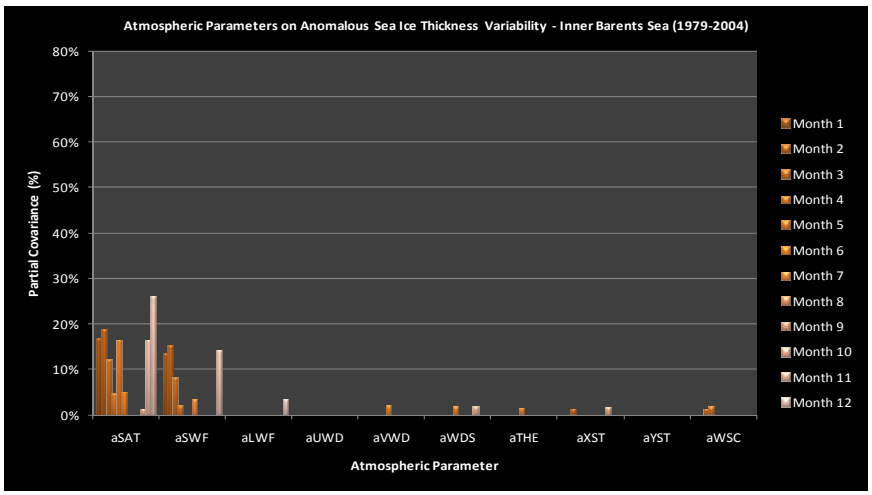

Figure 159. Anomalous Sea Ice Thickness Variability—Inner Barents Sea (1979-2004)

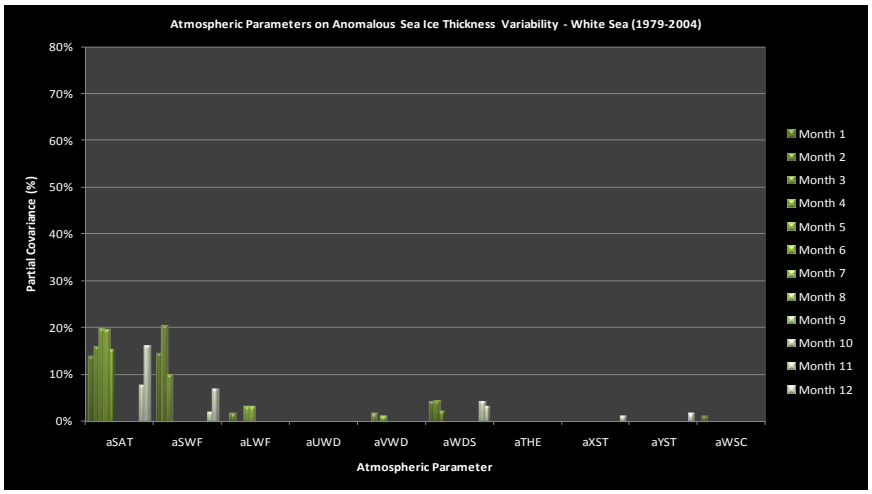

Figure 160. Anomalous Sea Ice Thickness Variability—White Sea (1979-2004)

C. ANOMALOUS SEA ICE AREA VARIABILITY

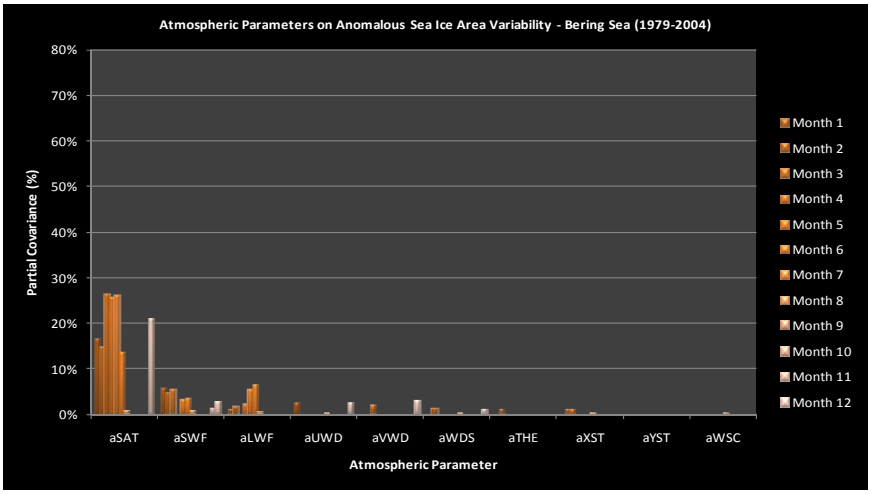

Figure 161. Anomalous Sea Ice Area Variability—Bering Sea (1979-2004) (same as Figure 43)

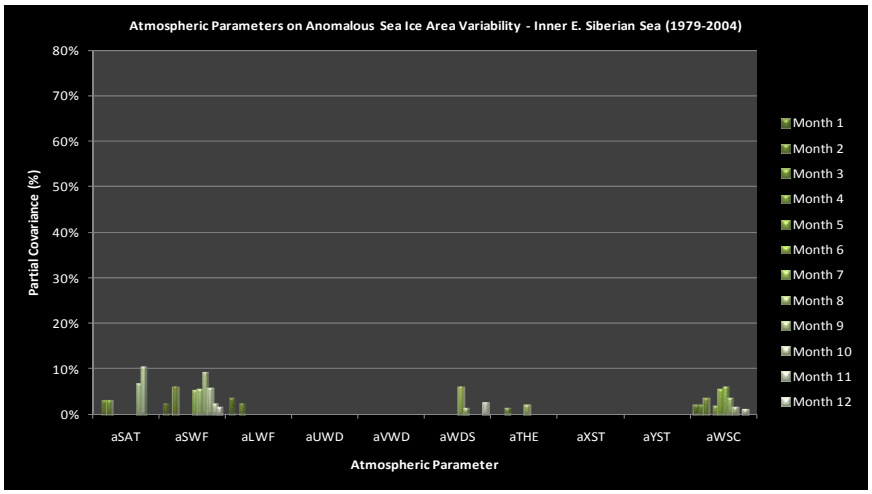

Figure 162. Anomalous Sea Ice Area Variability—Inner E. Siberian Sea (1979-2004)

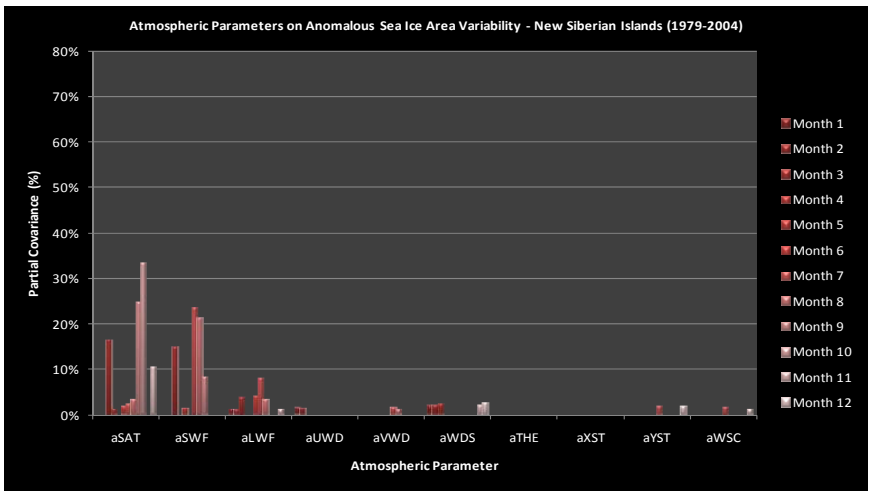

Figure 163. Anomalous Sea Ice Area Variability—New Siberian Islands (1979-2004)

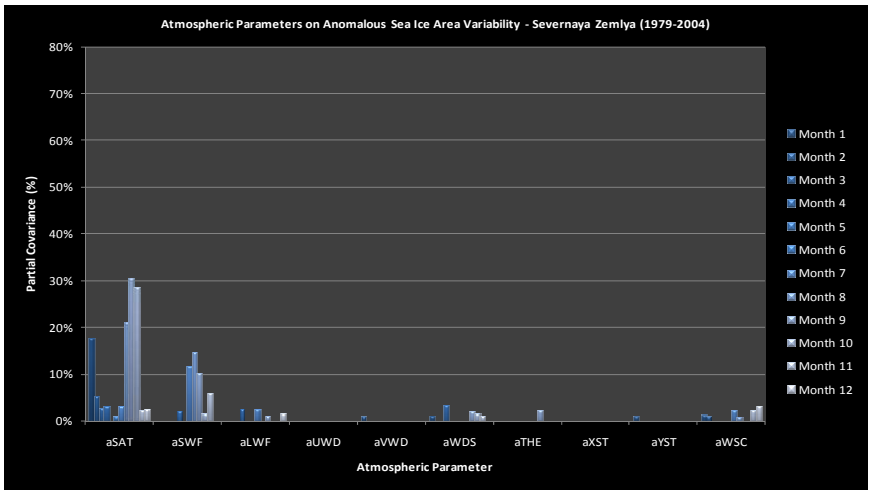

Figure 164. Anomalous Sea Ice Area Variability—Severnaya Zemlya (1979-2004)

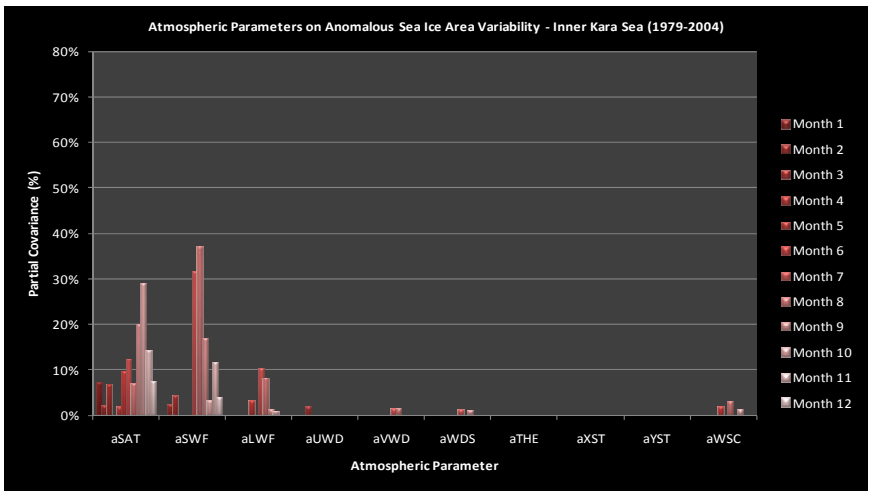

Figure 165. Anomalous Sea Ice Area Variability—Inner Kara Sea (1979-2004)

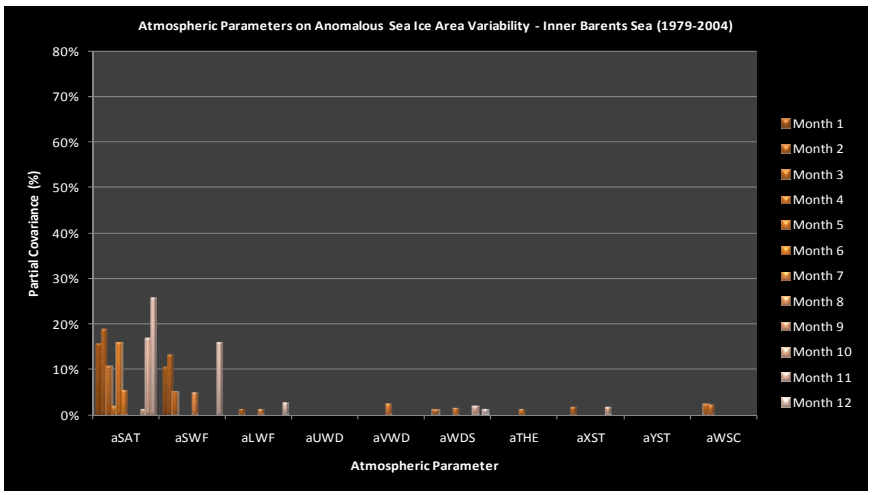

Figure 166. Anomalous Sea Ice Area Variability—Inner Barents Sea (1979-2004)

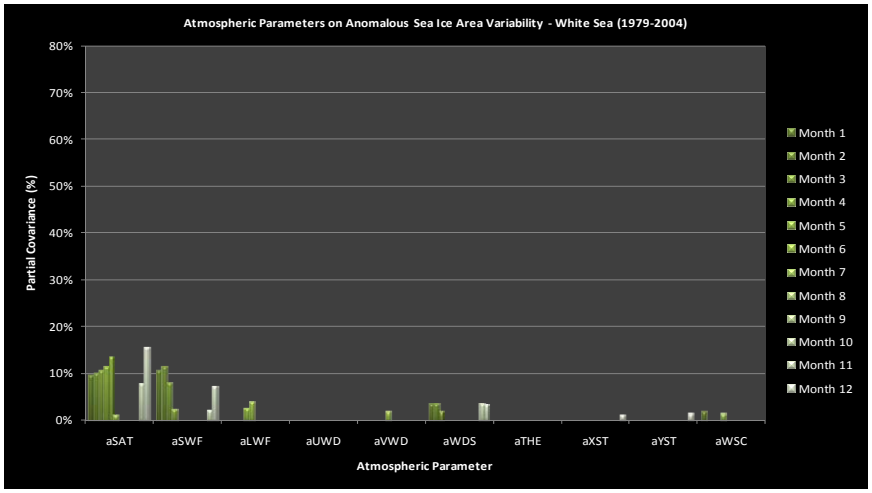

Figure 167. Anomalous Sea Ice Area Variability—White Sea (1979-2004)

THIS PAGE INTENTIONALLY LEFT BLANK

APPENDIX G: SUMMARY OF ATMOSPHERIC CONTRIBUTION TO ANOMALOUS SEA ICE VOLUME VARIABILITY IN THE CENTRAL ARCTIC

The following graphics provides summaries of the average, minimum, and maximum percentage of aSAT, aSWF, and aLWF contribute to aVOLv in the Central Arctic as well as their month(s) of occurrence. This is done for the entire data period, 1979–2004, first half of the data period, 1979–1991, and the second half of the data period, 1992–2004.

Two images make up each of the figures below (Figures 168-176). In both images, each square outlines a location in the Central Arctic. In the top image, each outlined location has a column of three numbers: the first number, the range in red, denotes the range of atmospheric forcing contribution to aVOLv during the warming months. The second number, in green, denotes the annual average of atmospheric forcing contribution to aVOLv. The third number, in blue, denotes the range of atmospheric forcing contribution to aVOLv during the cooling months. In the bottom image, each outlined location contain the warming and cooling months' maximum and minimum atmospheric forcing contribution to aVOLv along with their specific month(s) of occurrence.

A. 1979-2004

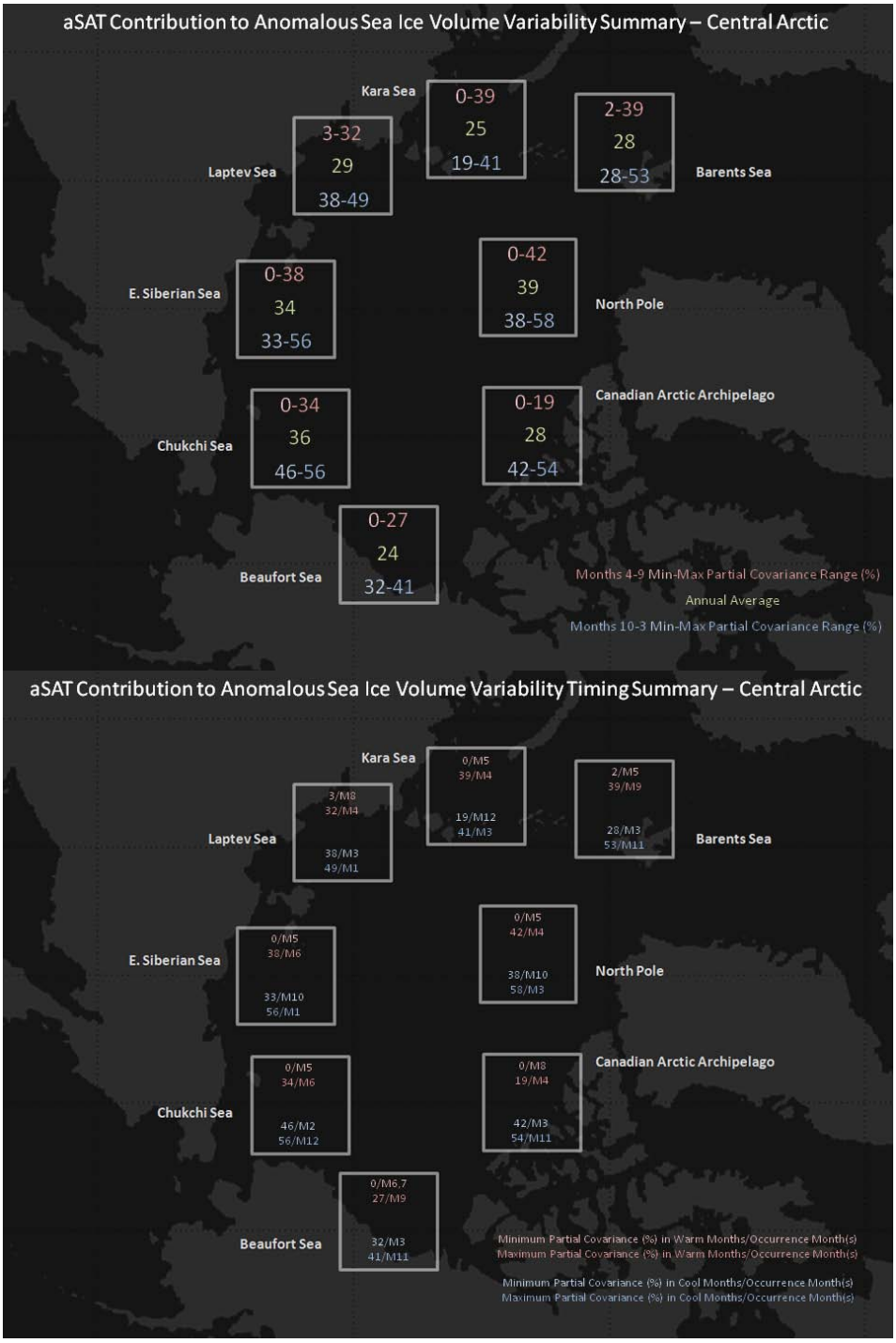

Figure 168. Average (green), Warming Months Minimum-Maximum Range (red), and Cooling Months Minimum-Maximum Range (blue) of aSAT Contribution to aVOLv (top) and Timing of Warming (red) and Cooling (blue) Minimum and Maximum (bottom)—Central Arctic (1979–2004) (same as Figure 44)

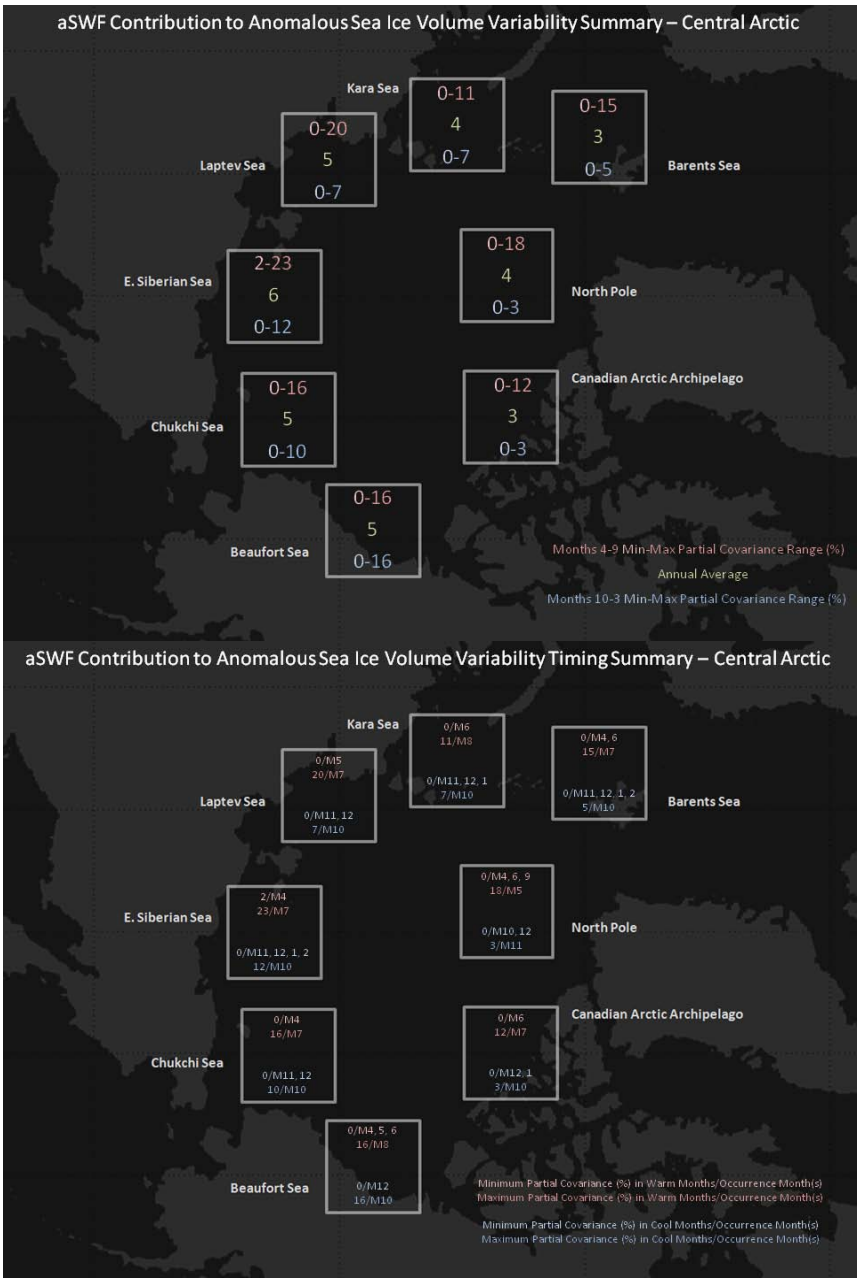

Figure 169. Average (green), Warming Months Minimum-Maximum Range (red), and Cooling Months Minimum-Maximum Range (blue) of aSWF Contribution to aVOLv (top) and Timing of Warming (red) and Cooling (blue) Minimum and Maximum (bottom)—Central Arctic (1979–2004)

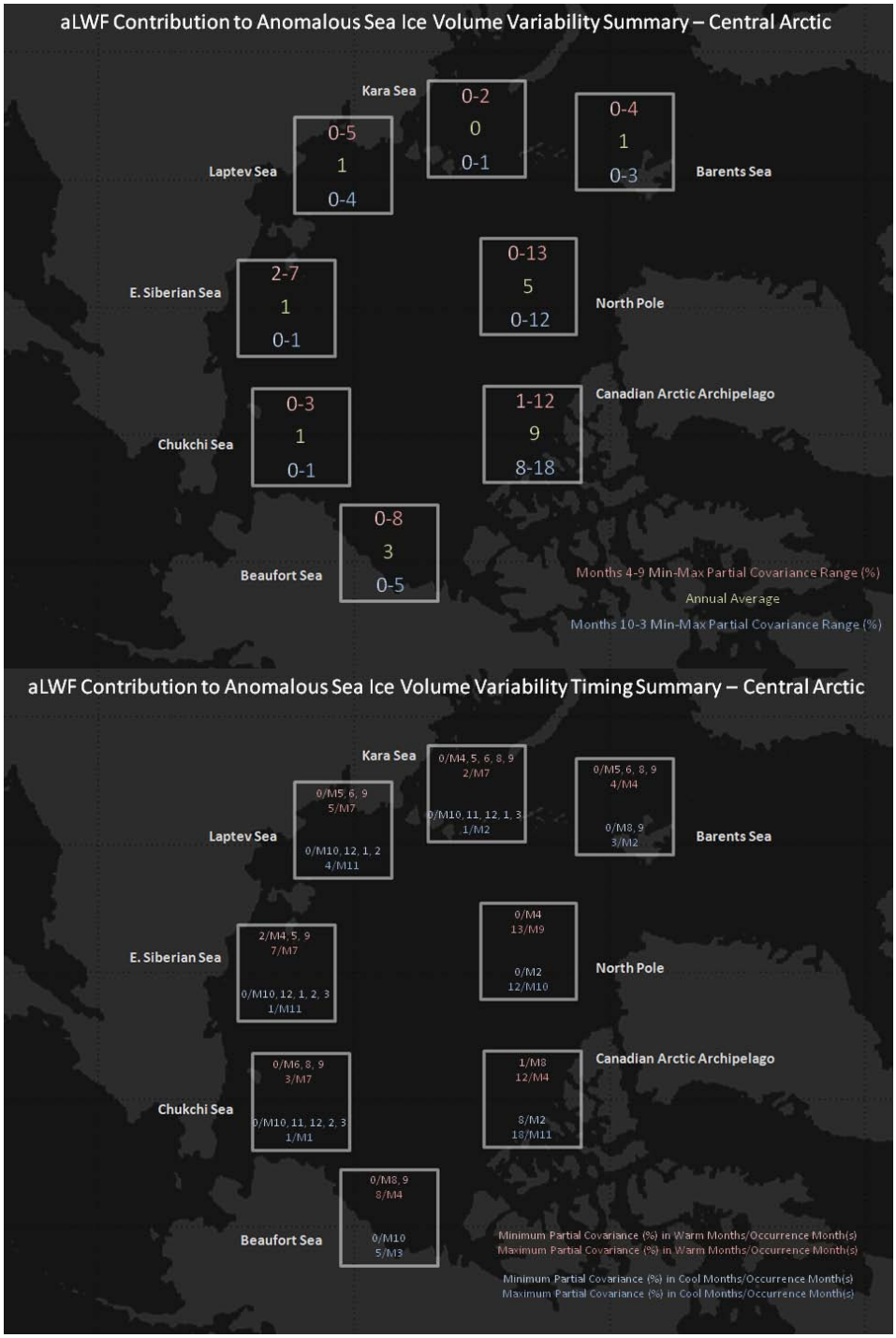

Figure 170. Average (green), Warming Months Minimum-Maximum Range (red), and Cooling Months Minimum-Maximum Range (blue) of aLWF Contribution to aVOLv (top) and Timing of Warming (red) and Cooling (blue) Minimum and Maximum (bottom)—Central Arctic (1979–2004)

B. 1979-1991

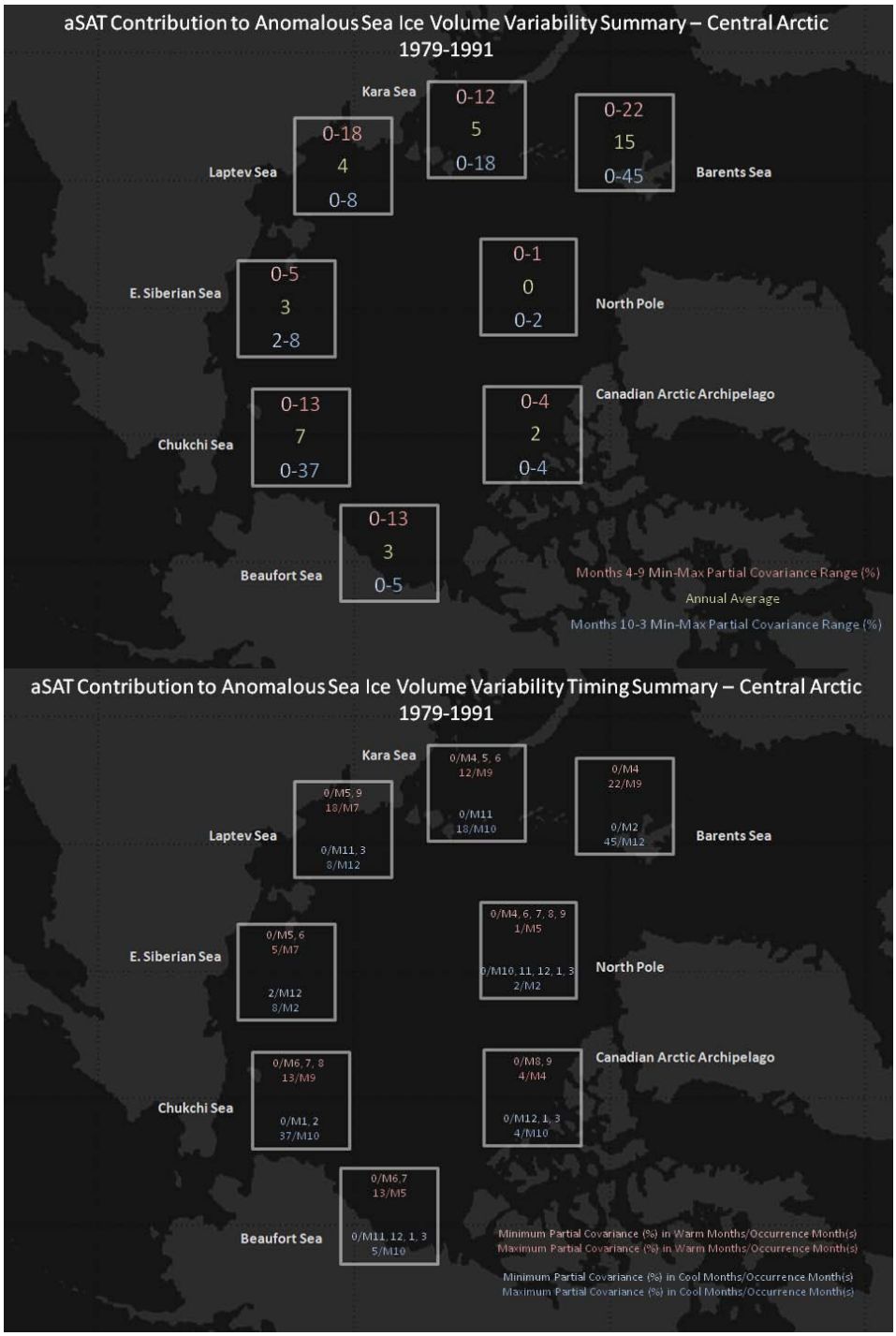

Figure 171. Average (green), Warming Months Minimum-Maximum Range (red), and Cooling Months Minimum-Maximum Range (blue) of aSAT Contribution to aVOLv (top) and Timing of Warming (red) and Cooling (blue) Minimum and Maximum (bottom)—Central Arctic (1979–1991)

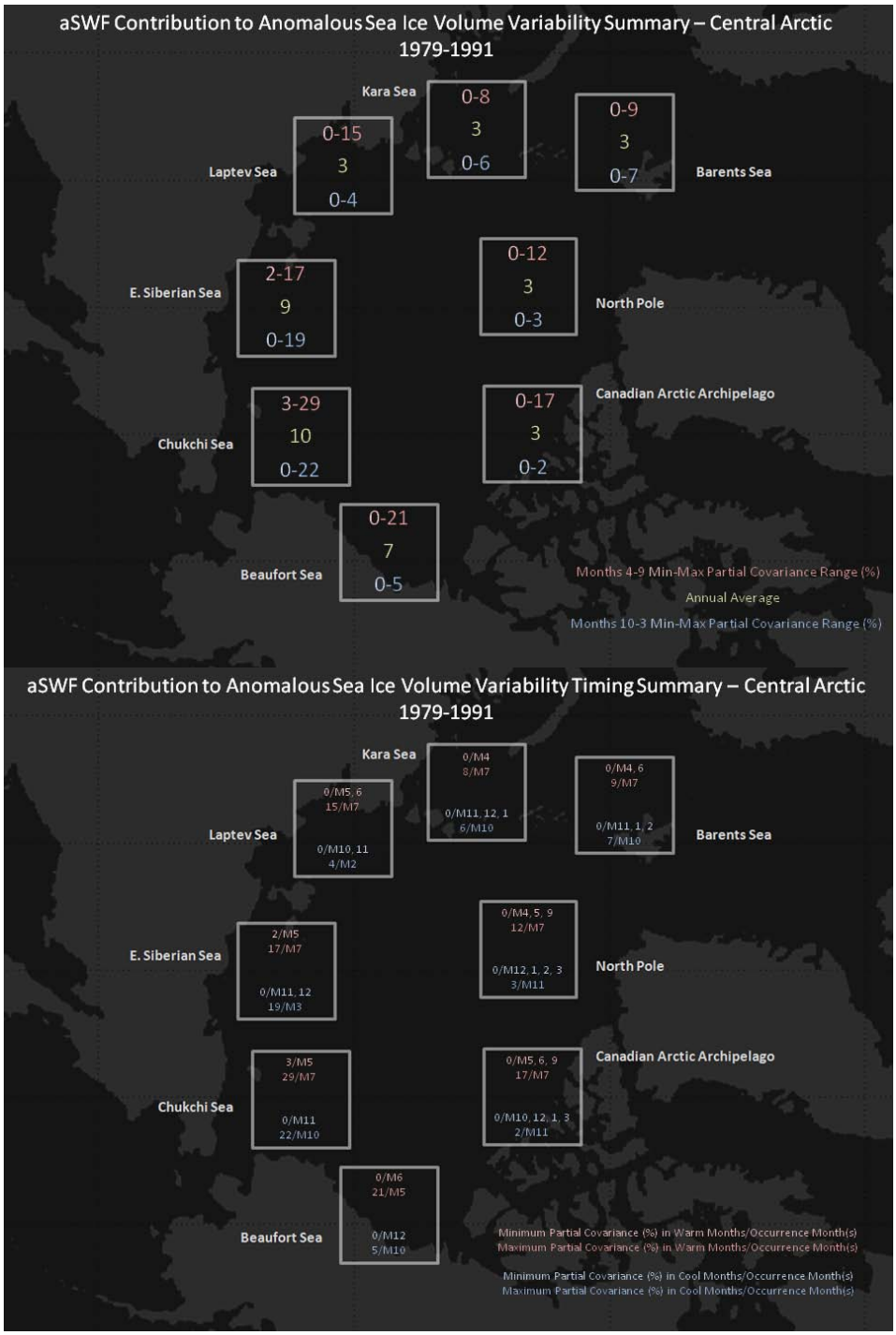

Figure 172. Average (green), Warming Months Minimum-Maximum Range (red), and Cooling Months Minimum-Maximum Range (blue) of aSWF Contribution to aVOLv (top) and Timing of Warming (red) and Cooling (blue) Minimum and Maximum (bottom)—Central Arctic (1979–1991)

Figure 173. Average (green), Warming Months Minimum-Maximum Range (red), and Cooling Months Minimum-Maximum Range (blue) of aLWF Contribution to aVOLv (top) and Timing of Warming (red) and Cooling (blue) Minimum and Maximum (bottom)—Central Arctic (1979–1991)

C. 1992-2004

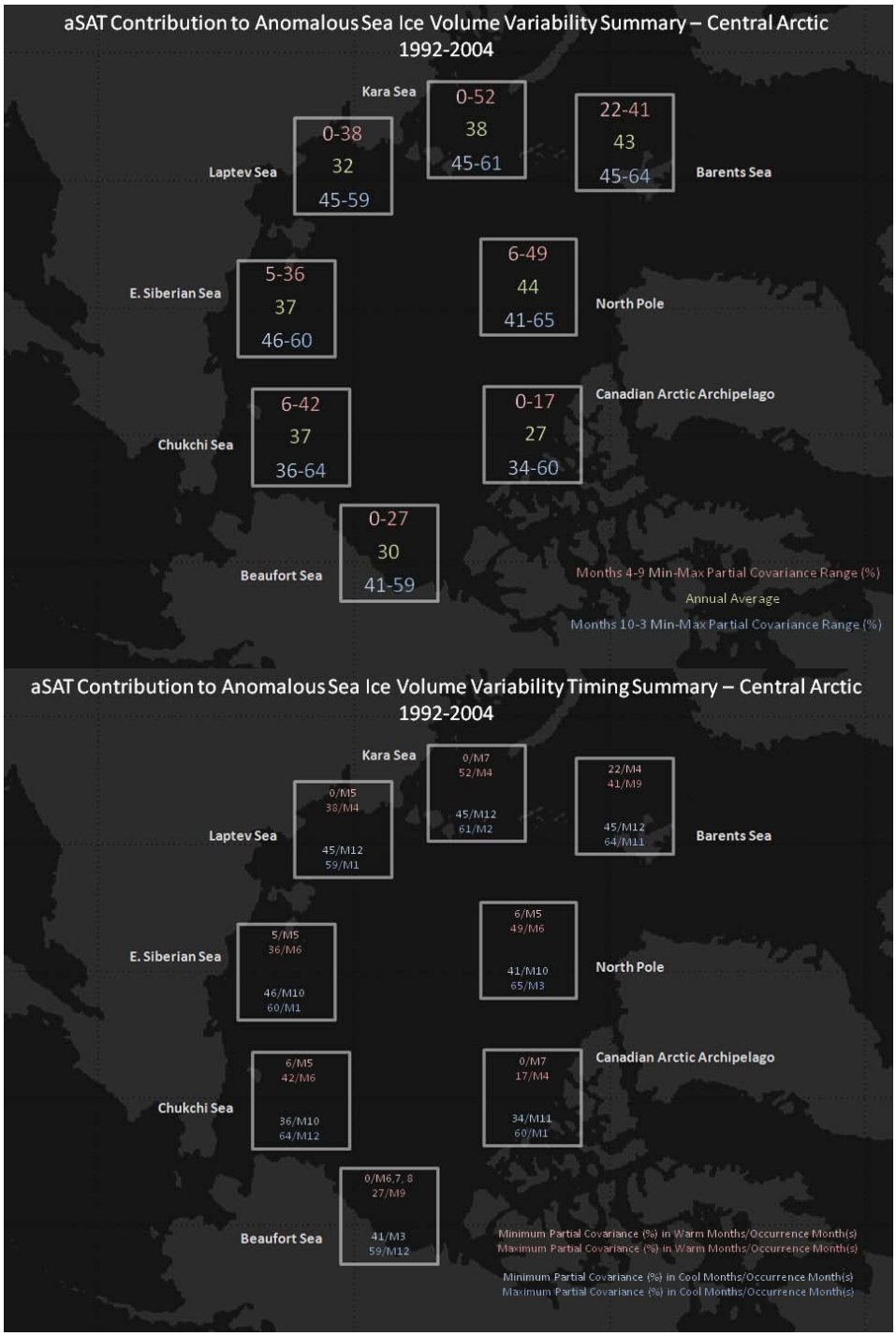

Figure 174. Average (green), Warming Months Minimum-Maximum Range (red), and Cooling Months Minimum-Maximum Range (blue) of aSAT Contribution to aVOLv (top) and Timing of Warming (red) and Cooling (blue) Minimum and Maximum (bottom)—Central Arctic (1992–2004)

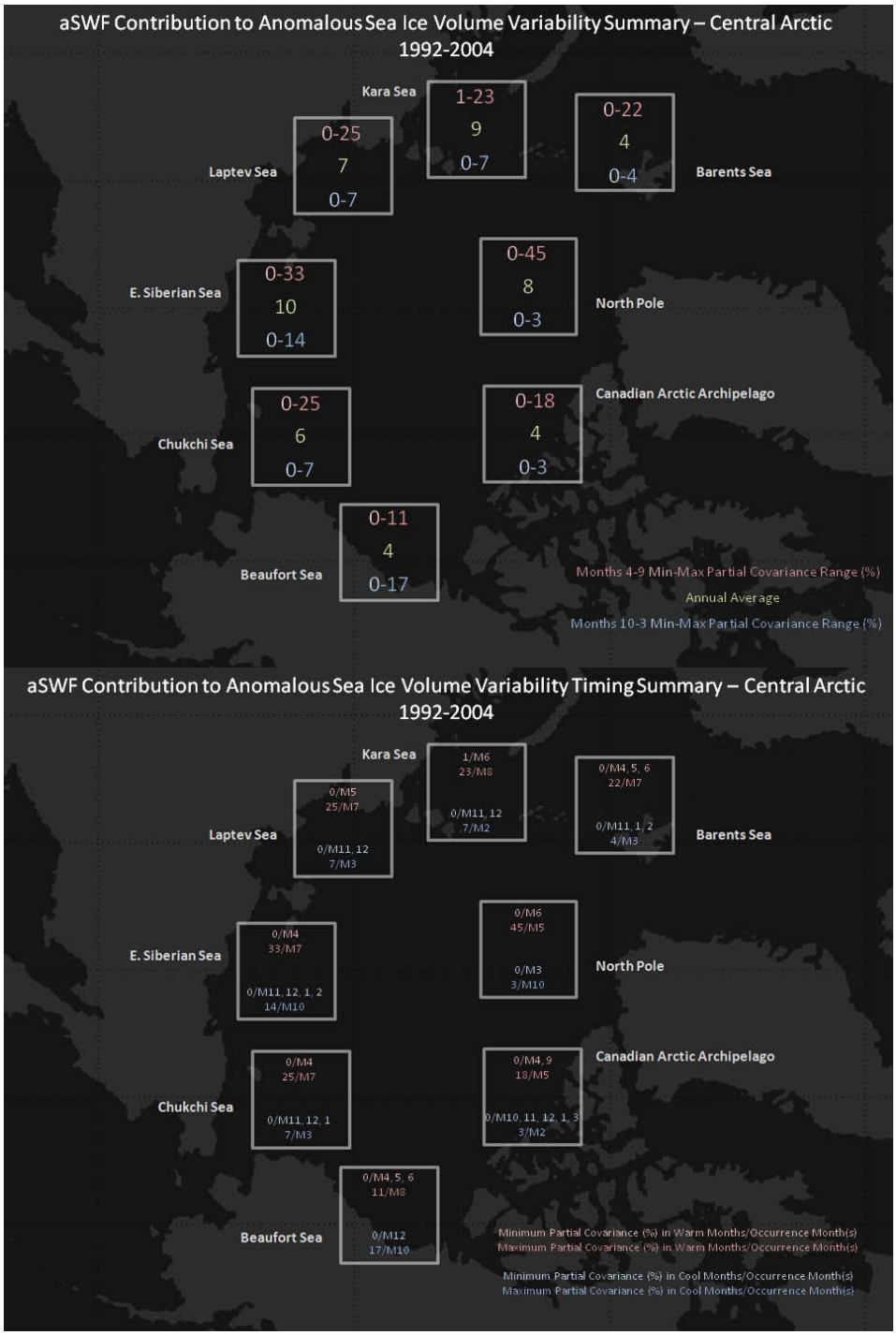

Figure 175. Average (green), Warming Months Minimum-Maximum Range (red), and Cooling Months Minimum-Maximum Range (blue) of aSWF Contribution to aVOLv (top) and Timing of Warming (red) and Cooling (blue) Minimum and Maximum (bottom)—Central Arctic (1992–2004)

Figure 176. Average (green), Warming Months Minimum-Maximum Range (red), and Cooling Months Minimum-Maximum Range (blue) of aLWF Contribution to aVOLv (top) and Timing of Warming (red) and Cooling (blue) Minimum and Maximum (bottom)—Central Arctic (1992–2004)

APPENDIX H: SUMMARY OF ATMOSPHERIC CONTRIBUTION TO ANOMALOUS SEA ICE THICKNESS IN THE CENTRAL ARCTIC

The following graphics provides summaries of the average, minimum, and maximum percentage of aSAT, aSWF, and aLWF contribute to aTHKv in the Central Arctic as well as their month(s) of occurrence. This is done for the entire data period, 1979–2004, first half of the data period, 1979–1991, and the second half of the data period, 1992–2004.

Two images make up each of the figures below (Figures 177-185). In the top image, each square outlines a location in the Central Arctic. Each has a column of three numbers: the first number, the range in red, denotes the range of atmospheric forcing contribution to aTHKv during the warming months. The second number, in green, denotes the annual average of atmospheric forcing contribution to aTHKv. The third number, in blue, denotes the range of atmospheric forcing contribution to aTHKv during the cooling months. In the bottom image, the warming and cooling months' maximum and minimum atmospheric forcing contribution to aTHKv is labeled along with their specific month(s) of occurrence.

A. 1979-2004

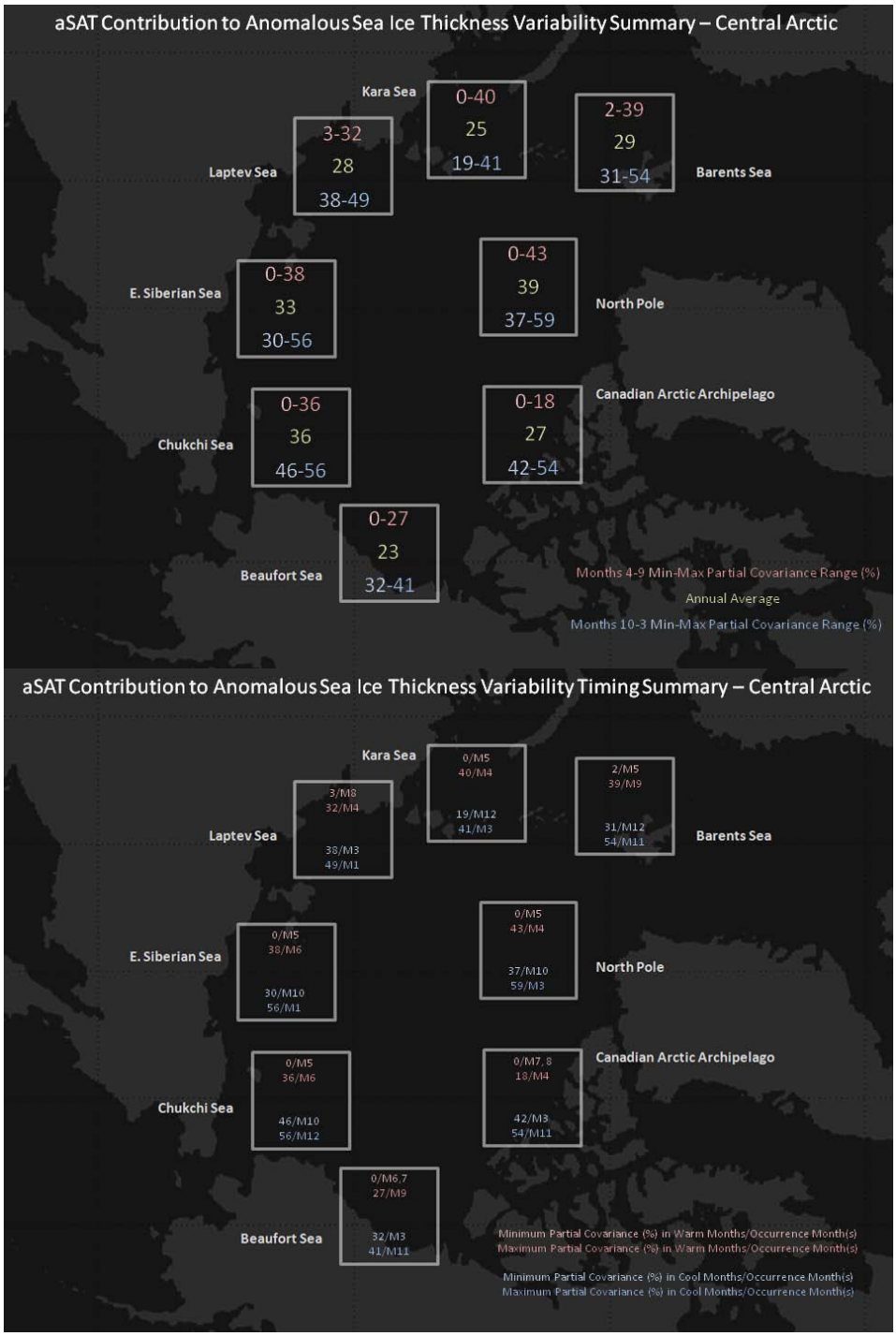

Figure 177. Average (green), Warming Months Minimum-Maximum Range (red), and Cooling Months Minimum-Maximum Range (blue) of aSAT Contribution to aTHKv (top) and Timing of Warming (red) and Cooling (blue) Minimum and Maximum (bottom)—Central Arctic (1979–2004)

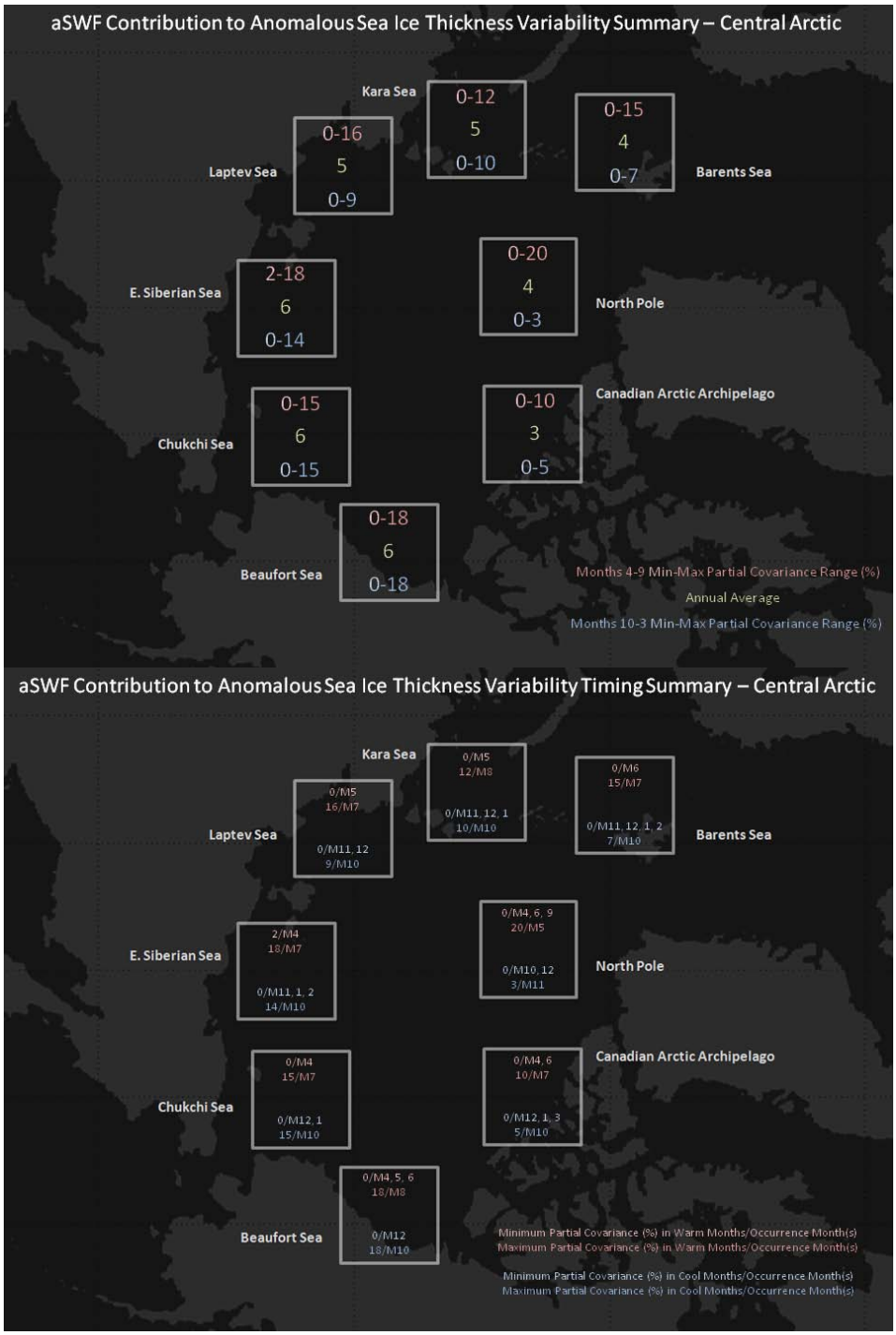

Figure 178. (Top) Average (green), Warming Months Minimum-Maximum Range (red), and Cooling Months Minimum-Maximum Range (blue) of aSWF Contribution to aTHKv (top) and Timing of Warming (red) and Cooling (blue) Minimum and Maximum (bottom)—Central Arctic (1979–2004)

Figure 179. Average (green), Warming Months Minimum-Maximum Range (red), and Cooling Months Minimum-Maximum Range (blue) of aLWF Contribution to aTHKv (top) and Timing of Warming (red) and Cooling (blue) Minimum and Maximum (bottom)—Central Arctic (1979–2004)

B. 1979-1991

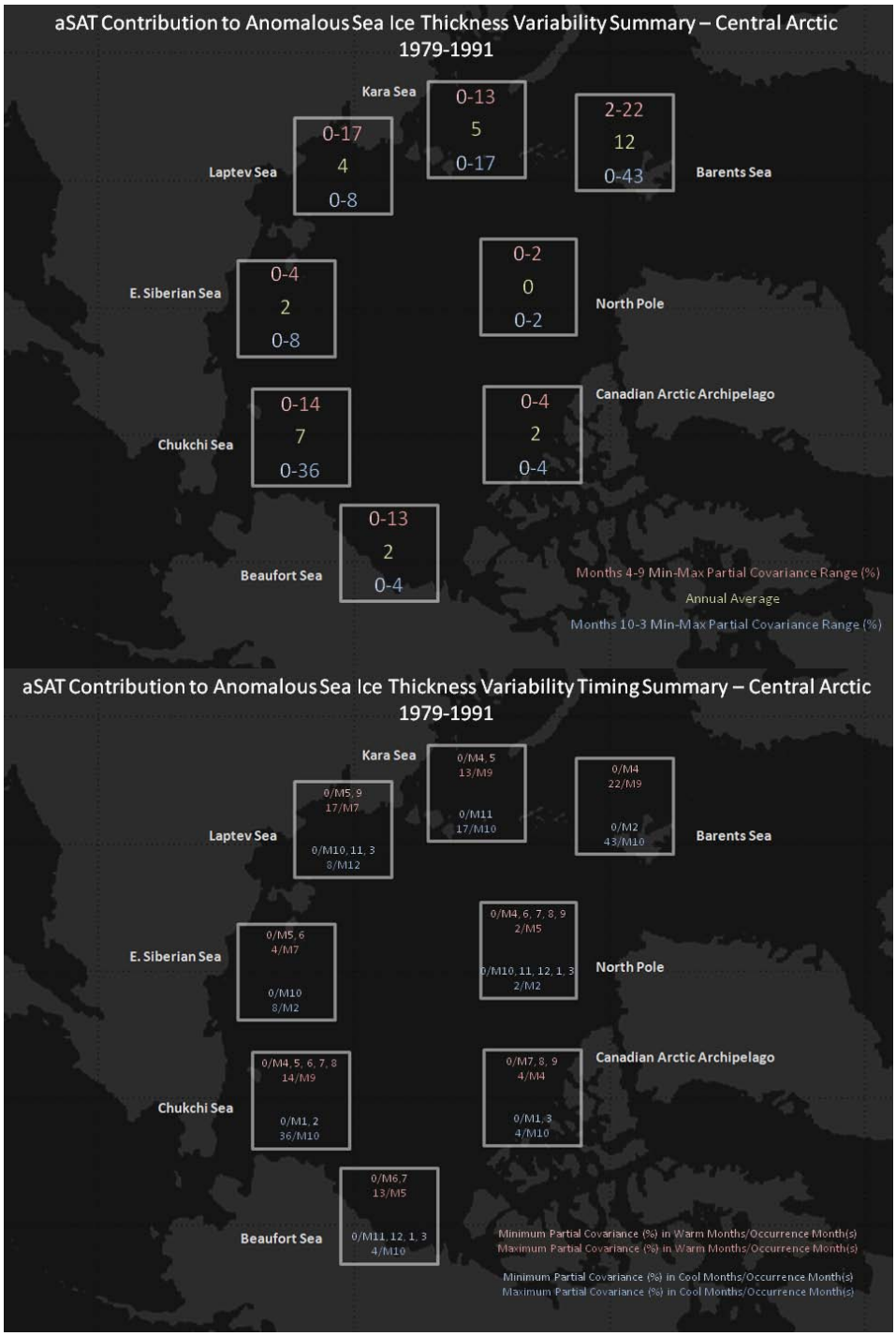

Figure 180. Average (green), Warming Months Minimum-Maximum Range (red), and Cooling Months Minimum-Maximum Range (blue) of aSAT Contribution to aTHKv (top) and Timing of Warming (red) and Cooling (blue) Minimum and Maximum (bottom)—Central Arctic (1979–1991)

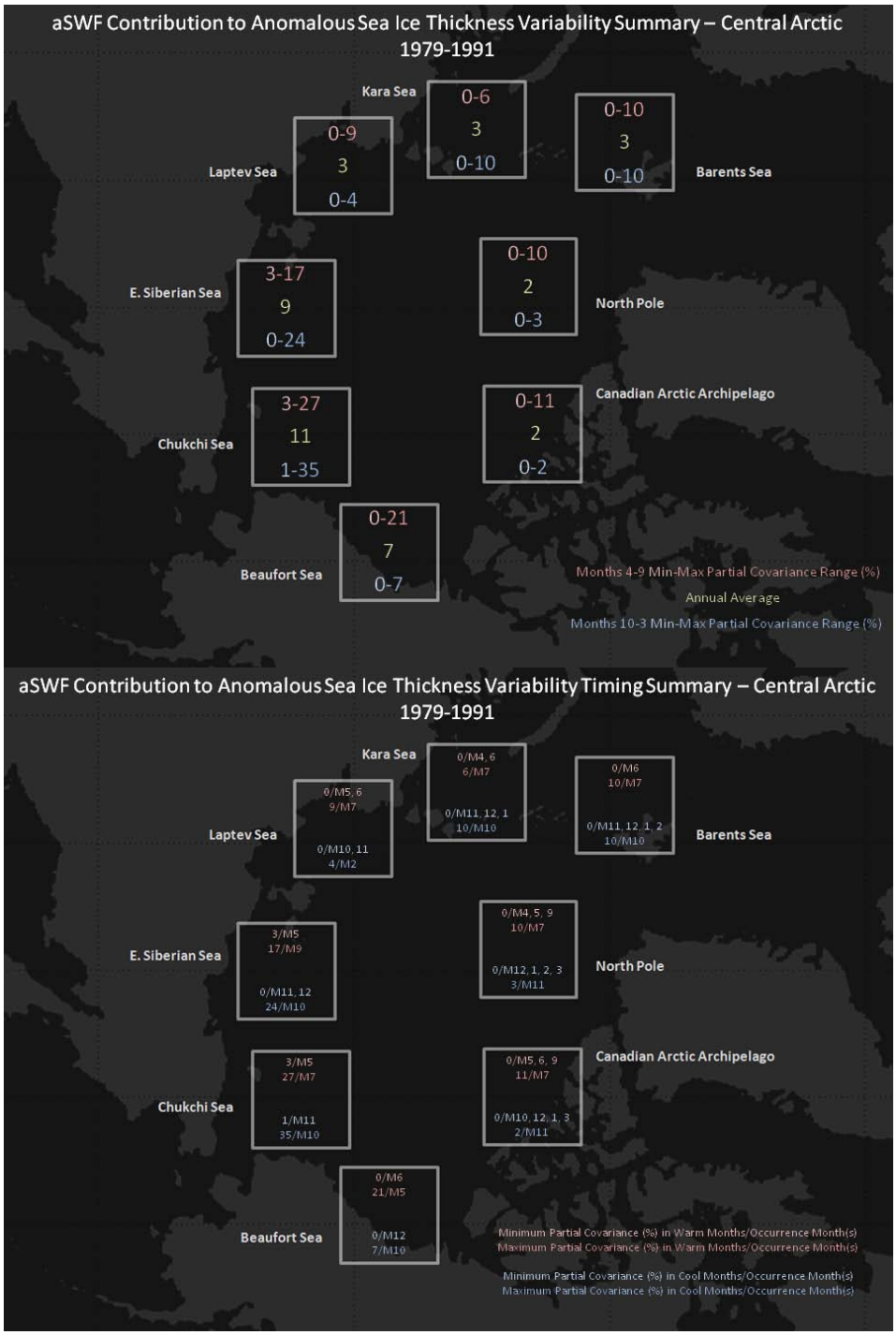

Figure 181. Average (green), Warming Months Minimum-Maximum Range (red), and Cooling Months Minimum-Maximum Range (blue) of aSWF Contribution to aTHKv (top) and Timing of Warming (red) and Cooling (blue) Minimum and Maximum (bottom)—Central Arctic (1979–1991)

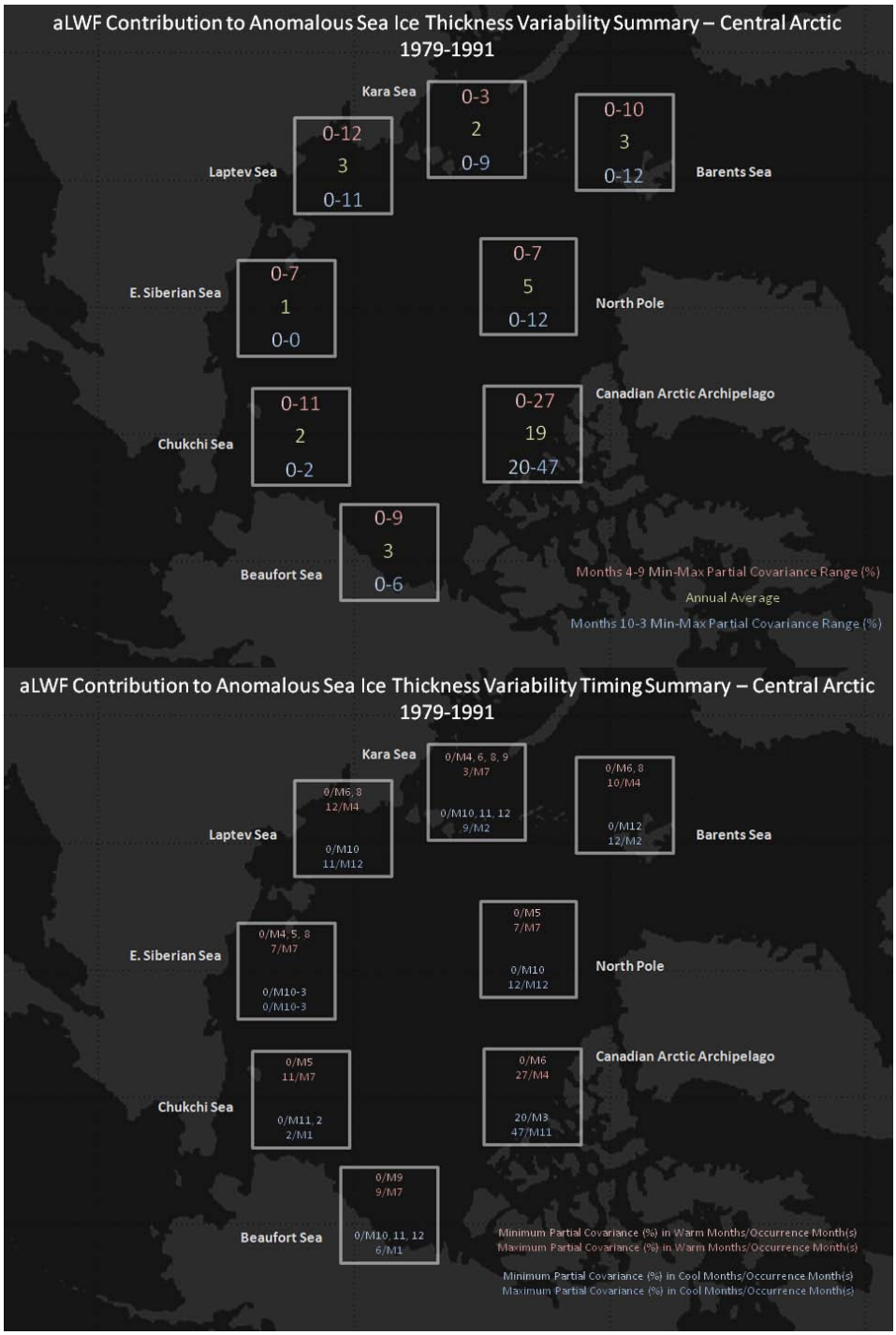

Figure 182. Average (green), Warming Months Minimum-Maximum Range (red), and Cooling Months Minimum-Maximum Range (blue) of aLWF Contribution to aTHKv (top) and Timing of Warming (red) and Cooling (blue) Minimum and Maximum (bottom)—Central Arctic (1979–1991)

C. 1992-2004

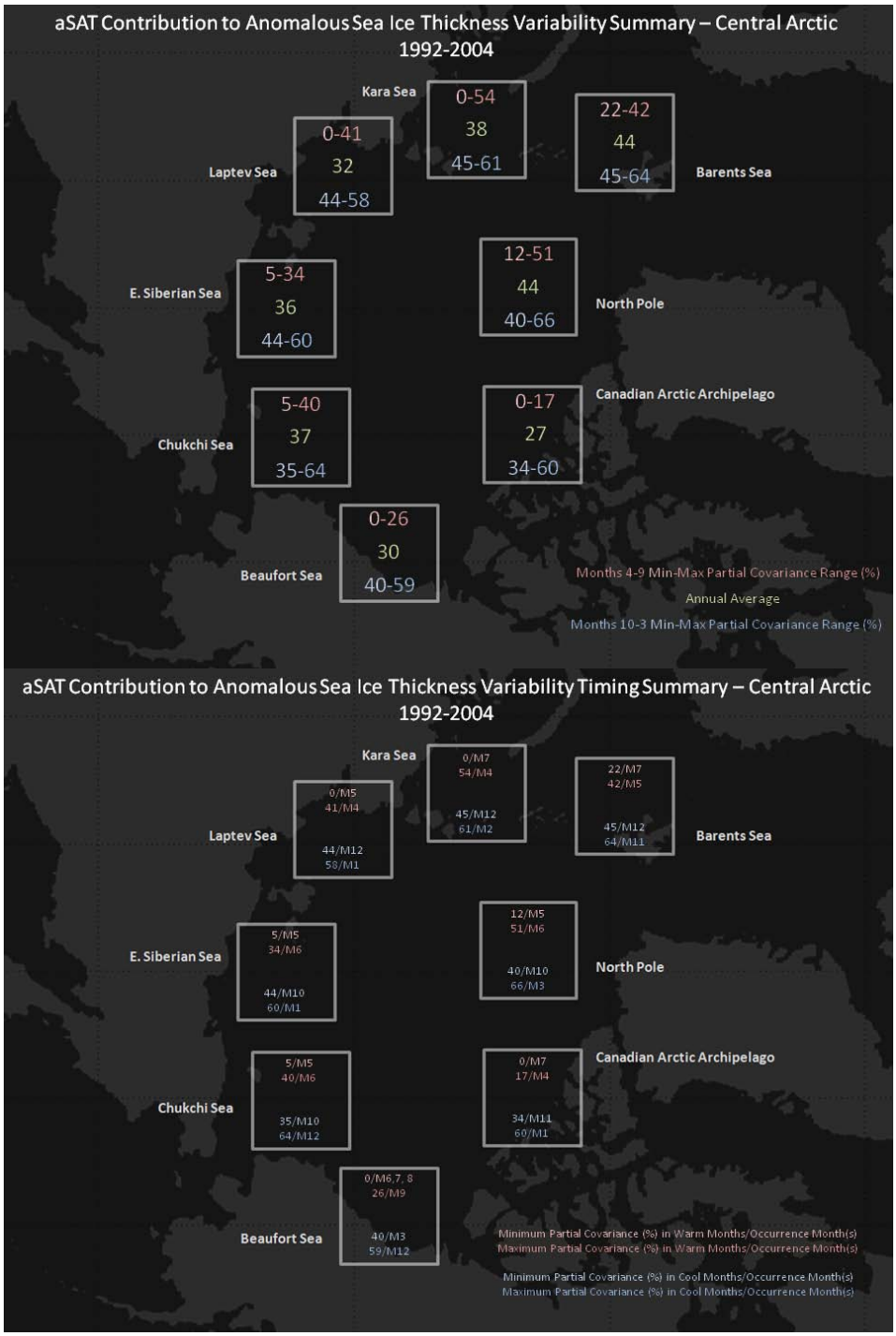

Figure 183. Average (green), Warming Months Minimum-Maximum Range (red), and Cooling Months Minimum-Maximum Range (blue) of aSAT Contribution to aTHKv (top) and Timing of Warming (red) and Cooling (blue) Minimum and Maximum (bottom)—Central Arctic (1992–2004)

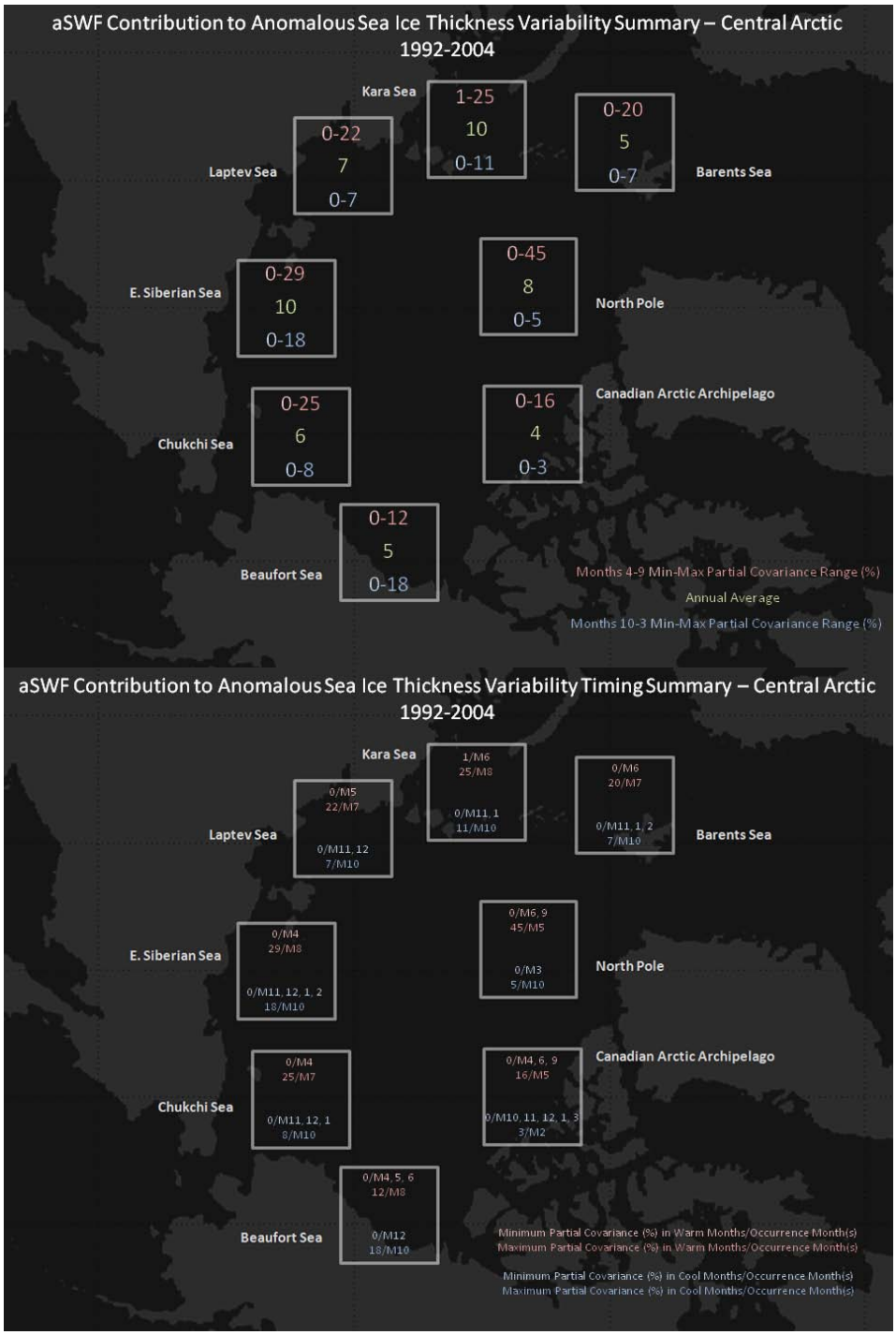

Figure 184. Average (green), Warming Months Minimum-Maximum Range (red), and Cooling Months Minimum-Maximum Range (blue) of aSWF Contribution to aTHKv (top) and Timing of Warming (red) and Cooling (blue) Minimum and Maximum (bottom)—Central Arctic (1992–2004)

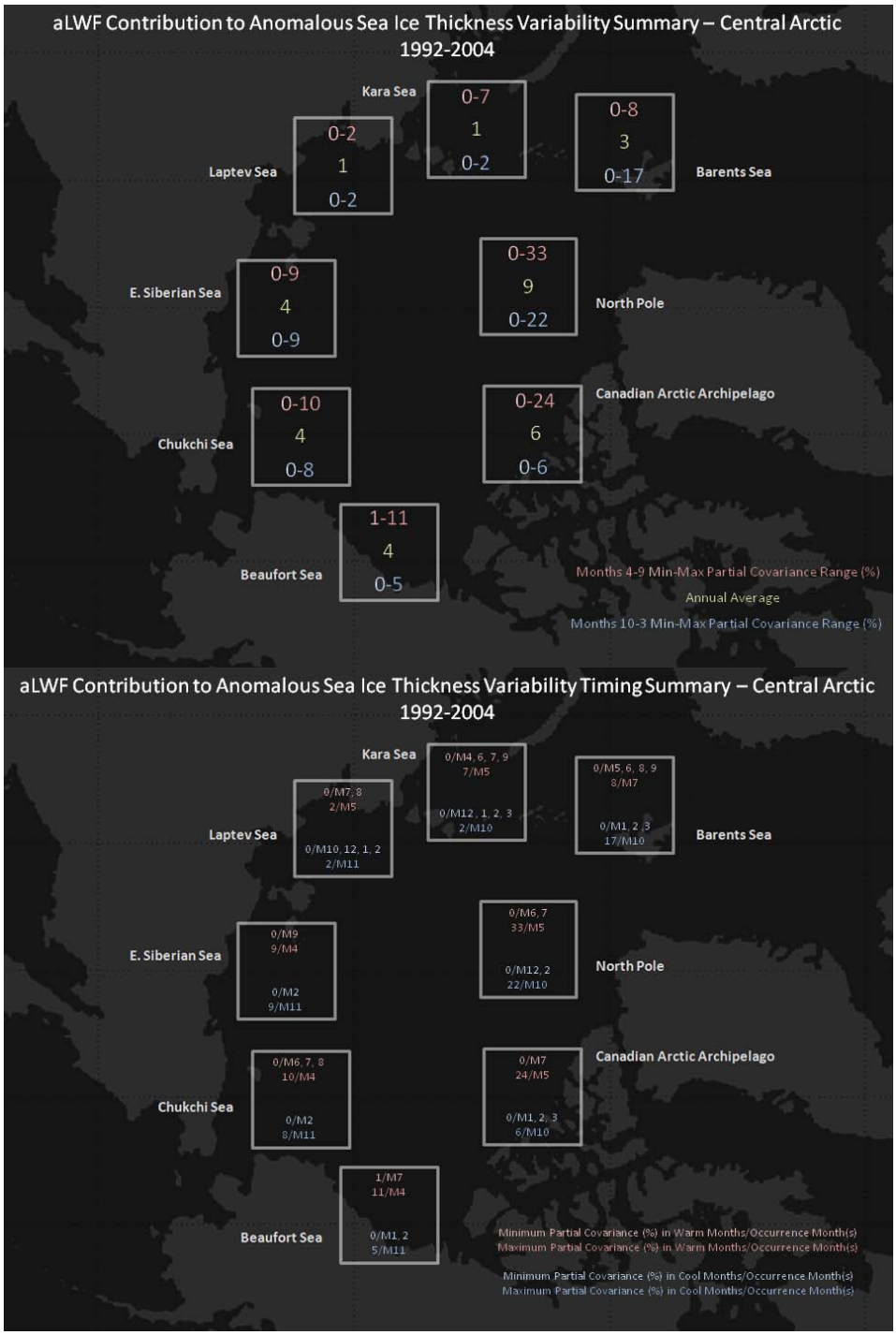

Figure 185. Average (green), Warming Months Minimum-Maximum Range (red), and Cooling Months Minimum-Maximum Range (blue) of aLWF Contribution to aTHKv (top) and Timing of Warming (red) and Cooling (blue) Minimum and Maximum (bottom)—Central Arctic (1992–2004)

APPENDIX I: SUMMARY OF ATMOSPHERIC CONTRIBUTION TO ANOMALOUS SEA ICE AREA VARIABILITY IN THE CENTRAL ARCTIC

The following graphics provides summaries of the average, minimum, and maximum percentage of aSAT, aSWF, and aLWF contribute to aARAv in the Central Arctic as well as their month(s) of occurrence. This is done for the entire data period, 1979–2004, first half of the data period, 1979–1991, and the second half of the data period, 1992–2004.

Two images make up each of the figures below (Figures 186-194). In the top image, each square outlines a location in the Central Arctic. Each has a column of three numbers: the first number, the range in red, denotes the range of atmospheric forcing contribution to aARAv during the warming months. The second number, in green, denotes the annual average of atmospheric forcing contribution to aARAv. The third number, in blue, denotes the range of atmospheric forcing contribution to aARAv during the cooling months. In the bottom image, the warming and cooling months' maximum and minimum atmospheric forcing contribution to aARAv is labeled along with their specific month(s) of occurrence.

A. 1979-2004

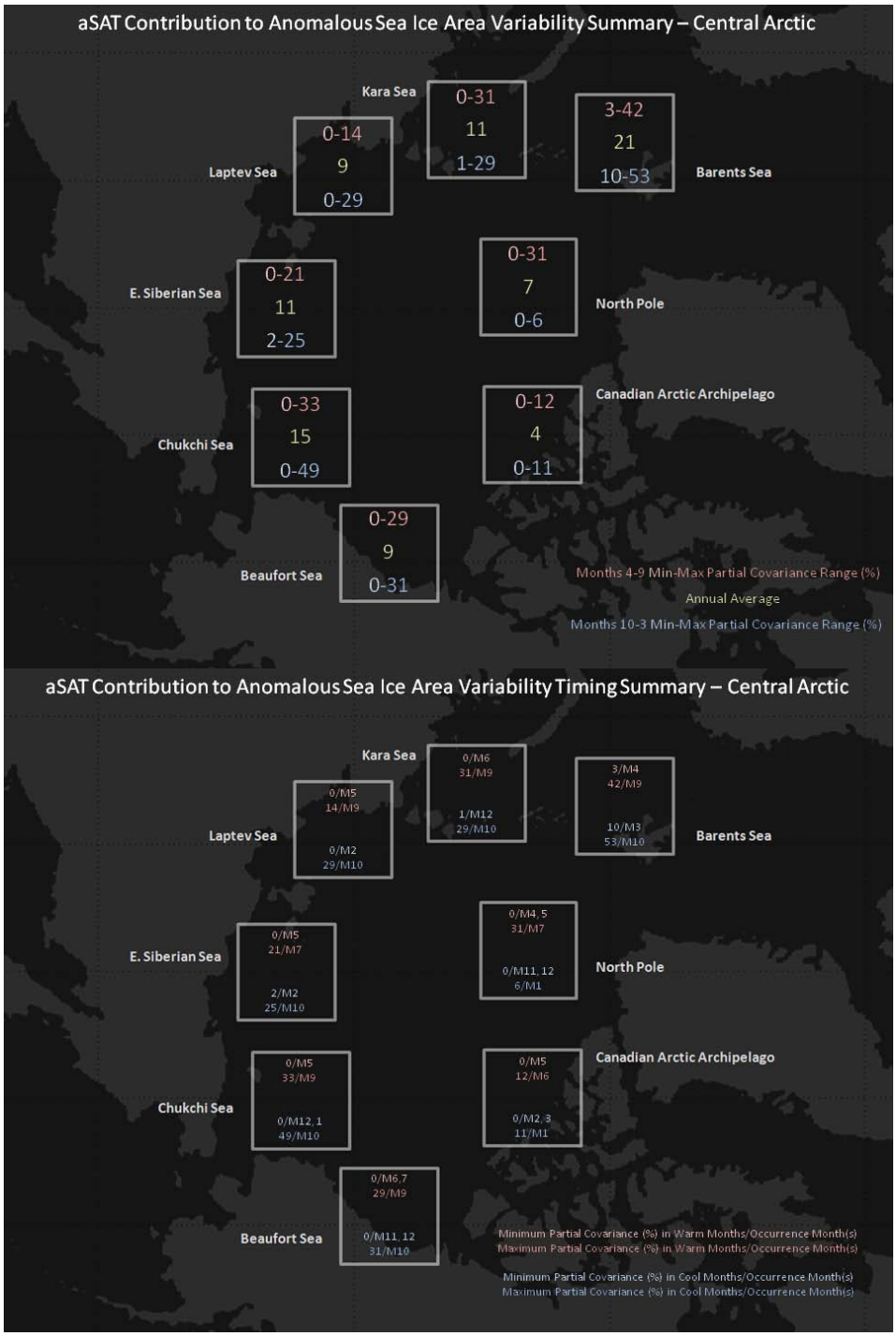

Figure 186. Average (green), Warming Months Minimum-Maximum Range (red), and Cooling Months Minimum-Maximum Range (blue) of aSAT Contribution to aARAv (top) and Timing of Warming (red) and Cooling (blue) Minimum and Maximum (bottom)—Central Arctic (1979–2004)

Figure 187. Average (green), Warming Months Minimum-Maximum Range (red), and Cooling Months Minimum-Maximum Range (blue) of aSWF Contribution to aARAv (top) and Timing of Warming (red) and Cooling (blue) Minimum and Maximum (bottom)—Central Arctic (1979–2004)

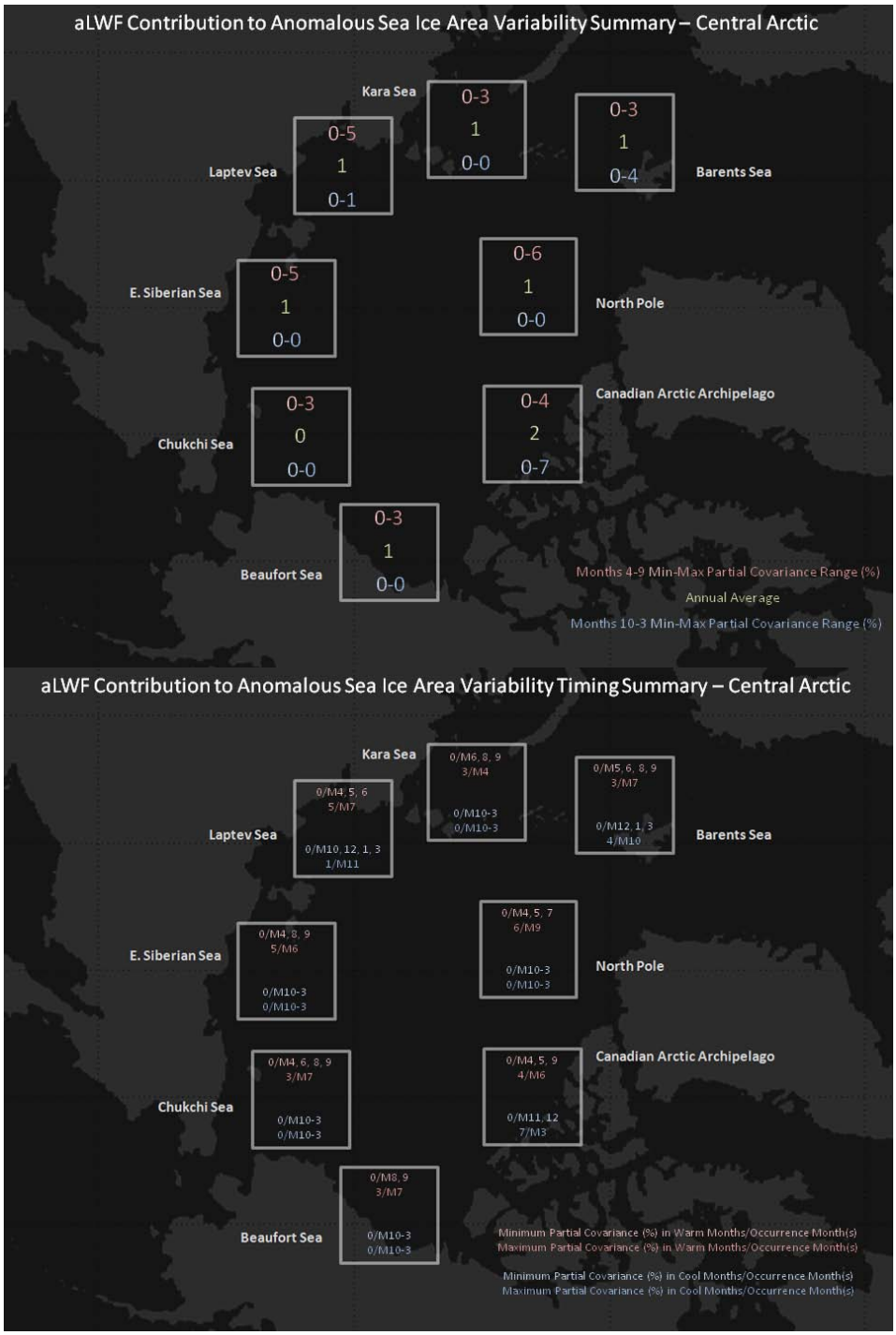

Figure 188. Average (green), Warming Months Minimum-Maximum Range (red), and Cooling Months Minimum-Maximum Range (blue) of aLWF Contribution to aARAv (top) and Timing of Warming (red) and Cooling (blue) Minimum and Maximum (bottom)—Central Arctic (1979–2004)

B. 1979-1991

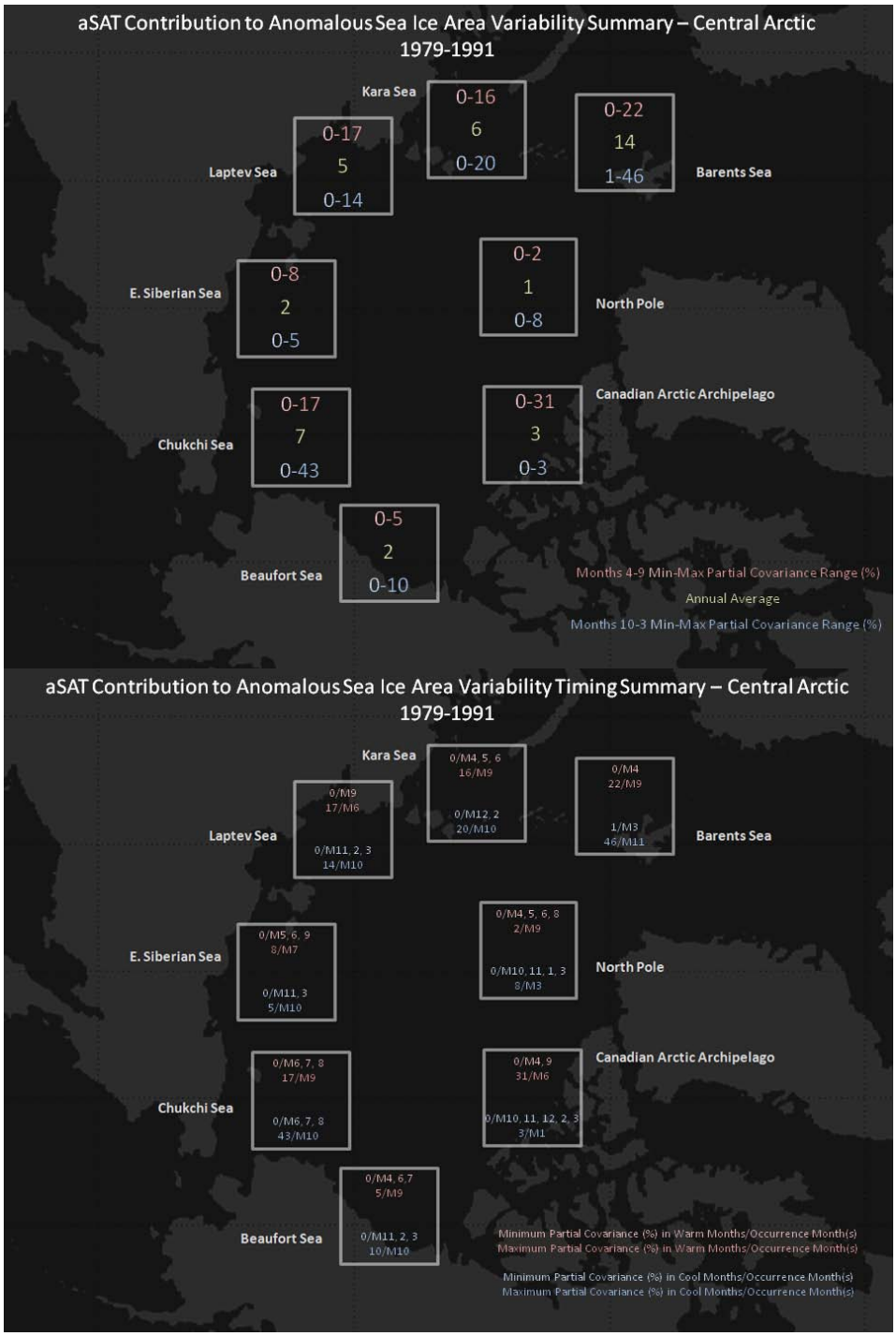

Figure 189. Average (green), Warming Months Minimum-Maximum Range (red), and Cooling Months Minimum-Maximum Range (blue) of aSAT Contribution to aARAv (top) and Timing of Warming (red) and Cooling (blue) Minimum and Maximum (bottom)—Central Arctic (1979–1991)

Figure 190. Average (green), Warming Months Minimum-Maximum Range (red), and Cooling Months Minimum-Maximum Range (blue) of aSWF Contribution to aARAv (top) and Timing of Warming (red) and Cooling (blue) Minimum and Maximum (bottom)—Central Arctic (1979–1991)

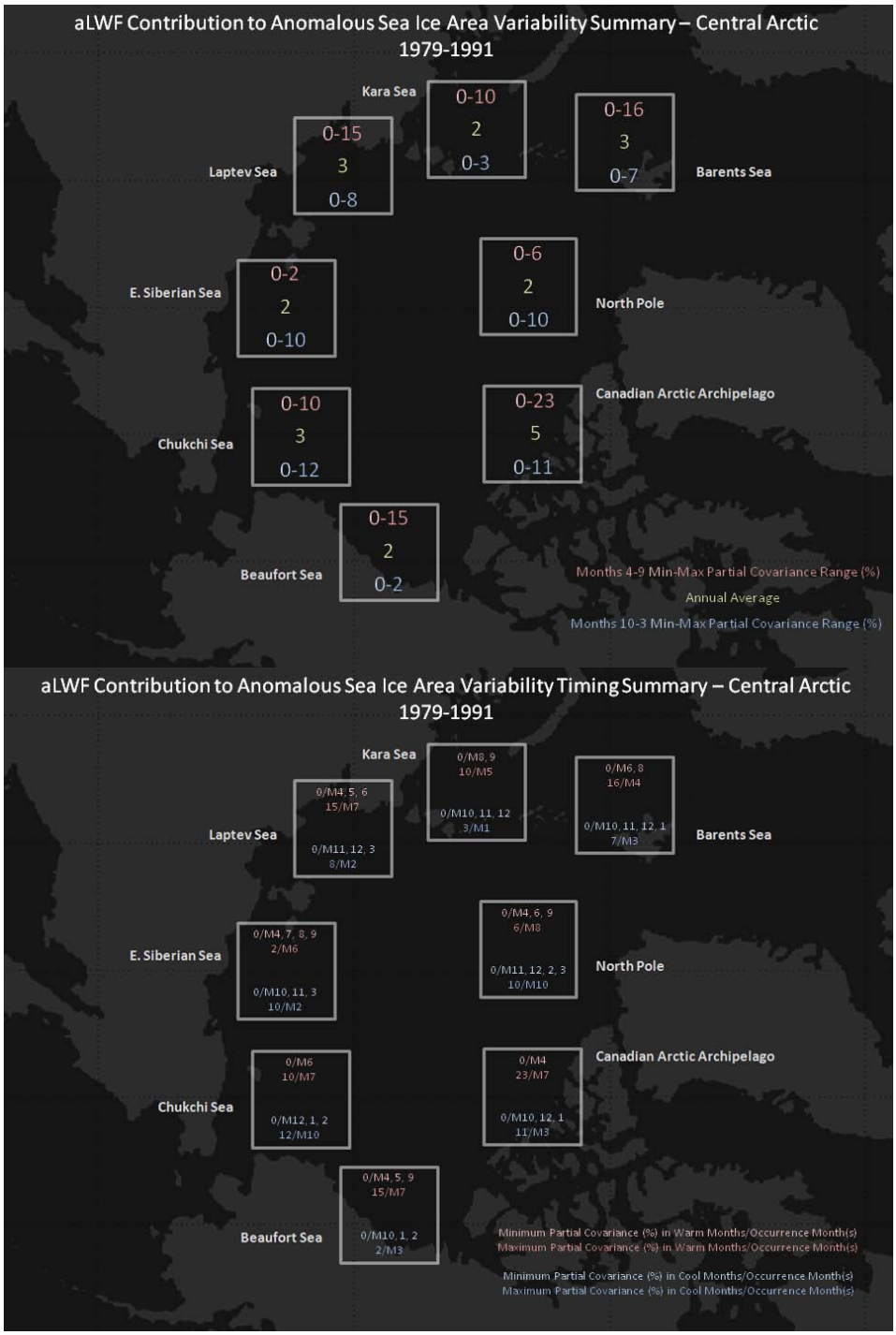

Figure 191. Average (green), Warming Months Minimum-Maximum Range (red), and Cooling Months Minimum-Maximum Range (blue) of aLWF Contribution to aARAv (top) and Timing of Warming (red) and Cooling (blue) Minimum and Maximum (bottom)—Central Arctic (1979–1991)

C. 1992-2004

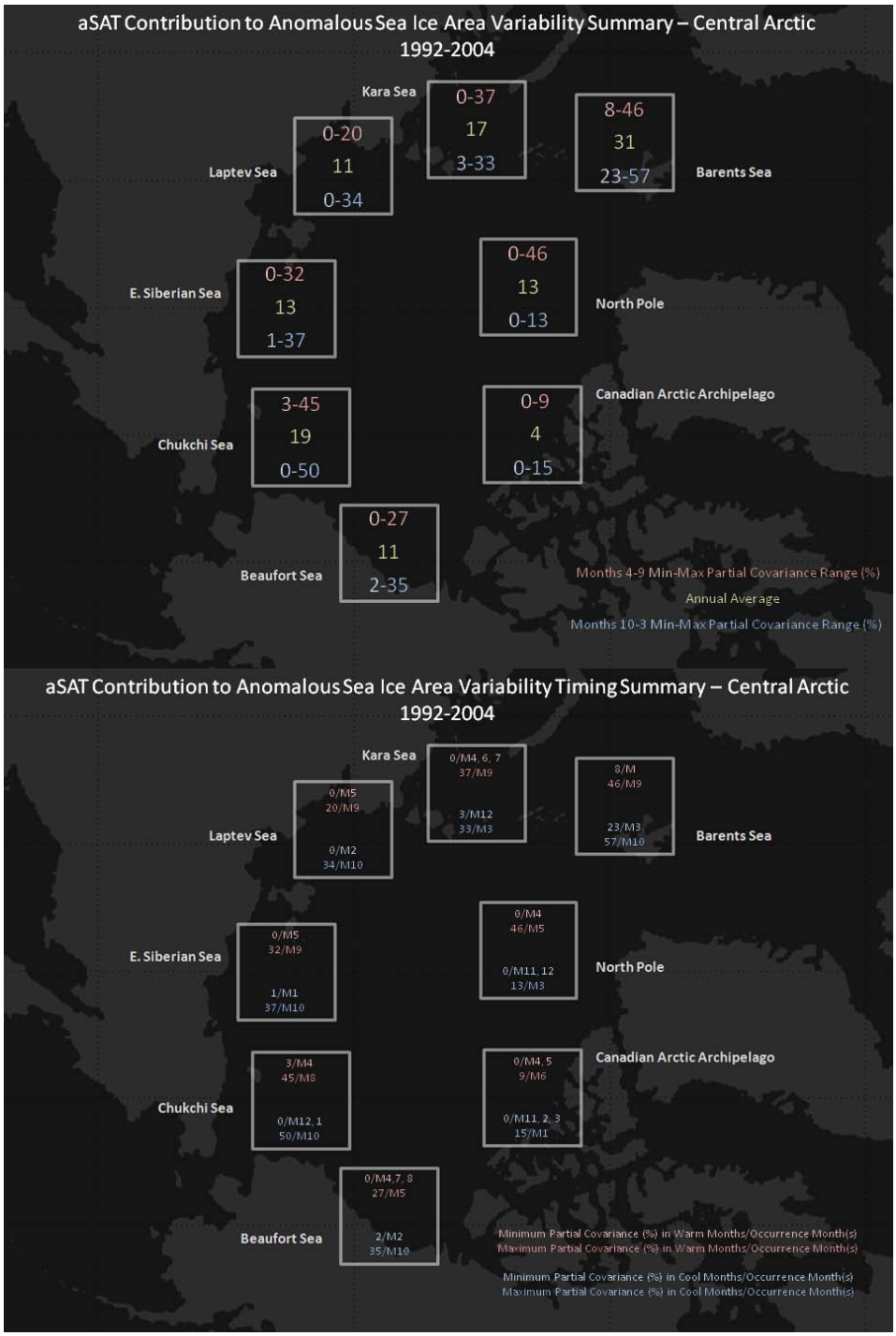

Figure 192. Average (green), Warming Months Minimum-Maximum Range (red), and Cooling Months Minimum-Maximum Range (blue) of aSAT Contribution to aARAv (top) and Timing of Warming (red) and Cooling (blue) Minimum and Maximum (bottom)—Central Arctic (1992–2004)

Figure 193. Average (green), Warming Months Minimum-Maximum Range (red), and Cooling Months Minimum-Maximum Range (blue) of aSWF Contribution to aARAv (top) and Timing of Warming (red) and Cooling (blue) Minimum and Maximum (bottom)—Central Arctic (1992–2004)

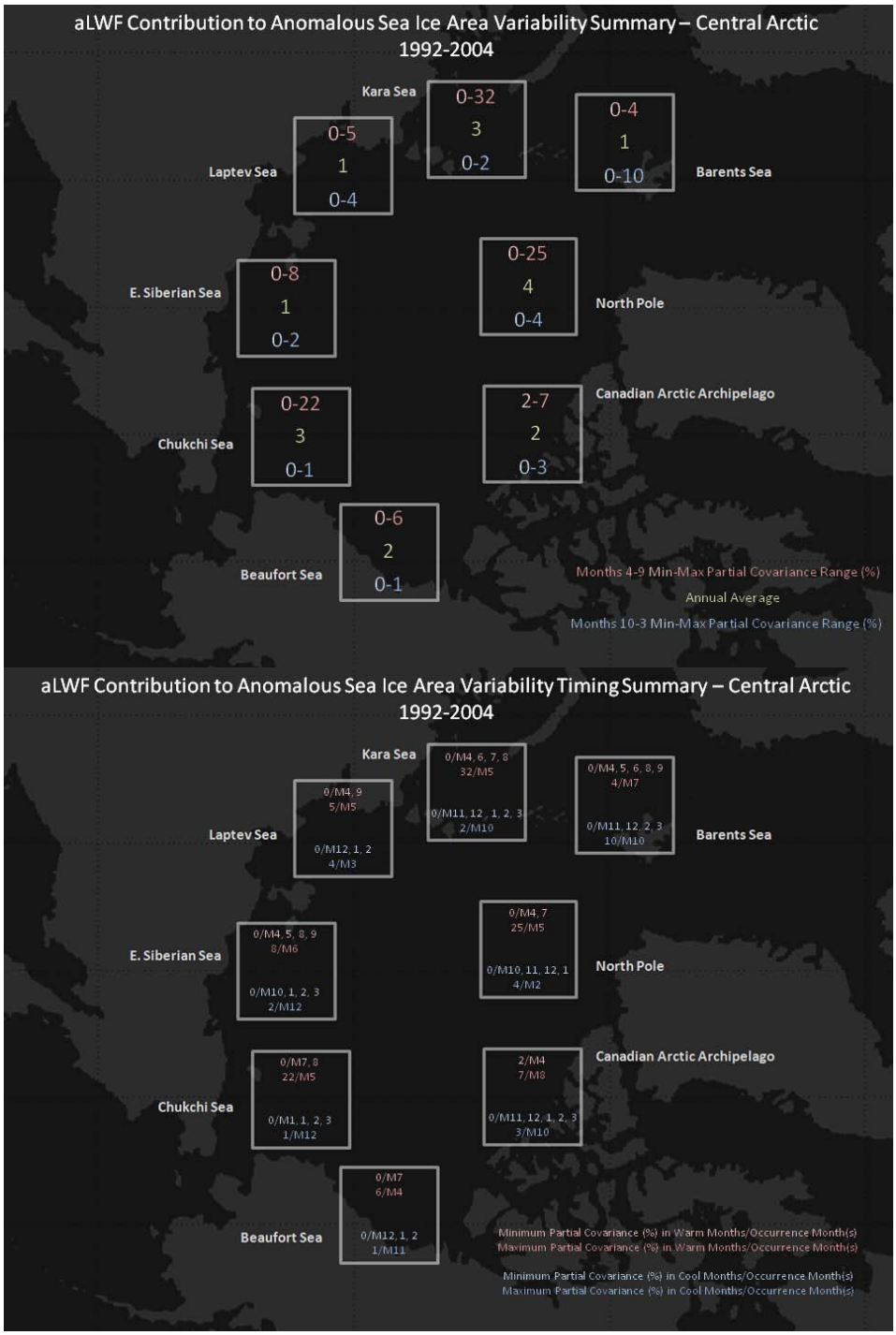

Figure 194. Average (green), Warming Months Minimum-Maximum Range (red), and Cooling Months Minimum-Maximum Range (blue) of aLWF Contribution to aARAv (top) and Timing of Warming (red) and Cooling (blue) Minimum and Maximum (bottom)—Central Arctic (1992–2004)

LIST OF REFERENCES

Ackerman, J. T., 2008: Climate Change, National Security, and the *Quadrennial Defense Review*: Avoiding the Perfect Storm. *Strategic Studies Quarterly*, 56–96.

Andres, R. B., 2009: Prospective U.S. Military Strategy in the Face of Military Tension in the Arctic Over Emerging Energy Resources. *Proc. 3rd Symposium on the Impact of an Ice-Diminishing Arctic on Naval and Maritime Operations*, U.S. Naval Academy, MD.

Barry, R. G., M. C. Serreze, J. A. Maslanik, and R. H. Preller, 1993: The Arctic sea ice-climate system: Observations and Modeling. *Reviews of Geophysics*, **31**, 397–422.

Belchansky, G.I., D.C. Douglas, and N.G. Platonov, 2004: Duration of the Arctic Sea Ice Melt Season: Regional and Interannual Variability, 1979–2001. *J. Climate*, **17**, 67–80.

Bernstein, I. H., C. P. Garbin, and G. K. Teng, 1988: Statistical Control: A First Look at Multivariate Relations. Springer-Verlag, 8 pp.

Bird, K. J., R.R. Charpentier, D.L. Gautier, D.W. Houseknecht, T.R. Klett, J.K. Pitman, T.E. Moore, C.J. Schenk, M.E. Tennyson, and C.J. Wandrey, 2008: Circum-Arctic Resource Appraisal: Estimates of Undiscovered Oil and Gas North of the Arctic Circle. U.S. Geological Survey Fact Sheet 2008-3049. Retrieved from http://pubs.usgs.gov/fs/2008/3049 (accessed 28 December 2009).

Bishop Allen Academy Model United Nations Conference, 2009: BAMUN 2009: Background Guide. Toronto, Ontario, BAMUN. Retrieved from http://www.bamun.org/docs/NATO%20-%20Arctic%20Sovereignty.pdf (accessed 29 December 2009).

Borgerson, S. G., 2008: Arctic Meltdown: The Economic Security Implications of Global Warming. *Foreign Affairs*, **8**, 63–77.

————, 2009: Statement of Scott G. Borgerson, Visiting Fellow for Ocean Governance at the Council on Foreign Relations, Before the Committee on Foreign Affairs, U.S. House of Representatives.

Bowles, D., 2010: Air Force, navy support functions begin merging into Joint Base Charleston. Retrieved from http://www.af.mil/news/story_print.asp?id=123189940 (accessed 10 February 2010).

Braithwaite, L., 2009: Changing Ice Conditions: The North American Ice Service (NAIS) Challenge. *Proc. 3rd Symposium on the Impact of an Ice-Diminishing Arctic on Naval and Maritime Operations,* U.S. Naval Academy, MD.

Broecker, W. S., 1999: What If the Conveyor Were to Shut Down? Reflections on a Possible Outcome of the Great Global Experiment. *GSA Today*, **9**, 1.

Clement, J. L., W. Maslowski, L. W. Cooper, J. M. Grebmeier, and W. Walczowski, 2005: Ocean circulation and exchanges through the northern Bering Sea - 1979-2001 model results. *Deep Sea Research Part II: Topical Studies in Oceanography,* **52**, 3509–3540, doi:10.1016/j.dsr2.2005.09.010.

CNA, 2009: Impact of Climate Change on Naval Operations in the Arctic.

Curry, J. A., J.L. Schramm, and E.E. Ebert, 1995: Sea Ice-Albedo Climate Feedback Mechanism. *J. Clim.*, **8**, 240–247.

Defense News, 2009: Time for Air-Sea Battle Concept. Retrieved from http://www.defensenews.com/story.php?i=4366297 (accessed 10 November 2009).

Delaney, J., 2004: Of Maps and Men: In Pursuit of a Northwest Passage: Exhibition. Retrieved from http://libweb5.princeton.edu/visual_materials/maps/websites/northwest-passage/titlepage.htm (accessed 1 January 2010).

Department of Defense, 2008: Joint Publication 3-0: Joint Operations. Executive Summary.

————, 2008: Joint Publication 3-59: Meteorological and Oceanographic Operations. Introduction-Execution of Meteorological and Oceanographic Forces in Joint Operations.

Deser, C., H. Teng, 2008: Evolution of Arctic sea ice concentration trends and the role of atmospheric circulation forcing, 1979–2007. *GRL*, **35**, doi:10.1029/2007GL032023.

Francis, J. A., 1994: Improvements to TOVS retrievals over sea ice and applications to estimating Arctic energy fluxes. *J. Geophys. Res.*, **99**, 10,395–10,408.

————, 1997: A method to derive downwelling longwave fluxes at the Arctic surface from TIROS operational vertical sounder data. *J. Geophys. Res.*, **102**, 1795–1806.

Francis, J. A., E. Hunter, 2006: New Insight Into the Disappearing Arctic Sea Ice. *Eos Trans. AGU*, **87**, 509–524.

————, ————, 2007: Drivers of declining sea ice in the Arctic winter: A tale of two seas. *Geophys. Res. Lett.*, **34**, doi:10.1029/2007GL030995.

Francis, J. A., E. Hunter, J. R. Key, and X. Wang, 2005: Clues to variability in Arctic minimum sea ice extent. *Geophys. Res. Lett.*, **32**, doi:10.1029/2005GL024376.

Gove, D., Rear Admiral, 2009: Arctic Melt: Reopening a Naval Frontier. *Proceedings Magazine*, **135/2**.

Guest, P., 2001: Vessel Icing: Description. Retrieved from http://www.weather.nps.navy.mil/~psguest/polarmet/vessel/description.html#effect (accessed 3 January 2010).

Hassol, S. J., 2004: Impacts of a Warming Arctic: Arctic Climate Impact Assessment (ACIA).

Hibler, W., 1979: A Dynamic Thermodynamic Sea Ice Model. *J. Phys. Oceanogr.*, **9**, 815–846.

Hu, A., C. Rooth, R. Bleck, and C. Deser, 2002: NAO influence on sea ice extent in the Eurasian coastal region. *Geophys. Res. Lett.*, **29**, doi:10.1029/2001GL014293.

Intergovernmental Panel on Climate Change (IPCC), 2007: Climate Change 2007: Synthesis Report. Cambridge University Press, 52 pp.

International Boundaries Research Unit, 2009: Maritime jurisdiction and boundaries in the Arctic region.

Köberle, C., R. Gerdes, 2003: Mechanisms Determining the Variability of Arctic Sea Ice Conditions and Export. *J. Climate*, **16**, 2843–2858.

Liu, Y., J. R. Key, J. A. Francis, and X. Wang, 2007: Possible causes of decreasing cloud cover in the Arctic winter, 1982-2000. *Geophys. Res. Lett.*, **34**, doi:10.1029/2007GL030042.

Maslowski, W., 2009: Oceanography 3212 Lecture Notes: Section 2, Lecture 4.

————, J.L. Clement, and J. Jakacki, 2008: Toward eddy resolving models of the Arctic Ocean. *Geophysical Monograph Series 177*, doi:10.1029/177GM16.

————, W.H. Lipscomb, 2003: High resolution simulations of Arctic sea ice, 1979-1993. *Polar Research*, **22(I)**, 67–74.

————, D. Marble, W. Walczowski, U. Schauer, J.L. Clement, and A.J. Semtner, 2004: On climatological mass, heat, and salt transports through the Barents Sea and Fram Strait from a pan-Arctic coupled ice-ocean model simulation. *J. Geophys. Res.*, **109**, doi:10.1029/2001JC001039.

————, B. Newton, P. Scholsser, A.J. Semtner, and D.G. Martinson, 2000: Modeling Recent Climate Variability in the Arctic Ocean. *Geophys. Res. Lett.*, **27(22)**, 3743–3746.

Maykut, G. A., N. Untersteiner, 1971: Some Results from a Time-Dependent Thermodynamic Model of Sea Ice. *J. Geophys. Res.*, **76**, 1550–1575.

Military Sealift Command, n.d.: Diego Garcia: A British Territory. Retrieved from http://www.msc.navy.mil/mpstwo/garcia.htm (accessed 1 January 2010).

Miller, J. R., Y. Chen, G. L. Russell, and J. A. Francis, 2007: Future regime shift in feedbacks during Arctic winter. *Geophys. Res. Lett.*, **34**, doi:10.1029/2007GL031826.

Mitchell, T., 2004: Arctic Oscillation (AO) Time Series, 1899-June 2002. Retrieved from http://jisao.washington.edu/ao/ (accessed 28 February 2010).

National Snow and Ice Data Center, n.d.: All About Sea Ice: Processes: Thermodynamics: Albedo. Retrieved from http://nsidc.org/seaice/processes/albedo.html (accessed 2 January 2010).

Ogi, M., J.M. Wallace, 2007: Summer minimum Arctic sea ice extent and the associated summer atmospheric circulation. *Geophys. Res. Lett.*, **34**, doi:10.1029/2007GL029897.

Overland, J. E., M. Wang, 2005: The Arctic climate paradox: The recent decrease of the Arctic Oscillation. *Geophys. Res. Lett.*, **32**, doi:10.1029/2004GL021752.

Perovich, D. K., J. A. Richter-Menge, K. F. Jones, and B. Light, 2008: Sunlight, water, and ice: Extreme Arctic sea ice melt during the summer of 2007. *Geophys. Res. Lett.*, **35**, doi:10.1029/2008GL034007.

Ramon, R., 2010: Bilateral training strengthens American, Japanese ties. Retrieved from http://aimpoints.hq.af.mil/display.cfm?id=37790 (accessed 25 February 2010).

Richeson, R., 2010: Dutch partnerships emphasizes innovations in training. Retrieved from http://aimpoints.hq.af.mil/display.cfm?id=37738 (accessed 22 February 2010).

Richter-Menge, J., E. and J.E. Overland, 2009: Arctic Report Card 2009.

————, ————, M. Svoboda, J. Box, M.J.J.E. Loonen, A. Proshutinsky, V. Romanovsky, D. Russell, C.D. Sawatzky, M. Simpkins, R. Armstrong, I. Ashik, L.-S. Bai, D. Bromwich, J. Cappelen, E. Carmack, J. Comiso, B. Ebbinge, I. Frolov, J.C. Gascard, M. Itoh, G.J. Jia, R. Krishfield, F. McLaughlin, W. Meier, N. Mikkelsen, J. Morison, T. Mote, S. Nghiem, D. Perovich, I. Polyakov, J.D. Reist, B. Rudels, U. Schauer, A. Shiklomanov, K . Shimada, V. Sokolov, M. Steele, M.-L. Timmermans, J. Toole, B. Veenhuis, D. Walker, J. Walsh, M. Wang, A. Weidick, and C. Zöckler, 2008: Arctic Report Card 2008.

Rigor, I. G., J. M. Wallace, 2004: Variations in the age of Arctic sea-ice and summer sea-ice extent. *Geophys. Res. Lett.*, **31**, doi:10.1029/2004GL019492.

————, ————, and R.L. Colony, 2002: Response of sea ice to the Arctic Oscillation. *J. Clim.*, **15**, 2648–2663.

Rolfsen, B., 2010: The Air Force has its marching orders. Retrieved from http://aimpoints.hq.af.mil/display.cfm?id=37718 (accessed 12 February 2010).

Rothrock, D. A., J. Zhang, and Y. Yu, 2003: The Arctic ice thickness anomaly of the 1990s: A consistent view from observation and models. *J. Geophys. Res.*, **108(C3)**, doi:10.1029/2001JC001208.

Schweiger, A.J., R.W. Lindsay, S. Vavrus, and J.A. Francis, 2008: Relationships between Arctic Sea Ice and Clouds during Autumn. *J. Climate*, **21**, 4799–4810.

Serreze, M. C., R. G. Barry, 2005: *The Arctic Climate System.* Cambridge, Cambridge University Press, 385 pp.

Stabeno, P.J., J.E. Overland, 2001: Bering sea shifts toward an earlier spring transition. *Eos Trans. AGU*, **82(29)**, 317.

Stroeve, J., M.M. Holland, W. Meier, T. Scambos, and M. Serreze, 2007: Arctic sea ice decline: Faster than forecast. *Geophs. Res. Lett.*, **34**, doi:10.1029/2007GL029703.

Stump, A.M., 2009: Top Air Force NCO Visits Canada to Develop Partnership. Retrieved from http://www.militaryconnection.com/news%5Cnovember-2009%5Cair-nco-canada.html (accessed 23 November 2009).

Sturm, M., T. Douglas, C. Racine, and G.E. Liston, 2005: Changing snow and shrub conditions affect albedo with global implications. *J. Geophys. Res.*, **110**, doi:10.1029/2005JG000013.

The White House Council on Environmental Quality Interagency Ocean Policy Task Force, 2009: The Interim Report of the Interagency Ocean Policy Task Force.

Thompson, D. W. J., J. M. Wallace, 1998: The Arctic Oscillation signature in the wintertime geopotential height and temperature fields. *Geophys. Res. Lett.*, **25**, 1297–1300.

————, ————, 2000: Annular modes in the extratropical circulation. Part I: Month-to-month variability. *J. Climate*, **13**, 1000–1016.

Titley, D., 2009: U.S. Navy Engagement in an Ice-Diminished Arctic. *Proc. 3rd Symposium on the Impacts of an Ice-Diminished Arctic on Naval and Maritime Operations*, U.S. Naval Academy, MD.

U.S. Department of State, n.d.: Purchase of Alaska. Retrieved from http://www.state.gov/r/pa/ho/time/gp/17662.htm (accessed 21 December 2009).

VanderKlippe, N., 2006: Northwest Passage gets political name change. *Ottawa Citizen.*

Wang, M., J. Overland, 2009: A sea ice free summer Arctic within 30 years? *Geophy. Res. Lett.*, **36**, doi:10.1029/2009GL037820.

Whelan, J., 2007: Understanding recent variability in the Arctic sea ice cover - synthesis of model results and observations.

Zhang, J., D. Rothrock, and M. Steele, 2000: Recent Changes in Arctic Sea Ice: The Interplay between Ice Dynamics and Thermodynamics. *J. Climate*, **13**, 3099–3114.

INITIAL DISTRIBUTION LIST

1. Defense Technical Information Center
   Ft. Belvoir, Virginia

2. Dudley Knox Library
   Naval Postgraduate School
   Monterey, California

3. Air Force Weather Technical Library
   151 Patton Ave, Room 120
   Asheville, North Carolina

4. CAPT Timothy Gallaudet, USN
   Task Force Climate Change, Office of Naval Research
   Washington, District of Columbia

5. Clara Deser, PhD
   Climate Analysis Section, National Center for Atmospheric Research
   Boulder, Colorado

6. Jennifer A. Francis, PhD
   Institute of Marine and Coastal Sciences, Rutgers University
   Shrewsbury, New Jersey

7. Wieslaw Maslowski, PhD
   Department of Oceanography, Naval Postgraduate School
   Monterey, California

8. CDR Rebecca E. Stone, PhD, USN
   Department of Oceanography, Naval Postgraduate School
   Monterey, California

9. Capt Hsien-Liang R. Tseng, USAF
   16th Weather Squadron, 2nd Weather Group
   Offutt Air Force Base, Nebraska